1 OF 2
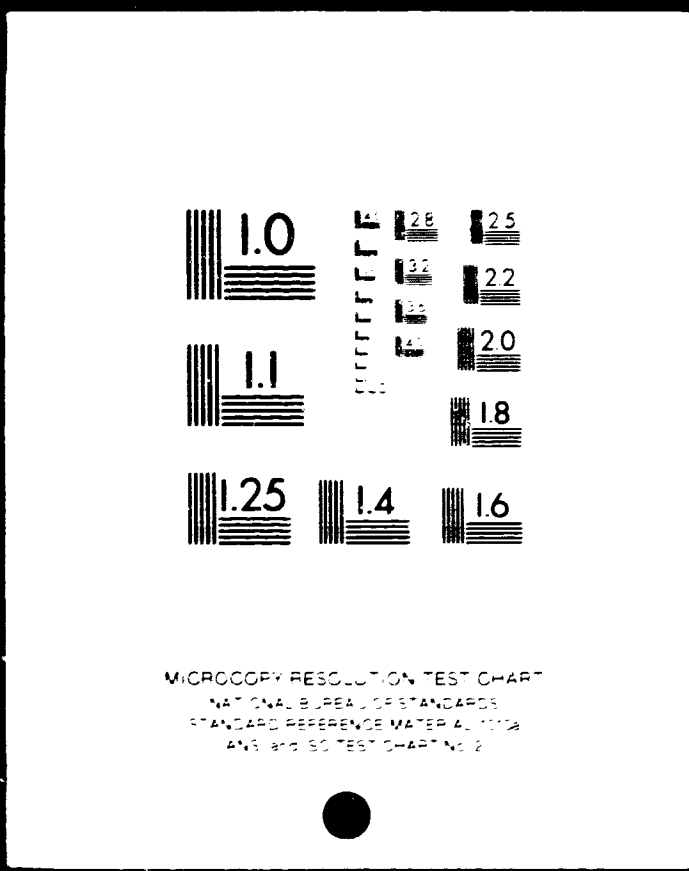
N90-28560 UNCLAS

P/65

#304586

ENERGY EFFICIENT ENGINE PROGRAM

ADVANCED TURBOFAN NACELLE DEFINITION STUDY

by

D. C. Howe and T. A. Wynosky

UNITED TECHNOLOGIES CORPORATION
Pratt & Whitney
Engineering Division

(NASA-CR-174942) ENERGY EFFICIENT ENGINE   N86-24586
PROGRAM ADVANCED TURBOFAN NACELLE DEFINITION
STUDY (PWA) 165 p   CSCL 21E
                                                             Unclas
                                                    G3/07 0304586

Prepared for

1. REPORT NO. NASA CR-174942	2. GOVERNMENT ACCESSION NO.	3. RECIPIENT'S CATALOG NO.

4. TITLE AND SUBTITLE Energy Efficient Engine Program Advanced Turbofan Nacelle Definition Study	5. REPORT DATE May 1985
	6. PERFORMING ORG. CODE

7. AUTHOR(S) D. C. Howe and T. A. Wynosky	8. PERFORMING ORG. REPT. NO. PWA-5594-315

9. PERFORMING ORG. NAME AND ADDRESS UNITED TECHNOLOGIES CORPORATION Pratt & Whitney Engineering Division East Hartford, CT 06108	10. WORK UNIT NO.
	11. CONTRACT OR GRANT NO. NAS3-20646

12. SPONSORING AGENCY NAME AND ADDRESS National Aeronautics and Space Administration Lewis Research Center 21000 Brookpark Road, Cleveland, Ohio 44135	13. TYPE REPT./PERIOD COVERED Topical Report
	14. SPONSORING AGENCY CODE

15. SUPPLEMENTARY NOTES
NASA Project Manager: Mr. E. T. Meleason
NASA-Lewis Research Center, 21000 Brookpark Road, Cleveland, OH 44135

16. ABSTRACT

Under the NASA-sponsored Energy Efficient Engine Program, Pratt & Whitney undertook the Advanced Turbofan Nacelle Definition Study to further define advanced, low-drag, nacelle configurations for some of the more promising propulsion systems identified in the earlier Benefit/Cost Study, to assess the benefits associated with these advanced technology nacelles and formulate programs for developing these nacelles and low-volume thrust reversers/spoilers to a state of technology readiness in the early 1990's. The study results established the design feasibility of advanced technology, slim-line nacelles applicable to advanced technology, high bypass ratio turbofan engines. Design feasibility was also established for two low volume thrust reverser/spoiler concepts that meet or exceed the required effectiveness for these engines. These nacelle and thrust reverser/spoiler designs were shown to be applicable in engines with takeoff thrust sizes ranging from 24,000 to 60,000 pounds. The reduced weight, drag, and cost of the advanced technology nacelle installations relative to current technology nacelles offer a mission fuel burn savings ranging from 3.0 to 4.5 percent (depending on mission) and direct operating cost plus interest improvements from 1.6 to 2.2 percent. Subcontractor evaluations by Douglas Aircraft Company utilizing these advanced engine/nacelle concepts indicated that up to 28% fuel burn savings on long range missions are attainable for an advanced widebody transport relative to currently available production engines/nacelles.

17. KEY WORDS (SUGGESTED BY AUTHOR(S)) Energy Efficient Engine Advanced Slim-Line Nacelle Low-Volume Thrust Reversers/Spoilers High Bypass Ratio Turbofans	18. DISTRIBUTION STATEMENT

19. SECURITY CLASS THIS (REPT) Unclassified	20. SECURITY CLASS THIS (PAGE) Unclassified	21. NO. PGS	22. PRICE *

FORWARD

The Energy Efficient Engine Component Development and Integration program is being conducted under parallel National Aeronautics and Space Administration contracts with Pratt & Whitney and General Electric Company. The overall project is under the direction of Mr. Carl C. Ciepluch. The Pratt & Whitney effort is under contract NAS3-20646, and Mr. Edward Meleason is the NASA Project Engineer responsible for the portion of the project described in this report. Mr. David E. Gray is Manager of the Energy Efficient Engine Program at Pratt & Whitney. This report was prepared by Mr. T. A. Wynosky and Mr. D. C. Howe of Pratt & Whitney.

TABLE OF CONTENTS

LIST OF ILLUSTRATIONS

LIST OF FIGURES (cont.)

LIST OF FIGURES (cont.)

LIST OF FIGURES (cont.)

LIST OF FIGURES (cont.)

LIST OF FIGURES (cont.)

LIST OF TABLES

LIST OF TABLES (cont.)

SECTION 1.0 SUMMARY

The National Aeronautics and Space Administration, under the Energy Efficient Engine Component Development and Integration Program, sponsored the Advanced Turbofan Nacelle Definition Study with the objectives of:

1) further defining the advanced nacelle configurations for some of the more promising propulsion systems identified in the earlier Energy Efficient Engine Benefit/Cost Study;

2) establishing in greater detail the viability, potential benefits, and technology requirements of these advanced nacelle concepts.

The Douglas Aircraft Company, as subcontractor, provided assistance in the design of the nacelle installations, conducted independent evaluations, and also assisted in the identification of technologies important to the success of these advanced nacelle concepts. Comments on the nacelle installations were also solicited and received from the Boeing Commercial Airplane Company and the Lockheed Corporation (Marietta, Georgia). Results of the study effort are summarized as follows:

o   Design feasibility of advanced technology, slim-line nacelles and low volume thrust reversers/spoilers was established for advanced turbofan engines ranging in takeoff thrust sizes from 106,756 to 266,892 Newtons (24,000 to 60,000 pounds).

o   When installed on advanced, high bypass ratio turbofan engines, the reduced weight, drag, and cost of advanced technology nacelles relative to current technology nacelles resulted in mission fuel burn savings ranging from 3.0 to 4.5 percent (depending on mission) and direct operating cost plus interest improvements ranging from 1.6 to 2.2 percent.

o   The predicted performance and economic advantages of geared fan engines relative to direct-drive fan engines were maintained with the more refined nacelle evaluations.

o   Douglas Aircraft Company evaluations utilizing the advanced technology nacelle and engine concepts on advanced, wide body transport concepts indicated that up to 28 percent fuel burn savings on long range missions are attainable, relative to currently available production engines and nacelles.

o   Preliminary noise estimates of the study turbofan engines incorporating advanced technology, slim-line nacelles indicated that it would be feasible to achieve FAR Part 36 Stage 3 noise limits.

o   Technology concepts requiring further analysis or test verification were identified, and a technology development program plan to address them was formulated.

SECTION 2.0 INTRODUCTION

The National Aeronautics and Space Administration has the objective of improving the energy efficiency of future United States commercial aircraft so that substantial savings in fuel can be realized. Toward this objective, NASA established the Energy Efficient Engine Component Development and Integration program in 1978 under contract NAS3-20646. Minimum goals for this program are a 12 percent reduction in thrust specific fuel consumption (TSFC) and a 5 percent reduction in direct operating costs (DOC) compared to the Pratt & Whitney JT9D-7A engine. In addition, FAR Part 36 (1978) noise rules and EPA-proposed 1981 exhaust emissions standards must be met.

The Energy Efficient Engine Component Development and Integration program is based on the results of the completed Energy Efficient Engine Preliminary Design and Integration Studies (Ref. 1). Through the extension of the technology base developed under this early program, The Energy Efficient Engine Component Development and Integration program will develop and demonstrate the technology for achieving higher overall efficiency (thermodynamic and propulsive) in future environmentally acceptable turbofan engines. To meet these program objectives, the current program consists of the following two tasks:

- o   Task 1 -- Flight Propulsion System analysis, design, and integration;
- o   Task 2 -- component analysis, design, and development.

More specifically, Task 1 provides for 1) the preliminary design of a flight propulsion system based on various iterative analyses and design updates, 2) propulsion system/aircraft integration evaluation, 3) program risk assessment, 4) a technology benefit/cost study, and 5) an advanced turbofan nacelle definition study -- the subject of this report.

The completed benefit/cost study (Ref. 2) identified several design characteristics that can maximize fuel savings beyond those projected for the refined Energy Efficient Engine evaluated in that study. One of several advanced concepts identified as contributing to fuel savings is a short, slim nacelle. The Advanced Turbofan Nacelle Definition Study was added to the Energy Efficient Engine program in December, 1983 to further define advanced nacelle configurations for some of the more promising propulsion systems identified in the benefit/cost study. The study focused on low external drag configurations with inlet designs that are thin-lipped and have short diffuser sections with minimum internal flow separation. Low volume thrust reverser/spoiler configurations were also considered. Installation drawings were prepared and supplied to the Douglas Aircraft Company which, as the subcontractor, conducted an independent evaluation of the refined nacelle installations. These drawings also formed the basis for refined weight and cost estimates used in an engine benefits evaluation. The Boeing and Lockheed Aircraft companies provided qualitative comments on the nacelle and installation designs.

This report describes the results of the Advanced Turbofan Nacelle Definition Study and includes a technology development plan for bringing the short, slim-line nacelle concept into a state of technology readiness.

SECTION 3.0 STUDY GROUND RULES

In conjunction with Douglas Aircraft Company, Pratt & Whitney carefully reviewed the aircraft, mission, economic, and nacelle related assumptions used in calculating benefits for advanced turbofan propulsion systems in the earlier Energy Efficient Engine Benefit/Cost Study.

As a result of this review, Pratt & Whitney recommended updating the Energy Efficient Engine (E^3) economic model for use in the Advanced Turbofan Nacelle Definition Study. The E^3 Benefit/Cost Study (Ref. 2) was completed using 1980 dollars with three fuel prices: $0.26, $0.40, and $0.53 per liter ($1.00, $1.50, and $2.00 per gallon). The recommendation was to re.ise the economic model to reflect 1983 dollars while continuing to use the same three fuel prices. Revised ground rules are shown in Tables 3-I and 3-II. Other than updating to 1983 dollars, the economic model and method of analysis are essentially unchanged. Figures 3-1 and 3-2 present information used in calculating crew costs.

The three airplanes described in Table 3-III were recommended for use in the evaluation. The short range, 150 passenger airplane is essentially identical to the one used in the earlier Benefit/Cost Study. The medium and long range airplanes have been updated to reflect the industry trend toward minimizing the number of engines for each aircraft/mission requirement. Thus, the domestic trijet shown in the reference becomes a twinjet, and the intercontinental quadjet is replaced with a trijet. These aircraft cover a wide range of possible applications for advanced technology engines and nacelles. The recommended updates were approved by the NASA program manager.

TABLE 3-I
Guidelines for E³ Direct Operating Cost (DOC) and DOC+Interest
Economic Analysis -- Recommended Revisions (1/84) for Nacelle Definition Study

Notes

Notes		
1, 2, 4	Crew Cost	1983 update of 1979 Boeing
3	Fuel	$0.26, 0.40, 0.53/liter ($1.00, 1.50, 2.00/gallon) in 1983 dollars
	Aircraft	
1, 2	o Price	PWA 1983
3, 2	o Utilization	1979 Boeing
1, 2	o Block Time	1979 Boeing
3	Insurance	1/2% flyaway per year
1, 2	Airframe Maintenance	1983 update of 1979 Boeing
3	Maintenance Burden	200% labor
3	Depreciation	Straight-line, 15 years to 10% residual
	o Spares	Airframe: 6%
		Engine: 30%
3	Engine Maintenance	Mature engine, no immaturity bump
		No derate
1	Year Dollars	1983
3	Interest Rate	15%

Notes: 1) Different from E³ Benefit/Cost Study
       2) Equations/explanation on next page
       3) No change from E³ Benefit/Cost Study
       4) Crew pay will be fixed for each airplane type
          (i.e., changes in gross weight caused by
          technology and/or propulsion system differences
          will not influence crew pay once the reference
          airplane configuration has been established).

TABLE 3-II
Recommended 1983 Economic Model Equations

•Crew Cost — Domestic = 1.455 $((33.7\ F_v + 28.08)\ F_u + 32.30$
(S/Block Hour)   (2 Crew)

Internatioal = 1.455 $((24.10\ F_v + 248.30)\ F_u + 81.00)$
(3 Crew)

Where F_v & F_u are attached

Aircraft Price — $0.8056\left(\dfrac{WAF}{1000}\right)^{0.7}$ $\times 10^6$ (Airframe)

$+\ 1.611\ (0.0089\ (\text{seats}) - 0.315)\ \times 10^6$ (Furnishings)

$+\ 1.611\ (0.0022\ (\text{seats}) + 1.81)\ \times 10^6$ (Avionics)

Utilization — Constant Trips/Year as Function of Range
(3200 @ 250 NM, 2200 @ 500 NM,
1400 @ 1000 NM, 850 @ 2000 NM)

Block Time — Taxi Times — Domestic 14 min
International 18 min

•Airframe Maintenance — Material = $0.3955\left(\dfrac{WAF}{1000}\right)$ /Block Time

$+\ 0.3172\left(\dfrac{WAF}{1000}\right)\left(\dfrac{\text{Flight Time}}{\text{Block Time}}\right)$

Labor $=\left[0.07365\left(\dfrac{WAF}{1000}\right)^{0.7908}\right.$ /Block Time

$\left.+\ 0.2048\left(\dfrac{WAF}{1000}\right)^{0.595}\left(\dfrac{\text{Flight Time}}{\text{Block Time}}\right)\right]$

$\times$ Labor Rate

WAF = Airframe Weight = OWE-Engine Weight

Labor Rate (Direct) = $15.15/Hour
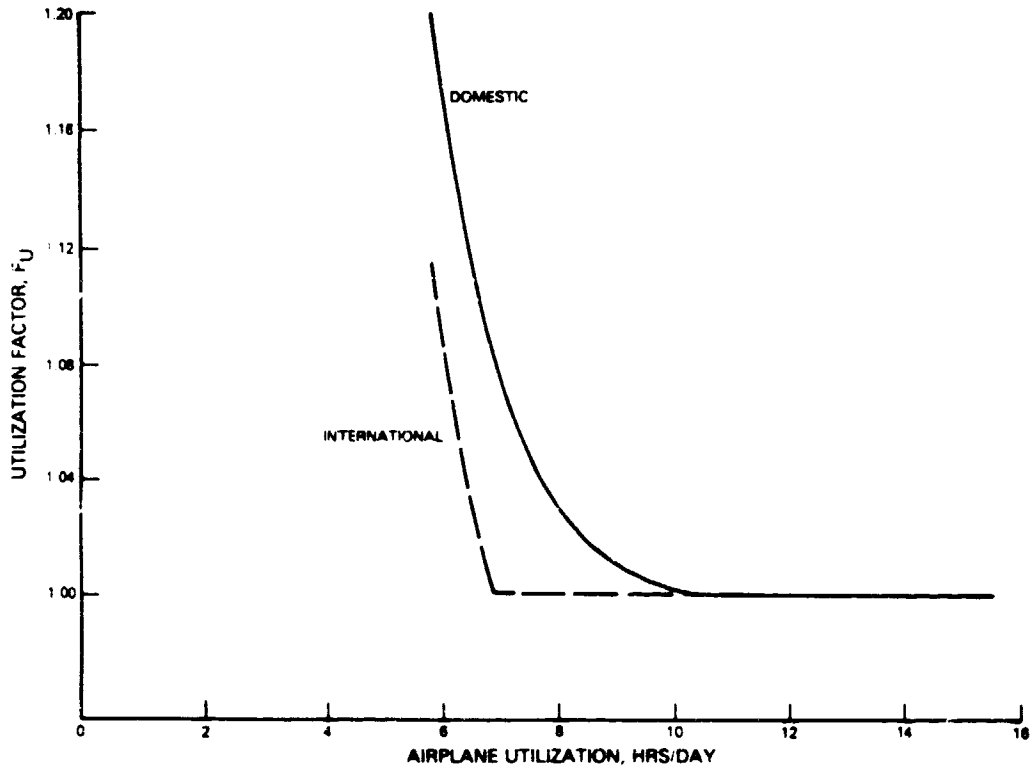
Figure 3-1   Crew Utilization Factor Used in Computing Crew Costs
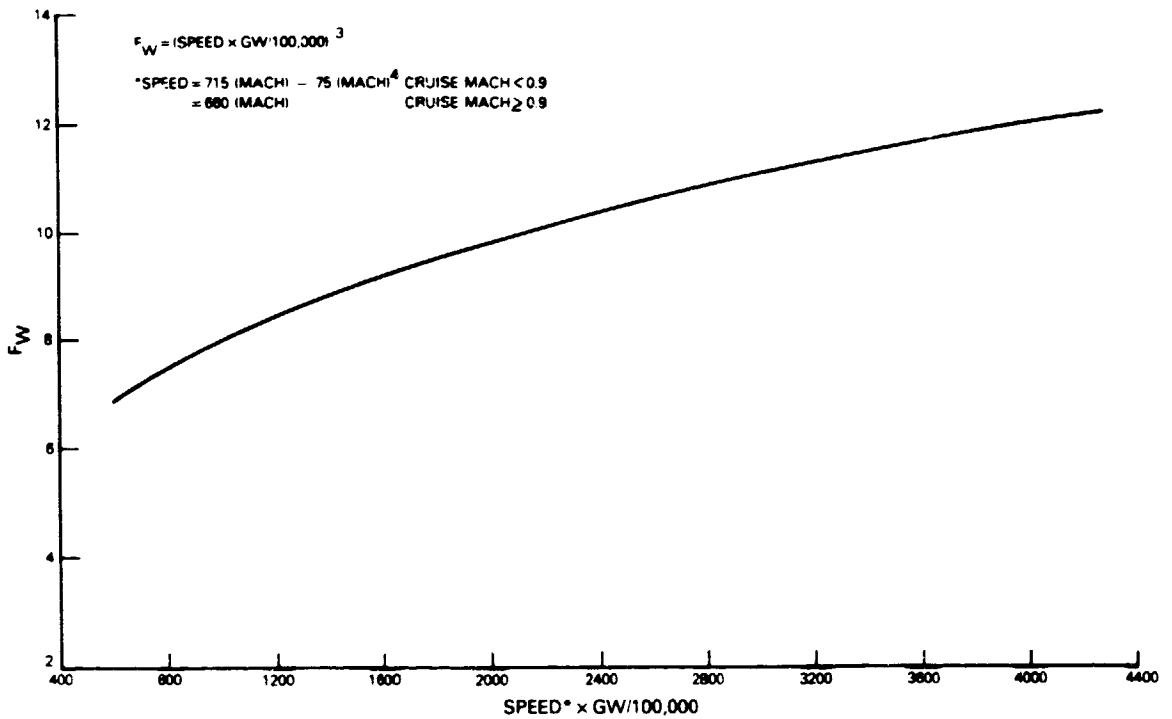
Figure 3-2   Airplane Speed/Gross Weight Factor Used in Calculating Crew Costs

6

TABLE 3-III
Recommended Pratt & Whitney Energy Efficient Engine Study Aircraft

PART 1: Recommended Missions

	Domestic	Domestic	Intercontinental
Design Range (NM)	1800	4000	6000
Typical Range (NM)	400	1000	2000
Design Payload (Passengers)	150	350	440
Cruise Mach Number	0.78	0.80	0.80
Initial Cruise Altitude, m (ft.)	11,887 (39,000)	11,887 (39,000)	10,058 (33,000)
Takeoff Field Length, m (ft.)	1,828 (6,000)	2,438 (8,000)	3,048 (10,000)

PART 2: Recommended Aircraft

	Domestic	Domestic	Intercontinental
TOGW Class, kg (lbs.)	61,234 (135,000)	199,546 (440,000)	306,173 (675,000)
Wing			
Aspect Ratio	10	12	12
Quarter Chord Sweep (degrees)	23	25	25
Fuselage			
Diameter, cm (in.)	391 (154)	601 (237)	601 (237)
Seating (# first/tourist)	12/138	54/296	44/396
Seating (A/B first/tourist)	4/6	6/9	6/9
Engine			
Number	2	2	3
Location	Wing	Wing	Wing/Tail
Takeoff Thrust Class, N (lbs.)	93,412 (21,000)	266,892 (60,000)	200,169 (45,000)

SECTION 4.0   CONFIGURATION SELECTION

4.1   ENGINE CYCLE SELECTION

The approved airplane and economic models referred to in Section 3.0 were used to generate trade factors showing the effects of TSFC, weight, costs, and maintenance costs on mission fuel burn and economics for each airplane at each of the three fuel prices. These trade factors were then used to evaluate a matrix of direct drive, geared, mixed flow, and separate flow engines (incorporating year 2000-2010 technology levels) which were originally evaluated in the Benefit/Cost Study. Engines with bypass ratios ranging from 7 to 17 and both advanced and current technology nacelle designs were evaluated. Only isolated pod performance was considered: potential interference drag and/or ground clearance, etc., problems arising from specific airplane applications were not addressed. Engines were sized at cruise and all had adequate take-off thrust to meet field length requirements.

Results of the updated screening evaluations are shown in Figures 4.1-1 through 4.1-3 for $0.40/liter ($1.50/gal.) fuel price. Lowering fuel price to $0.26/liter ($1.00/gal.) has little effect on cycle selection, as shown in Figure 4.1-3, where $0.40 and $0.26/liter ($1.50 and $1.00/gal.) results are compared. Likewise, Figure 4.1-1 shows that raising fuel prices to $0.53/liter ($2.00/gal.) has very little effect on the trends. DOC and fuel burn trends are quite similar to those of the original Benefit/Cost Study, as a comparison of Figure 4.1-4 with Figure 4.1-1 shows. Geared, separate-flow engines provide best DOC+I and fuel burn regardless of airplane type. For these engines, the optimum bypass ratio appears to be approximately 13.0 for minimum DOC+I. The short-range twin optimizes somewhat below 13.0, and the long range trijet optimizes slightly above. Minimum fuel burn, however, occurs at the highest bypass ratio investigated for all three airplane types. The best direct-drive engine is also separate-flow and has an optimum bypass ratio near 10.0.
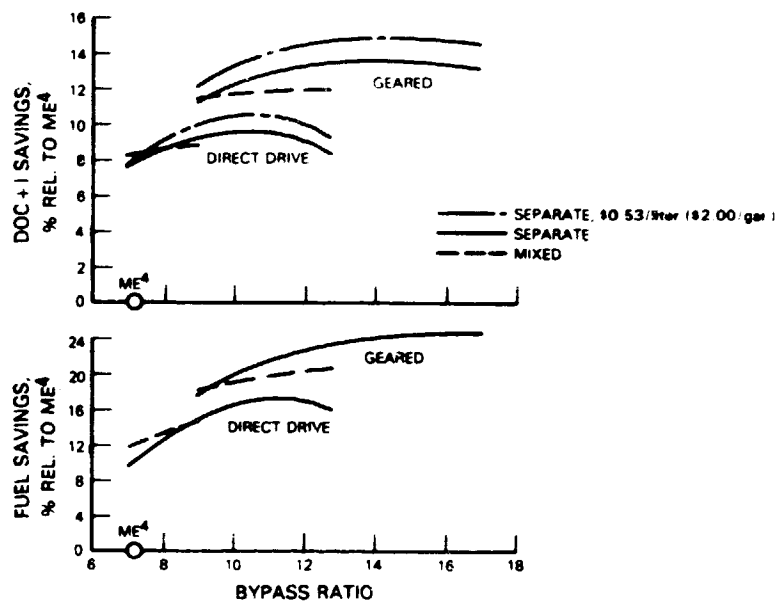
Figure 4.1-1   Bypass Ratio Effect on DOC+I and Fuel Burn, 440 Pax Trijet @ 2000 NM, $0.40/1 ($1.50/gal.) Fuel

8

DOC + I SAVINGS, % REL TO ME^4

12
10
8
6
4
2
0

GEARED

DIRECT DRIVE

ME^4

SEPARATE
MIXED

FUEL SAVINGS, % REL TO ME^4

24
20
16
12
8
4
0

GEARED

DIRECT DRIVE

ME^4

6   8   10   12   14   16   18
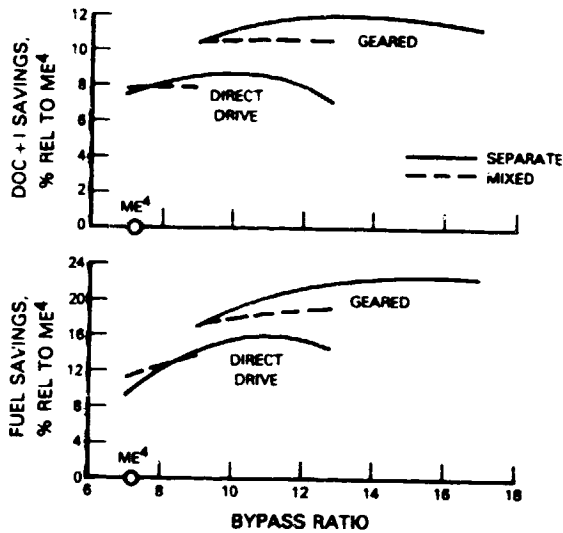
BYPASS RATIO

Figure 4.1-2 Bypass ratio Effect on DOC+I and Fuel Burn, 350 Pax Twinjet, 1000 NM, $0.40/1 ($1.50/gal.) Fuel

DOC + I SAVINGS, % REL TO ME^4

12
10
8
6
4
2
0

GEARED

DIRECT DRIVE

ME^4

$0.26/1 ($1.00/GAL)
FUEL, SEPARATE
SEPARATE
MIXED

FUEL SAVINGS, % REL TO ME^4

24
20
16
12
8
4
0

GEARED

DIRECT DRIVE

ME^4

6   8   10   12   14   16   18
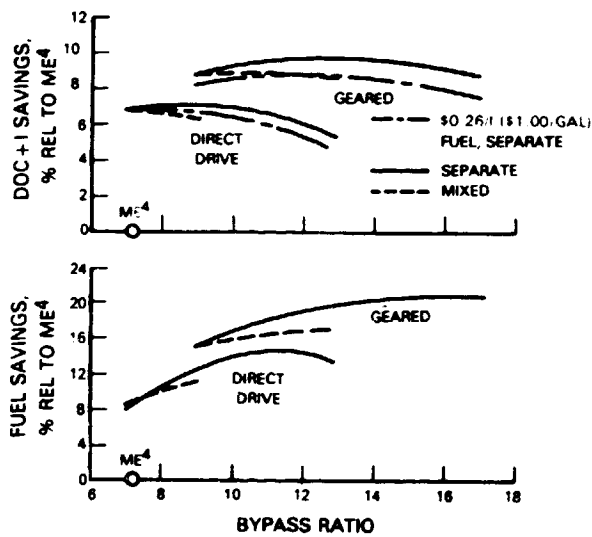
BYPASS RATIO

Figure 4.1-3 Bypass Ratio Effect on DOC+I and Fuel Burn: 150 Pax Twinjet @ 400NM, $0.40/1 ($1.50/gal.) Fuel
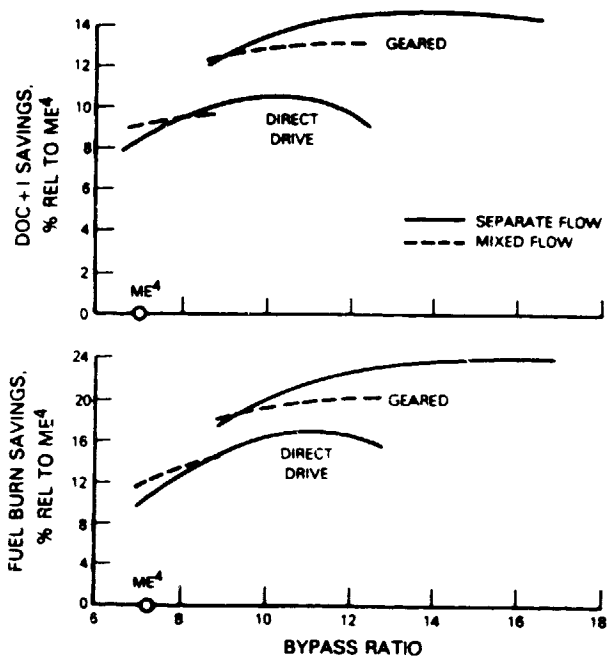
Figure 4.1-4   Bypass Ratio Effect on Fuel Burned and DOC+I, 500 Passenger
Quadjet @ 2000 NM, $0.40/l ($1.50/gal.) Fuel

Based on the updated screening study results, the engine cycles shown in Table
4.1-I were recommended and approved for use in the preliminary design phase of
the study. They encompass airplane thrust requirements ranging from the small
domestic twin to the large domestic twin and represent minimum DOC+I and mini-
mum fuel burn bypass ratios, as shown in Figures 4.1-5 and 4.1-6. The refe-
rence engine for comparative purposes is the Maximum Efficiency Energy Effi-
cient Engine (ME[4]) that was defined in Reference 2.

TABLE 4.1-I
Recommended Engine Cycles

	ME[4]	STF654	STF653	STF653-DD
Fan Drive	Direct	Geared	Geared	Direct
Take-Off Thrust, N (lbs.)	177,928	106,756	257,995	222,410
	(40,000)	(24,000)	(58,000)	(50,000)
Bypass Ratio (M_{CR})	7.2	11.8	12.8	9.6
Fan Pressure Ratio (M_{CR})	1.65	1.56	1.53	1.70
Overall Pressure Ratio (M_{CR})	38.6	55.0	64.0	64.0
Combustor Exit Temperature, Max °C (Max °F)	1,435 (2,616)	1,482 (2,700)	1,482 (2,700)	1,482 (2,700)
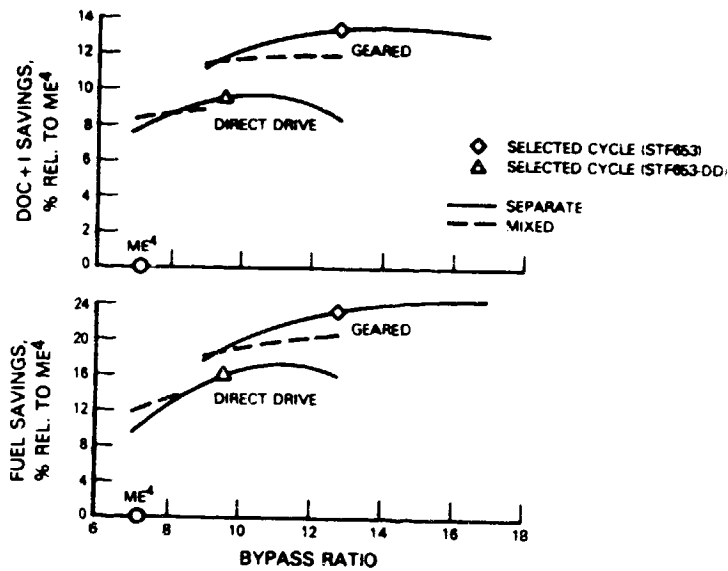
Figure 4.1-5 Bypass Ratio Effect on DOC+I and Fuel Burn: 440 Pax Trijet @ 2000 NM, $0.40/1 ($1.50/gal.) Fuel: Engine Cycle Selection
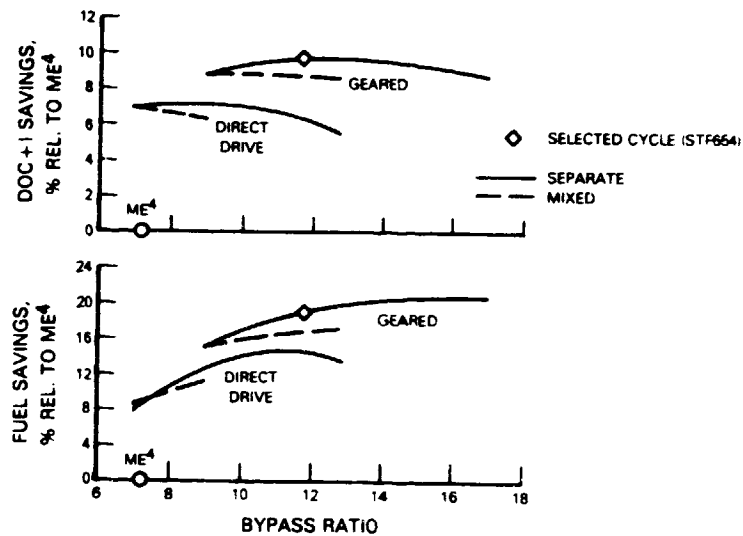
Figure 4.1-6 Bypass Ratio Effect on DOC+I and Fuel Burn: 150 Pax Twinjet @ 400 NM, $0.40/1 ($1.50/gal.) Fuel: Engine Cycle Selection

4.2 NACELLE CONCEPT SELECTION

Aerodynamics

Nacelle concept selection was based upon the principle of defining the ideal geometric configuration from an aerodynamic standpoint and then assessing the factors that might compromise the ideal configuration. Engine installation features affecting the application of this principle were considered in the selection of the recommended engine cycles described in Section 4.1. For example, the STF653 engine with a bypass ratio of 12.8 is amenable to "clean" nacelle contours, as shown in Figure 4.2-1, and can accommodate core-mounted accessories. However, an engine with essentially the same bypass ratio in a smaller thrust size (STF654) may have essentially the same ideal nacelle aerodynamic contours (see Figure 4.2-2) but may require installation of engine

11

accessories in the cowl if there is not sufficient room for them in the engine core. This possibility could significantly compromise the nacelle geometry and needs to be explored. The advanced technology nacelle contours recommended for further analysis are shown in Figures 4.2-1 through 4.2-3.
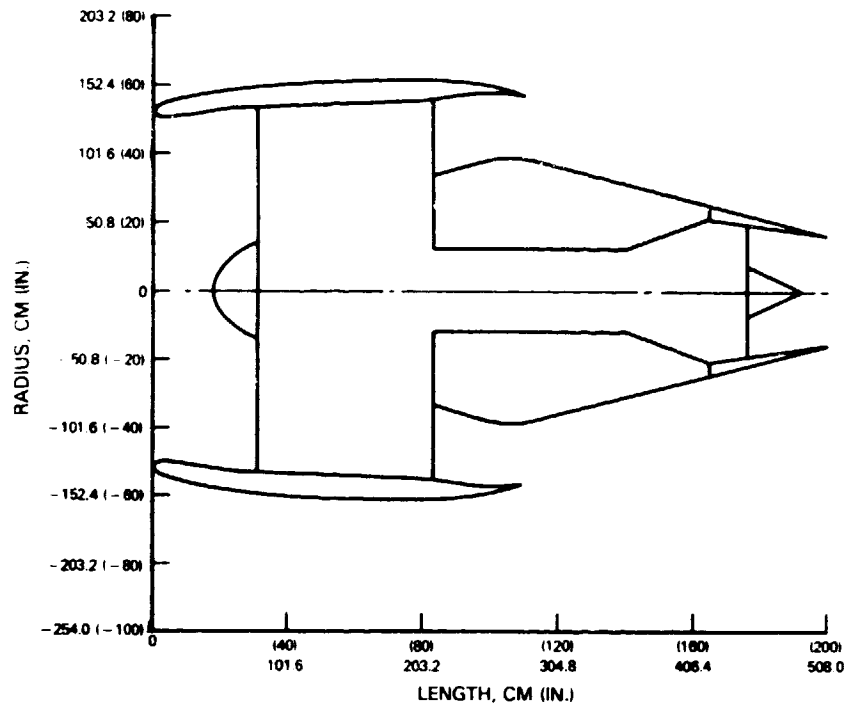
Figure 4.2-1 STF653 Advanced Technology Nacelle Contours Recommended for Further Analysis
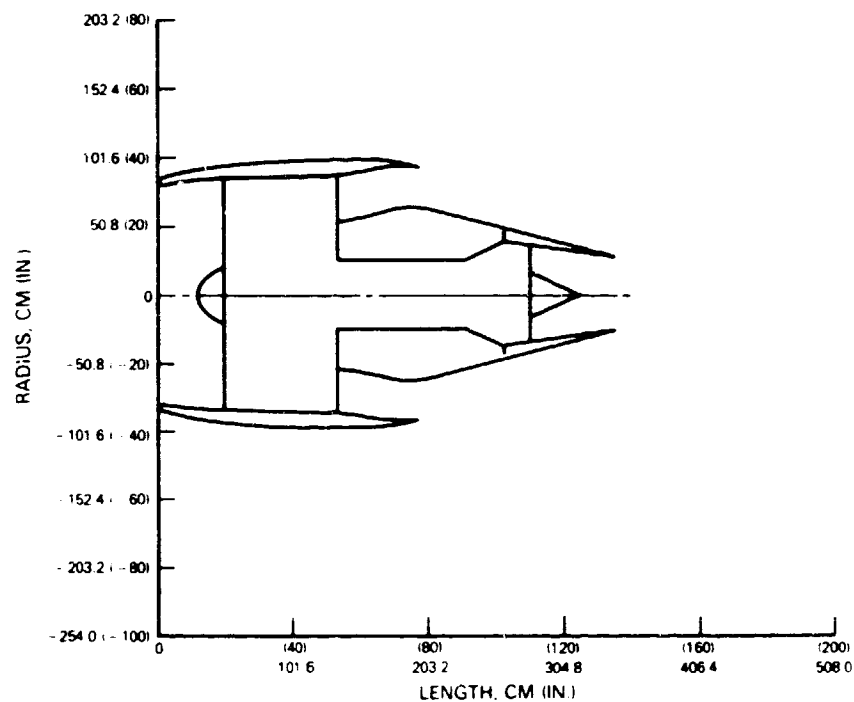
Figure 4.2-2 STF654 Advanced Technology Nacelle Contours Recommended for Further Analysis

12
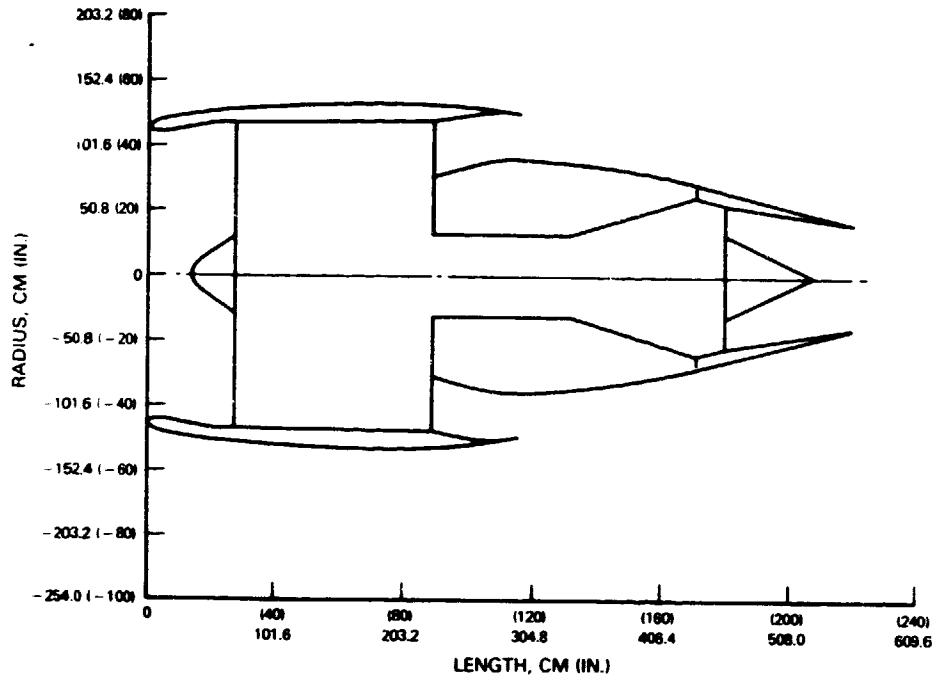
Figure 4.2-3 STF653-DD Advanced Technology Nacelle Contours Recommended for Further Analysis

A comparison of the nacelle contours resulting from the application of advanced and current technology aerodynamic concepts is illustrated in Figure 4.2-4, along with the impact of advanced technology on nacelle design features. The principal nacelle characteristics which differentiate each nacelle concept are listed in Figure 4.2-5, and the design-point aerodynamic conditions are listed in Table 4.2-I. Preliminary estimates of nacelle installation losses for the advanced concepts relative to current concepts are shown in Figure 4.2-6.
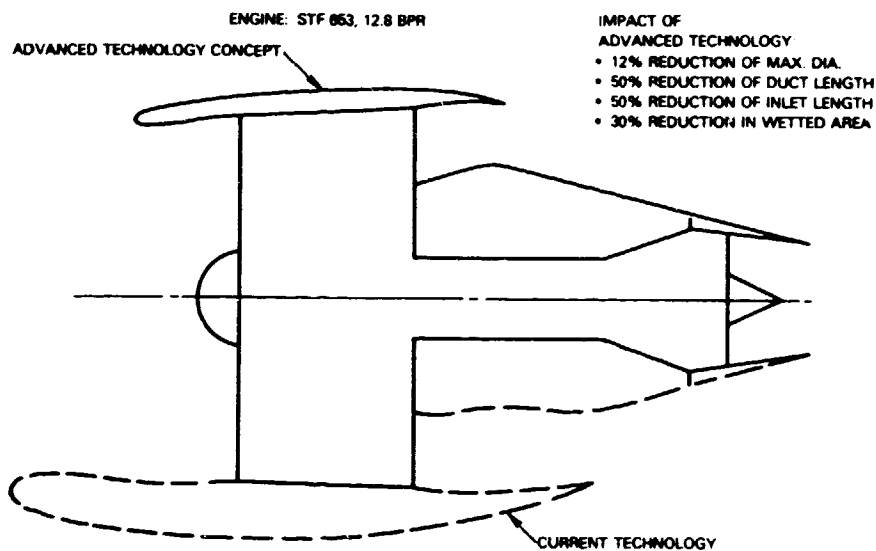
Figure 4.2-4 A Comparison of Advanced and Current Technology Designs Illustrates the Potential Impact of Design Innovation and Advanced Aero Technology

13
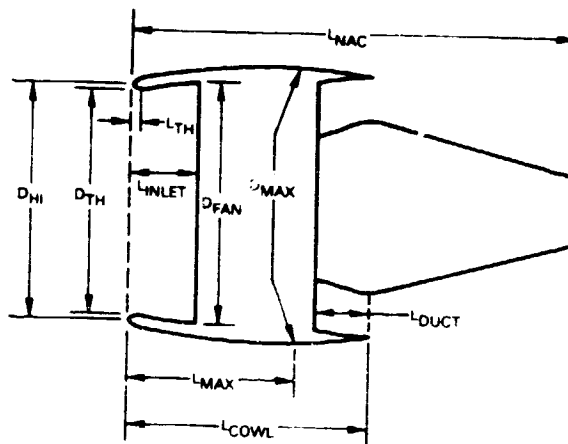
TECHNOLOGY	ADVANCED	ADVANCED	ADVANCED	CURRENT
ENGINE	STF653	STF653-DD	STF654	STF653
$D_{FAN(REFERENCE)}$	106.800 IN. (271.272 CM.)	93.84 IN (238.354 CM.)	67.800 IN (172.212 CM.)	106.8 IN (271.272 CM.)
D_{MAX}	122.471 IN. (311.076 CM.)	106.00 IN (269.240 CM.)	78.293 IN (198.864 CM.)	139.9 IN (355.346 CM.)
D_{HI}/D_{MAX}	0.846	0.858	0.839	0.828
D_{TH}/D_{FAN}	0.944	0.944	0.944	0.963
L_{TH}/D_{FAN}	0.0313	0.0313	0.0313	0.1404
L_{MAX}/D_{MAX}	0.672	0.755	0.798	0.565
L_{NAC}/D_{FAN}	1.864	2.331	1.989	2.205
L_{DUCT}/D_{FAN}	0.255	0.285	0.350	0.505
L_{INLET}/D_{FAN}	0.291	0.291	0.291	0.637
L_{COWL}/D_{FAN}	1.522	1.225	1.131	1.620

Figure 4.2-5   Preliminary Nacelle Geometric Characteristics

TABLE 4.2-I
Nacelle Design Point Conditions

Mach Number: 0.80
Altitude: 10.67 km (35,000 ft.)

Engine	STF653	STF653-DD	STF654
Fan Nozzle Pressure Ratio	2.32	2.57	2.36
Primary Nozzle Pressure Ratio	1.80	1.86	1.78
Maximum Corrected Flow in kg (lbs.)/sec $\dfrac{Wa\sqrt{\theta}_{t_2}}{\delta_{t_2}}$	1,239 (2733)	957 (2110)	498 (1100)
Mass Flow Ratio (MFR)	0.94	0.94	0.94

14
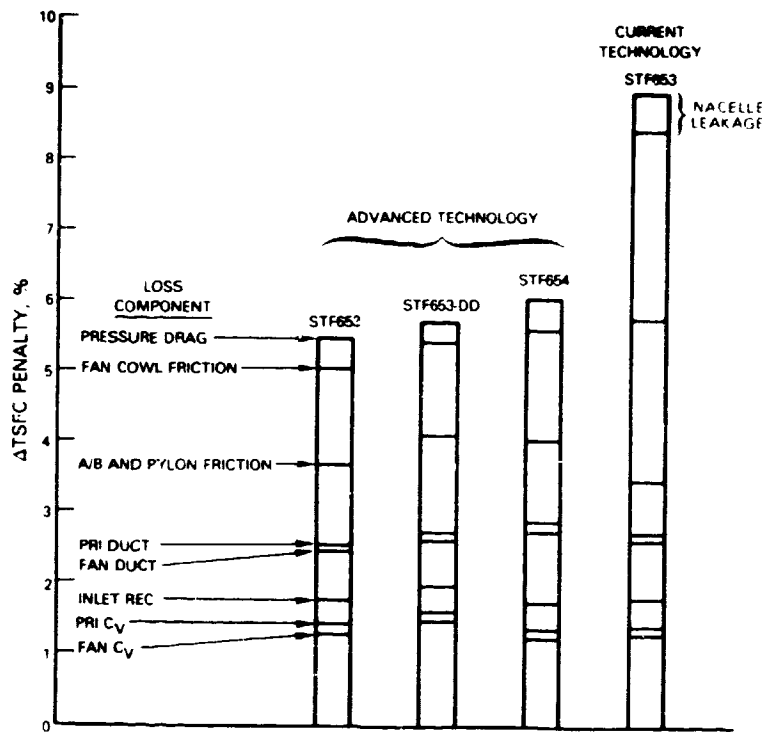
Figure 4.2-6 Preliminary Nacelle Installation Loss Comparison at Design Point Aerodynamic Conditions

Acoustics

Acoustic treatment requirements are another potential source of compromise to the nacelle aerodynamic contours. The recommended nacelle contours were subjected to a qualitative assessment based on the amount of surface area available for acoustic treatment. The JT9D-7R4 nacelle was used as a reference. Comparisons were done in terms of the length-to-height (L/H) ratio of the inlet, fan duct and tailpipe. Results are summarized in the following table:

TABLE 4.2-II
Approximate L/H Available For Treatment Relative to JT9D-7R4

ENGINE	INLET	FAN DUCT	TAILPIPE
STF653	50%	60%	110%
STF653-DD	50%	50%	120%
STF654	50%	40%	80%

Principal areas of concern are the inlet and fan duct, because the areas available for treatment of fan and low pressure compressor noise are considerably less than in the JT9D-7R4 nacelle. Areas available in the tailpipe for treatment of turbine noise are comparable and are expected to be less of a concern. In view of the cursory nature of this evaluation, the results were not weighed too heavily in the selection process. However, future study efforts investigating acoustic emissions must consider the following:

o   minimization of pylon disturbances at the fan;
o   cambered rather than conventional drooped inlet to minimize distortions;
o   provision for as much treatment as possible in nacelle and engine (e.g., in the fan case and in the "goose-neck" flowpath leading to the low pressure compressor).

4.3 REVERSER CONCEPT SELECTION

High bypass ratio cycles require less reverser effectiveness than current cycles due to increased ram drag (larger fan diameter and flow) and higher fan gross thrust to total net thrust ratio. The increased ram drag becomes increasingly potent at increased 'down-the-runway' aircraft velocities. Figure 4.3-1 presents results obtained in the earlier Benefit/Cost Studies. The studies show that the 12.8 bypass ratio engine requires approximately half the JT9D reverser effectiveness to supply the same reverse thrust as a percentage of forward thrust. This result was based on an assumed takeoff turbine temperature and also assumed no fan or gas generator match point shift from forward to reverse operation. Evaluating a range of design bypass ratio cycles at an average 'down-the-runway' condition of 100 knots flight velocity, the minimum effectiveness to meet the JT9D reverse thrust level decreases as bypass ratio is increased (Figure 4.3-2). This leads to the objective of achieving the simplest reverser mechanical design that will provide the required effectiveness, with minimum or no compromise to the nacelle aerodynamic design.
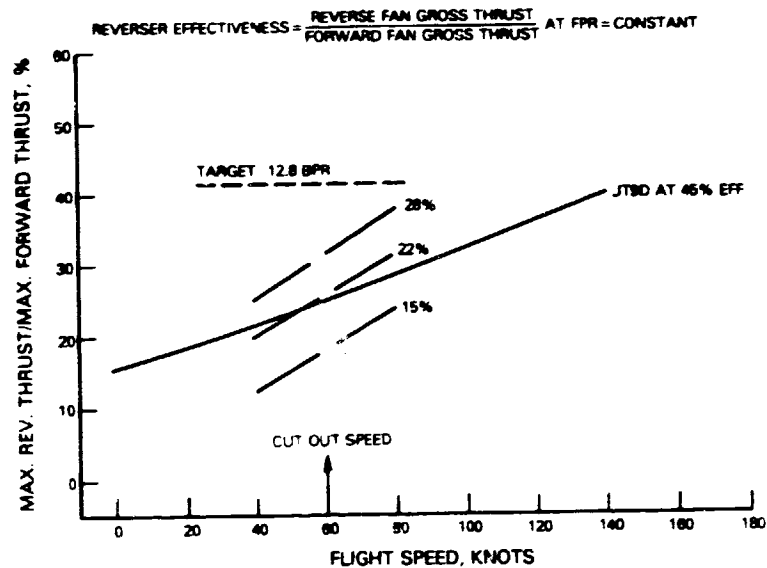
Figure 4.3-1 Comparison of Reverse Thrust Requirements for Advanced High Bypass Ratio Turbofan Engine and Current JT9D

16
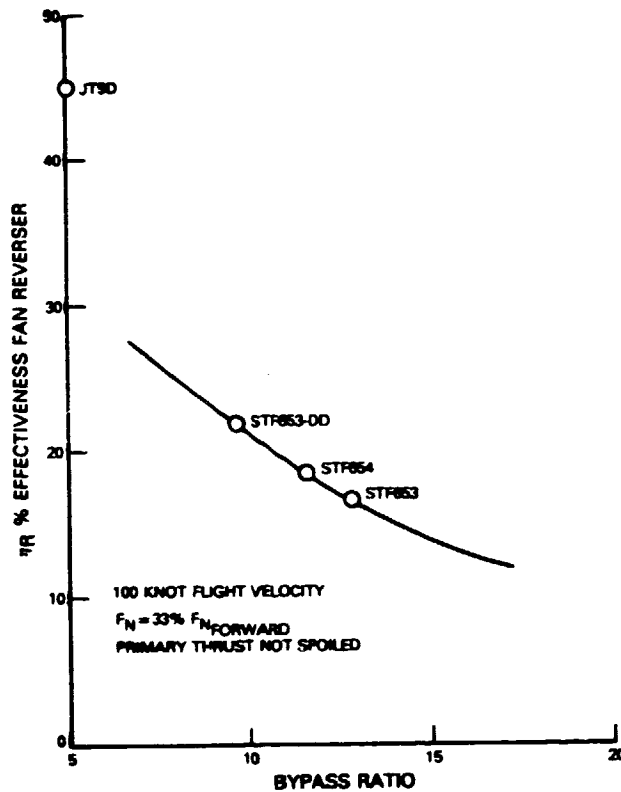
Figure 4.3-2 Projected Reverser Thrust Effectiveness Requirements as a Function of Engine Bypass Ratio

The literature identifies many reverser concepts. The most successful types generally fall into one of two categories: cascade reversers and target reversers. Figures 4.3-3 through 4.3-6 identify examples of design concepts that embody the two kinds of reversers recommended for evaluation in the preliminary design phase of the study. Figure 4.3-3 is the baseline reference system and is representative of the type of fan reverser scheme used in current technology nacelles. It is a proven design that features a translating cowl, blocker doors to divert the fan air, and turning vanes (cascades) to provide efficient reversal of the fan flow. Figure 4.3-4 is a simple variant of the scheme shown in Figure 4.3-3, which eliminates the use of cascades. Flow turning will not be as efficient without cascades, and reverser effectiveness will be less than that for the reference scheme. However, it has the advantages of not requiring space in the cowl for the cascade trays and opens up the reverser passage flow area, thereby reducing the actuator stroke. These features offer reduced weight and complexity.
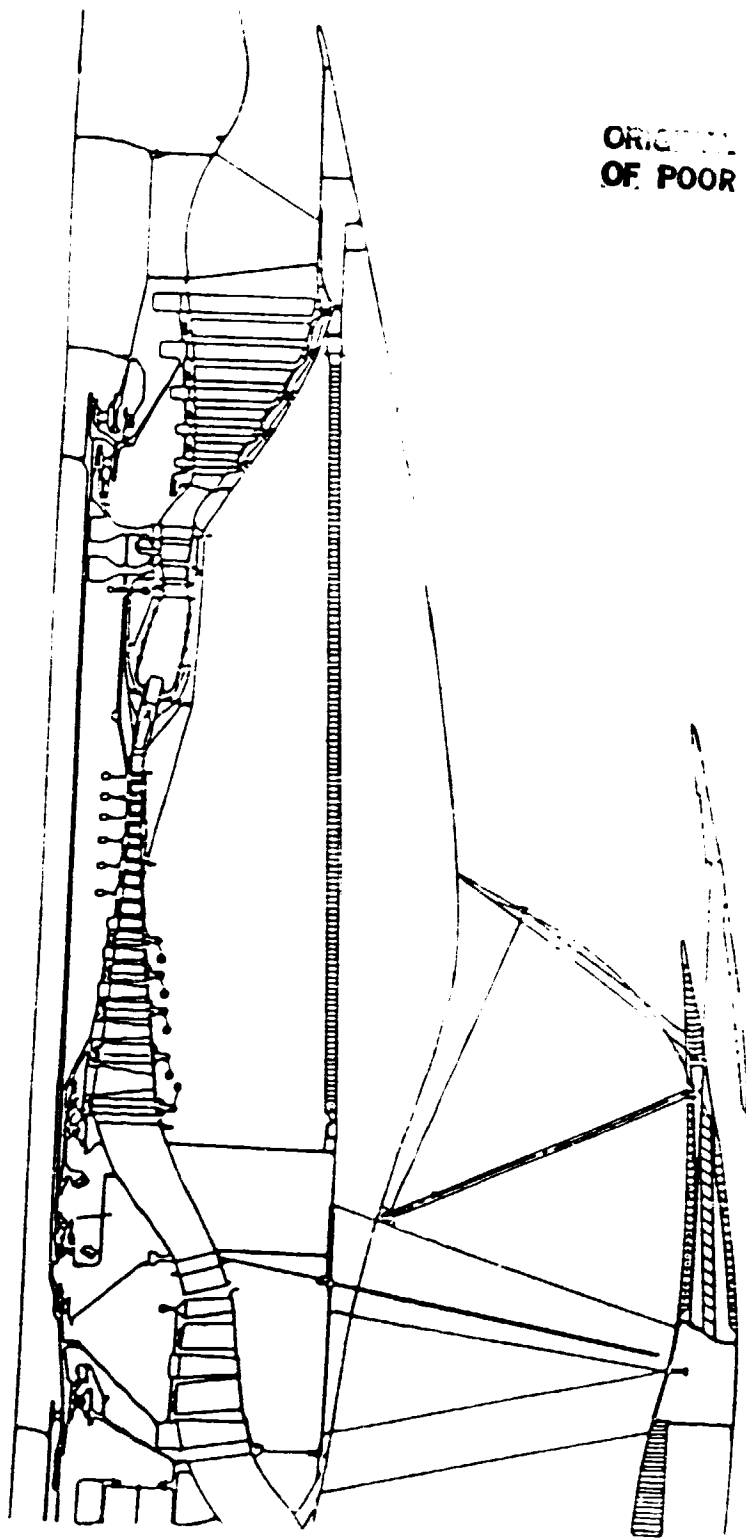
Figure 4.3-3   Typical Cascade Reverser Representative of Current Designs
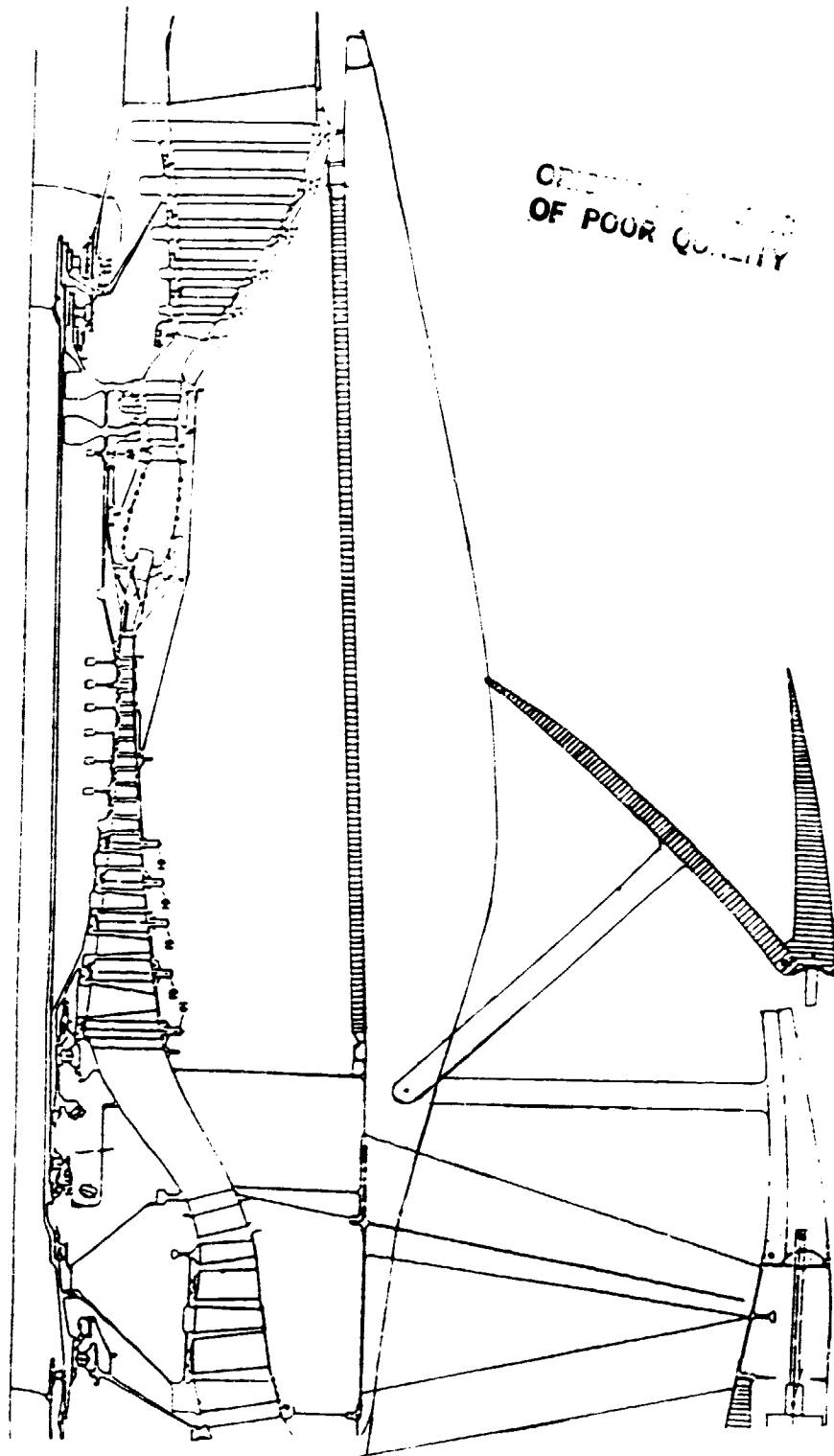
Figure 4.3-4 Simple Variant of the Cascade Reverser Concept Where the Cascades Have Been Eliminated

19
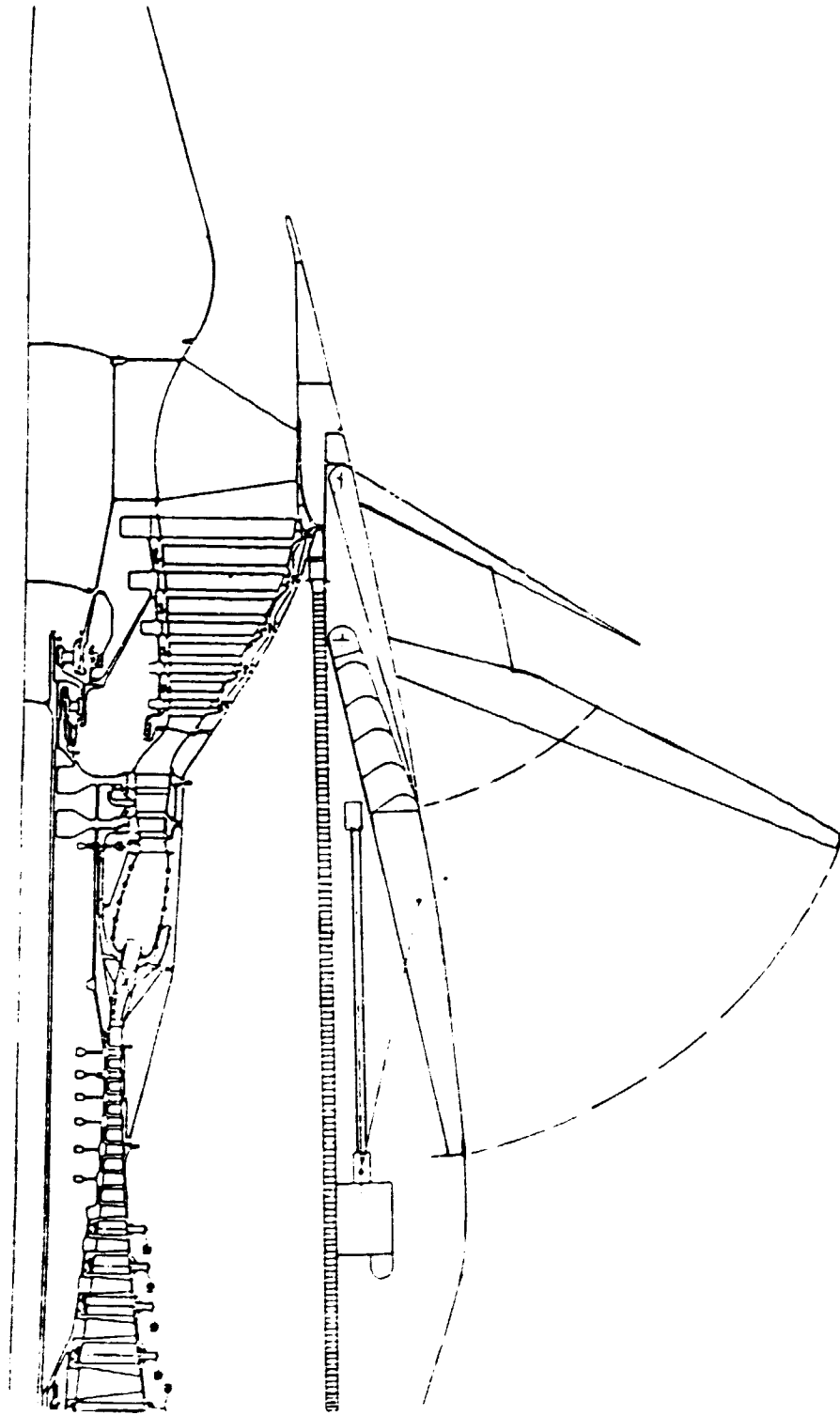
Figure 4.3-5 Possible Core-Mounted Target Reverser Concept for Diverting Fan Flow
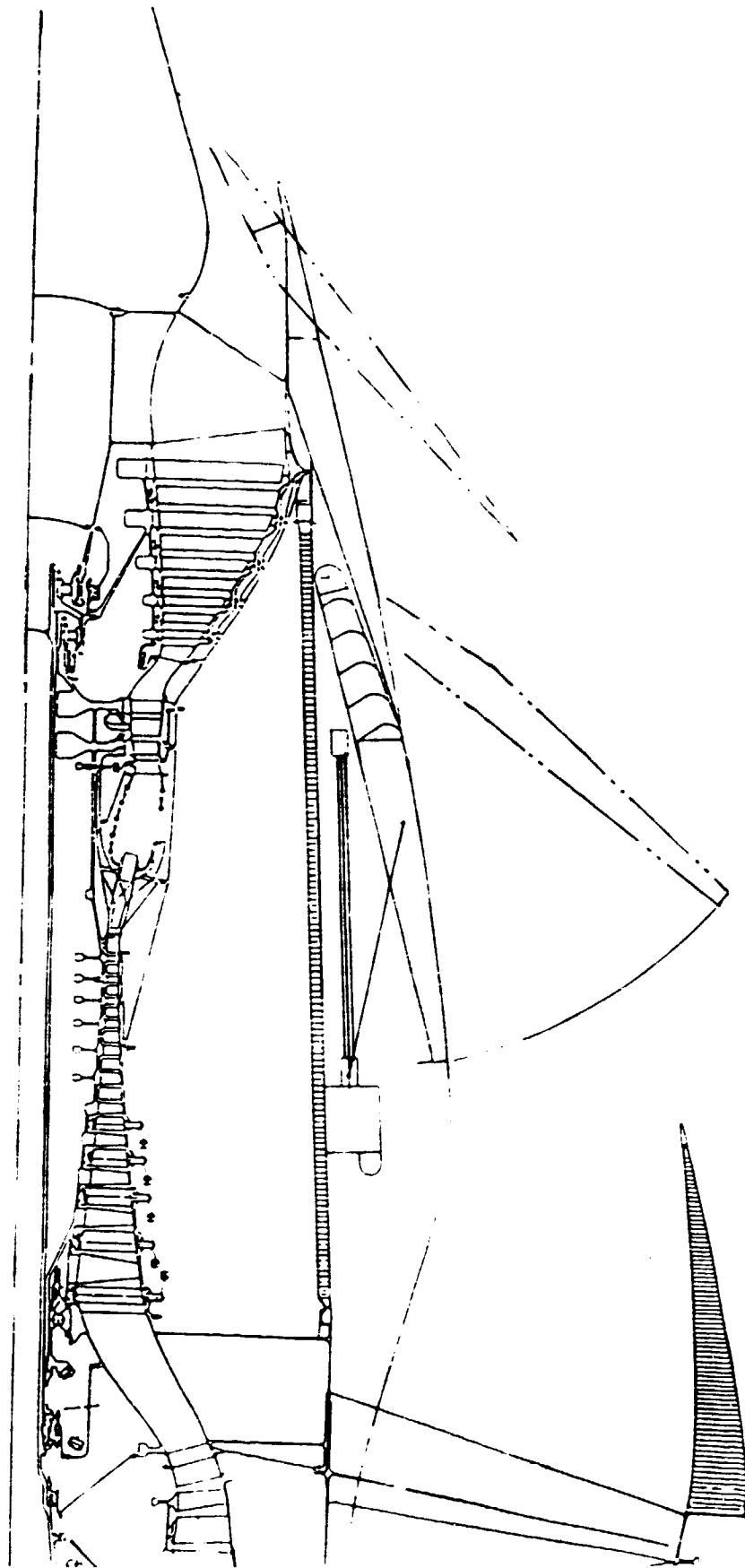
Figure 4.3-6   Possible Core-Mounted Target Reverser Concept for Diverting Both
Fan and Primary Stream Flow

Figures 4.3-5 and 4.3-6 illustrate core-mounted reverser schemes that typify target reversers. These could be employed should fan cowl mounted systems unduly compromise the nacelle aerodynamic design. Figure 4.3-5 identifies a system of blocker doors that effectively diverts and/or reverses the fan flow. Turning vanes may be included in the upstream doors if flow turning efficiency is shown to be an important criterion. Figure 4.3-6 is a variant of the scheme shown in Figure 4.3-5 and includes reversal of the primary (core) flow as well as the fan flow. This scheme has the potential of improved reverser effectiveness over the scheme shown in Figure 4.3-5. Reversible-pitch fan blades are also potential reverser candidates, but studies have indicated that they are not viable in the range of fan pressure ratios and fan tip speeds of interest.

The two advanced reverser designs evaluated during the nacelle preliminary design activity were refinements of these representative schemes and incorporate necessary fail-safe features.

SECTION 5.0
NACELLE AND THRUST REVERSER/SPOILER AERODYNAMIC DESIGN

Following approval of the recommended Engine/Nacelle conceptual configurations discussed in Section 4.0, further analyses were conducted to refine the geometric contours of current and advanced technology nacelles to meet aerodynamic requirements at both on and off-design conditions. Included in these analyses were low-volume thrust reversers (or spoilers). Analysis techniques and the resultant nacelle contours are discussed in the following sections.

5.1 CURRENT TECHNOLOGY NACELLE AERODYNAMIC DESIGN

A standardized analysis procedure which calculates absolute nacelle performance was used to formulate current technology nacelle contours for the contract study engine installations. The procedure comprises three general areas of analysis: definition of nacelle geometry, computation of external flow effects (drag), and computation of internal losses. Figure 5.1-1 shows the activities in each area and how each area is integrated to predict a final nacelle performance level for a given design point. The procedure begins with engine frame definition, which includes clearance requirements, accessory envelope, and key cycle parameters. This information (described in Figure 5.1-2) is combined with experienced-based nacelle geometric parameters (shown in Figure 5.1-3) and technology level assumptions and is used as input to the Nacelle Geometry and Performance Program (NACPERF). The nacelle wrap methodology utilized in this program incorporates elipses, circular arcs, and straight lines to speed the analysis and define the major nacelle characteristics for the candidate engine installations.
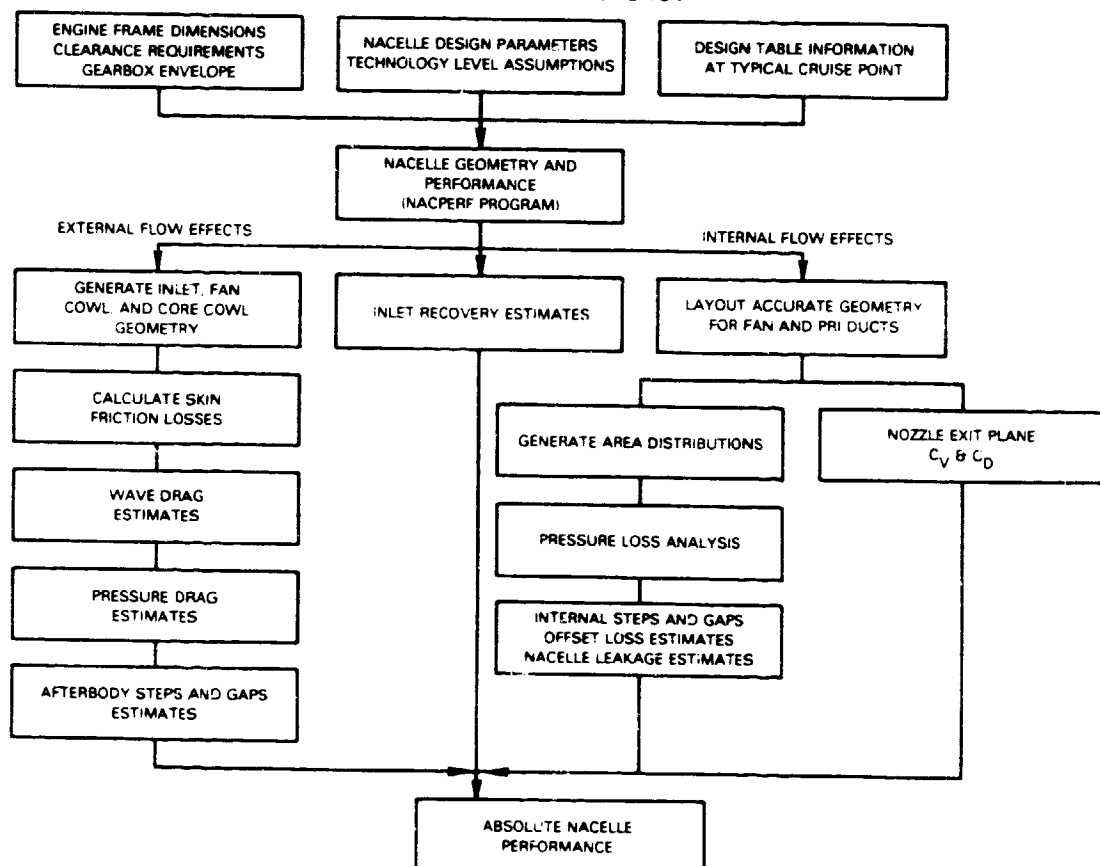
Figure 5.1-1 NACPERF Nacelle Design and Performance System

ENGINE DIMENSIONS
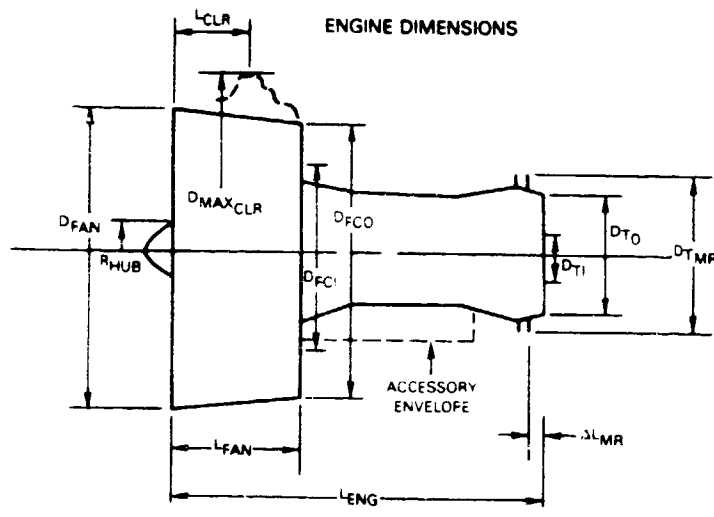
REQUIRED ENGINE PARAMETERS
(AT 90% CRUISE EXCEPT AS NOTED*)

M_∞ – MACH NUMBER
ALT – ALTITUDE
W_A – ACTUAL FLOW
W_{AT2}* MAX CORRECTED FLOW
BPR – BYPASS RATIO
THRUST – CRUISE NET THRUST

FAN NOZZLE AND PRIMARY NOZZLE

T_T – TOTAL TEMPERATURE °R
P_T/P_{AMB} – NOZZLE PRESSURE RATIO
AREA – JET

$$C_{D_L} - \frac{\Delta V_J/V_J}{\Delta P_{T9}/P_{T9}} \cdot \frac{F_G}{F_N}$$

$D_{MAX_{CLR}}$	MAX DIA. FOR NACELLE CLEARANCE	D_{TI}	LPT EXIT I.D
D_{FAN}	FAN TIP DIAMETER	L_{FAN}	FAN CASE LENGTH
R_{HUB}	HUB RADIUS	L_{ENG}	TOTAL ENGINE LENGTH
D_{FCO}	FAN EXIT O.D	L_{CLR}	LOCATION OF CLEARANCE PT
D_{FCI}	FAN EXIT I.D	ΔL_{MR}	LOCATION OF MOUNT RING
D_{TO}	LPT EXIT O.D	$D_{T_{MR}}$	MOUNT RING DIAMETER

Figure 5.1-2 Principal Engine Geometric and Performance Parameters Required to Initiate Nacelle Definition

THROAT AREA (A_{TH}) SIZED AT $M_N \leq 0.76$
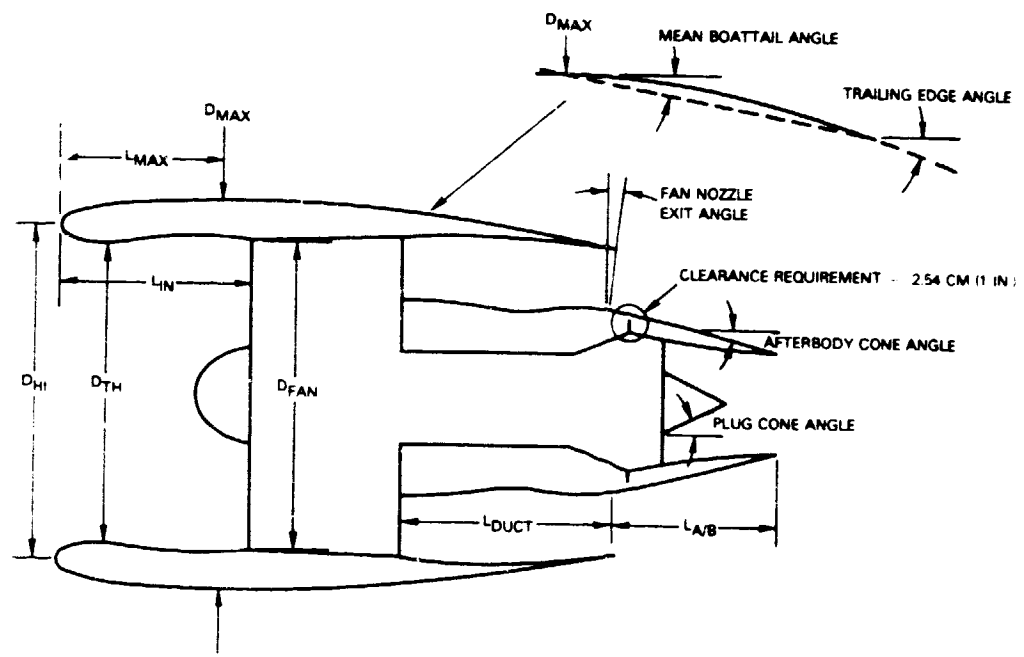
L_{IN}/D_{FAN}	– INLET LENGTH/FAN TIP DIAMETER	
A_{HI}/A_{TH}	– HIGHLIGHT AREA/THROAT AREA = $(D_{HI}/D_{TH})^2$	
D_{HI}/D_{MAX}	– HIGHLIGHT DIA./MAXIMUM DIA.	
L_{MAX}/D_{MAX}	– LENGTH TO D_{MAX}/MAXIMUM DIA.	

L_{DUCT} – FAN DUCT LENGTH
$L_{A/B}$ – AFTERBODY LENGTH

Figure 5.1-3 Critical Geometric Parameters Used in the Calculation of Nacelle Performance

24

The nacelle design procedure is illustrated in figures 5.1-4 through 5.1-8 and can be separated into a progression of sections as an entire nacelle is formed. The sequence of figures is intended to show each major section and a method used to determine the nacelle wrap requirements for that section. Figure 5.1-4 shows the definition of the plug which is initially defined as a cone. The core cowls are shown in Figure 5.1-5 and are essentially conical with a maximum angle limit that historically has ensured attached flow on the boattail. The core cowl must clear the turbine clearance point and extend rearward until the required primary jet area is achieved. The initial core cowl angle is set perpendicular to the fan nozzle exit angle, and the contour curvature increases until the maximum angle is reached (again, the maximum angle limit is based on experience). The outer contour of the primary duct is assumed to be a straight line from the outside diameter of the turbine exhaust case to the end of the primary cowl.

The fan duct, shown in Figure 5.1-6 is designed to minimize pressure loss from the fan exit guide vanes to the duct exit, while providing sufficient length for acoustic treatment requirements. As shown, the fan duct exit outside diameter is established to provide the required fan duct exit area while accounting for the pylon width at the fan duct exit. Pylon width is typically on the order of 47.62 cm (18.75 in.) for current large engine designs. The interior inlet contour definition is shown in Figure 5.1-7. The contour is defined by an ellipse, two circular arcs, and a straight section between the arcs while providing sufficient length for acoustic treatment requirements. The slope of the straight section defines the maximum local diffusion angle. The throat area is designed to provide a throat Mach number less than 0.76 at maximum corrected flow. This provides some margin for future thrust growth through increased fan airflow capacity. The fan cowl contour from the highlight to the maximum diameter, Figure 5.1-8, is defined by a semi-cubic parabola with the length, radial offset, and equation constants selected to minimize wave drag. The contour from the maximum point to the end of the fan cowl is defined by a circular arc as shown in Figure 5.1-9. The maximum contour (boattail) angle occurs at the exit and is based on preventing flow separation on the fan cowl.
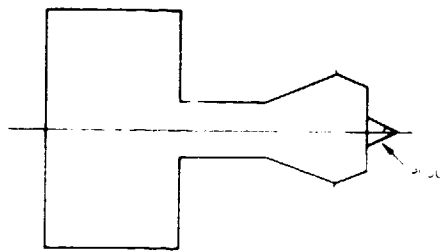
Figure 5.1-4   Exhaust Nozzle Plug -- Essentially Conical in Shape
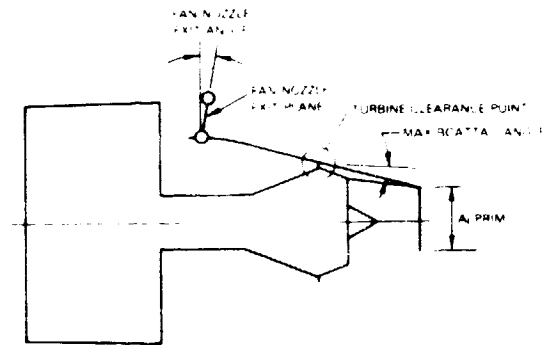
Figure 5.1-5   Core Cowl Contour Definition
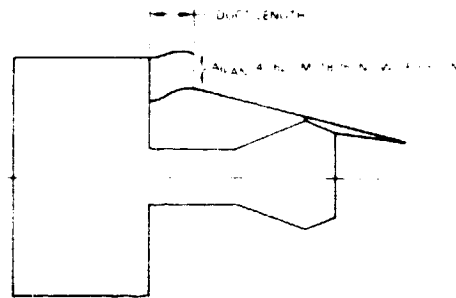
Figure 5.1-6   Fan Duct Exit Contour Definition
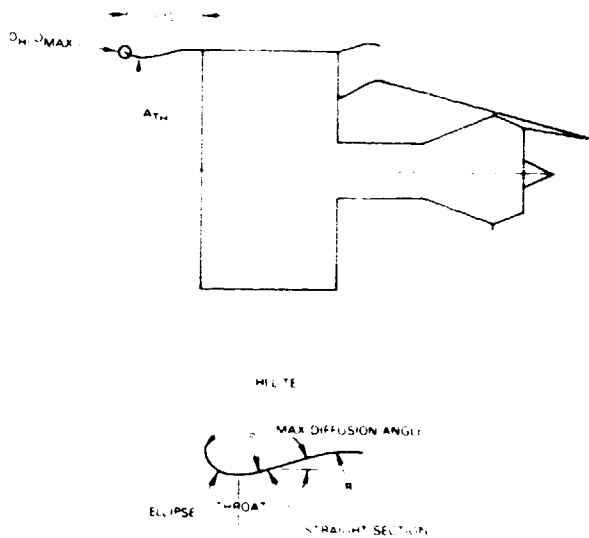
26   Figure 5.1-7   Fan Duct Interior Inlet Contour Definition

MINIMUM WAVE
DRAG CONTOUR
$F(D_{HI}/D_{MAX}, L_{MAX}/D_{MAX})$
DEFINED BY A
SEMI-CUBIC PARABOLA
$R = \sqrt{A + BX + CX^2 + DX^3}$

L_{MAX}

MINIMUM
CLR

R_{HI}

R_{MAX}
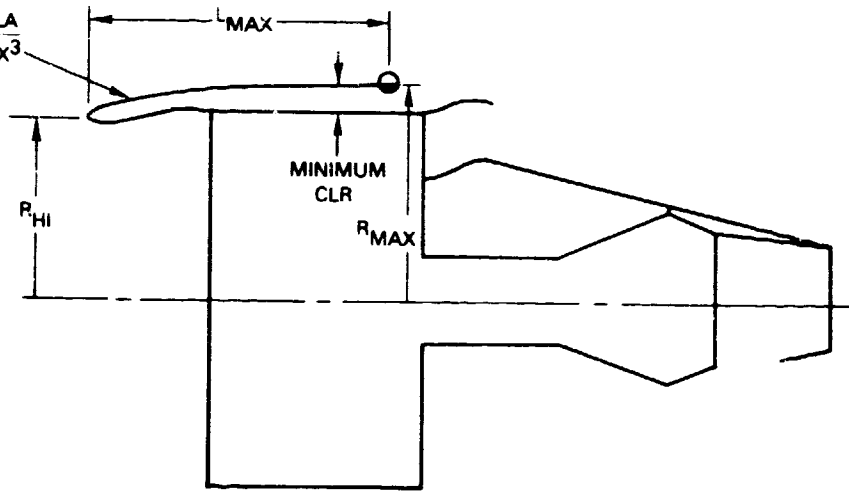
Figure 5.1-8   Forward Fan Cowl Outer Contour Definition

CIRCULAR ARC

MAX BOATTAIL
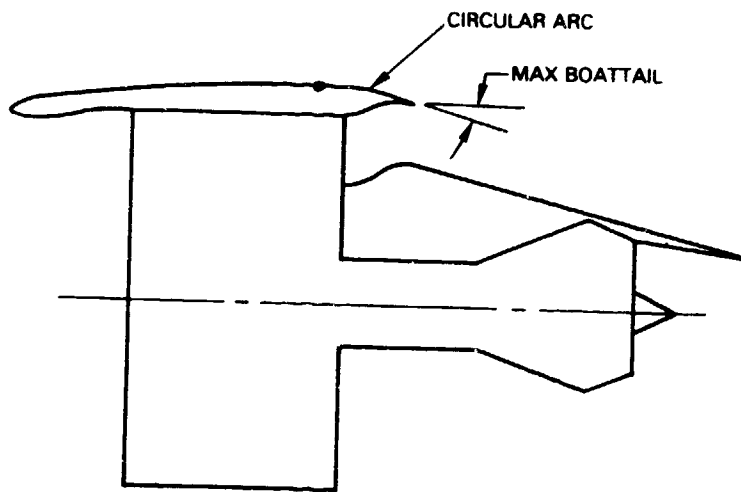
Figure 5.1-9   Fan Cowl Afterbody Outer Contour Definition

27

Once the nacelle geometry has been defined, computation of external flow effects (drag) and internal losses outlined in Figure 5.1-10 can begin. External drag estimates begin with the calculation of a cowl wetted area (A_{wet}) scrubbed by the freestream flow. This area is used to calculate a flat plate skin friction drag.
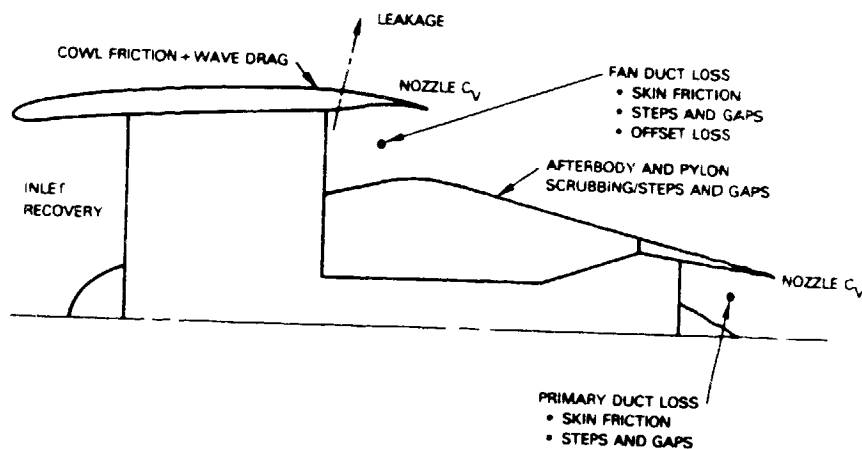
Figure 5.1-10   Aerodynamic Losses Factored into Nacelle Design

Model test data have shown that true integrated fan cowl friction drag levels are approximately 98% of the flat plate skin friction value. As a result, the equation for fan cowl friction drag becomes:

$$\text{Drag fan cowl} = 0.98 \, (\text{Drag})_{flat\ plate} \tag{1}$$

Afterbody drag is calculated based on wetted area scrubbed by fully expanded fan flow (the shadowing of the pylon is subtracted from the afterbody wetted area). A flat plate skin friction drag is calculated assuming that boundary layer growth starts upstream of the fan exit.

Pylon wetted areas are calculated from the area scrubbed by a constant area, unexpanded fan flow. The pylon is assumed to close out to a knife edge at the primary exit plane. Pylon drag is calculated as:

$$\text{Drag}_{pylon} = \text{Drag}_{afterbody} \times \left[\frac{A_{wet}\ \text{pylon}}{A_{wet}\ \text{afterbody}} \right] \tag{2}$$

An additional loss is bookkept on the afterbody to include steps and gaps over and above the flat plate friction calculation.

In addition to skin friction drag, shock losses (wave drag) may occur if the flow over the cowl surface becomes locally supersonic and aerodynamic contour displacement drag (form or pressure drag) will occur as a result of boundary layer viscous effects. Wave drag carpet plots (as a function of D_H/D_{max} and L/D_{max} were generated for a range of mass flow ratios and free stream Mach numbers, using a transonic inlet analysis, to determine the region of shock free contours or minimum wave drag (see Figure 5.1-11). The design intent for the current technology nacelles was to have shock free contours by

28

ensuring that D_H/D_{max} and L/D_{max} were optimized. A correlation was then developed that related pressure drag to skin friction plus wave drag and is a function of nacelle fineness ratio. The correlation shown in Figure 5.1-12 is based on nacelle test data and estimates of skin friction drag and wave drag using the methods described earlier. The value of C_D pressure/C_D friction + C_p wave is applied to the friction drag to determine nacelle pressure drag. Pressure and skin friction drag are then combined to obtain the" external flow effects" drag.
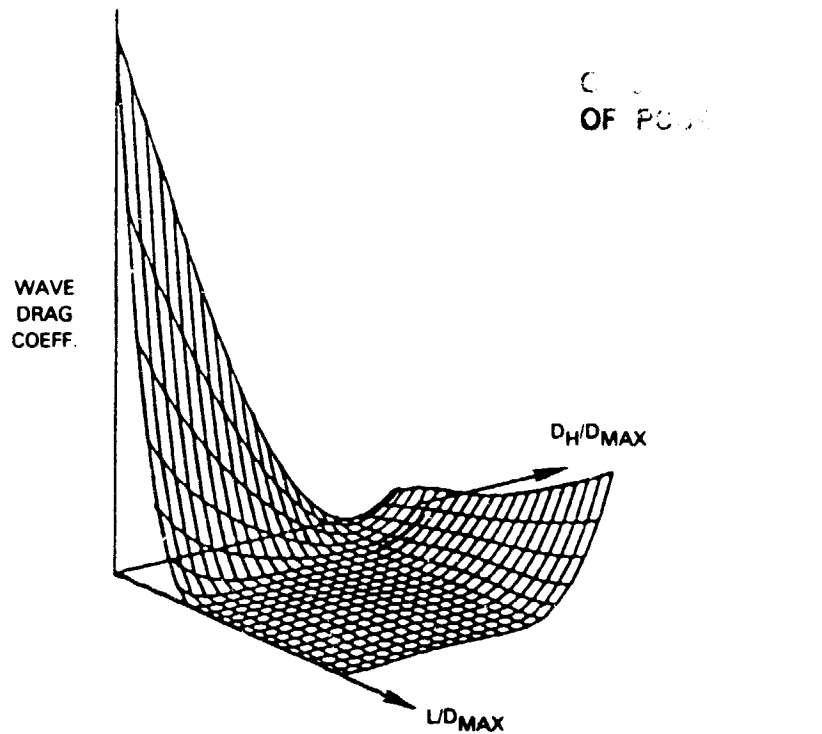
Figure 5.1-11   Wave Drag Carpet Plot Defines Region of Shock-Free Contours
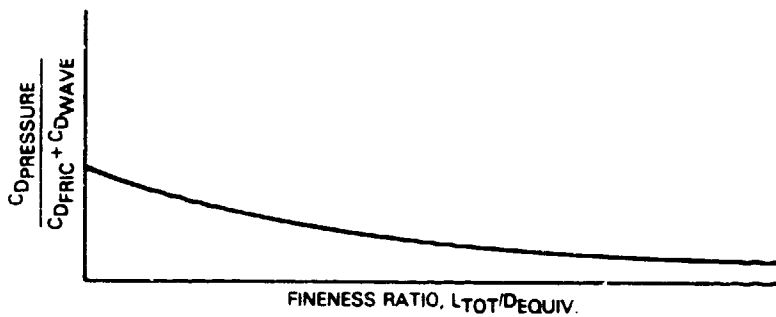
Figure 5.1-12   Shock-Free Nacelle Drag Coefficient Correlation

Computation of internal losses includes inlet recovery, duct losses, duct flow leakage, and nozzle efficiency. Inlet recovery estimates are based on inlet scale model tests and the recovery (P_{T2}/P_T) vs. corrected airflow to inlet throat area (W_c/A_t) correlation shown in Figure 5.1-13. Fan and primary duct pressure loss calculations are made using a one-dimensional skin friction analysis. Fan ducts are assumed to be hardwall or incorporate Dynarohr^R sound treatment material, which elevates the friction coefficient. The primary ducts are assumed to have porous plate sound treatment material with a 17% porosity. Fan duct pressure loss also included offset loss (Figure 5.1-14) which relates to the amount of outward displacement of the flow through the duct from the case exit to the nozzle exit. An additional pressure loss, used to account for duct steps and gaps, is included in both the fan and the primary duct pressure loss. To account for losses associated with leakage of reverser seals and fan duct door seals, a percentage of fan duct flow, based on full scale test experience, is assumed to be lost in a radial direction. Finally, nozzle efficiency or nozzle exit plane thrust coefficients are used to account for losses associated with non-uniform velocity profiles at the nozzle exit. These coefficients, shown in Figure 5.1-15 for fan and primary nozzles, are based on extensive model data.

$$\frac{P_{T2}}{P_{T_\infty}} W_{AT} = W_{AF} \frac{P_{T_F}}{P_{T_\infty}} + W_{AP}$$
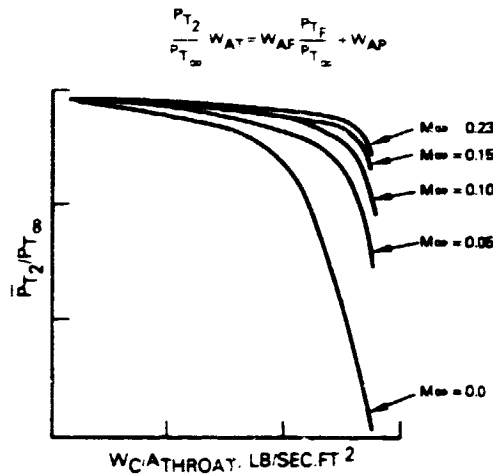
Figure 5.1-13   Inlet Total Pressure Recovery Correlation
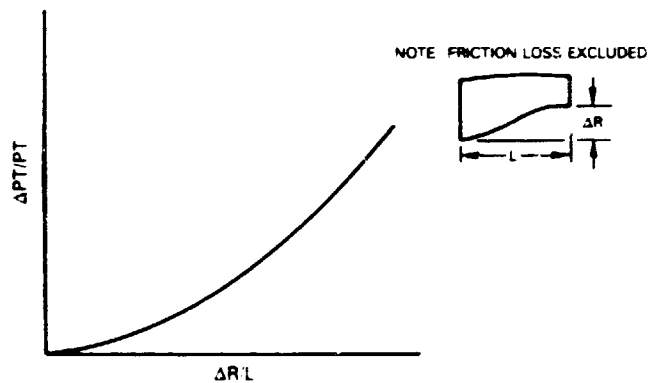
Figure 5.1-14   Fan Duct Offset Loss Correlation

30
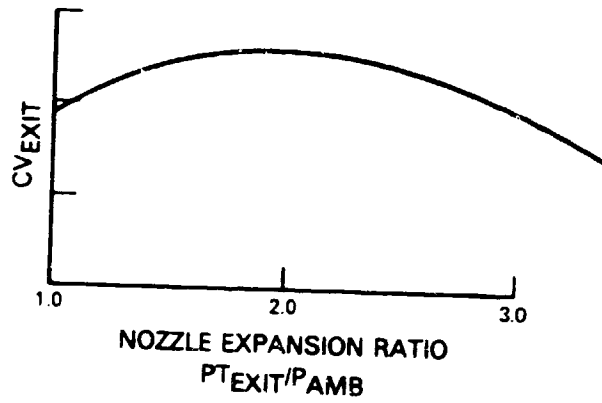
Figure 5.1-15   Fan and Primary Nozzle Gross Thrust Coefficient

Utilizing these procedures, aerodynamic contours were established for the current technology nacelles wrapped around the three candidate advanced technology engines (STF653, STF653-DD, STF654) described in section 6.1. Characteristics of these nacelles are summarized in figure 5.1-16. These contours formed the reference point for the engine and nacelle integration efforts described in section 6.0
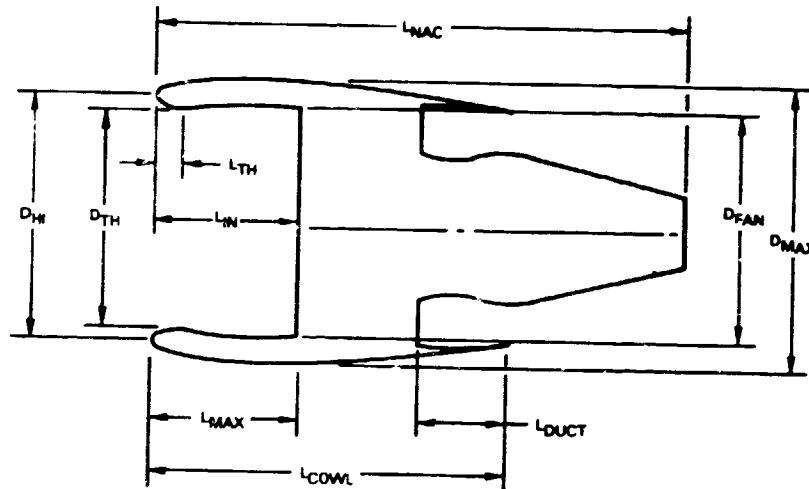
	STF653	STF653-DD	STF654
D_{FAN}	106.800 IN.	93.840 IN.	67.800 IN.
	271.272 CM.	238.354 CM.	172.212 CM.
D_{MAX}	133.302 IN.	117.128 IN.	84.570 IN.
	338.588 CM	297.505 CM.	214.808 CM.
D_{HI}/D_{MAX}	0.889	0.889	0.889
D_{TH}/D_{FAN}	0.9701	0.9701	0.9695
L_{TH}/D_{FAN}	0.1431	0.1431	0.1431
L_{MAX}/D_{MAX}	0.400	0.400	0.400
L_{NAC}/D_{FAN}	2.190	2.058	2.315
L_{DUCT}/D_{FAN}	0.4307	0.4902	0.678
L_{IN}/D_{FAN}	0.617	0.617	0.617
L_{COWL}/D_{FAN}	1.525	1.767	1.767

Figure 5.1-16   Preliminary Current Technology Nacelle Aerodynamic Contour Definition

31

5.2 ADVANCED TECHNOLOGY NACELLE AERODYNAMIC DESIGN

The previous section described the Nacelle design procedures and design criteria that have proven successful in service. Application of this design process to a series of turbofan engines with increasing fan diameters, indicated that nacelle installation losses increased in direct proportion to the nacelle diameter. It became apparent that the potentially large fuel savings associated with increased bypass ratio could be offset by these losses unless growth in nacelle diameter and cowl wetted area could be controlled. This led to the definition of the short, slim-line nacelle concepts described in section 4.2, which challenge the state-of-the-art in nacelle aerodynamic technology. Aerodynamic analysis of these advanced technology nacelles focused on inlet and fan duct flow concerns and the elimination of wave drag on the nacelle cowl.

5.2.1 Inlet and Duct Fan Analysis

The critical geometric parameter controlling nacelle diameter for a fan with given diameter is fan cowl thickness. This is normally dictated by aerodynamic and structural concerns as well as the volume requirement for accessories, plumbing and thrust reversers. Taking into account advancements in 1) materials technologies, 2) improved load carrying, 3) structural arrangements, and 4) reductions in accessory, plumbing and thrust reverser volume requirements, a minimum cowl thickness over the fan cases of 12.7 cm (5 in.) was established as a starting point in the formation of the advanced technology nacelle geometric configurations.

Attention was then focused on the inlet lip thickness (Figure 5.2-1). Reducing the maximum diameter while still holding the fan diameter and the maximum climb airflow constant creates an aerodynamic concern at the inlet lip. The reduced maximum diameter requires that the inlet highlight diameter be reduced in order to insure low wave drag at cruise. However, holding constant maximum climb airflow Mach number through the inlet throat also requires that the throat diameter be held constant. Consequently, the highlight closes down onto the throat. This creates a sharp internal lip, which introduces concern over flow separation at angels of attack (lower lip) and at static/low speed, high power conditions, especially with crosswind. In order to provide relief, the maximum inlet throat Mach number at the top of climb was increased. The increased flow velocity reduced the inlet throat diameter and permitted an increase in the radius of curvature around the internal lip, which provided some relief to the internal flow separation concern at the throat. To further balance the aerodynamic threats, the highlight diameter to maximum diameter ratio for shock-free (no wave drag) inlet designs was increased slightly to provide more relief on the internal lip, which created a slight threat to the zero wave drag performance assumption. This threat is discussed in Section 5.2.2.

There are potential concerns arising from design modifications to reduce the inlet throat diameter. First, the inlet internal diffusion task is made more difficult. The fan face Mach number stays fixed, but the inlet throat Mach number has increased, necessitating more throat-to-fan face diffusion. This in turn implies that more inlet length is required to control the magnitude of the adverse pressure gradients. This has not been a problem to date because inlet length has traditionally been set by acoustic treatment requirements, where the acoustic treatment surface areas and/or length to duct height ratios over-shadowed the diffusion requirements.

32

CONVENTIONAL WRAP
TIGHT WRAP

REDUCING THE NACELLE DIAMETER
LEADS TO THIN INLETS

D_{HILITE}

D_{THROAT}

D_{MAX}

C_L
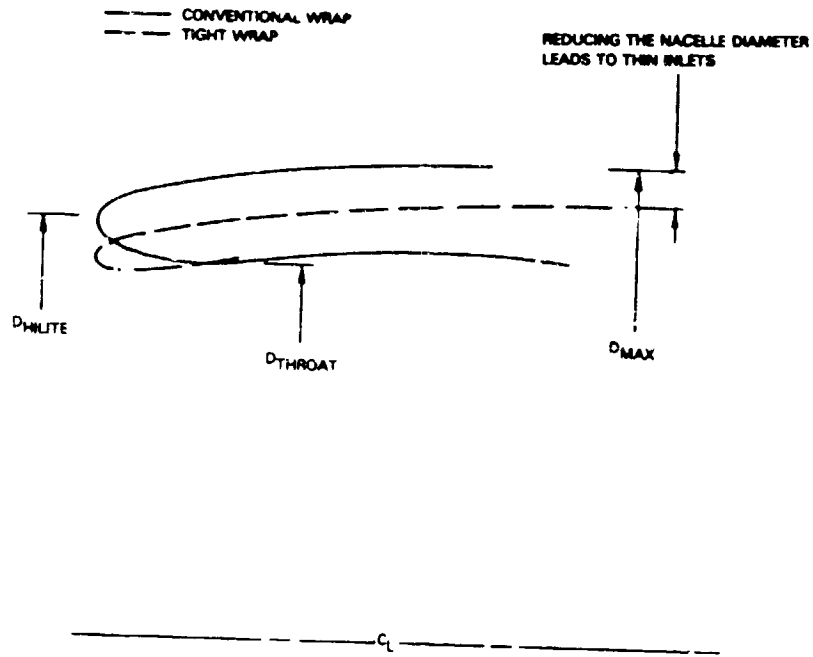
Figure 5.2-1   Inlet Thickness Comparison

CONVENTIONAL NACELLE WITH
ACOUSTIC TREATMENT

ADVANCED NACELLE
INLET LENGTH
SET BY DIFFUSER
REQUIREMENTS
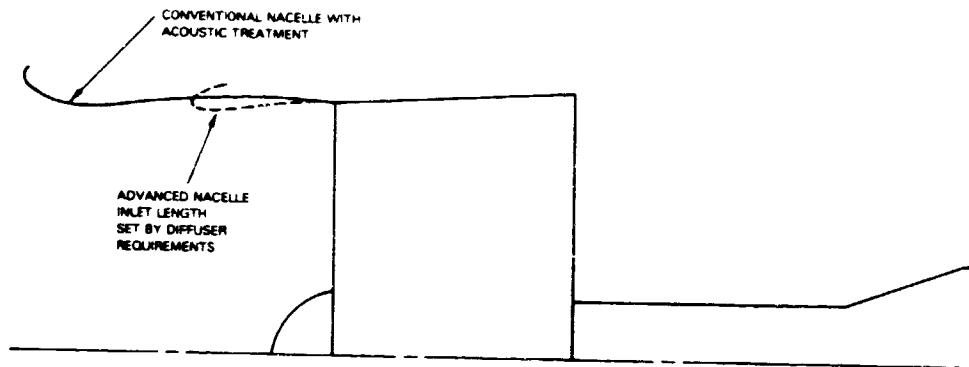
Figure 5.2-2   Comparison of Inlet Diffuser Lengths

Using diffuser data correlations, it was determined that, even with the elevated throat Mach numbers, the advanced nacelle diffusers would maintain attached flow with inlet lengths considerably shorter than those of conventional nacelles (see Figure 5.2-2). Acoustic assessments, discussed in Section 6.5, showed that advanced high bypass ratio, low nozzle pressure ratio engines have the potential to meet the present FAR 36 rule with the shorter, advanced technology inlets.

The second concern related to reduced inlet throat area is the loss of engine growth. Experience has shown that when a new engine enters service, the customers will be looking eventually for more thrust. Increased payload, more aggressive mission requirements, etc., usually lead to a family of engines within one model. For example the JT8D-1, 9, 15, and 17 were successively higher thrust models of the JT8D. Similarly the JT9D-7, 7Q, 7R4, 7R4-H cover a thrust range from nominally 177 to 266 thousand Newtons (40-60 thousand lbs.). From an economic point of view, it is desirable to accomplish this growth without changing the nacelle. The throat Mach number of the conventional nacelle was selected to provide margin for increasing the inlet airflow without changing the nacelle. With the advanced nacelle there is little or no margin for increasing inlet airflow because the inlet throat Mach number is near the design limit. Therefore, increasing thrust by increasing airflow would require a larger diameter fan, which in turn requires a new inlet. Since the inlet must be re-designed, the consequences of opening up the throat at that time are minimal. Thrust growth without nacelle change could be accomplished by increasing the jet velocity via increased fan pressure ratio or increased exhaust gas temperature at constant inlet airflow.

The aerodynamic design from the fan duct aft is made easier by the tight wrap (minimum cowl thickness) philosophy. The maximum mean boattail angle from the maximum diameter to the fan nozzle exit sets the required duct length needed to avoid incurring flow separation and a drag penalty. This same limiting angle was used for both the current technology nacelles and the more tightly wrapped advanced technology nacelles (see Figure 5.2-3). For the same nozzle area, the tight wrap will result in a shorter fan duct, as shown in the figure.
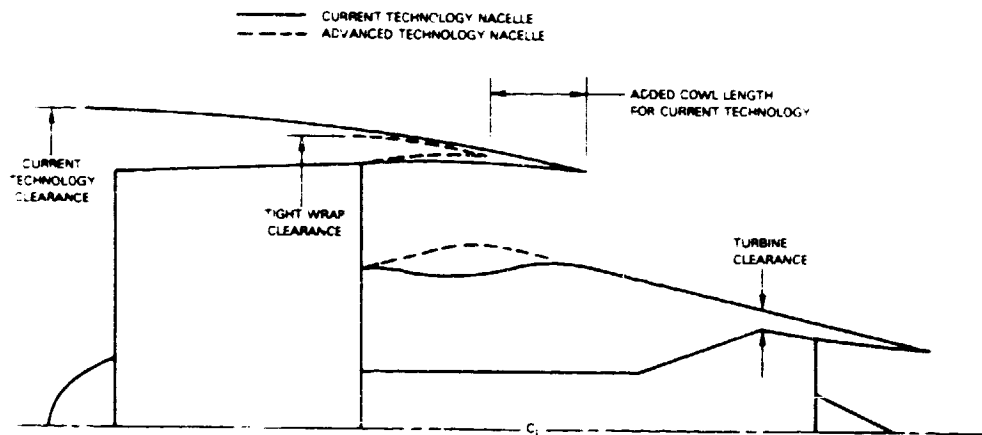
Figure 5.2-3   Comparison of Fan Cowl Lengths

This feature is extremely important because advanced engines with their high component efficiencies, high overall pressure ratios, and high cycle temperature will have significantly shorter and smaller diameter cores than current technology engines. The tight wrap of the advanced technology nacelle around the fan case enables the achievement of the desired fan nozzle while at the same time maintaining a tight afterbody wrap around the turbine case. The overall benefit is a reduction in nacelle wetted area. The current technology fan case wrap and the boattail angle limits, however, require either a longer fan duct (higher duct pressure loss), or an afterbody shape that is displaced radially outward to keep the fan duct length under control (see Figure 5.2-4). The later design approach is also limited because of the constraints on the maximum afterbody angle. Locating the fan throat at a larger mean radius leads to inordinately large afterbody wetted areas and subsequent friction drag penalties.
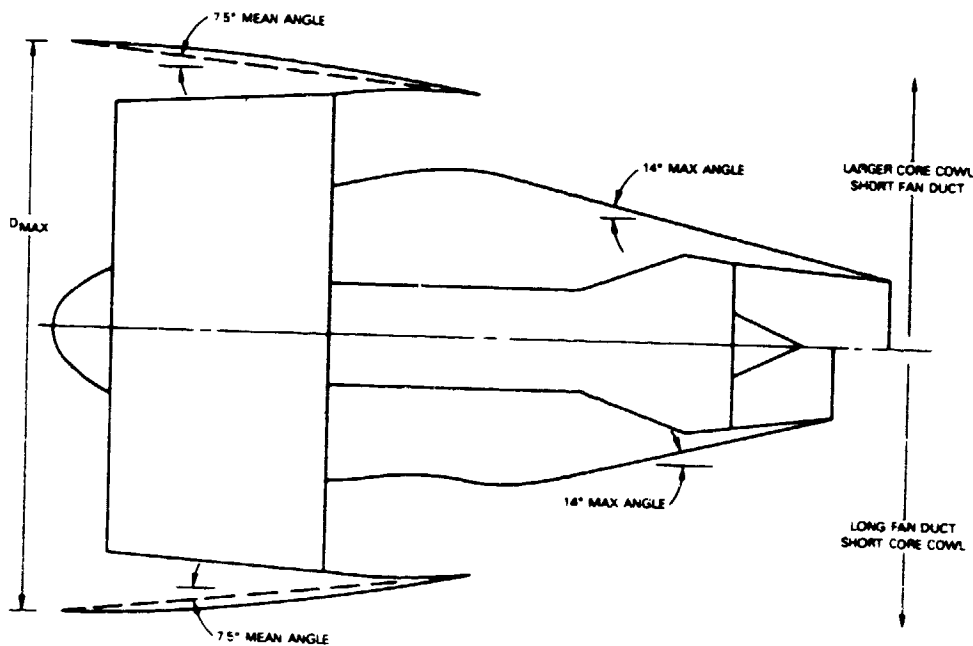
Figure 5.2-4   Current Technology Case Wrap Leads to a Long Fan Duct or Large Core Cowl

5.2.2 External Wave Drag Analysis

The design process described in Section 5.2.1 indicated that the tight wrap philosophy used to configure the advanced technology nacelles resulted in configurations that a) had compact aft ends that stayed within conventional closure angle limits, and b) lead to thin inlet lips which threatened off-design performance and challenged the "zero wave drag" assumption. This section describes the analytical work performed under the present contract to address the "zero wave drag at cruise assumption". Section 8.0 describes concepts and recommended technology programs to further address both of these concerns.

The analysis used in this study is an adaptation of the Euler Solution originally developed for transonic cascades (Ref. 3). A computational grid was developed by Pratt & Whitney that allows application of this analysis to the complete nacelle (Figure 5.2-5), or for sections of the nacelle, such as the inlet (Figure 5.2-6). Pratt & Whitney has had great success in the use of this code, and through experience has developed confidence in its accuracy. For high speed cruise problems, the angle of attack is small enough that the axisymmetric version of the code can be used. At take-off rotation angles, second segment climb, or at cruise with modest angles of attack, the three-dimensional version of the analysis is required. In all cases, the code has shown its accuracy and versatility as evidenced by the following prediction vs. static pressure data comparisons for the Pratt & Whitney JT9D-7R4 nacelle at the top, side, and bottom of the nacelle, both inside and outside for the following diverse range of operating conditions:

Mach Number	Angle of Attack	Inlet Mass Flow Ratio	Fig.
0.01	0.0°	High Power	5.2-7A
0.2	24°	Windmill	5.2-7B
0.25	16°	High Power	5.2-7C
0.6	4°	Typical Cruise	5.2-7D
0.6	4°	Maximum Cruise	5.2-7E
0.8	0.0°	Typical Cruise	5.2-7F
0.8	0.0°	Maximum Cruise	5.2-7G

Exercising the three-dimensional version of the code was outside the scope of the present contract effort, so off-design condition angle of attack problems were not addressed. However, the flow field at high speed (Mn = 0.8), zero angle of attack with the axisymmetric version of the code was analyzed in some detail. Initial analyses of 'thin lip' configurations, using a semi-cubic parabola to define the external inlet contour resulted in high external inlet Mach numbers and shock strengths. Peak Mach numbers were as high as 1.5, with strong multiple shocks (Figure 5.2-8). The conventional semi-cubic parabola was subsequently abandoned in favor of contour refinement using a full potential transonic analysis. After many iterations, a contour was formulated that virtually eliminated the lip shock, keeping the peak Mach numbers to 1.1, thereby virtually eliminating any wave drag (Figure 5.2.9). Consequently, Pratt & Whitney has concluded that, through use of Transonic Computational Fluid Dynamics (CFD), 'slim-line' nacelles can be designed to achieve low cruise drag.
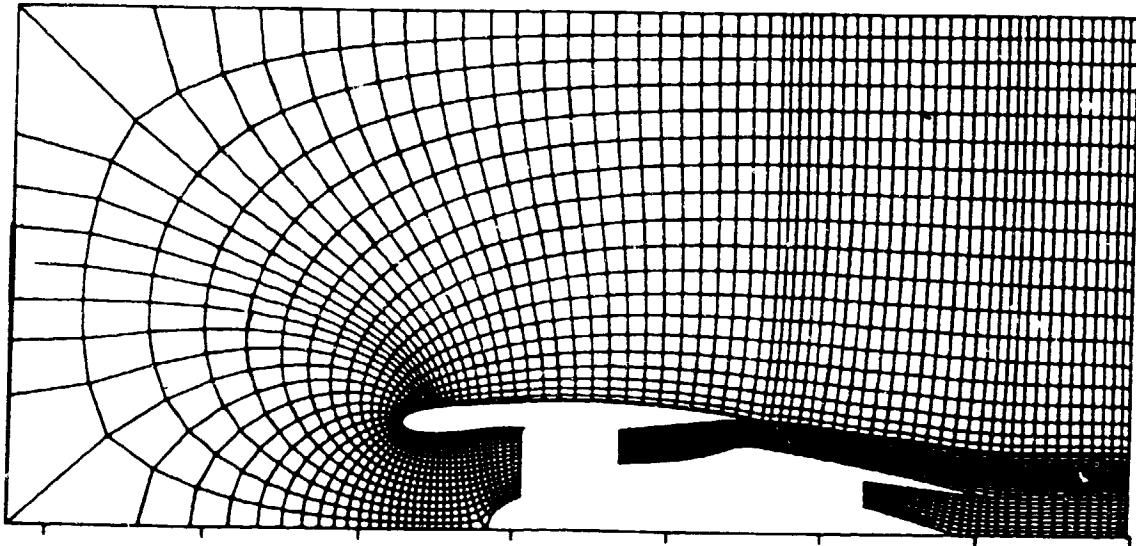
Figure 5.2-5   Full Nacelle Computational Grid
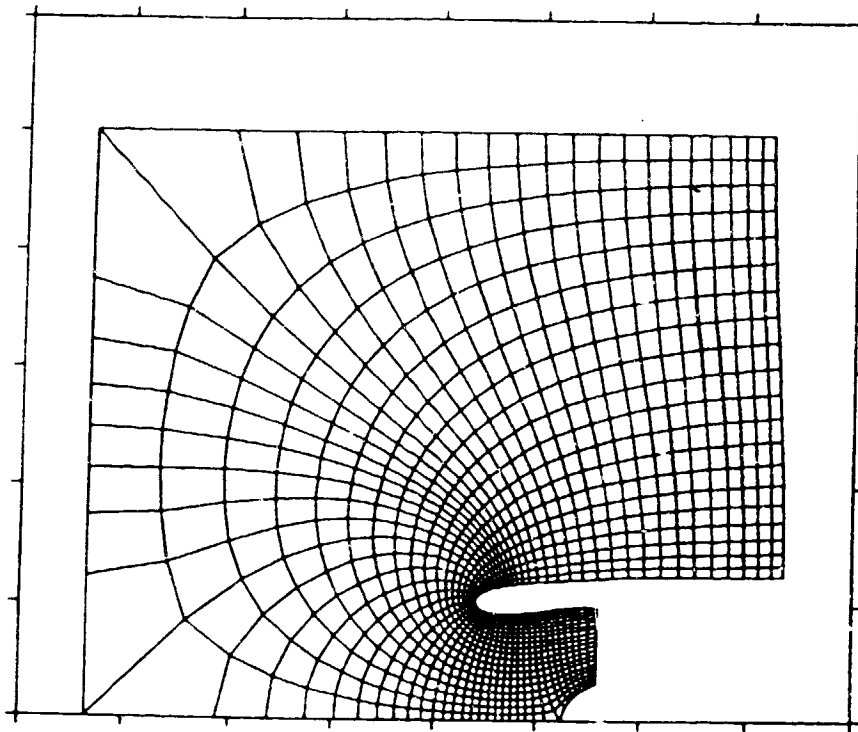
Figure 5.2-6   Isolated Inlet Computational Grid

φ = 0° AT TDC

ENGINE CENTERLINE

X = AXIAL DISTANCE
ASYMMETRIC (DROOPED) INLET

STREAMLINES IN PLANE OF SYMMETRY
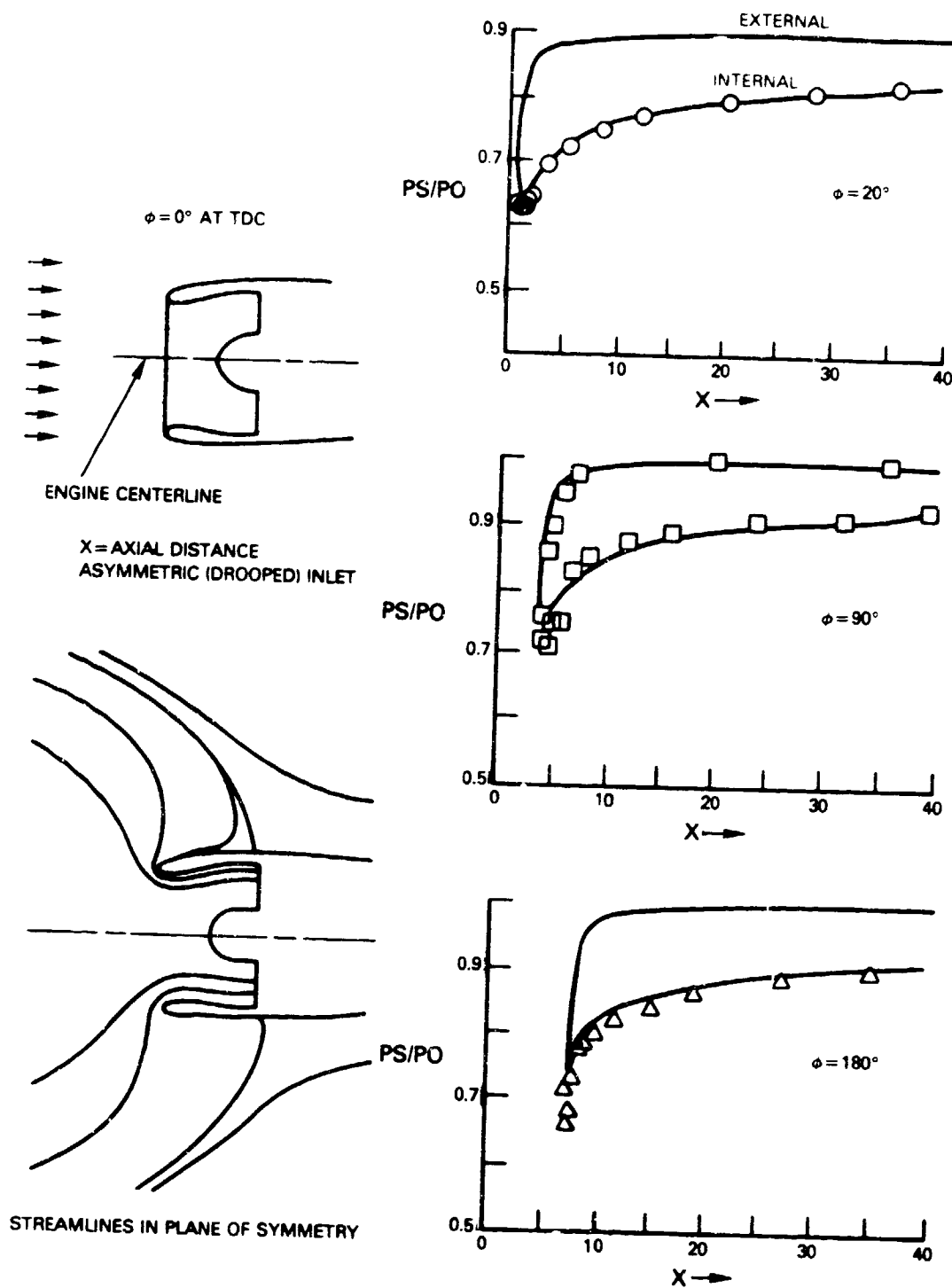
Figure 5.2-7A   Inlet Euler Code Results: Mn = 0.01, Angle of Attack = 0.0°,
Inlet Corrected Flow, kg/sec (lb/sec) = 476.7 (1051)

φ = 0° AT TDC

ENGINE CENTERLINE

X = AXIAL DISTANCE
ASYMMETRIC (DROOPED) INLET

STREAMLINES IN PLANE OF SYMMETRY
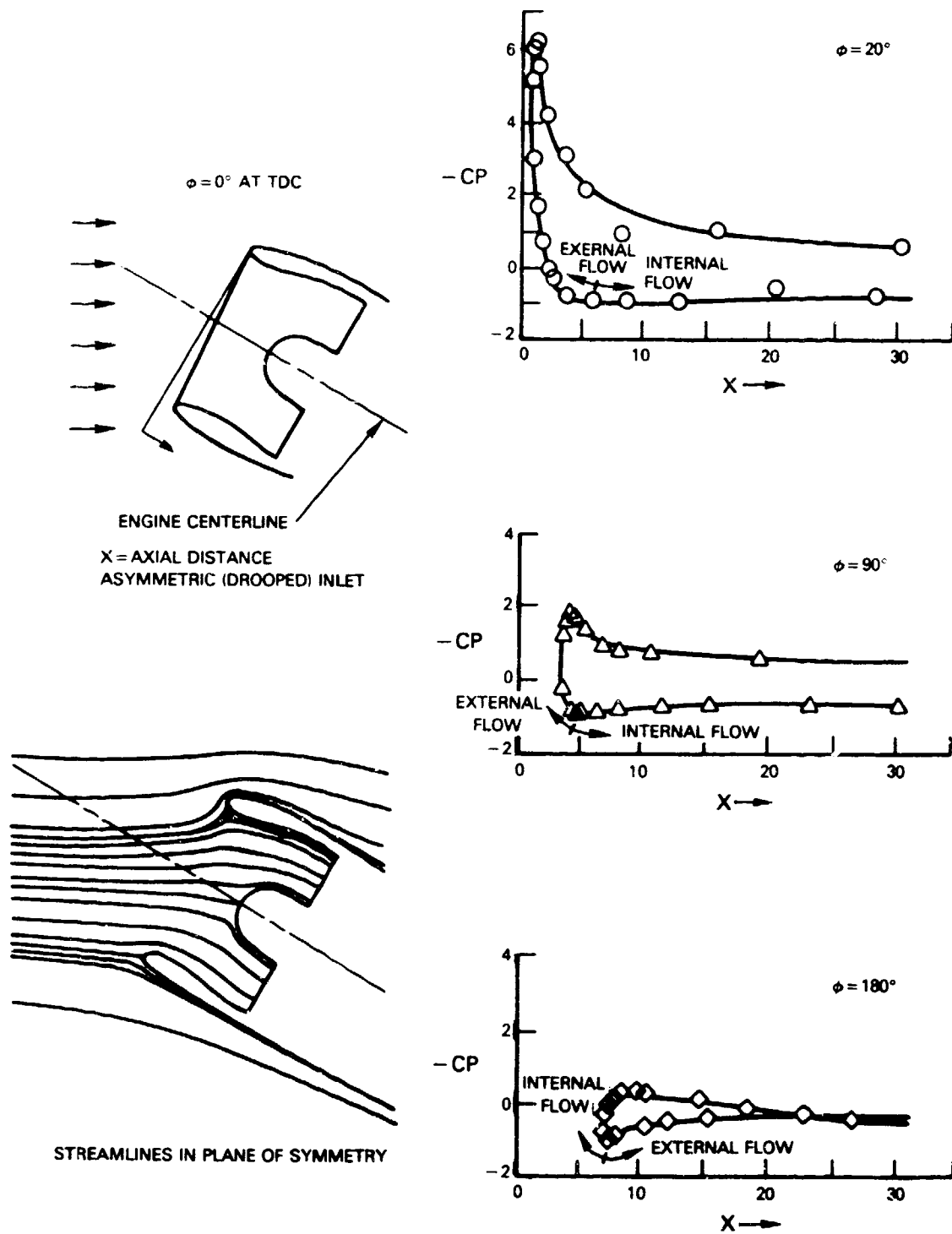
Figure 5.2-7B   Inlet Euler Code Results: Mn = 0.201, Angle of Attack = 24.12°, Inlet Corrected Flow, kg/sec (lb/sec) = 173.0 (381.45)

φ = 0° AT TDC

ENGINE CENTERLINE

X = AXIAL DISTANCE
ASYMMETRIC (DROOPED) INLET

STREAMLINES IN PLANE OF SYMMETRY

φ = 20°

φ = 90

φ = 180°
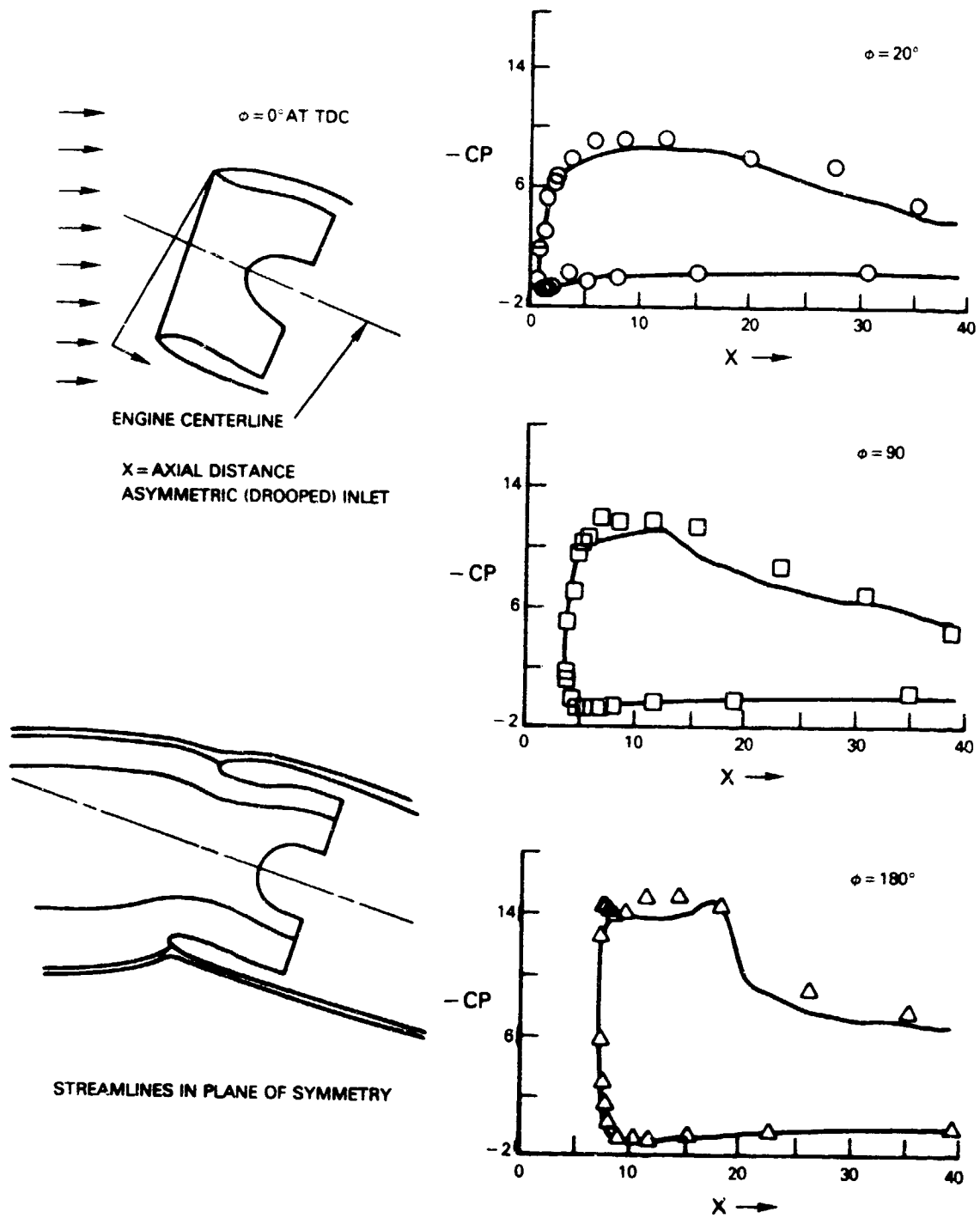
Figure 5.2-7C   Inlet Euler Code Results: Mn = 0.2501, Angle of Attack = 16.001°, Inlet Corrected Flow kg/sec (lb/sec) = 799.2 (1762)
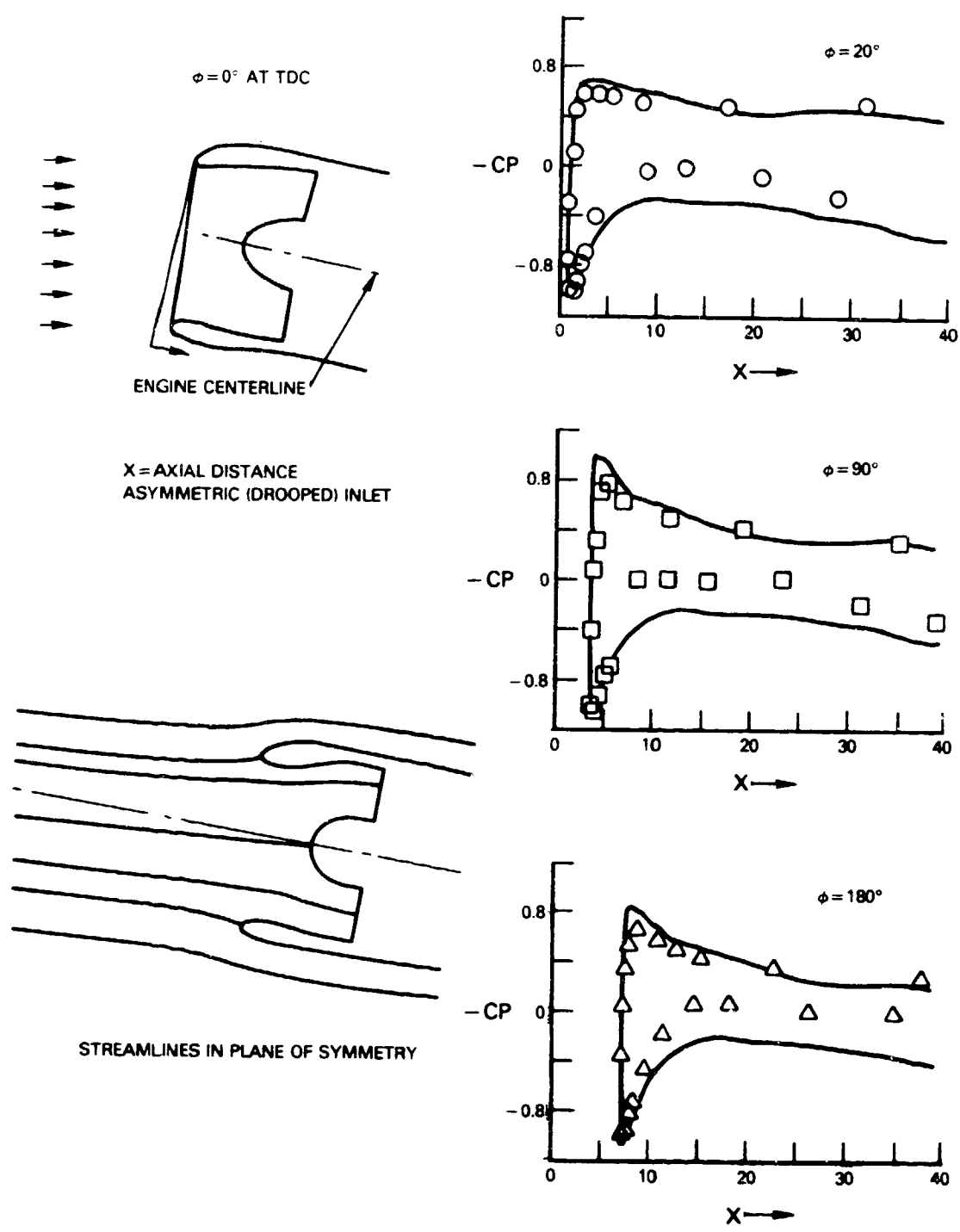
Figure 5.2-7D   Inlet Euler Code: Mn = 0.602, Angle of Attack = 4.05°, Inlet
                 Corrected Flow kg/sec (lb/sec) = 593.8 (1309.04)

ENGINE CENTERLINE

X = AXIAL DISTANCE
ASYMMETRIC (DROOPED) INLET

STREAMLINES IN PLANE OF SYMMETRY
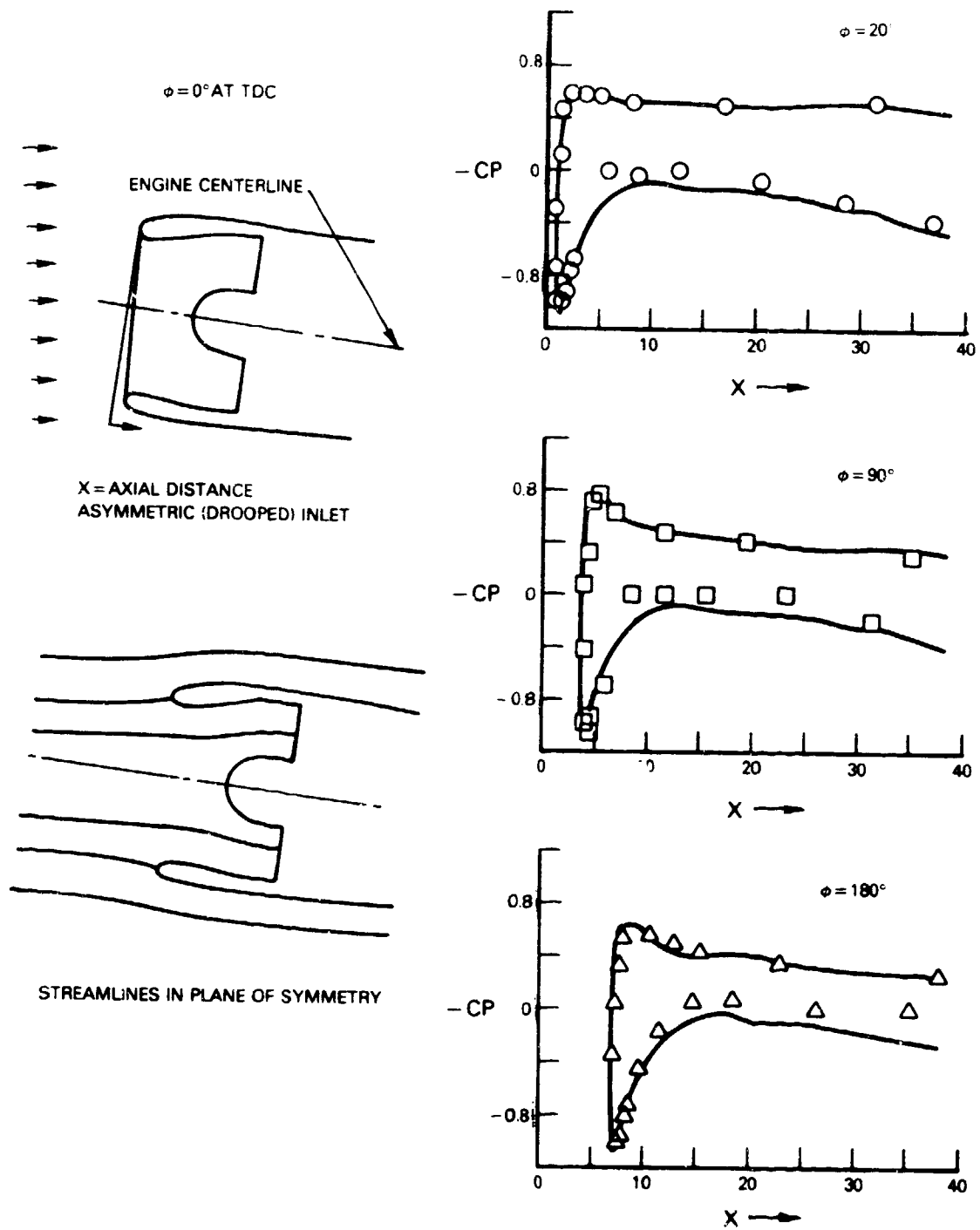
Figure 5.2-7E   Inlet Euler Code Results: Mn = 0.602, Angle of Attack = 4.05°,
Inlet Corrected Flow kg/sec (lb/sec) = 617.3 (1361)
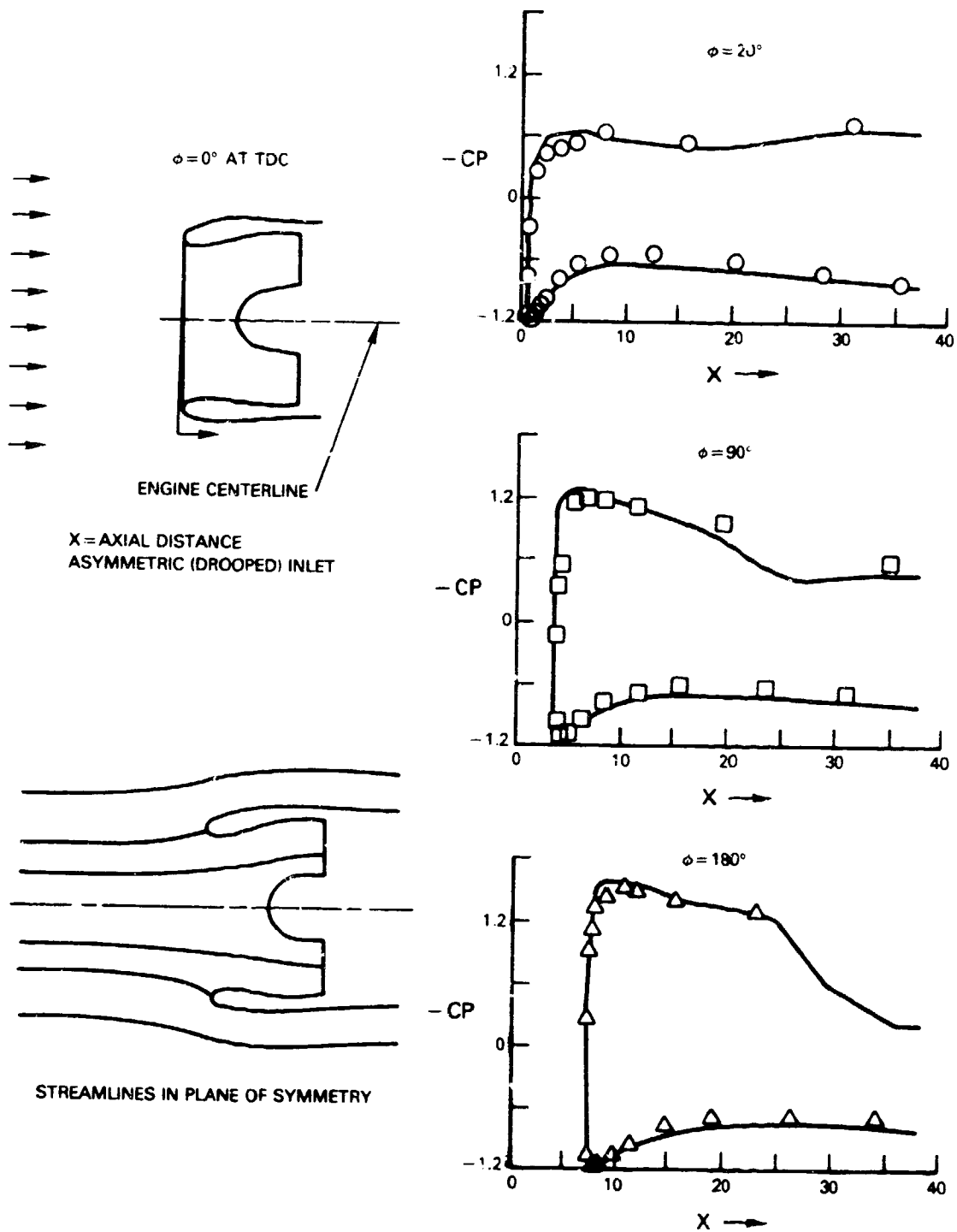
Figure 5.2-7F   Inlet Euler Code Results: Mn = 0.801, Angle of Attack = 0.01°,
Inlet Corrected Flow kg/sec (lb/sec) = 551.5 (1215.9)
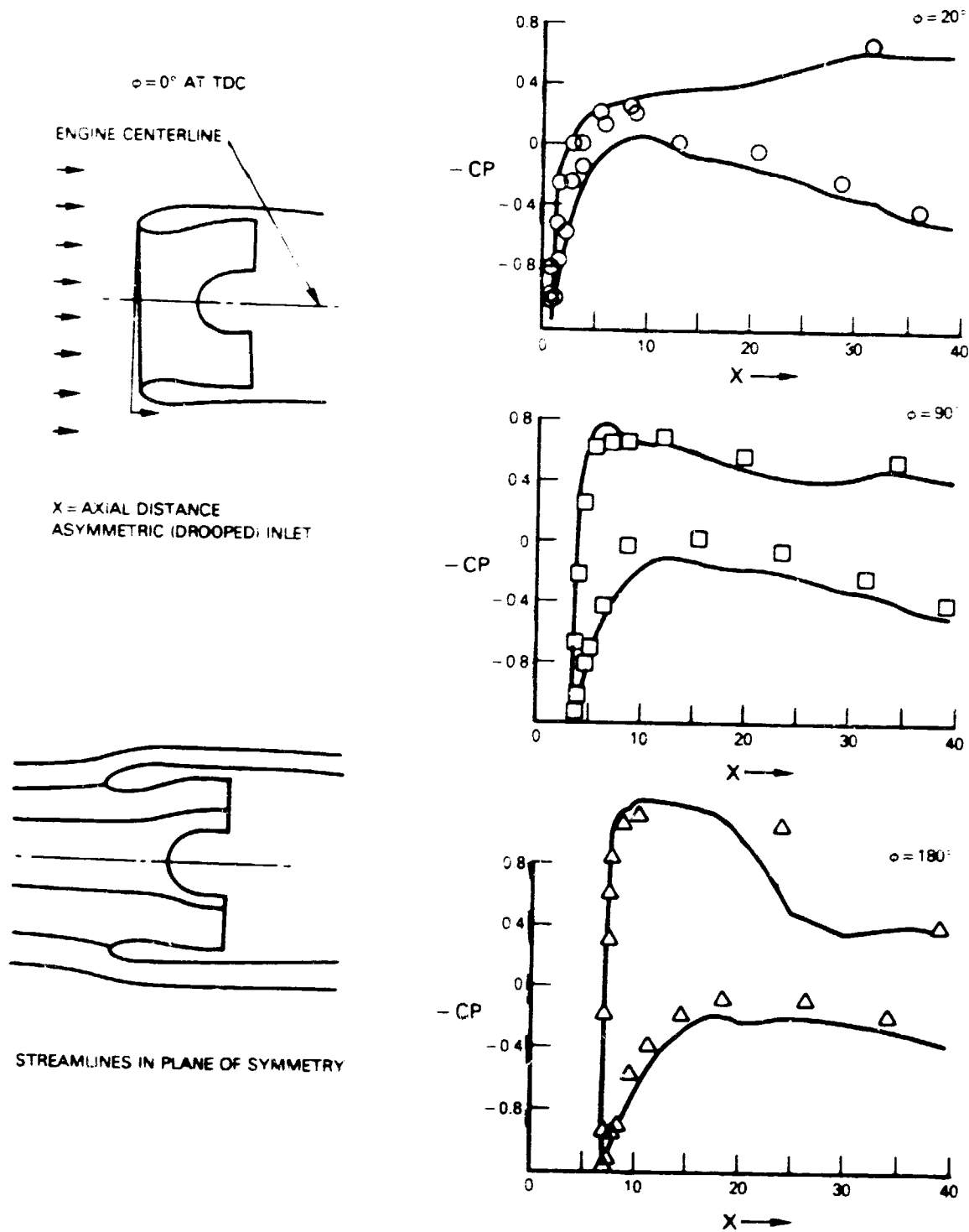
Figure 5.2-7G   Inlet Euler Code Results: Mn = 0.801, Angle of Attack = 0.06°.
Inlet Corrected Flow kg/sec (lb/sec) = 736.6 (1623.9)
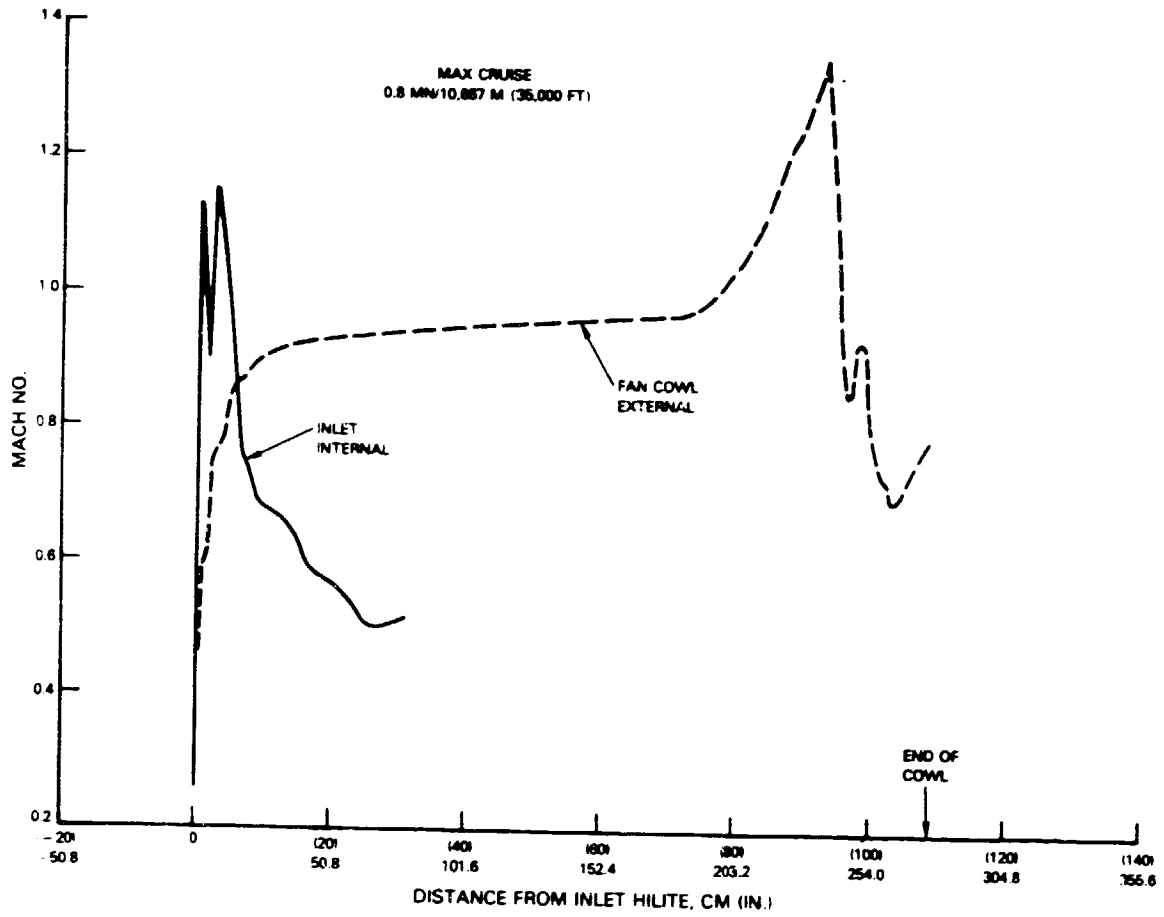
Figure 5.2-8   Original Inlet Contour Would Have Had Strong Shocks and Large
                Wave Drag Losses
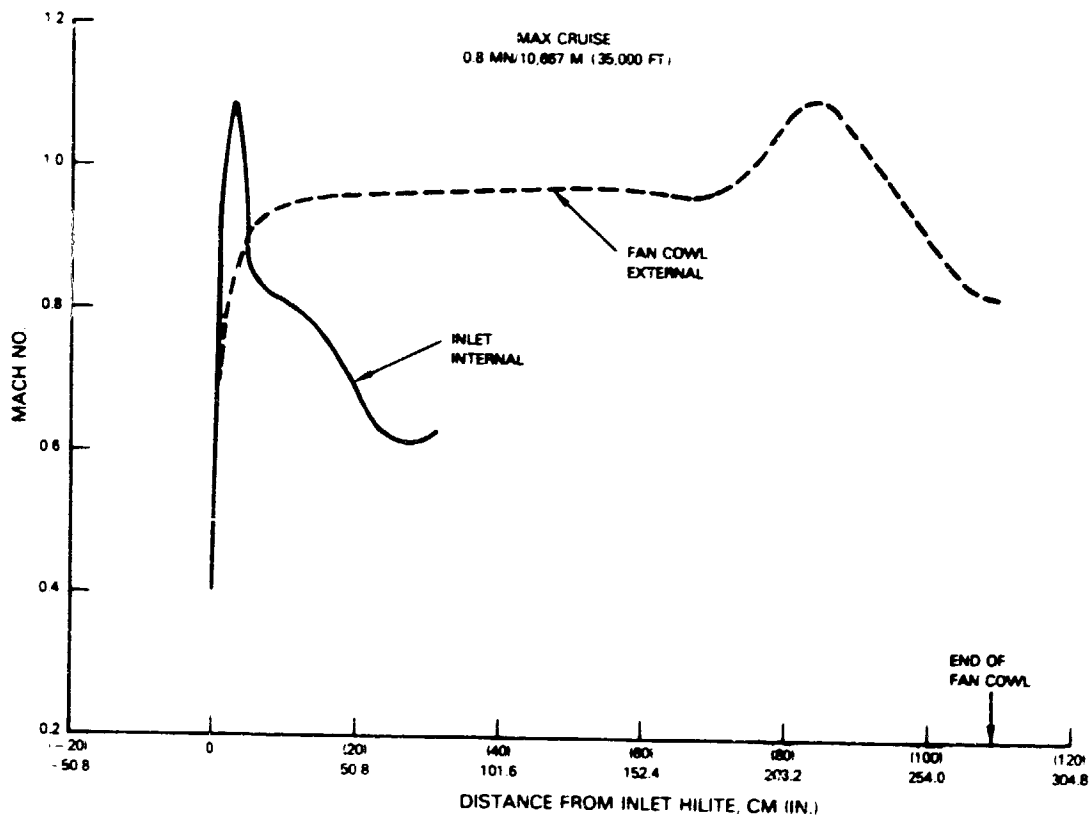
Figure 5.2-9   Contour Refinements Reduced Shock Strength and Eliminated Wave
                Drag

45

5.2.3 Advanced Technology Nacelle Definition

Utilizing the procedures described in sections 5.1, 5.21 and 5.2.2, ideal aerodynamic contours were established for the advanced technology nacelles wrapped around the three advanced technology engines (STF653, STF653-DD, STF654) described in section 6.1. Characteristics of these nacelles are summarized in Figure 5.2-10. These idealized contours formed the reference point for the engine and nacelle integration efforts described in Section 6.0.

ENGINE	STF653	STF653-DD	STF654
$D_{FAN(REFERENCE)}$	106.800 IN.	93.84 IN.	67.800 IN.
	(271.272 CM.)	(238.354 CM.)	(172.212 CM.)
D_{MAX}	122.471 IN.	106.00 IN.	79.019 IN.
	(311.076 CM.)	(269.240 CM.)	(200.708 CM.)
D_{HI}/D_{MAX}	0.853	0.866	0.839
D_{TH}/D_{FAN}	0.9526	0.9526	0.9520
L_{TH}/D_{FAN}	0.0313	0.0313	0.0313
L_{MAX}/D_{MAX}	0.672	0.755	0.825
L_{NAC}/D_{FAN}	1.864	2.331	2.039
L_{DUCT}/D_{FAN}	0.255	0.285	0.388
L_{INLET}/D_{FAN}	0.291	0.291	0.291
L_{COWL}/D_{FAN}	1.023	1.225	1.223

Figure 5.2-10   Preliminary Advanced Technology Nacelle Aerodynamic Contour Definition

46

5.3 THRUST REVERSER AERODYNAMIC DESIGN

As shown in section 4.3, the reverser effective requirements for high bypass ratio turbofans are significantly lower than those required for current engines due to increased ram drag (large fan diameter) and higher fan gross thrust to total net thrust ratio. The increased ram drag becomes increasingly potent at higher 'down-the-runway' aircraft velocities. The thrust reverser effectiveness required for each of the three study engines is shown in Figure 5.3-1 at an average 'down-the-runway' condition of 100 knots flight velocity without the primary thrust spoiled. The minimum effectiveness to meet the JT9D reverser thrust level decreases as bypass ratio increases.
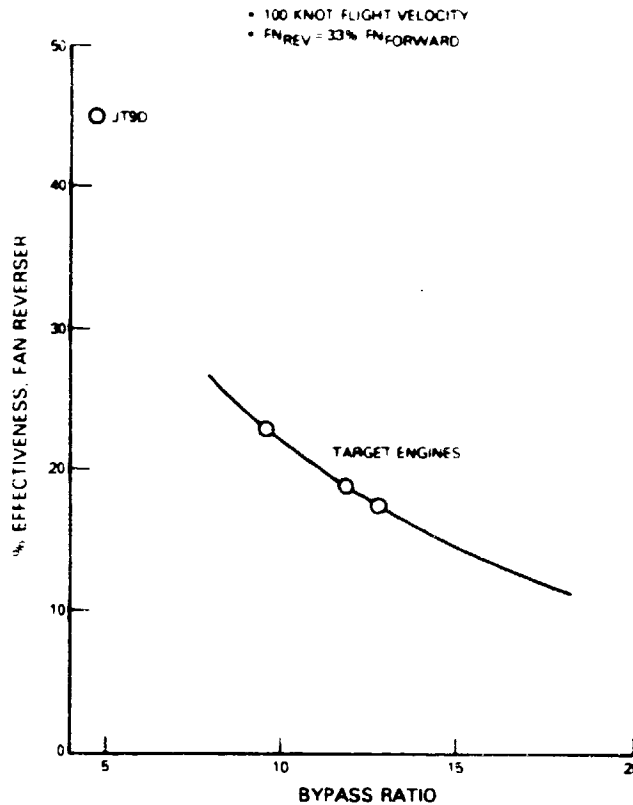
Figure 5.3-1   Reverser Effectiveness Requirements

The two types of fan reversers selected for further evaluation were cascade reversers and target reversers. Several principal physical parameters were selected for each type of reverser so that the overall dimensions and key characteristics of each configuration could be defined to meet a specified reverser effectiveness and effective flow area. For the cascade reversers, the principal physical parameters were defined as the following:

  1) cascade length (l_c);
  2) cascade diameter (D_c);
  3) the included angle of the cascade circumference (α_c);
  4) cascade discharge angle (β);
  5) cascade chord (c);
  6) cascade pitch/chord ratio (S/C).

These parameters are illustrated in Figure 5.3-2. For the target reversers, the principal physical parameters (as illustrated in Figure 5.3-3) were defined as:

1) reverser spacing (1_r);
2) reverser size (h'/H);
3) reverser angle (Θ);
4) discharge angle (β).

The length (L) of each cascade reverser was sized using the following equation:

$$L = \frac{K \ (AJCD)_{FAN}}{(C_D \ cascade) \ (Cos \ \beta) \ \pi \ D_c \ (\alpha_c/360)}$$

where $(AJCD)_{FAN}$ is the fan nozzle effective flow area in the non-reverse mode. C_D is the cascade discharge coefficient ($C_D = 0.95$), and K is the factor to account for compressor bleed margin and blockage of rails and vanes (K = 1.1).

The reverser effectiveness (η_R) was calculated as:

$$\eta_R = Cos \ (90 - \beta_{EFF})$$

where β_{EFF} is the effective reverser discharge angle.

CASCADE PROFILE

END VIEW
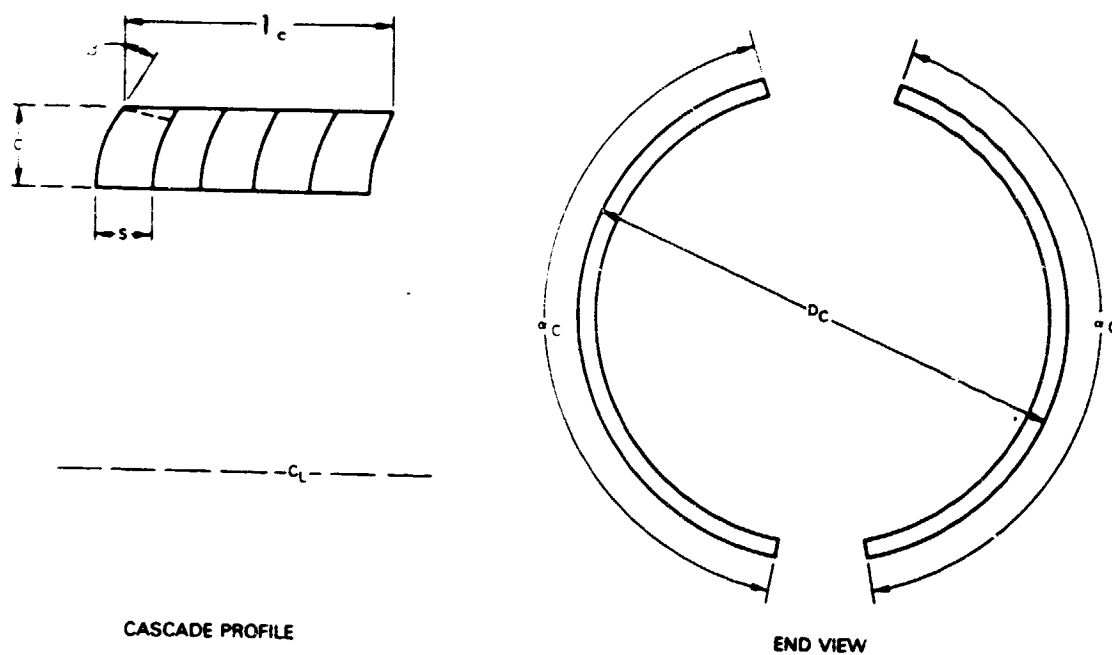
Figure 5.3-2   Principal Cascade Physical Parameters

THROAT PLANE

90°

BULLNOSE

← FLOW DIRECTION

C_L
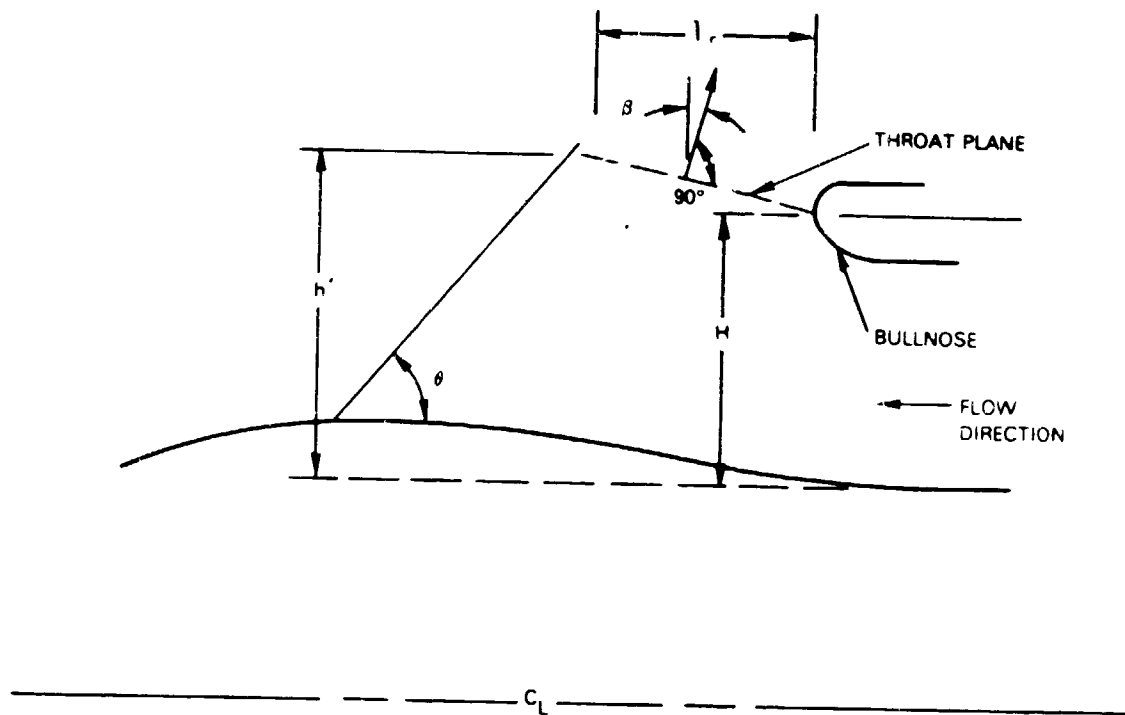
Figure 5.3-3   Principal Annular Target Reverser Parameters

The cascade discharge angle was set at 22 degrees to avoid excessive diffusion through the vanes which could result in flow separation and a loss of reverser efficiency. With a typical deviation angle of 3 degrees (aero vs. vane geometry), the effective flow discharge angle becomes 19 degrees, which results in a reverser effectiveness of 32.5 percent. This effectiveness exceeds the effectiveness required for each engine to match JT9D capability. The principal physical parameters of the cascade reverser for each engine are tabulated in Table 5.3-I. Also tabulated is the reverser effectiveness needed to achieve a reverse thrust that equals 33 percent of the forward thrust. Having this excess reverse thrust with a 22 degree cascade discharge angle opens two options:

1) reducing the cascade exit angle an appropriate amount to match the JT9D capability; this reduces the length of the cascade tray and the size of the blocker doors, resulting in a small weight savings;

2) lowering the engine thrust setting in reverse; this will pay off in turbine life and durability -- of the two, this option was chosen.

TABLE 5.3-I
Cascade Reverser Parameters

Engine	Required Effectiveness η_R	$(A_{JR})_{EFF}$ cm (in.)	l_c cm(in.)	D_c cm(in.)	β_{EFF} deg.	S/C
STF653	16.7 %	16,860 (6638)	46.17 (18.18)	299 (118)	19°	0.70
STF654	18.4 %	6,654 (2620)	29.33 (11.55)	195 (77)	19°	0.70
STF653-DD	21.8 %	11,652.2 (4587.5)	35.78 (14.09)	270.5 (106.5)	19°	0.70

In the case of the target reversers, the reverser discharge angle was defined as perpendicular to the throat plane defined by the reverser blocker door and the bull nose. The orientation of the throat plane to produce the desired reverser effectiveness was selected with the aid of a data correlation relating reverser effectiveness to the discharge angle. This correlation, which is shown in Figure 5.3-4, was obtained from the "Final Report STOL Transport Thrust Reverser/Vectoring Program" (Ref. 4). The reverser effective area was defined as:

$$A_{JR} = \frac{(AJCD)_{FAN}}{C_D (1-K)}$$

where C_D is the discharge coefficient ($C_D = 0.80$) and K is the factor to account for compressor bleed margin and blockage (K = 0.06).
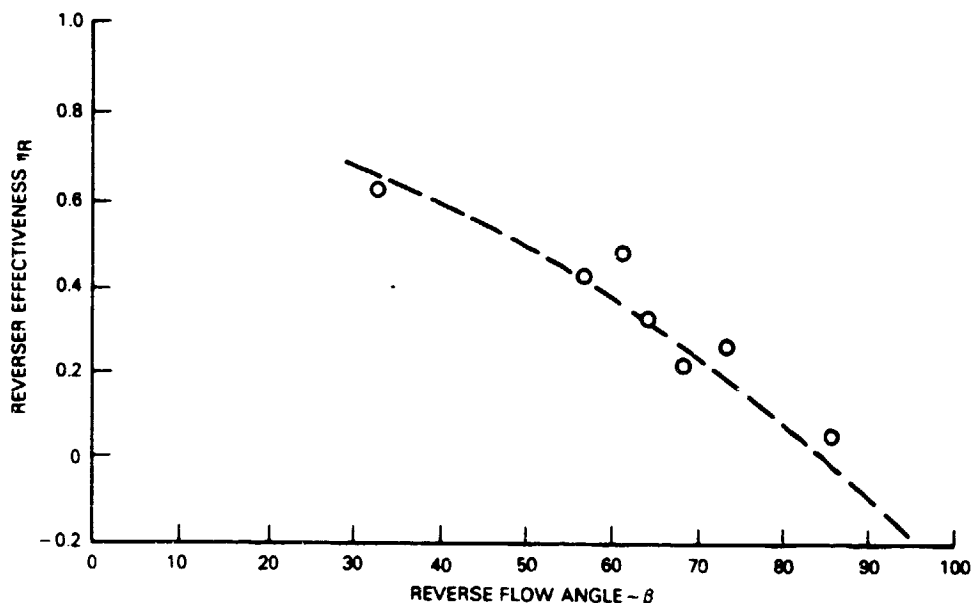
Figure 5.3-4   Reverser Effectiveness vs. Discharge Angle for Target Reversers

The target reverser parameters h'/H, H, Θ, and l_R were selected to produce the desired throat plane area and discharge angle. The principal physical parameters for the long flap and pivot blocker door target reversers are shown in Table 5.3-II.

The data shown in Tables 5.3-I and 5.3-II were utilized to assess the impact of reverser volume requirements on the ideal aerodynamic contours for the current and advanced technology nacelles. The results of this assessment are discussed in section 6.0.

TABLE 5.3-II
Target Reverser Parameters

Long Flap Reversers

Engine	Required Reverser Effectiveness η_R	$(A_{JR})_{EFF}$ cm (in.)	l_r cm(in.)	h'/H	H cm(in.)	Θ deg.	β deg.
STF653	16.7%	6,654 (2620)	42.04 (16.55)	1.196	63.402 (24.961)	50°	16.5°
STF654	18.4%	6,654 (2620)	25.96 (10.22)	1.207	39.958 (15.731)	50°	17.5°
STF653-DD	21.8%	11,652.2 (4587.5)	33.27 (13.10)	1.248	48.769 (19.200)	50°	20.0°

Pivot Blocker Door Reverser

Engine	Required Reverser Effectiveness η_R	$(A_{JR})_{EFF}$ cm (in.)	l_r cm(in.)	h'/H	H cm(in.)	Θ deg.	β deg.
STF653	16.7%	16,860 (6638)	43.94 (17.30)	1.253	63.400 (24.961)	50°	20.0°
STF654	18.4%	6,654 (2620)	26.92 (10.60)	1.273	39.956 (15.731)	50°	22.0°
STF653-DD	21.8%	11,652.2 (4587.5)	34.29 (13.50)	1.313	48.768 (19.200)	50°	24.0°

51

SECTION 6.0 ENGINE AND NACELLE INTEGRATION

Following definition of the aerodynamic contours for the current and advanced technology nacelle installations, further analyses were conducted to assess the degree to which these contours might be affected by engine installation requirements. These analyses included:

1) engine configuration and flowpath definition for the recommended engine cycles;

2) mechanical design and analysis of sufficient depth to ensure that the resultant nacelle and reverser/spoiler configurations were mechanically and structurally feasible;

3) investigation of airframe-engine interface requirements;

4) integration of the resultant engine/nacelle/reverser configuration into isolated nacelle installations for airframe subcontractor evaluation and mission benefits analysis;

5) a preliminary assessment of the noise characteristics of these installations.

These efforts are discussed in the following sections.

6.1 ENGINE CONFIGURATION AND FLOWPATH DEFINITION

The three engine cycles selected for study in section 4.0 encompass two airplane thrust level requirements, with two low spool design philosophies in the larger thrust size. Significant engine parameters affecting nacelle aerodynamic design are compared in Table 6.1-I. Detailed information on cycle evaluation and flowpath studies is available in Volume II of Reference 2.

TABLE 6.1-I
Propulsion System Characteristics Summary

	STF653	STF653-DD	STF654
Cycle			
Takeoff Thrust Size, N (lbs.)	257,995	222,410	106,756
	(58,000)	(50,000)	(24,000)
Fan Pressure Ratio (MCR)	1.53	1.70	1.56
Bypass Ratio (MCR)	12.8	9.6	11.8
Overall Pressure Ratio	64	64	55
Configuration			
Compression System	Axial	Axial	Axi-Centrifugal
Staging	1-3-11-2-5	1-5-11-2-7	1-3-6+C-2-4
Fan Drive	Geared	Direct	Geared
Geometry			
Fan Tip Dia, cm (in.)	271.2	238.2	172.2
	(106.8)	(93.8)	(67.8)
Low Turbine Max Dia, cm (in.)	106.4	124.2	76.9
	(41.9)	(48.9)	(30.3)
Compression System Length, cm	236.09	235.4	141.9
(in.)	(92.95)	(92.7)	(55.9)
Overall Engine Length, cm (in.)	366.2	385.0	232.1
	(144.2)	(151.6)	(91.4)

The choice between direct drive and gear driven fan systems affects the cycle selection as well as the flowpath, both of which affect the nacelle design. Compromise in the low rotor speed selection in a direct drive turbofan results in cycle optimization at higher fan pressure ratios and lower bypass ratios as shown in the screening studies. This also requires an increase in low pressure turbine stage number and elevation, increasing both the afterbody length and diameter (Figure 6.1-1). Reduced bypass ratio cycles require more effective thrust reversing designs to meet a given airplane requirement. All of these factors introduce variations between the STF653 and STF653-DD, which influence the optimum nacelle design.
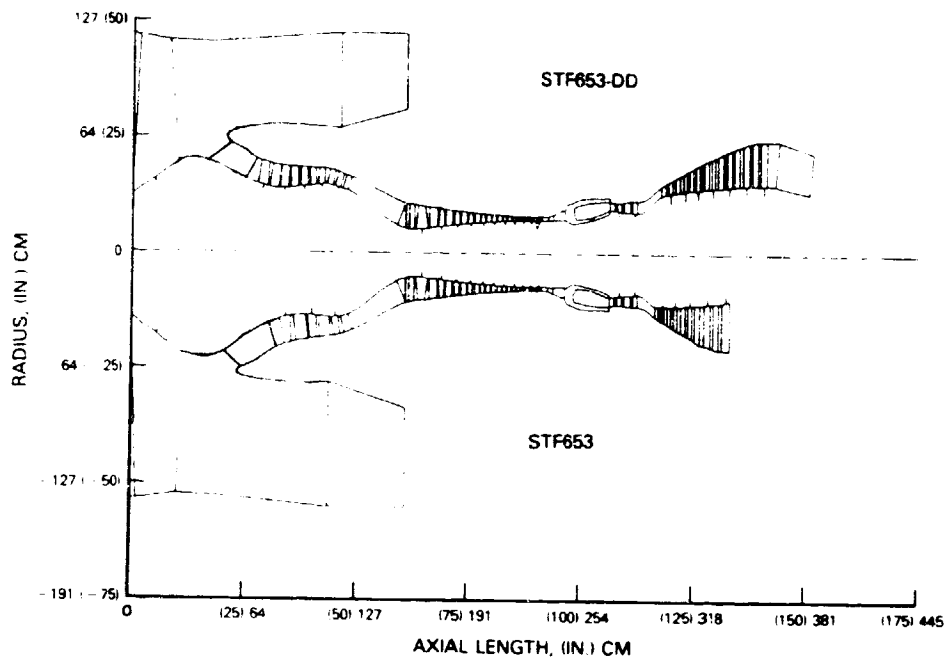
Figure 6.1-1   Comparison of Direct-Drive and Gear-Driven Fan Engine Flowpaths

Small thrust size engines offer several different challenges to nacelle design relative to large engines. Design minimums may be encountered in both engine and nacelle systems which prevent pure 'scaling down' of large engine results. Table 6.1-I shows that the overall pressure ratio of the STF654 was reduced relative to the large thrust size; this results from the adverse effect of small flow size on performance as engines are scaled down. The choice of an axial-centrifugal high-pressure compressor configuration is a direct conse- quence of high pressure ratio and small compressor exit corrected flow size. This compact high spool with a radial bulge in the mid-section (Figure 6.1-2) could affect engine accessory size and placement, warranting cowl-mounted accessories and attendant nacelle aerodynamic compromise. Conventional fan cowl thrust reversing systems could also present "packaging" difficulties in a small, high bypass ratio turbofan. These are discussed further in the fol- lowing section. Engine configuration and flowpath definitions resulting from this effort were used in establishing the ideal nacelle aerodynamic contours discussed earlier in section 5.0 as well as in establishing the installed pro- pulsion system performance discussed in section 6.4.
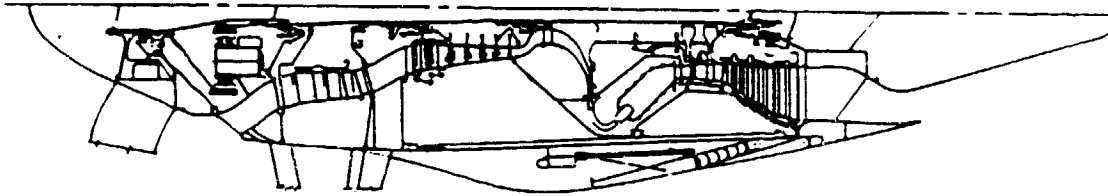
Figure 6.1-2   Flowpath of Gear-Driven Fan Engine with a Centrifugal
Compressor Stage

6.2   NACELLE AND REVERSER MECHANICAL DESIGN CONSIDERATIONS

6.2.1   Overview

The overall benefit of the advanced nacelle concepts described in Sections 4.0
and 5.0 is best measured in the context of what is best for the airline cus-
tomer. This means that not only must nacelle aerodynamic characteristics be
taken into consideration, but weight, cost and maintainability as well. Me-
chanical design analysis was therefore conducted 1) to establish the nacelle
and reverser design definition necessary to enable preliminary weight and cost
estimates, 2) to assure mechanical feasibility of the recommended configura-
tions, and 3) to provide installation drawings for use by the airframe sub-
contractor.

To establish a reference for quantifying the benefits of advanced nacelle and
reverser technologies, each of the advanced engines was first configured with
a nacelle and reverser representative of current (mid-1980's) technology. They
were subsequently configured with an advanced, slim-line nacelle to which was
applied two candidate advanced, low-volume reverser designs, which were
refinements of the concepts described in section 4.3. The high bypass ratios
of the selected engines put a premium on controlling nacelle cowl diameter.
This was achieved, in part, by utilizing minimum thickness nacelle sections.
The resultant slim-line design, while providing aerodynamic benefits, also
created a space constraint that would preclude the use of cascade-type thrust
reversers typical of current designs. Offsetting this concern is the fact that
ram drag characteristics of very high bypass ratio engines may require only
spoiling or moderate reversal of fan thrust for aircraft deceleration. The two
advanced reverser concepts investigated take advantage of this relaxed
requirement.

High fan bypass ratios do pose challenges in the thrust reverser designs. The
larger flowpath area requires larger blocker doors and longer drag links com-
pared to current engine designs. Sufficient analysis was accomplished to
assure that proper thrust reverser areas were attained and that critical fea-
tures such as drag links and blocker panels were properly sized.

One other potential constraint on achieving optimum slim-line nacelle contours
is the mount location of engine accessories. For ease of maintenance, acces-
sories are customarily mounted on the fan case or on the engine core case, if
space permits. However, mounting accessories on the fan case means com-
promising the optimum fan cowl geometry. Consequently, accessory location was
investigated in the design analysis.

55

6.2.2 Cascade Reverser Mechanical Design

The reverser design concept shown in Figure 6.2-1 is representative of all the Current Nacelle Technology reverser designs. This design concept is basically the same as the one used on current high bypass ratio production engines, with slight modifications. It consists of a fixed cascade ring covered by a translating outer shroud to which are attached twelve hinged blocker panels. A hinged drag link attaches to each of the panels and crosses the flow path to a hinge on the inner fan duct cowl. The outer shroud is translated by four synchronized ball screw drives.

To adapt this reverser concept to the advanced technology "slim-line" nacelle geometry, the ball screw drives must be located in the same diametral plane as the cascade ring, which requires an integral clearance annulus in the cascade ring. In the current production design, the ball screw drive is inside of the cascade ring. These minor changes to the reverser design did affect the optimum nacelle aerodynamic lines to some degree as shown in Figure 6.2-2. A more detailed review of the thrust reverser design is recommended to further reduce the reverser geometry to fit within the optimum aerodynamic nacelle lines.

DRAG LINK

CASCADE

BLOCKER PANELS AND OUTER
SHROUD IN REVERSE POSITION
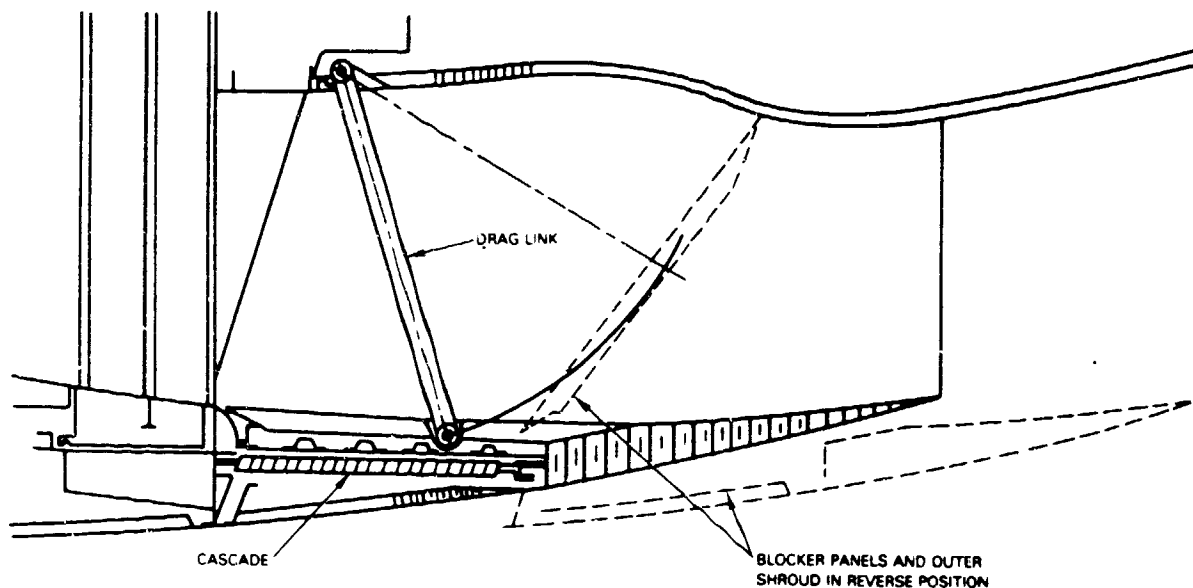
Figure 6.2-1   Current Technology Cascade Reverser Design Concept

56

6.2.3 Target Reverser Mechanical Design

As noted in Section 6.2.1. two low-volume, target type, reverser/spoiler con-
cepts were investigated which would meet thrust reverse requirements and still
fit within the optimum slim-line nacelle cowl geometry. The thrust spoiler
design concepts shown in Figure 6.2-3 are representative of all the Advanced
Thrust Spoiler designs. The primary Advanced Spoiler design shown in Figure
6.2-3A is similar to the Current Nacelle Reverser discussed in section 6.2.2,
except that the cascade has been deleted, which creates a thrust spoiler
rather than a thrust reverser. This requirement became necessary due to the
thin nacelle cowl contour which minimized the space necessary to install a
cascade thrust reverser design. The blocker panels, however, were designed to
provide some forward thrust out of the reverser opening. The rest of the sys-
tem -- including the * 'nslating cowl, ball screw actuators, blocker panels
and drag links --   ns basically the same as in the current technology
nacelle reverser　　　.

The alternate Thrust Spoiler design shown in Figure 6.2-3B consists of a
translating cowl connected by links to four blocker panels. The blocker panels
are supported by pins located in fixed 'strings,' or beams, located between
the panels. When the cowl is translated, the blocker panels are rotated
through the links into the fan duct where they turn the fan stream outward and
forward. A feature of this design not found in the other designs is that the
links do not extend across the fan duct. Further detailed design study and
analysis is recommended for this particular configuration to fully optimize
nacelle aerodynamic lines and confirm feasibility.
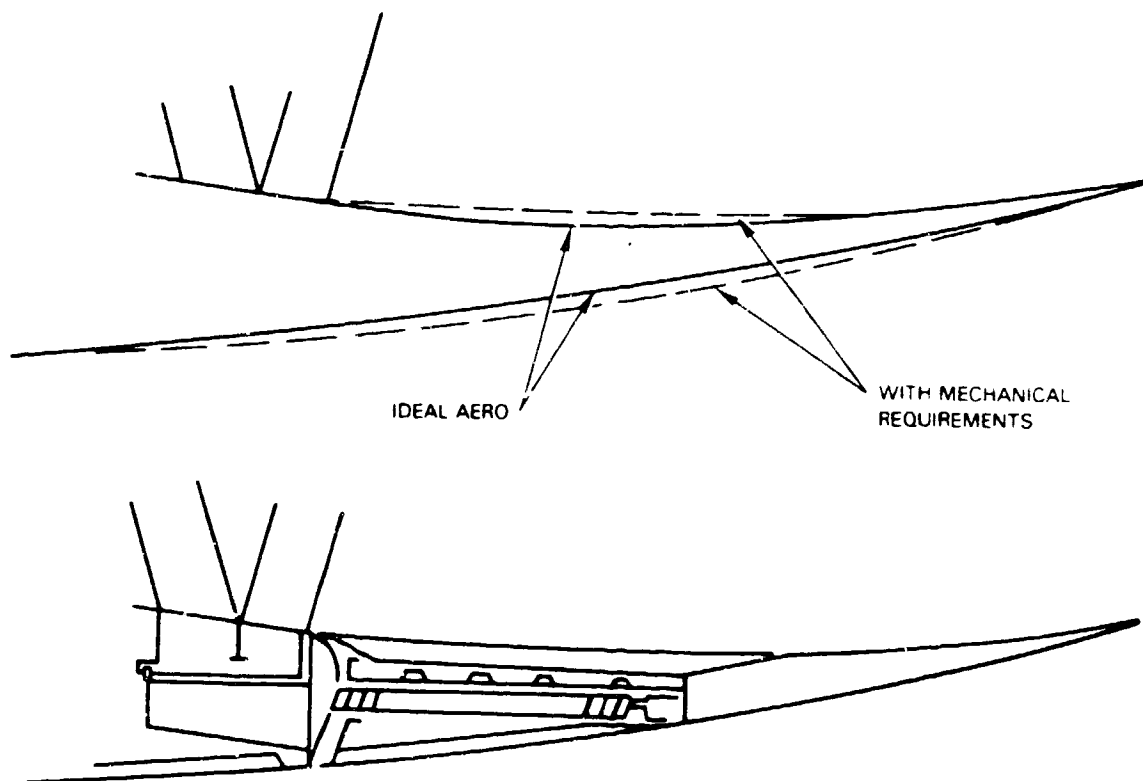
Figure 6.2-2   Effect of Current Technology Cascade Reverser Volume
Requirements on Ideal Aerodynamic Nacelle Cowl Contours
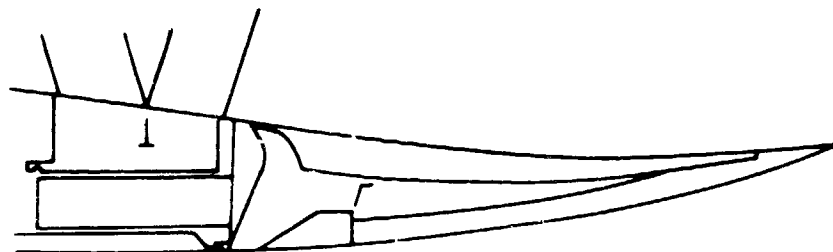
(A) ADVANCED TECHNOLOGY – LONG FLAP TARGET REVERSER
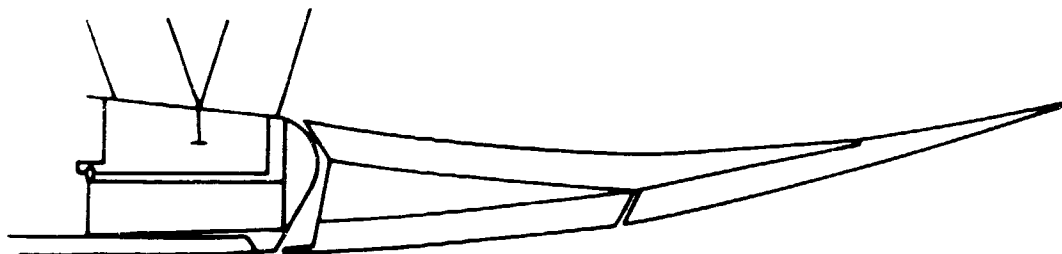
(B) ADVANCED TECHNOLOGY – FOUR-PIECE PILOT BLOCKER DOOR TARGET REVERSER

Figure 6.2-3   Target Reverser Concepts for Advanced Technology Nacelle Applications

6.2.4   <u>Nacelle Configuration and Accessory Mount Location Analysis</u>

The large engines (STF653 and STF653-DD) in both the Current and Advanced Technology Nacelle configurations utilize a core-mounted gearbox. This type of installation is possible due to the amount of space that is available based on the nacelle aerodynamic lines. Core-mounted installations are typical of current high bypass ratio production engines.

The smaller engine (STF654) is unable to utilize a core-mounted gearbox due to the minimal space available and requires an alternate gearbox installation. A fan duct mounted gearbox was selected for the Current Technology Nacelle installation. This type of installation is possible due to the longer inlet cowl and afterbody lines of the nacelle which in turn allow acceptable nacelle geometry to be faired over the gearbox.

The Advanced Technology Nacelle configuration for the STF654 engine included the added constraints of a shorter cowl and afterbody. The fan-duct mounted gearbox installation could not be utilized since acceptable nacelle lines could not be faired over the gearbox. Core-mounting of all accessories was not possible because use of a centrifugal stage in the high-pressure compressor limits the volume available for accessories. The final installation configuration, shown in Figure 6.4-9, was accomplished by reducing accessory sizes to account for advancements in technology and placing the accessories in two locations. The airframe accessories, which include the IDGS, Hydraulic Pump and the EEC, were located on the fan duct, at the top vertical centerline of the engine. These accessories would be covered by pylon fairings in the aircraft installation. The engine accessories were located in the core location

58

of the engine, as in the current technology nacelle configuration. This arrangement may not be acceptable to the aircraft owner. However, it should be noted that more detailed studies may show that an all-axial compressor is competitive in the engine size noted. This possibility, combined with advancements in accessory technology and packaging techniques, may make the core-mounting of accessories feasible.

6.3 ENGINE-AIRFRAME INTEGRATION CONSIDERATIONS

In addition to the concerns about accessory size and location discussed in section 6.2.4, other engine-airframe interface concerns include:

1) bleed and horsepower extraction requirements for customer air and engine starting;
2) plumbing and maintainability considerations;
3) nacelle de-icing requirements;
4) thrust reverser/spoiler targeting requirements;
5) engine mount location and associated pylon-nacelle interactions.

All of these have the potential for affecting the the optimum nacelle aerodynamic contours. A detailed assessment of these points was not within the scope of the study effort, although the airframe subcontractor (appendix A) did conduct a preliminary assessment of engine mount location. These issues have been suggested for future investigation (see section 8.0).

6.4 INSTALLED PROPULSION SYSTEM DEFINITION

Finalization of the installed propulsion system performance, weight and geometric characteristics was an iterative process between the nacelle aerodynamic design and mechanical design activities to arrive at nacelle aerodynamic contours that properly accounted for the effects of thr st reverser/spoiler installations as well as accessory requirements. The approach was to define initial installations with "ideal" nacelle aerodynamic contours to establish a reference point, (see Section 5.0) then modify these contours as necessary to accommodate thrust reverser/spoiler and accessory requirements and assess the performance and weight changes caused by these modifications. Installation drawings of the finalized configurations were subsequently prepared for use in the airframe subcontractor evaluations (Appendix A) and for estimating the propulsion system weight, performance, and cost information necessary for the benefits assessment discussed in Section 7.0.

6.4.1 Thrust Reverser/Spoiler and Accessory Location Effects on Propulsion System Characteristics

Iteration of the current and advanced nacelle aerodynamic designs to accommodate accessory and thrust reverser/spoiler volume requirements yielded the modifications discussed in the following paragraphs. For the STF653 and STF653-DD engines, the volume available around the engine was sufficient to permit core-mounted accessories without the need to modify the aerodynamic contours of the core nacelle wrap. Similarly, the volume available in the nacelle cowl was sufficient to accommodate the current technology cascade reverser design. Hence, the ideal aerodynamic contours for the current technology nacelles, described in Section 5.1 were preserved.

Nacelle cowl volume in the advanced technology nacelle was not sufficient to accommodate either of the advanced technology reverser/spoiler designs without modifying the ideal aerodynamic contours. Incorporating the long flap target reverser design required a 5.0 cm (2 inch) increase in nacelle maximum diameter as shown in Figure 6.4.1(a). The blocker door thrust spoiler required not only a 5.0 cm (2 inch) increase in nacelle maximum diameter, but a 23.6 cm (9.3 inch) increase in fan cowl length, as shown in Figure 6.4.1(b). The effects of these changes on the principal nacelle dimensions as the ideal contours, are shown in Table 6.4-I and their effects on nacelle performance are summarized in Table 6.4-II along with the performance of current and advanced technology nacelles with ideal aerodynamic contours.

(A) ADVANCED TECHNOLOGY   LONG FLAP TARGET REVERSER

(B) ADVANCED TECHNOLOGY   FOUR-PIECE PILOT BLOCKER DOOR TARGET REVERSER
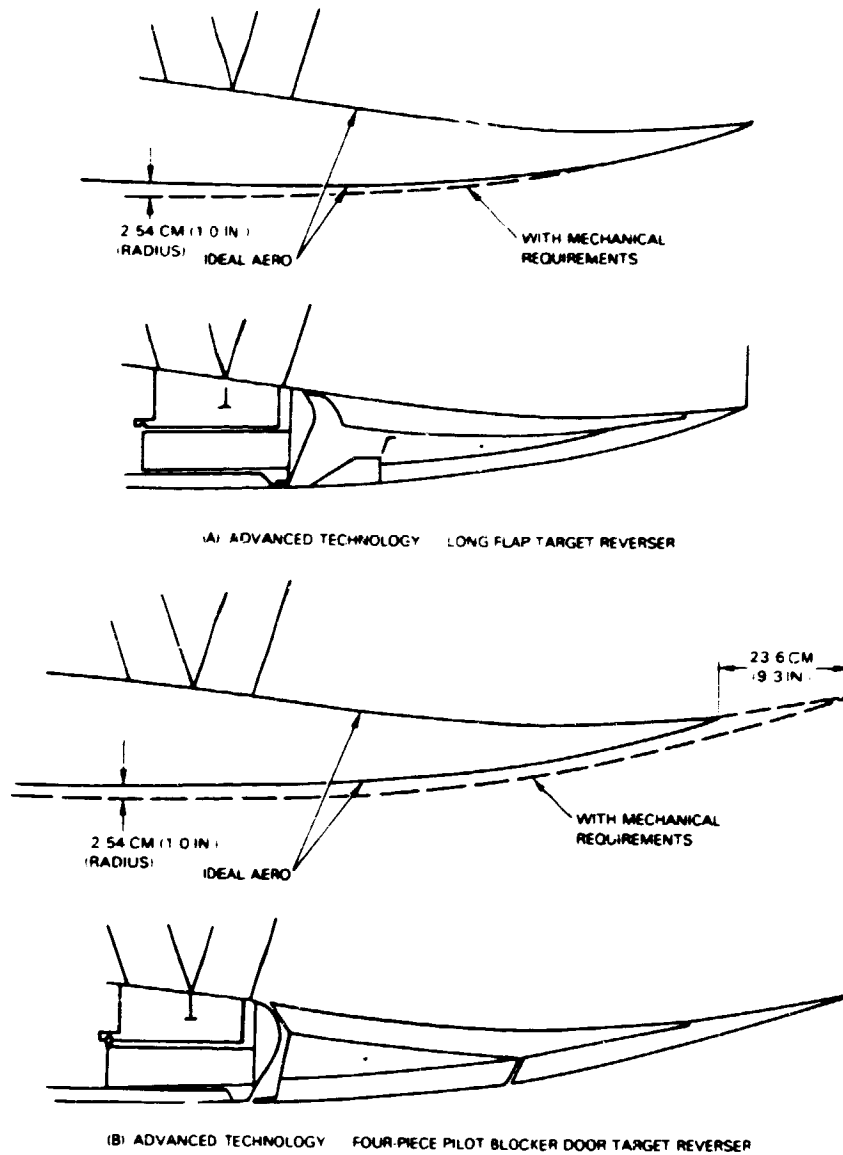
Figure 6.4-1   Long Flap Target Reverser and Four-Piece Pivot Blocker Door

		REVISED AERO. CONTOURS	
	IDEAL AERO. CONTOURS	Long Flap Reverser (+5.0 cm, 2.0 in. D_{MAX})	Four Piece Pivot Blocker Door Reverser (+5.0 cm, 2.0 in. D_{MAX}, +23.6 cm, 9.3 in. Fan Cowl Length)
D_{FAN}	106.8 in. 271.272 cm.	106.8 in. 271.272 cm.	106.8 in. 271.272 cm.
D_{MAX}	122.471 in. 311.076 cm.	124.470 in. 316.154 cm.	124.470 in. 316.154cm.
D_{HI}/D_{MAX}	0.853	0.83906	0.83906
D_{TH}/D_{FAN}	0.9526	0.9526	0.9526
L_{TH}/D_{FAN}	0.0313	0.0313	0.0313
L_{MAX}/D_{MAX}	0.672	0.6174	0.6174
L_{NAC}/D_{FAN}	1.864	1.864	1.864
L_{DUCT}/D_{FAN}	0.255	0.255	0.342
L_{IN}/D_{FAN}	0.291	0.291	0.291
L_{COWL}/D_{FAN}	1.023	1.0231	1.110

TABLE 6.4-II
Summary of Nacelle Performance Characteristics
STF653
Maximum Cruise 0.8MN/10.67 km, (35,000 ft) Altitude

	CURRENT TECHNOLOGY Ideal Aero. Contours	ADVANCED TECHNOLOGY Ideal Aero. Contours	ADVANCED TECHNOLOGY Revised Aero. Contours	
			Long Flap Reverser	Four-Piece Pivot Blocker Door Reverser
Pressure Drag, N (lbs.)	306.4 (68.9)	223.2 (50.2)	257.9 (58.0)	250.8 (56.4)
Fan Cowl Friction, N (lbs.)	1,080.9 (243.0)	729.0 (163.9)	738.4 (166.0)	788.2 (177.2)
AfterBody and Pylon Friction, N (lbs.)	449.2 (101.0)	577.8 (129.9)	573.8 (129.0)	491.9 (110.6)
After Body Steps and Gaps, N (lbs.)	206.3 (46.4)	0.0 (0.0)	0.0 (0.0)	0.0 (0.0)
Total Drag, N (lbs.)	2,043.0 (459.3)	1,530.1 (344.0)	1,570.2 (353.0)	(1,531.0 344.2)
Nacelle Leakage (% of Flow)	0.2%	0.0	0.0	0.0
Primary Duct Loss(%$\Delta P_T/P_T$)	0.48	0.412	0.412	0.412
Fan Duct Loss (%$\Delta P_T/P_T$)	0.58	0.468	0.469	0.562
Inlet Recovery ($P_{T2}/P_{T\infty}$)	0.9975	0.9982	0.9982	0.9982
Primary CV	0.9957	0.9957	0.9957	0.9957
Fan CV	0.9953	0.9953	0.9953	0.9953

TABLE 6.4-III
Summary of Nacelle Performance Characteristics
STF653-DD
Maximum Cruise 0.8MN/10.67 km (35,000 ft) Altitude

	CURRENT TECHNOLOGY Ideal Aerodynamic Contours	ADVANCED TECHNOLOGY Ideal Aerodynamic Contours
Pressure Drag, N (lbs.)	237.9 (53.5)	135.2 (30.4)
Fan Cowl Friction, N (lbs.)	973.2 (218.8)	661.0 (148.6)
AfterBody and Pylon Friction, N (lbs.)	560.4 (126.0)	692.1 (155.6)
AfterBody Steps and Gaps, N (lbs.)	168.5 (37.9)	0.0 (0.0)
Total Drag, N (lbs.)	1,940.3 (436.2)	1,488.3 (334.6)
Nacelle Leakage (% of Flow)	0.2	0.0
Primary Duct Loss (%$\Delta P_T/P_T$)	0.636	0.538
Fan Duct Loss (%$\Delta P_T/P_T$)	0.918	0.591
Inlet Recovery ($P_{T2}/P_{T\infty}$)	0.9976	0.9982
Primary CV	0.9958	0.9958
Fan CV	0.9937	0.9937

A similar detailed assessment of the reverser/spoiler impact on the STF653-DD engine was not undertaken. However, the modifications to the ideal aerodynamic contours are expected to be similar to those for the STF653. Table 6.4-III compares the performance of the current and advanced technology nacelles with ideal aerodynamic contours as installed on the STF653-DD engine.

For the STF654 engine, insufficient volume precluded mounting of all accessories on the core. As a consequence, the decision was made to mount the accessories on the fan case for the current technology nacelle and to split the accessories between two locations as discussed earlier in Section 6.2.4 for the advanced technology nacelle. To accommodate the fan case mounted accessories, the current technology nacelle ideal contours were revised from a circular cross-section to an unsymmetrical fan cowl shape with a constant D_{max} upper half and a super-elliptical shape for the lower half. This modification is illustrated in Figure 6.4.-2(a) and the corresponding revised contours relative to the ideal contours are compared in Table 6.4-IV. Cowl volume with ideal aerodynamic contours was adequate to house the cascade thrust reverser in the current technology nacelle.

Splitting the accessory locations for the advanced technology nacelle eliminated the need to modify the ideal contours to accommodate accessory volume requirements. However, to incorporate either of the advanced thrust reversers required a 10.1 cm (4.0 inch) increase in D_{max} and a 0.2 cm (0.1 inch) increase in the core cowl diameter at the turbine elevation clearance point as shown in Figure 6.4.-2(b). The corresponding revised contours relative to the ideal contours are shown in Table 6.4-V. Table 6.4-VI compares the performance of the current and advanced technology nacelles with ideal aerodynamic contours and as modified to accommodate accessory and thrust reverser volume requirements.
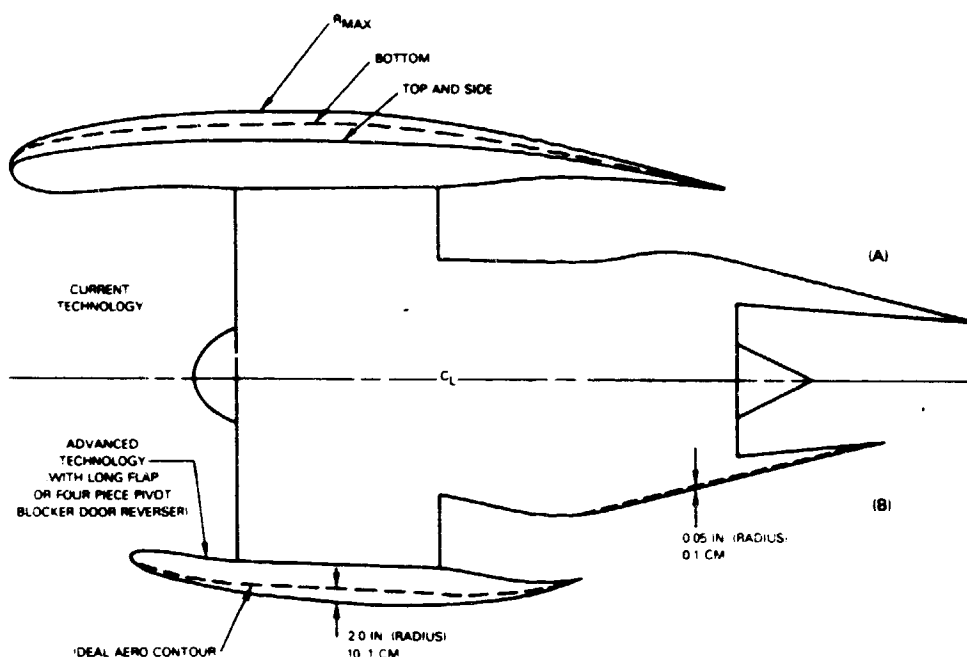
Figure 6.4-2   Comparison of Modified Current and Advanced Technology STF654 Nacelles

63

TABLE 6.4-IV
Nacelle Dimensions for STF654 with Current Technology Nacelle

	Ideal Aero. Contours	Revised Aero. Contours (Fan Case Mounted Accessories) Circumferential Location			
		Top	Side	Max. Radius'	BOTTOM
D_{FAN}	67.8 in. 172.212 cm.	67.8 in. ----------------------------------▶ 172.212 cm. ----------------------------------▶			
D_{MAX}	84.570 in. 214.808 cm.	85.954 in. -------▶ 218.323 cm. -------▶		97.165 in. 246.799 cm.	92.250 in. 234.315 cm.
D_{HI}/D_{MAX}	0.869	0.855	0.865	0.777	0.819
D_{TH}/D_{FAN}	0.9695	0.9695 ----------------------------------▶			
L_{TH}/D_{FAN}	0.1431	0.1431 ----------------------------------▶			
L_{MAX}/D_{MAX}	0.400	0.582 ------------▶		0.520	0.543
L_{NAC}/D_{FAN}	2.315	2.604 ----------------------------------▶			
L_{DUCT}/D_{FAN}	0.678	0.767 ----------------------------------▶			
L_{IN}/D_{FAN}	0.617	0.617 ----------------------------------▶			
L_{COWL}/D_{FAN}	1.787	1.930 ----------------------------------▶			

NOTE (1): At 36.576 Degrees From Bottom Dead Center

TABLE 6.4-V
Nacelle Dimensions for STF654 with Advanced Technology Nacelle

	Ideal Aero Contours	Revised Aero Contours
		Long Flap and Four Piece Pivot Blocker Door Reverser (+10.1 cm, +4.0 in. D_{MAX} and +0.2 cm, +0.1 in. at Turbine Elevation Clearance Pt.)
D_{FAN}	67.8 in. 172.212 cm.	67.8 in. 172.212 cm.
D_{MAX}	79.019 in. 200.708 cm.	83.10 in. 211.074 cm.
D_{HI}/D_{MAX}	0.839	0.79732
D_{TH}/D_{FAN}	0.9520	0.9520
L_{TH}/D_{FAN}	0.0313	0.0313
L_{MAX}/D_{MAX}	0.825	0.65102
L_{NAC}/D_{FAN}	2.039	2.045
L_{DUCT}/D_{FAN}	0.386	0.388
L_{IN}/D_{FAN}	0.291	0.291
L_{COWL}/D_{FAN}	1.223	1.224

TABLE 6.4-VI
Summary of Nacelle Performance Characteristics
STF654
Max. Cruise: 0.8MN/10.67 km (35,000 ft.) Altitude

	CURRENT TECHNOLOGY NACELLES		ADVANCED TECHNOLOGY NACELLES	
	IDEAL AERO. CONTOURS	REVISED AERO. CONTOURS	IDEAL AERO. CONTOURS	REVISED AERO. CONTOURS
Pressure Drag, N (lbs.)	123.2 (27.7)	161.9 (36.4)	98.3 (22.1)	148.5 (33.4)
Fan Cowl Friction, N (lbs.)	532.8 (119.8)	603.6 (135.7)	372.7 (83.8)	388.7 (87.4)
Afterbody and Pylon Friction, N (lbs.)	143.6 (32.3)	185.4 (41.7)	241.0 (54.2)	243.3 (54.7)
Afterbody Steps and Gaps, N (lbs.)	83.6 (18.8)	83.6 (18.8)	0.0 (0.0)	0.0 (0.0)
Total Drag, N (lbs.)	883.4 (198.6)	1,034.6 (232.6)	712.1 (160.1)	780.6 (175.5)
Nacelle Leakage (% Flow)	0.2	0.2	0.0	0.0
Primary Duct Loss (%$\Delta P_t/P_t$)	0.645	0.858	0.548	0.551
Fan Duct Loss (%$\Delta P_t/P_t$)	0.852	1.015	0.775	0.739
Inlet Recovery (P_t/P_t)	0.9975	0.9975	0.9982	0.9982
Primary C_v	0.9957	0.9957	0.9957	0.9957
Fan C_v	0.9952	0.9952	0.9951	0.9951

The weight and performance benefits associated with the finalized advanced technology nacelle contours, as compared to the current technology nacelles, are summarized in Table 6.4-VII. These preliminary results favor the long flap target reverser. As noted earlier, the STF653-DD nacelle contours are ideal aerodynamic shapes. Consequently, the performance benefit shown is slightly higher than that for the STF653. In reality, it would be on the order of the 1.7 percent shown for the STF653.

6.4.2 Engine Performance Definition

Once the nacelle geometry had been established, the performance characteristics of the propulsion system installations was determined for use in mission analyses by P&W and the Douglas Aircraft Company subcontractor. Table 6.4-VIII provides a summary of the propulsion systems and their performance as installed in current technology nacelles with cascade thrust reversers and advanced technology nacelles with long flap target thrust reversers/spoilers. The current technology nacelle for the STF654 is as modified to accommodate fan case mounted accessories. The table includes cycle variations, engine and nacelle dimensions, weights, installation losses, and performance at both maximum cruise and take-off power settings.

66

TABLE 6.4-VII
Weight and Performance Benefits of Advanced Technology Nacelles

TSFC Improvement Relative To
Current Technology Nacelle, %

ENGINE	CURRENT TECHNOLOGY NACELLES	ADVANCED TECHNOLOGY NACELLES		Weight Savings Relative to Current Technology Nacelle, kg (l s)	
		Rev. 1	Rev. 2	Rev. 1	Rev. 2
STF653	Base	1.7	1.6	306 (675)	215 (475)
STF654	Base	2.2	2.2	286 (630)	222 (490)
STF653-DD	Base	1.8⁽*⁾	-	299 (660)	213 (470)

Rev. 1   Long Flap Reverser

Rev. 2   Four Piece Pivot Blocker Door Reverser

(*)   With Ideal Aerodynamic Contours

The significant cycle variations between the selected engines, along with the dimensional and weight information, can be found for both current and advanced technology nacelle definitions. The advantages in the advanced technology nacelle drag and installation losses are also tabulated vs. the current technology definitions. The summary of the maximum cruise uninstalled and isolated pod thrust specific fuel consumption shows an advantage for the higher bypass ratio engines. Also, the advantage for advanced technology relative to current technology nacelle is increasing as bypass ratio increases.

The even-larger benefit for the STF654 small turbofan advanced technology nacelle includes the effects of relocation and scale-down of the accessories. The current technology installation has fan-case mounted accessories, which have been scaled down 10% and split between a core and pylon mount for the advanced technology nacelle. Takeoff thrust-to-weight ratio is improved with the advanced technology nacelles, primarily because of their smaller size and attendant weight savings. Installation drawings depicting these propulsion systems and their principal characteristics are shown in Figures 6.4-3 tnrough 6.4-9.

TABLE 6.4-VIII
Propulsion System Characteristics Summary

Nacelle Technology	STF631 Current	STF653DD Current	STF653DD Advanced	STF653 Current	STF653 Advanced	STF654 Current	STF654 Advanced
Cycle							
BPR	7.2	9.6	9.6	12.8	12.8	11.78	11.78
FPR	1.65	1.7	1.7	1.53	1.53	1.56	1.56
OPR	38.6	64	64	64	64	55	55
HPC Exit Corrected Flow	8.3	5.5	5.5	5.5	5.5	2.75	2.75
VJI/VJE	-	0.789	0.789	0.781	0.781	0.782	0.781
PTD/PTE	1.032	1.36	1.36	1.29	1.29	1.33	1.33
Configuration	AXIAL	AXIAL		AXIAL		AXI-CENT	
Staging	1-4-10-2-5	1-5-11-2-7		1-3-11-2-5		1-3-6+0-2-4	
Fan Tip Diameter cm (in)	215.84	238.2	238.2	271.2	271.2	172.2	172.2
	(84.98)	(93.8)	(93.8)	(106.8)	(106.8)	(67.6)	(67.6)
Max Nacelle Diameter cm (in)	257.50	297.4	269	338.5	311.1	226.3	198.8
	(101.38)	(117.1)	(106)	(133.3)	(122.5)	(89.1)	(78.3)
Engine Length cm (in)	331.7	385.0	385.0	366.2	366.2	232.1	232.1
	(130.6)	(151.6)	(151.6)	(144.2)	(144.2)	(91.4)	(91.4)
Nacelle Length cm (in)	680.2	633.4	555.7	594.1	505.5	448.5	351.2
	(267.8)	(249.4)	(218.8)	(233.9)	(199.05)	(176.6)	(138.3)
Engine Weight kg (lbs.)	3,549	3,517	3,517	4,222	4,222	1,839	1,839
	(7826)	(7755)	(7755)	(9310)	(9310)	(4055)	(4055)
Nacelle Weight kg (lbs.)	1,485	1,503	1,204	1,583	1,276	1,188	902
	(3274)	(3315)	(2655)	(3490)	(2815)	(2620)	(1990)
Total Propulsive System Weight kg (lbs.)	5,034	5,021	4,721	5,805	5,499	3,027	2,741
	(11100)	(11070)	(10410)	(12800)	(12125)	(6675)	(6045)
Performance *							
FN Uninstalled, N (lbs.)	41,230	50,536	50,718	53,756	53,849	22,418	22,512
	(9,269)	(11,361)	(11,402)	(12,085)	(12,106)	(5,040)	(5,061)
TSFC Uninstalled	0.5261	0.4764	0.4745	0.4441	0.4426	0.4698	0.468
FN Isolated, POD, N (lbs.)	39,762	48,285	49,179	51,309	52,266	21,386	21,756
	(8,939)	(10,855)	(11,056)	(11,535)	(11,750)	(4,808)	(4,891)
% TSFC Isolated POD	BASE .5455	-8.6	-10.4%	-14.7%	-16.4%	-9.1%	-11.3%
Installation Losses							
Inlet Recovery	0.9976	0.9976	0.9982	0.9975	0.9982	0.9975	0.9982
Nacelle Leakage % WAD	0.2	0.2	-	0.2 -	0.2	-	
ΔP/P Duct	0.0088	0.00918	0.00591	0.0058	0.00468	0.01015	0.00779
ΔP/P Duct Mixer	0.0018	-	-	-	-	-	-
ΔP/P Primary Mixer	0.0062	-	-	-	-	-	-
ΔP/P Tailpipe	0.0055	0.00636	0.00538	0.0048	0.00412	0.00858	0.00548
CV Duct	-	0.9937	0.9937	0.9953	0.9953	0.9952	0.9951
CV Primary	-	0.9959	0.9959	0.9957	0.9957	0.9957	0.9957
CV Mixed	0.9933**	-	-	-	-	-	-
Drag Afterbody & Pylon Friction, N (lbs.)	-	560.4	692.1	449.2	577.8	185.3	241.7
	-	(126)	(155.6)	(101)	(129.9)	(41.66)	(54.3)
Drag Afterbody Steps & Gaps, N (lbs.)	-	165.9	-	206.8	-	83.3	-
	-	(37.3)	-	(46.5)	-	(18.74)	-
Drag External Flow Effects, N (lbs.)	1,303.3	1,209.9	796.2	1,387.8	951.9	765.0	470.3
	(293)	(272)	(179)	(312)	(214)	(172.10)	(105.68)
Fan Cowl Friction, N (lbs.)	1,187.6	973.2	661.0	1,080.9	729.0	603.6	372.7
	(267)	(218.8)	(148.6)	(243)	(163.9)	(135.7)	(83.8)
Pressure Drag, N (lbs.)	115.6	237.9	135.2	306.4	223.2	162.0	98.2
	(26)	(53.5)	(30.4)	(68.9)	(50.2)	(36.43)	(22.08)
Total Drag, N (lbs.)	1,303.3	1,939.4	1,490.1	2,043.9	1,529.7	1,034.2	712.3
	(293)	(436)	(335)	(459.5)	(343.9)	(232.5)	(160.1)
Total Drag, FN Uninstalled, %	3.20%	3.80%	2.90%	3.80%	2.80%	4.60%	3.16%
Sea Level TakeOff							
MAX CET, °C (°F)	1,435	1,482	1,482	1,482	1,482	1,482	1,482
	(2616)	(2700)	(2700)	(2700)	(2700)	(2700)	(2700)
Static FN, Installed, N (lbs.)	176,122	223,940	224,896	223,806	255,460	106,254	106,743
	(39,594)	(50,344)	(50,559)	(50,314)	(57,430)	(23,887)	(23997)
Static FN, Inst./Iso. Pod Weight	3.57	4.55	4.86	4.48	4.74	4.58	3.97
FN, Isolated POD @ 0.2 MN, N (lbs.)	142,547	179,133	180,547	199,314	200,493	83,532	842,133
	(32,046)	(40271)	(40,589)	(44,808)	(45,073)	(18,779)	(18,932)

* 10.67 km (35,000 ft)/.80 Mn/Std. Day Max Cruise Rating, No Customer Bleed or Power Extraction
** Includes 82% Mixing
*** Fan Case Mounted Accessories; all others core-mounted.
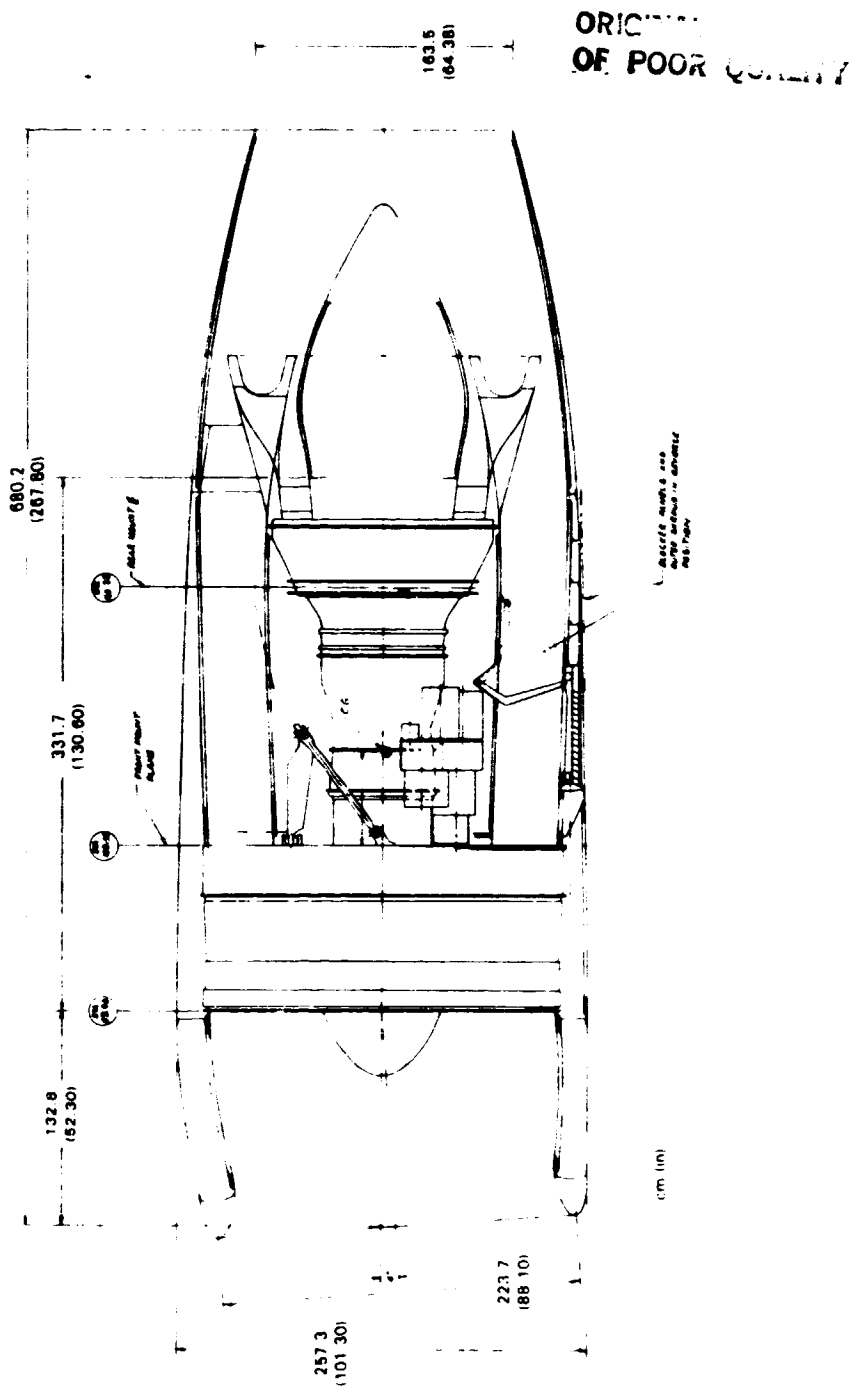
Figure 6.4-3   STF631 Reference Engine Installation Drawing

Figure 6.4-4   STF653-DD Installation with Current Technology Nacelle and Thrust Reverser
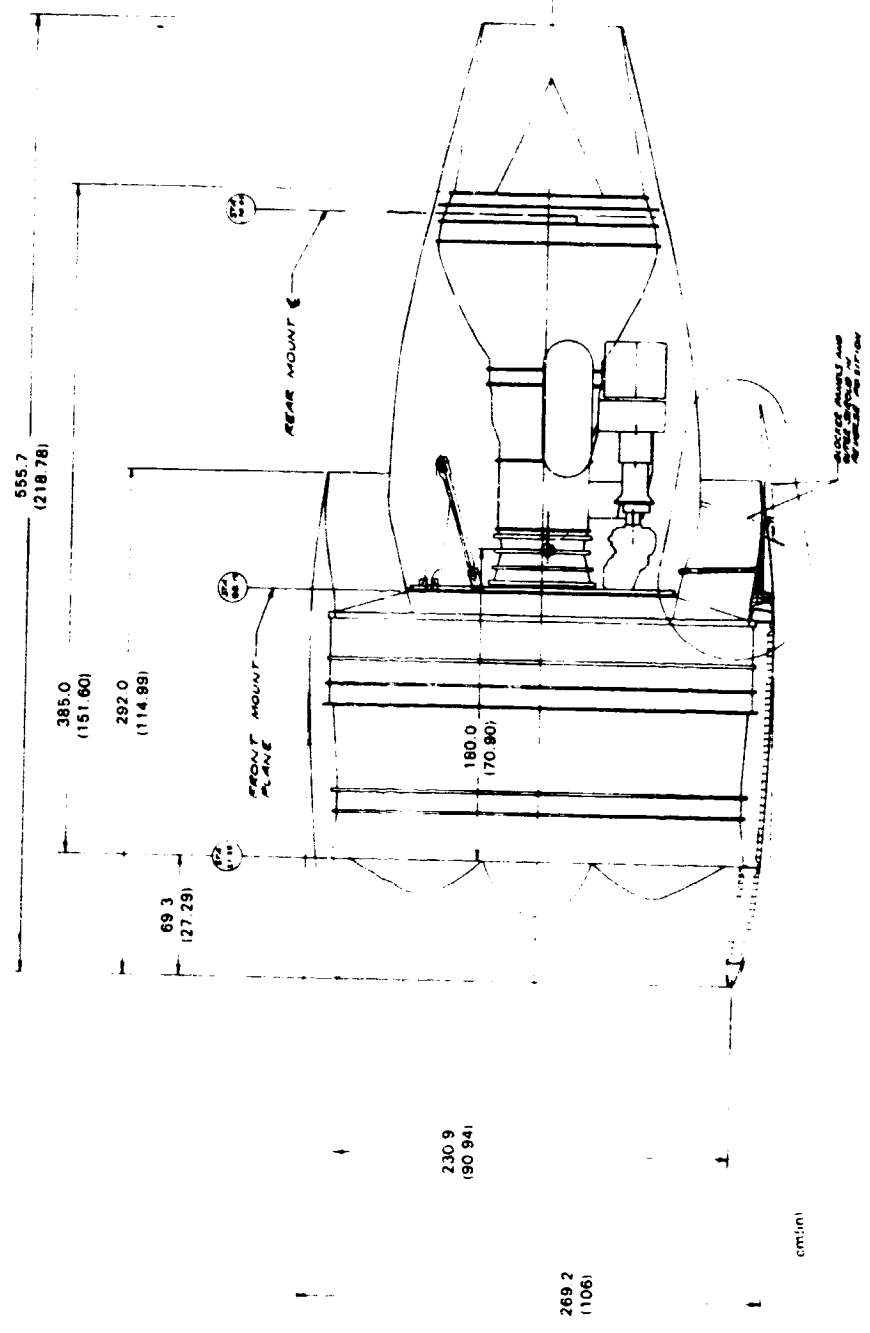
Figure 6.4-5   STF653-DD Installation with Advanced Technology Nacelle and Long Flap Target Thrust Reverser
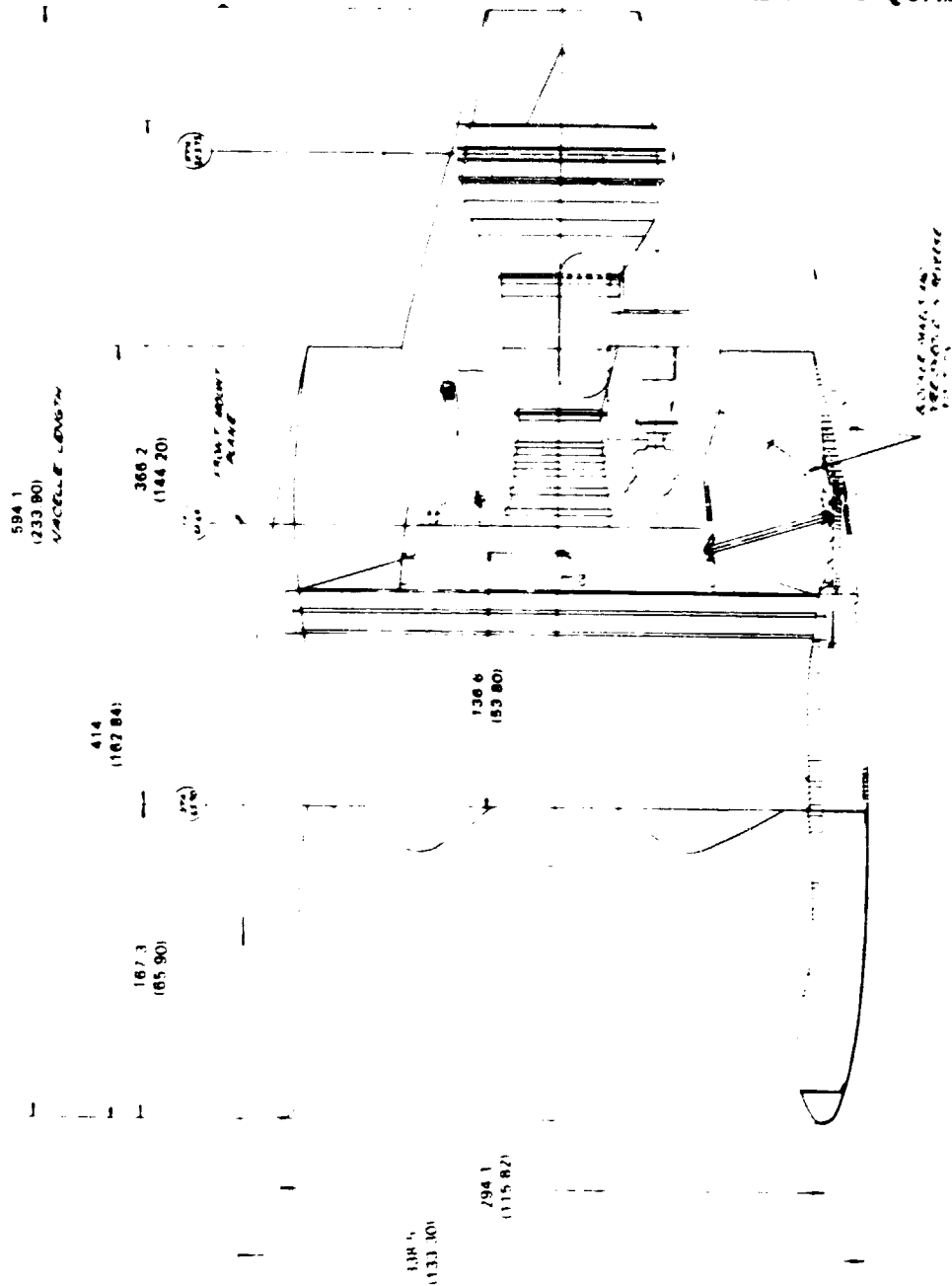
Figure 6.4-6   STF653 Installation with Current Technology Nacelle and Thrust
Reverser
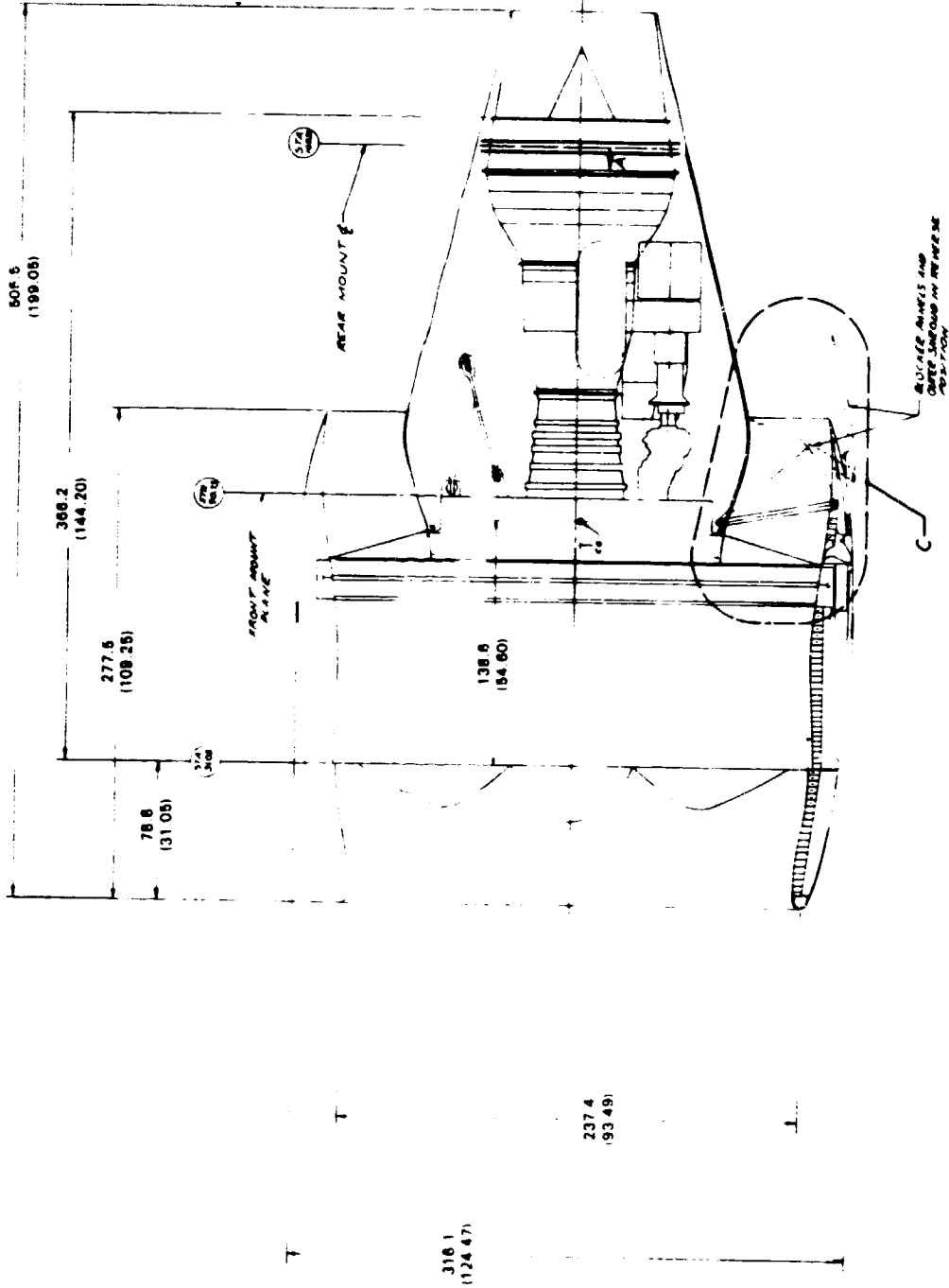
Figure 6.4-7   STF653 Installation with Advanced Technology Nacelle and Long
Flap Target Thrust Reverser
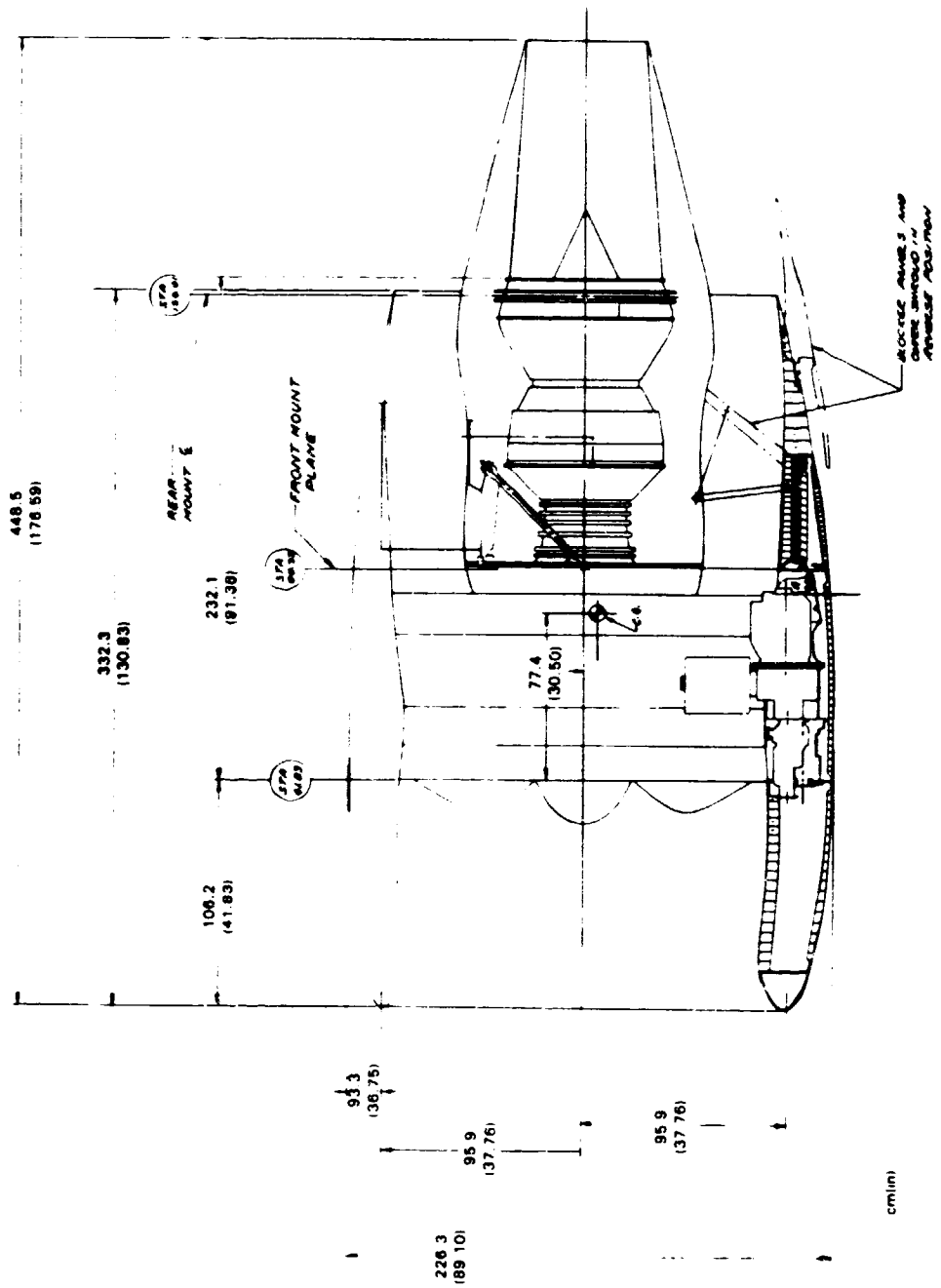
Figure 6.4-8   STF654 Installation with Current Technology Nacelle and Thrust Reverser

74
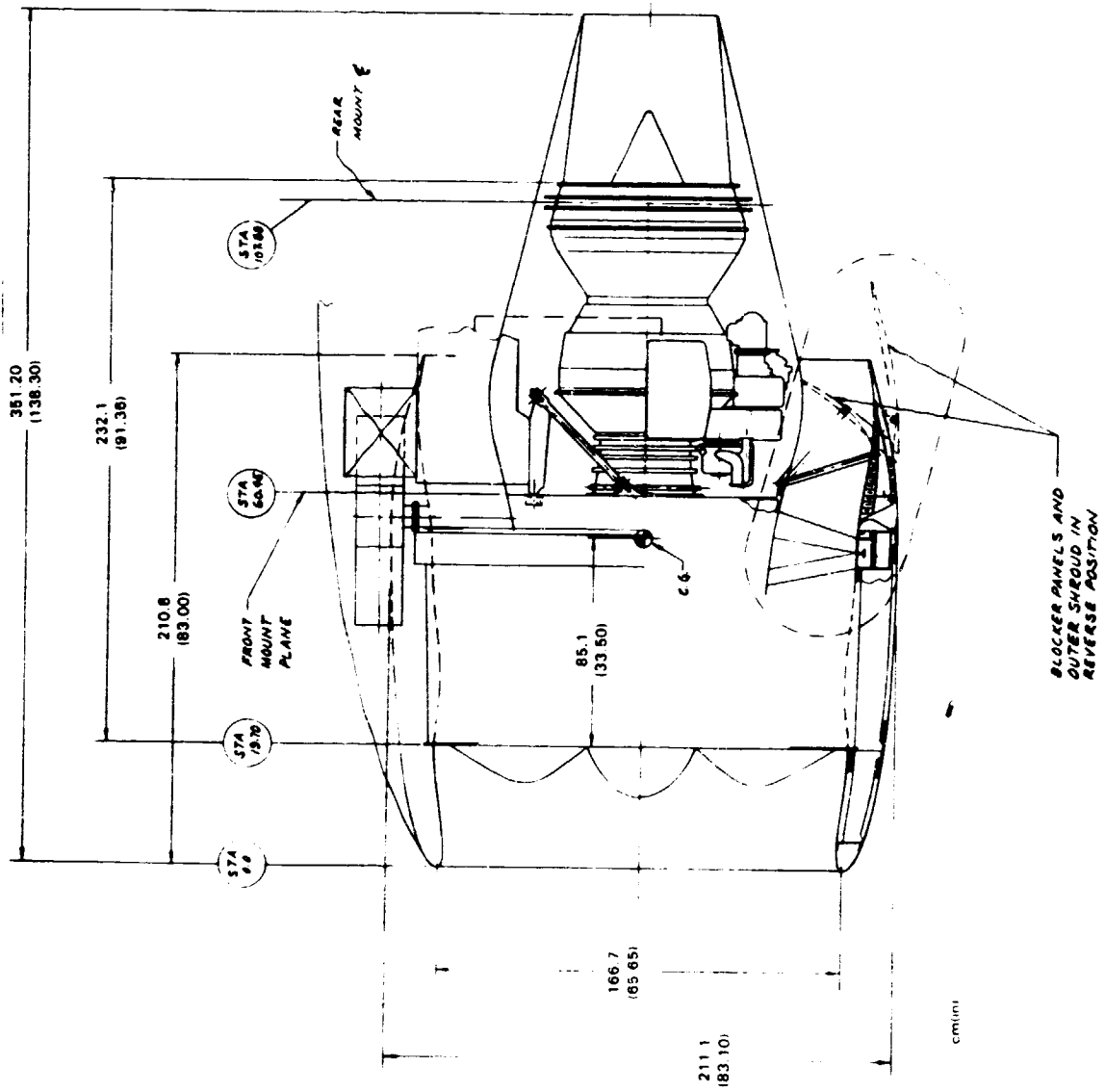
Figure 6.4-9   STF654 Installation with Advanced Technology Nacelle and Long
Flap Target Thrust Reverser

75

6.5 PRELIMINARY NOISE ASSESSMENT

Preliminary noise estimates for the configurations described in section 6.4 were conducted in order to assess the ability of these installations to comply with FAR Part 36 Stage 3 noise limits. Noise limit compliance was a concern because of the small length-to-diameter ratio of the advanced technology nacelles relative to current technology nacelles and the reduction in surface area available for sound absorbing materials.

Airplane and flight profile assumptions used for the noise assessment are shown in Table 6.5-I. These take off, gross weight, and flight profile data are based on early study results; they are, therefore, somewhat conservative relative to the final airplane definitions discussed in section 7.0.

TABLE 6.5-I
Preliminary Noise Assessment
Airplane and Flight Profile Assumptions

Engine	STF653 Geared (scaled)	STF654 Geared (scaled)	STF653 Direct Drive (scaled)
Thrust Size, N (lbs.)	225,448 (50,683)	98,839 (22,220)	225,448 (50,683)
No. of Engines	3	2	3
Takeoff Gross Wgt., kg (lbs.)	306,445 (675,600)	59,284 (130,700)	306,445 (675,600)
Takeoff Altitude, m (ft.)	297 (976)	764 (2507)	297 (976)
Cutback Takeoff Alt., m (ft.)	272 (893)	722 (2369)	272 (893)
Cutback -- Percent Thrust	, '	69	71
Approach -- Percent Thrust	31	30	31

Hardwall (untreated) nacelle noise levels were estimated for both the twinjet and the trijet at the three FAA noise certification test conditions: takeoff, cutback, and approach. Noise levels for nacelles with sound absorbing treatment installed were estimated only for the study trijet powered by the STF653 geared engine. Treated nacelles on the twinjet would be expected to provide noise attenuations of about the same magnitude of those predicted for the trijet. The same applies to the STF653 direct drive powered trijet. Estimated noise levels are summarized in Table 6.5-II. Although there are uncertainties associated with the noise estimates because of the need to extrapolate from current data bases to predict noise for geared fan engines, it appears feasible for advanced nacelle installations to comply with Stage 3 noise limits.

TABLE 6.5-II
Preliminary Noise Assessment: Noise Estimates (EPNdB)

| Engine | STF653 (geared) | | STF654 (geared) | STF653 (direct drive) |
	Hardwall	Treated	Hardwall	Hardwall
Takeoff Noise	104.2	101.9	89.4	107.5
FAR Part 36	102.7	102.7	90.2	102.7
Δ REL. Rule	+1.5	-0.8	-0.8	+4.8
Cutback Takeoff Noise	101.6	99.5	86.0	107.3
FAR Part 36	102.7	102.7	90.2	102.7
Δ REL. Rule	-1.1	-3.2	-4.2	+4.6
Sideline Noise	96.1	94.1	87.1	99.7
FAR Part 36	102.0	102.0	95.9	102.0
Δ REL. Rule	-5.9	-7.9	-8.8	-2.3
Approach Noise	104.5	102.6	98.6	106.2
FAR Part 36	105.0	105.0	99.8	105.0
Δ REL. Rule	-0.5	-2.4	-1.2	+1.2

Noise levels were obtained by separately estimating noise levels for each engine component (noise source) and combining them through the use of analytical codes. The relative importance of the different noise sources and the benefit of sound absorbing treatment is illustrated for the trijet at takeoff and approach conditions in Figures 6.5-1 and 6.5-2. Note that the total noise is influenced predominantly by the fan at both operating conditions; any further benefits from treatment and/or reductions in fan source noise would lower the total noise.
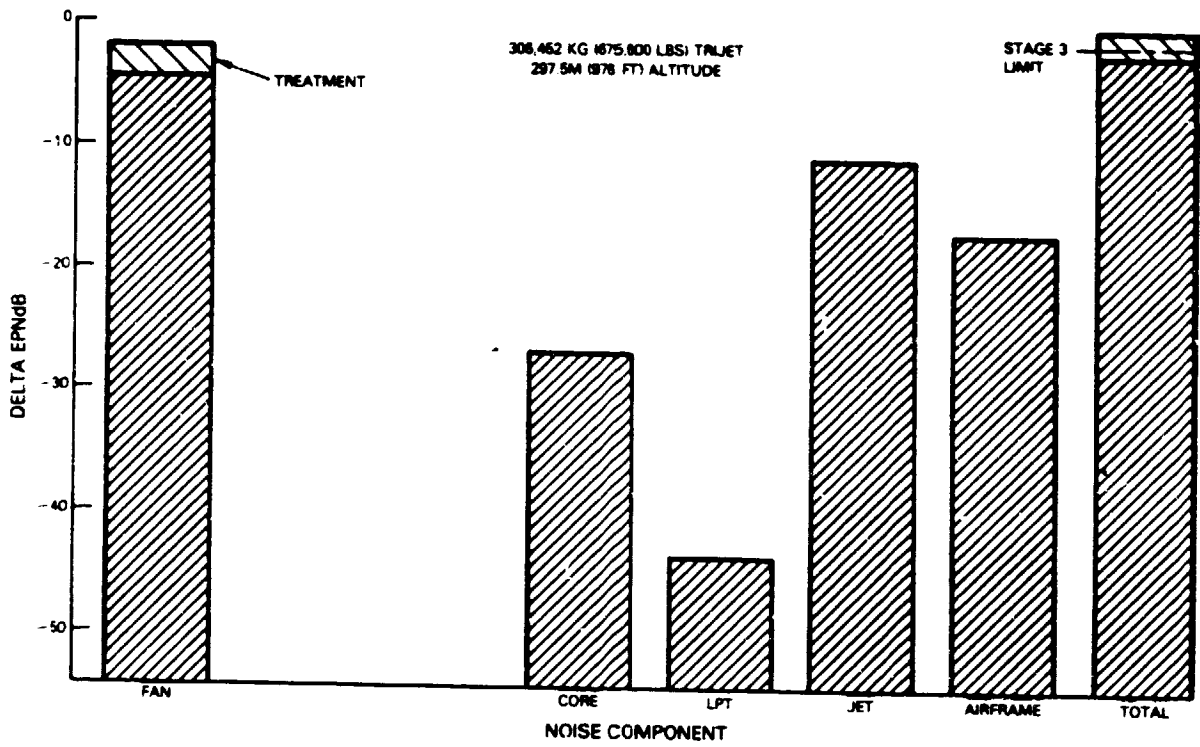
Figure 6.5-1   STF653 Geared Fan: Relative Levels of Noise Components at Takeoff Conditions
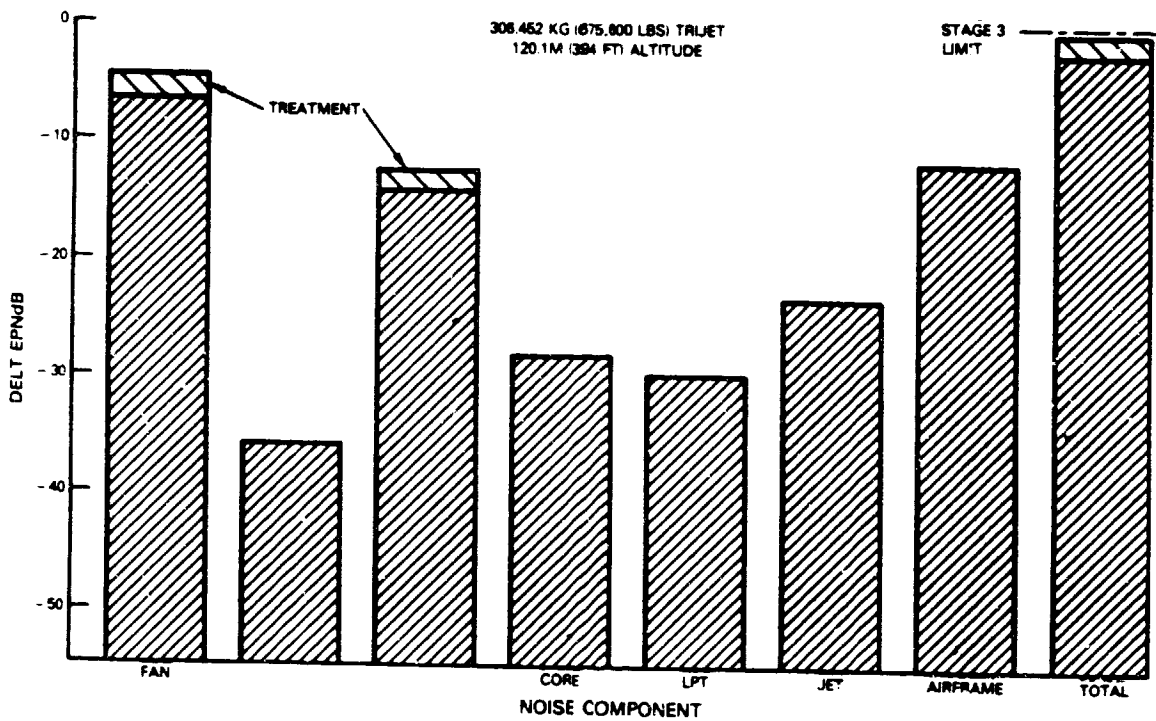
Figure 6.5-2   STF653 Geared Fan: Relative Levels of Noise Components at Approach Conditions

78

7.0 PROPULSION SYSTEM AIRCRAFT INTEGRATION

The specific engine and nacelle combinations described in Section 6 were evaluated in airplanes by both Pratt & Whitney and Douglas. This Section will describe the Pratt & Whitney evaluation and summarize the Douglas Company results. The complete Douglas final report is in Appendix A.

The Propulsion System Aircraft Integration evaluation consisted of evaluating the airplane performance and economics of the engine and nacelle combinations developed during Nacelle Preliminary Design. Airplanes and evaluation ground rules used are described in Section 3. Figures of merit for this evaluation were mission fuel burn and direct operation cost.

7.1 METHOD OF EVALUATION

This task used a more detailed evaluation procedure compared to the configuration selection Task (Section 4). In the first Task (performed by Pratt & Whitney only), configuration selection was based on a trade factor evaluation of weight, cost, drag and cruise TSFC trends over a wide range of bypass ratio, engine types and nacelle types. In this Task, a detailed airplane mission analysis was performed for each engine/nacelle combination. The analysis was based on specific weight, cost, drag estimates, and a mission matrix of thrust and TSFC. The ME^4 (STF631) served as baseline in all three Pratt & Whitney airplanes. STF653 geared and direct drive engines were evaluated with current and advanced nacelles in the long range trijet and medium range large twinjet airplanes. The STF654 was evaluated with current and advanced nacelles in the small twinjet only, since its thrust size was not adequate for the larger airplanes.

Propulsion System Aircraft Integration evaluations done by Pratt & Whitney used isolated pod performance. Aerodynamic interactions between the airplane and engine (interference drag, etc.) were not considered. However, Douglas included an interference drag penalty of 3% of airplane drag for all cases.

Douglas evaluated the STF653 and STF653DD relative to the STF631 in a long range trijet aircraft, Model D967C-209. This airplane incorporated a number of advanced technologies, including a high aspect ratio, supercritical wing, an advanced tail, longitudinal stability augmentation, and advanced structures. Wing size and thrust loading were optimized for minimum fuel burn, and the airplane was resized to to keep constant payload/range for each engine. Details on the airplane may be found in Appendix A.

7.2 RESULTS AND CONCLUSIONS

All of the TARGET engines (the geared STF653, the directly driven STF653, and the STF654) showed large fuel burn and DOC + I advantages over the ME^4 baseline engine in the Pratt & Whitney evaluation, as summarized in Figures 7.2-1 and 7.2-2. Including the benefits of advanced nacelles, typical mission fuel burn savings ranged from 18% on the small twin to 23% on the large twin for the geared engines. DOC + I savings ranged from 9 to 13% at a $0.40 per liter ($1.50/gal.) fuel price.
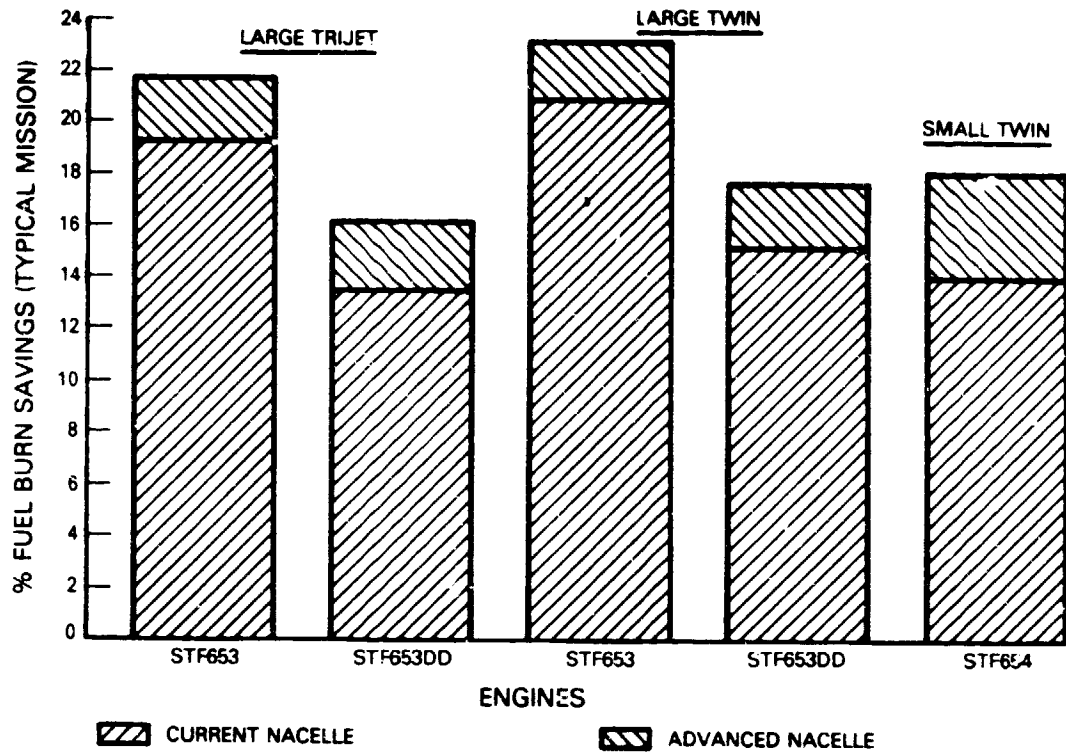
Figure 7.2-1   Fuel Burn Savings Relative to ME^4 Base
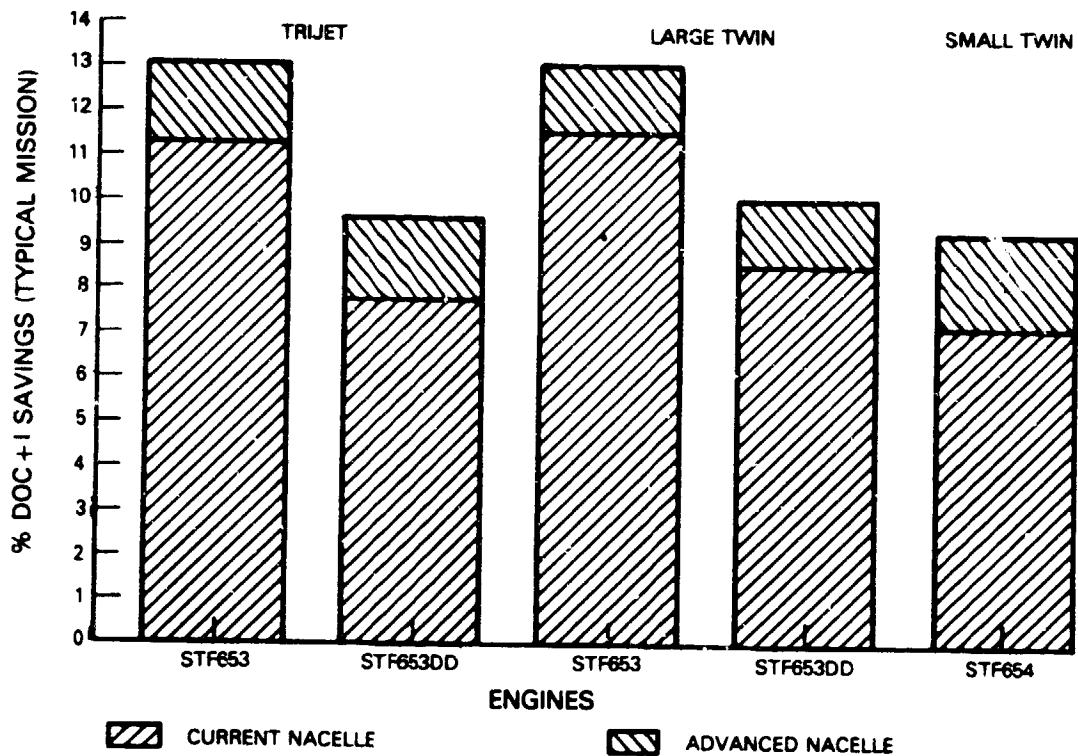
Figure 7.2-2   DOC+I savings rel. to ME^4 base

Douglas results were similar to the Pratt & Whitney large trijet results, as shown in Figure 7.2-3. The STF653 with advanced nacelle had a 22% fuel b rn advantage over the STF631, while the STF653DD showed a 16% advantage. Douglas did not evaluate operating costs.
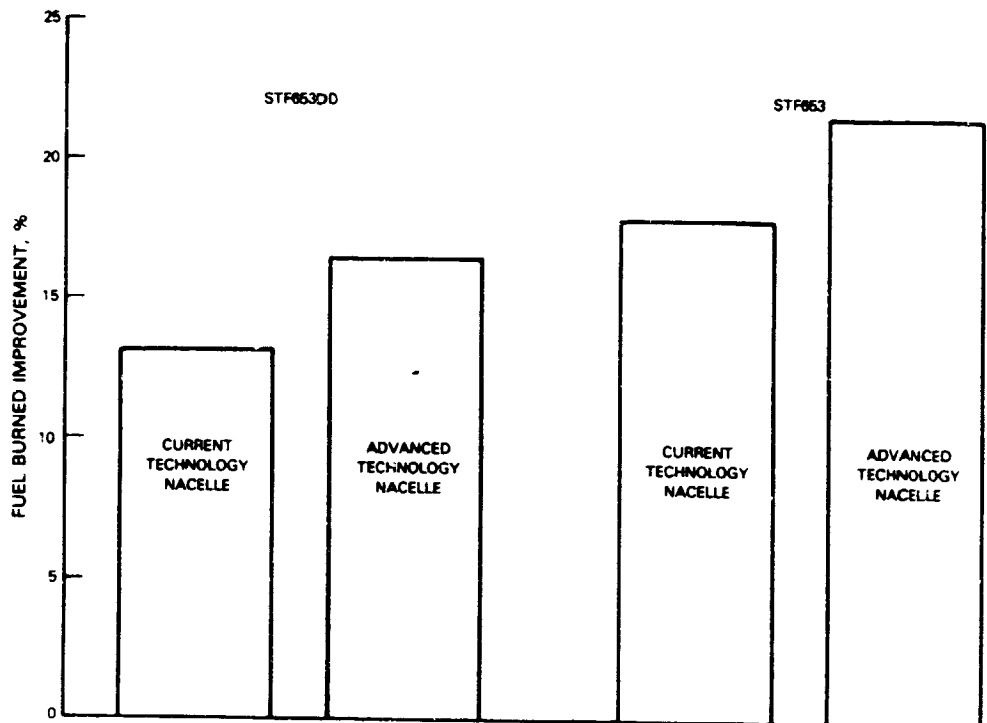
Figure 7.2-3   Improvements from Advanced Propulsion Systems Relative to ME^4 Base (Douglas Results)

Considering only the advanced engines, Figures 7.2-4 and 7.2-5 show the advantages of advanced nacelles relative to current configurations. Advanced nacelles on both STF653 engines offer fuel burn advantages of about 3% regardless of airplane. The STF654 shows more savings with an advanced nacelle: almost 5% in fuel burn. This increased advantage results from accessory location. On the large STF653 engines, accessories are core-mounted for both current and advanced nacelles, allowing both to have a fairly slim nacelle. The STF654 engine with the current technology nacelle features fan-case mounted accessories, however, which the fan cowl must clear. The STF654 engine with the advanced nacelle has core-mounted accessories. Since the fan cowl does not encompass the accessories, nacelle weight and drag are reduced. Thus, the efficiency of the advanced nacelle combines with the advantageous accessory location to result in greater savings relative to the STF653 configurations.
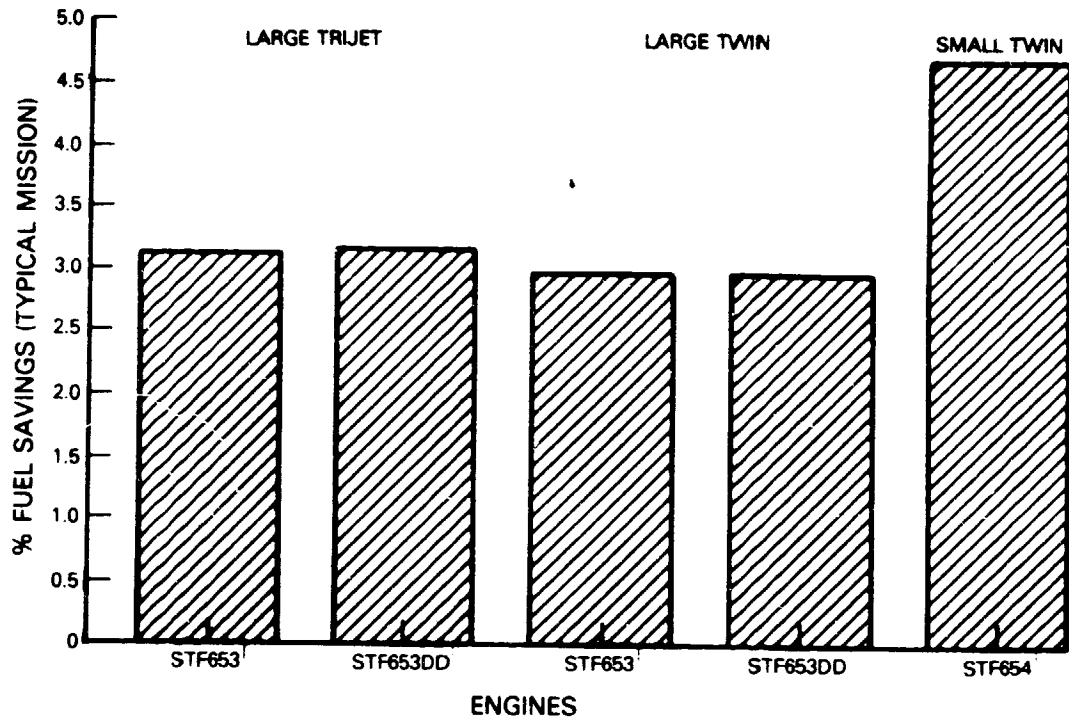
Figure 7.2-4   Advanced Nacelle Fuel Burn Advantage
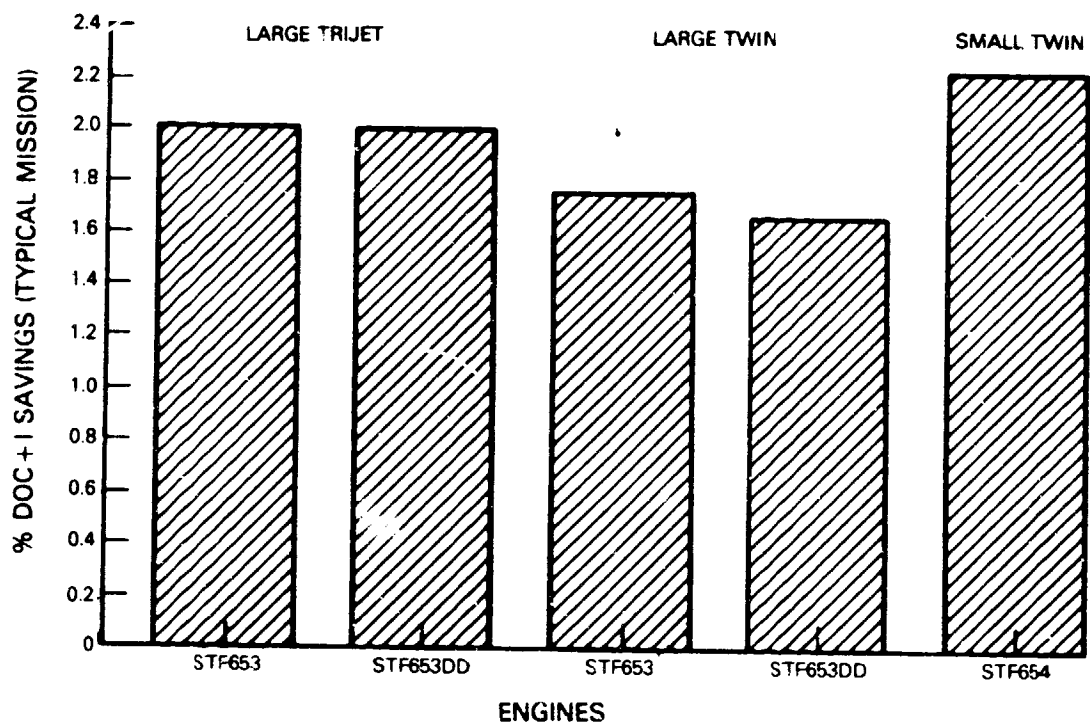
Figure 7.2-5   Advanced Nacelle DOC+I Advantage

82

Fuel burn advantages of 3 to 4% for advanced over current nacelles were also shown by Douglas. Figure 7.2-6 is a breakdown of this advantage. The bottom three items -- reverser/nozzle, cowl and pylon drag, and weight -- correspond to the isolated pod performance considered in Pratt & Whitney's evaluation. Interference drag and environmental control system effects were not considered by Pratt & Whitney. The Douglas breakdown shows that these factors may have significant impact on fuel burn. No assessment was made, however, of whether these factors would have different effects on current nacelles as compared to advanced nacelles.
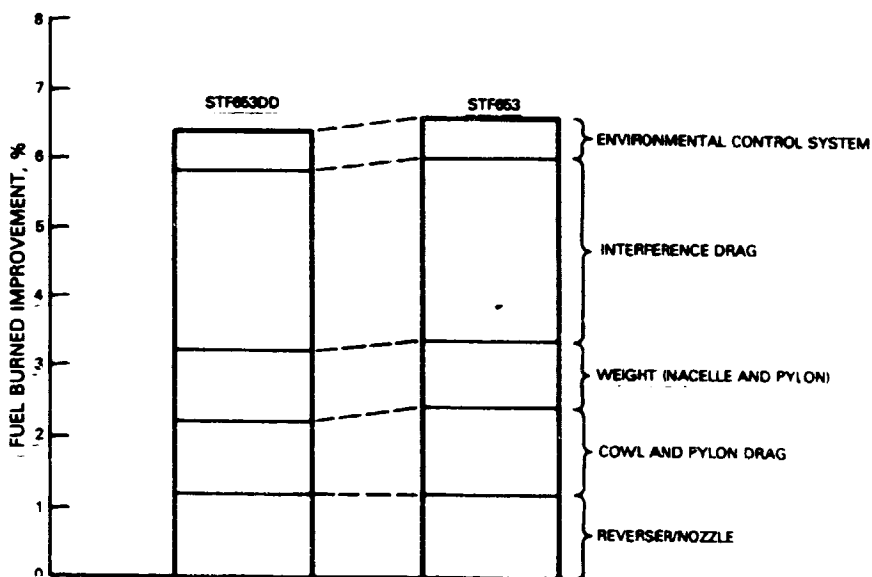
Figure 7.2-6   Installation Integration Technology Perspective Relative to Current Technology (Douglas Results)

DOC + interest evaluations show the same trend discussed above, though to a lesser degree. The economics of the small twin are somewhat less sensitive to fuel burn than those of the longer range airplanes. Fuel makes up a smaller portion of the small twin operating costs, as can be seen from Figure 7.2-7, which shows a comparison of the DOC + I breakdowns of all these airplanes with advanced nacelle, geared engines.
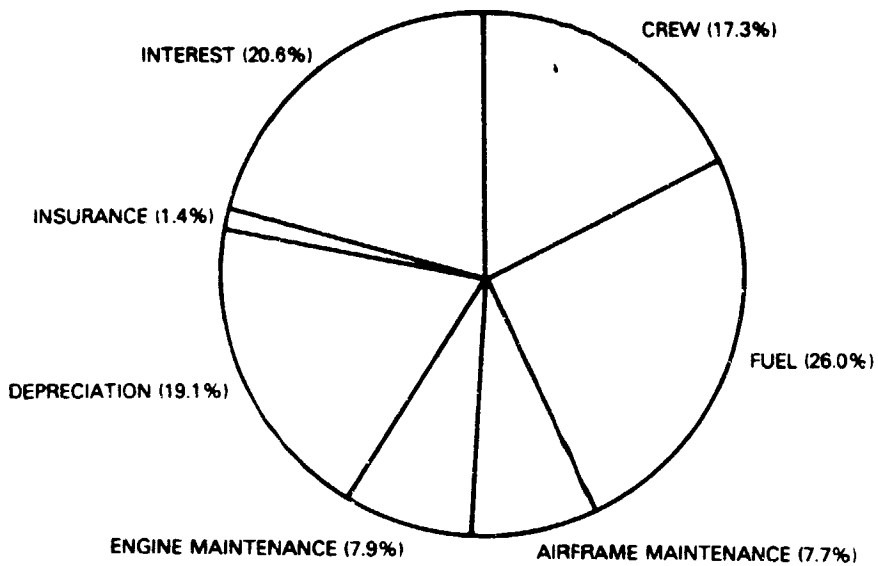
Figure 7.2-7A   DOC+I Breakdown, 150 Pax Twin @ 400 NM, $0.40/1 ($1.50/gal.) Fuel
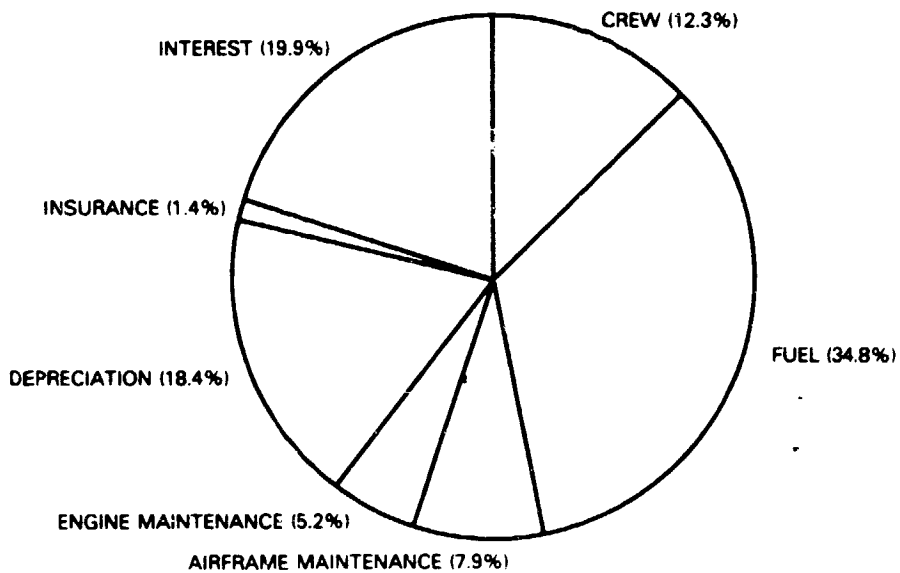
Figure 7.2-7B   DOC+I Breakdown: 350 Pax Twinjet @ 1000 NM, $0.40/1 ($1.50/gal.) Fuel

INTEREST (16.7%)

CREW (15.4%)

INSURANCE (1.2%)

DEPRECIATION (15.4%)

ENGINE MAINTENANCE (5.1%)

AIRFRAME MAINTENANCE (7.2%)

FUEL (39.0%)
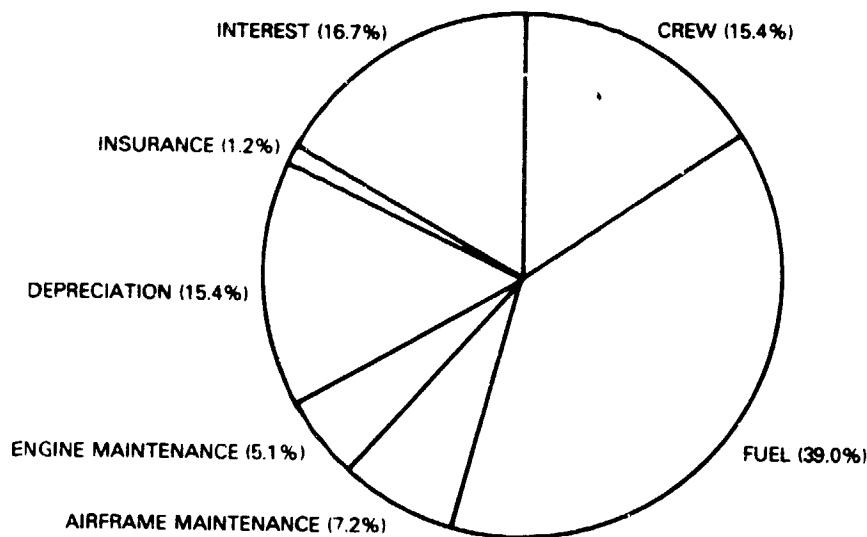
Figure 7.2-7C   DOC+I   Breakdown: 440   Pax   Trijet   @   2000   NM, $0.40/1
($1.50/gal.) Fuel

Mission analysis results are detailed in Tables 7.2-I, 7.2-II, and 7.2-III.
Engine and nacelle weights are shown in base thrust size and in the size
required by the airplane (scaled). Since this was a "rubber" airplane evalua-
tion -- i.e., the airplane was resized to produce the same payload/range for
each engine -- the thrust required to fly the airplane varies from engine to
engine. Thrust size is quoted in terms of sea level static, standard plus
25°F, installed take-off rating. Quoting thrust size at take-off when some of
the engine/airplane combinations are sized by cruise causes the reference
engine (ME^4) to appear to be a relatively smaller engine than it is (see
small twin scaled thrust sizes). This is caused by its having a higher cruise
to take-off thrust ratio than the higher bypass ratio STF653 and 654 engines.
Rating differences also contribute to the thrust ratio difference.
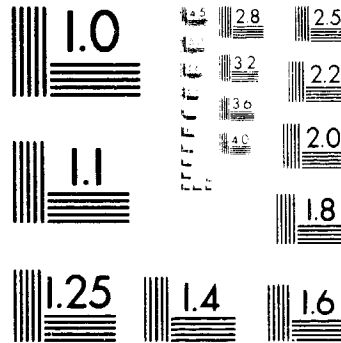
MICROCOPY RESOLUTION TEST CHART
NATIONAL BUREAU OF STANDARDS
STANDARD REFERENCE MATERIAL 1010a
(ANSI and ISO TEST CHART No. 2)

TABLE 7.2-I

Mission Analysis Results for the Small Twin-Engined Aircraft (PW)

Engine	ME4 Direct	STF654 Geared	STF654 Geared
Nacelle	Current	Current	Advanced
Base Thrust Size, N (lbs)	131,640 (29,594)	106,654 (23,977)	106,654 (23,977)
Base Engine Weight, kg (lbs)	3,549 (7826)	1,839 (4055)	1,839 (4055)
Base Nacelle Weight, kg (lbs)	1,485 (3274)	1,188 (2620)	902 (1990)
Engine Scale Factor	0.528	0.987	0.942
Scaled Thrust Size, N (lbs)	92,994 (20,906)	105,266 (23,665)	10,244 (22,586)
Scaled Engine Weight, kg (lbs)	1,781 (3928)	1,818 (4010)	1,745 (3849)
Scaled Nacelle Weight, kg (lbs)	731 (1612)	1,172 (2584)	845 (1864)
Scaled Propulsion System Cost, %	Base	-18	-24
Scaled Propulsion System Maintenance Cost, %	Base	-18	-19
MTOGW, kg (lbs)	57,895 (127,639)	58,073 (128,030)	56,493 (124,548)
OEW, kg (lbs)	33,645 (74,176)	34,967 (77,090)	33,874 (74,680)
ICAC, m (ft)	12,073 (39,611)	11,968 (39268)	11,970 (39,274)
TOFL @ MTOGW, m (ft)	1,819 (5969)	1,618 (5311)	1,637 (5371)
Design Range, NM	1800	1800	1800
Cruise Altitude, km (1000 ft)	10.7/11.9 (35/39)	10.7/11.9 (35/39)	10.7/11.9 (35/39)
Mach Number	0.78	0.78	0.78
Fuel Burn, kg (lbs)	7,851 (17,310)	7,003 (15,441)	6,655 (14,672)
delta % Fuel Burn	BASE	-10.8	-15.2
TYPICAL MISSION			
Range, NM	400	400	400
Cruise Altitude, m (ft)	11,887 (39,000)	11,887 (39,000)	11,887 (39,000)
Fuel Burn, kg (lbs)	2,096 (4622)	1,802 (3973)	1,717 (3787)
delta % Fuel Burn	BASE	-14.0	-18.1
ECONOMICS			
Range, NM	400	400	400
Fuel Price, $/1 ($/gal.)	0.26 (1.00)	0.26 (1.00)	0.26 (1.00)
DOC, cents/seat st. mi.	3.676	3.414	3.345
Delta DOC, %	BASE	-7.1	-9.0
DOC+I, cents/seat st. mi.	4.708	4.406	4.318
Delta DOC+I, %	BASE	-6.4	-8.3
Fuel Price, $/1 ($/gal.)	0.40 (1.50)	0.40 (1.50)	0.40 (1.50)
DOC, cents/seat st. mi.	4.175	3.843	3.754
Delta DOC, %	BASE	-8.0	-10.1
DOC+I, cents/seat st. mi.	5.208	4.835	4.727
Delta DOC+I, %	BASE	-7.2	-9.2
Fuel Price, $/1 ($/gal.)	0.53 (2.00)	0.53 (2.00)	0.53 (2.00)
DOC, cents/seat st. mi.	4.674	4.273	4.163
Delta DOC, %	BASE	-8.6	-10.9
DOC+I, cents/seat st. mi.	5.707	5.265	5.136
Delta DOC+I, %	BASE	-7.7	-10.0

TABLE 7.2-II

Mission Analysis Results for the Large Twin-Engined Aircraft (PW)

Engine	ME4 Direct	STF653 Geared	STF653 Geared	STF653 Direct	STF653 Direct
Nacelle	Current	Current	Advanced	Current	Advanced
Base Thrust Size, N (lbs)	176,122 (39,594)	254,944 (57,314)	255,460 (57,430)	223,940 (50,344)	224,896 (50,559)
Base Engine Weight, kg (lbs)	3,549 (7,826)	4,222 (9,310)	4,222 (9,310)	3,517 (7,755)	3,517 (7,755)
Base Nacelle Weight, kg (lbs)	1,485 (3,274)	1,583 (3,490)	1,276 (2,815)	1,503 (3,315)	1,204 (2,655)
Engine Scale Factor	1.459	0.965	0.937	1.0375	1.0149
Scaled Thrust Size, N (lbs)	256,963 (57,768)	246,021 (55,308)	239,366 (53,812)	232,338 (52,232)	228,246 (51,312)
Scaled Engine Weight, kg (lbs)	5,377 (11,855)	4,093 (9,024)	3,987 (8,792)	3,638 (8,022)	3,566 (7,862)
Scaled Nacelle Weight, kg (lbs)	2,247 (4,954)	1,522 (3,357)	1,188 (2,621)	1,565 (3,451)	1,224 (2,699)
Scaled Propulsion System Cost, %	Base	-23	-29	-17	-22
Scaled Propulsion System Maintenance Cost, %	Base	-13	-14	-9	-10
MTOGW, kg (lbs)	191,467 (422,115)	174,589 (384,907)	171,764 (378,677)	177,045 (390,321)	174,428 (384,550)
OEW, kg (lbs)	108,637 (239,506)	101,481 (223,729)	99,961 (220,378)	101,073 (222,829)	99,837 (220,105)
ICAC, m (ft)	11,918 (39,103)	11,447 (37,556)	11,448 (37,562)	11,478 (37,659)	11,513 (37,773)
TOFL @ MTOGW, m (ft)	2,438 (8,000)	2,300 (7,546)	2,321 (7,615)	2,438 (8,000)	2,438 (8,000)
Design Range, NM	4000	4000	4000	4000	4000
Cruise Altitude, km (1000 ft)	10.7/11.9 (35/39)	10.7/11.9 (35/39)	10.7/11.9 (35/39)	10.7/11.9 (35/39)	10.7/11.9 (35/39)
Mach Number	0.8	0.8	0.8	0.8	0.8
Fuel Burn, kg (lbs)	43,099 (95,019)	34,850 (76,832)	33,738 (74,381)	37,325 (82,288)	36,148 (79,695)
Delta % Fuel Burn	BASE	-19.1	-21.7	-13.4	-16.1
TYPICAL MISSION					
Range, NM	1000	1000	1000	1000	1000
Cruise Altitude, m (ft)	11,887 (39,000)	11,887 (39,000)	11,887 (39,000)	11,887 (39,000)	11,887 (39,000)
Fuel Burn, kg (lbs)	11,139 (24,558)	8,821 (19,449)	8,560 (18,873)	9,449 (20,833)	9,169 (20,215)
Delta % Fuel Burn	BASE	-20.8	-23.1	-15.2	-17.7
ECONOMICS					
Range, NM	1000	1000	1000	1000	1000
Fuel Price, $/l ($/gal.)	0.26 (1.00)	0.26 (1.00)	0.26 (1.00)	0.26 (1.00)	0.26 (1.00)
DOC, cents/seat st. mi.	2.368	2.102	2.067	2.171	2.138
Delta DOC, %	BASE	-11.2	-12.7	-8.3	-9.7
DOC+I, cents/seat st. mi.	3.017	2.712	2.668	2.790	2.749
Delta DOC+I, %	BASE	-10.1	-11.6	-7.5	-8.9
Fuel Price, $/l ($/gal.)	0.40 (1.50)	0.40 (1.50)	0.40 (1.50)	0.40 (1.50)	0.40 (1.50)
DOC, cents/seat st. mi.	2.823	2.462	2.417	2.557	2.512
Delta DOC, %	BASE	-12.8	-14.4	-9.4	-11.0
DOC+I, cents/seat st. mi.	3.472	3.072	3.018	3.176	3.123
Delta DOC+I, %	BASE	-11.5	-13.1	-8.5	-10.1
Fuel Price, $/l ($/gal.)	0.53 (2.00)	0.53 (2.00)	0.53 (2.00)	0.53 (2.00)	0.53 (2.00)
DOC, cents/seat st. mi.	3.278	2.823	2.767	2.943	2.887
Delta DOC, %	BASE	-13.9	-15.6	-10.2	-11.9
DOC+I, cents/seat st. mi.	3.927	3.432	3.367	3.561	3.497
Delta DOC+I, %	BASE	-12.6	-14.3	-9.3	-10.9

TABLE 7.2-III

Mission Analysis Results for the Large Trijet Aircraft (PW)

Engine	ME4 Direct	STF653 Geared	STF653 Geared	STF653 Direct	STF653 Direct
Nacelle	Current	Current	Advanced	Current	Advanced
Base Thrust Size, N (lbs)	176,122 (39,594)	254,944 (57,314)	255,460 (57,430)	223,940 (50,344)	224,896 (50,559)
Base Engine Weight, kg (lbs)	3,549 (7,826)	4,222 (9,310)	4,222 (9,310)	3,517 (7,755)	3,517 (7,755)
Base Nacelle Weight, kg (lbs)	1,485 (3,274)	1,583 (3,490)	1,276 (2,815)	1,503 (3,315)	1,204 (2,655)
Engine Scale Factor	1.165	0.822	0.795	0.895	0.866
Scaled Thrust Size, N (lbs)	205,182 (46,127)	209,563 (47,112)	203,091 (45,657)	200,426 (45,058)	194,759 (43,784)
Scaled Engine Weight, kg (lbs)	4,198 (9,257)	3,556 (7,840)	3,453 (7,614)	3,180 (7,012)	3,083 (6,799)
Scaled Nacelle Weight, kg (lbs)	1,755 (3,871)	1,277 (2,816)	993 (2,190)	1,332 (2,937)	1,027 (2,266)
Scaled Propulsion System Cost, %	Base	-21	-27	-15	-20
Scaled Propulsion System Maintenance Cost, %	Base	-11	-13	-7	-9
MTOGW, kg (lbs)	294,835 (650,004)	265 (585,198)	260,034 (573,282)	272,057 (599,788)	266,579 (587,711)
OEW, kg (lbs)	148,792 (328,034)	139,799 (308,206)	137,355 (302,819)	140,006 (308,663)	137,741 (303,669)
ICAC, m (ft)	10,342 (33,932)	10,187 (33,423)	15,165 (33,435)	15,253 (33,628)	10,249 (33,628)
TOFL @ MTOGW, m (ft)	2,964 (9,727)	2,472 (8,111)	2,492 (8,176)	2,608 (8,557)	2,625 (8,615)
Design Range, NM	6000	6000	6000	6000	6000
Cruise Altitude, km (1000 ft)	9.4/10.7/11.9 ------------------------------- (31/35/39) -------------------------------				
Mach Number	0.8	0.8	0.8	0.8	0.8
Fuel Burn, kg (lbs)	90,764 (200,102)	72,962 (160,855)	70,409 (155,227)	78,626 (173,343)	75,859 (167,243)
Delta % Fuel Burn	BASE	-19.6	-22.4	-13.4	-16.4
TYPICAL MISSION					
Range, NM	2000	2000	2000	2000	2000
Cruise Altitude, km (1000 ft)	11.9 (39)	11.9 (39)	10.7/11.9 (35/39)	11.9 (39)	10.7/11.9 (35/39)
Fuel Burn, kg (lbs)	27,854 (61,409)	22,498 (49,601)	21,794 (48,048)	24,113 (53,162)	23,350 (51,479)
Delta % Fuel Burn	BASE	-19.2	-21.8	-13.4	-16.2
ECONOMICS					
Range, NM	2000	2000	2000	2000	2000
Fuel Price, $/l ($/gal.)	0.26 (1.00)	0.26 (1.00)	0.26 (1.00)	0.26 (1.00)	0.26 (1.00)
DOC, cents/seat st. mi.	2.190	1.954	1.917	2.028	1.990
Delta DOC, $	BASE	-10.8	-12.5	-7.4	-9.1
DOC+I, cents/seat st. mi.	2.684	2.416	2.372	2.501	2.456
Delta DOC+I, %	BASE	-10.0	-11.6	-6.8	-8.5
Fuel Price, $/l ($/gal.)	0.40 (1.50)	0.40 (1.50)	0.40 (1.50)	0.40 (1.50)	0.40 (1.50)
DOC, cents/seat st. mi.	2.642	2.319	2.271	2.420	2.369
Delta DOC, %	BASE	-12.2	-14.0	-8.4	-10.3
DOC+I, cents/seat st. mi.	3.136	2.782	2.726	2.893	2.835
Delta DOC+I, %	BASE	-11.3	-13.1	-7.7	-9.6
Fuel Price, $/l ($/gal.)	0.53 (2.00)	0.53 (2.00)	0.53 (2.00)	0.53 (2.00)	0.53 (2.00)
DOC, cents/seat st. mi.	3.095	2.685	2.625	2.811	2.748
Delta DOC, %	BASE	-13.2	-15.2	-9.2	-11.2
DOC+I, cents/seat st. mi.	3.588	3.147	3.080	3.285	3.214
Delta DOC+I, %	BASE	-12.3	-14.2	-8.4	-10.4

DOC evaluations show more benefit for the advanced engines than DOC + I does because fuel cost is a larger portion of DOC (see Figure 7.2-8). Increasing fuel cost also increases the benefit for advanced engines and nacelles. Direct operating cost and DOC plus interest are summarized for each engine at three fuel prices in the tables. Relative engine plus nacelle acquisition and maintenance costs are also included.
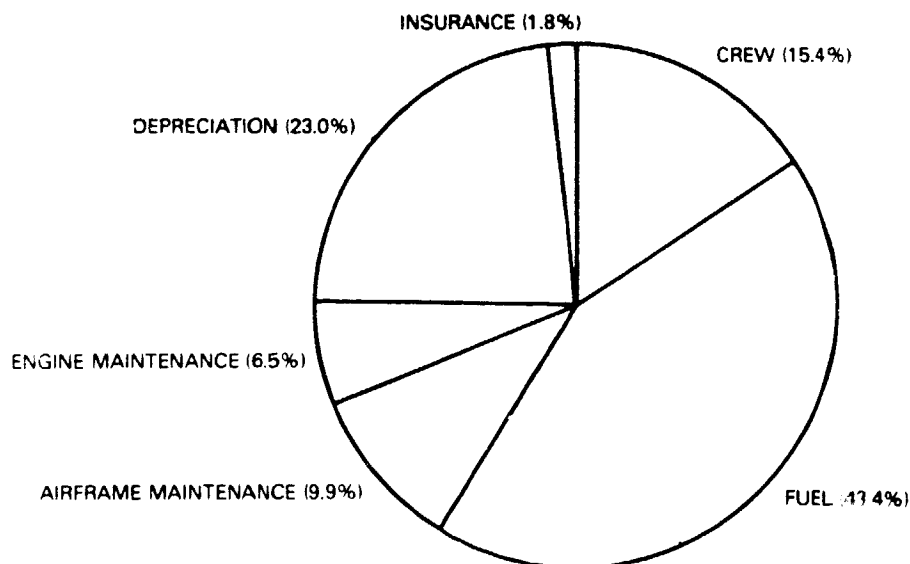
Figure 7.2-8A   DOC Breakdown: STF653G, 350 Pax Twin @ 1000 NM, $0.40/1 ($1.50/gal.) Fuel
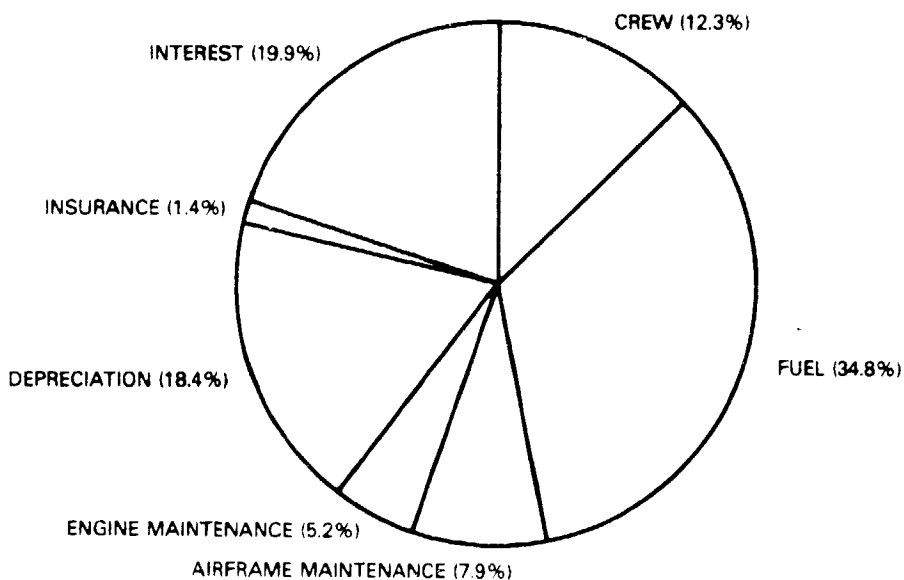
Figure 7.2-8B   DOC+I Breakdown: STF653G, 350 Pax twin @ 1000 NM, $0.40/1 ($1.50/gal.) Fuel

Figures 7.2-9 to 7.2-14 show how the specific engine/nacelle combinations evaluated in this Task compared to the trends established in the configuration selection Task. On the long range trijet the geared STF653 performed slightly worse than what was predicted relative to the ME^4, while the direct drive engine was slightly better. The medium range, large twin-engine aircraft performed better than predicted -- in both geared and direct drive configurations. The small twin-engine airplane with the geared STF654 performed slightly worse than predicted. Overall, the agreement between the two evaluations is quite good, which tends to confirm the trends found in the configuration selection task.
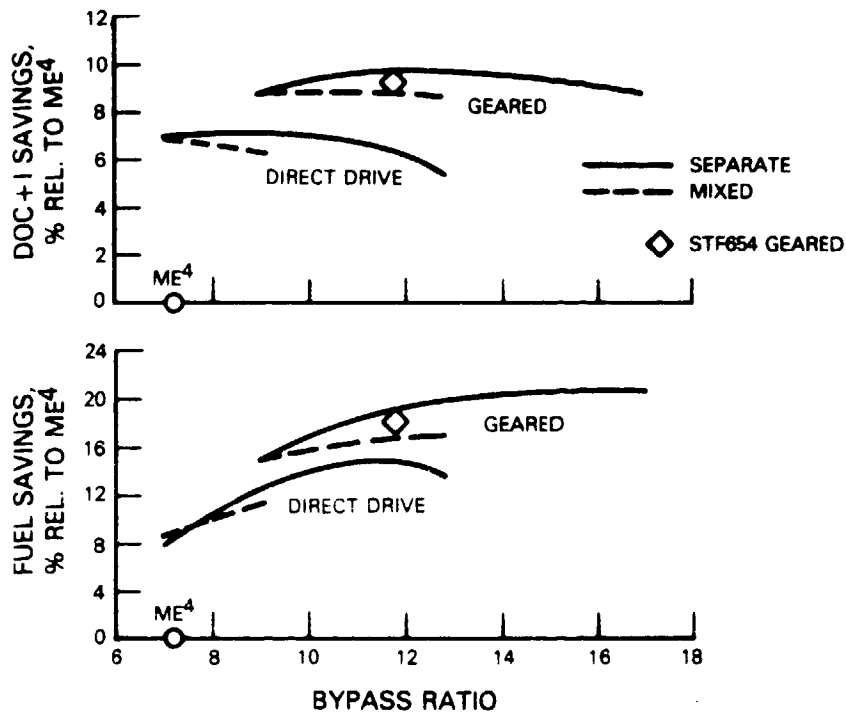
Figure 7.2-9   Bypass Ratio Effect on DOC+I and Fuel Burn: 150 Pax Twinjet @ 400 NM, $0.40/1 ($1.50/gal.) Fuel (advanced technology nacelles)

90

Figure 7.2-10   Bypass Ratio Effect on DOC+I and Fuel Burn: 150 Pax Twinjet
                       @   400 NM, $0.40/l ($1.50/gal.) Fuel (current technology
                       nacelles)
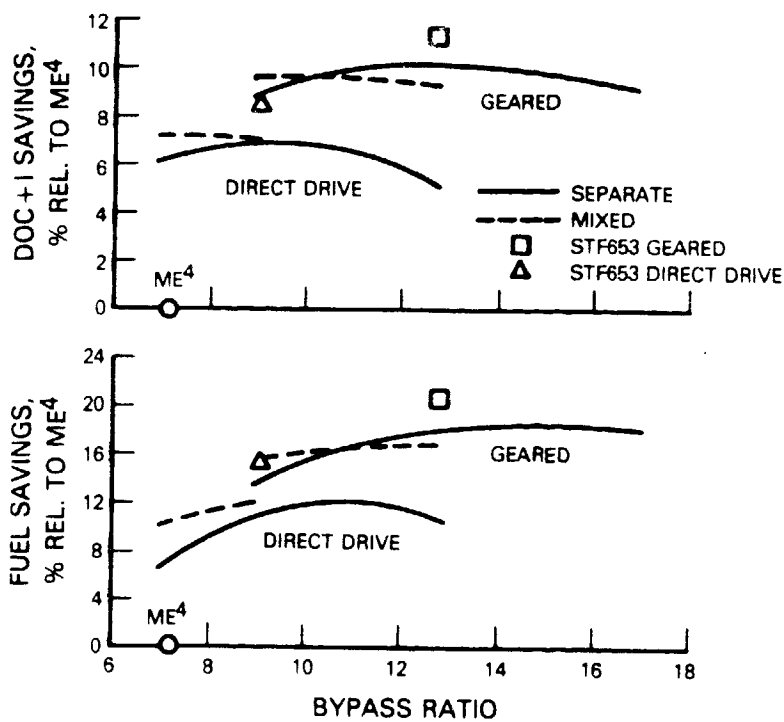
Figure 7.2-11   Bypass Ratio Effect on DOC+I and Fuel Burn: 350 Pax Twinjet
                       @ 1000 NM, $0.40/l ($1.50/gal.) Fuel (current technology
                       nacelles)
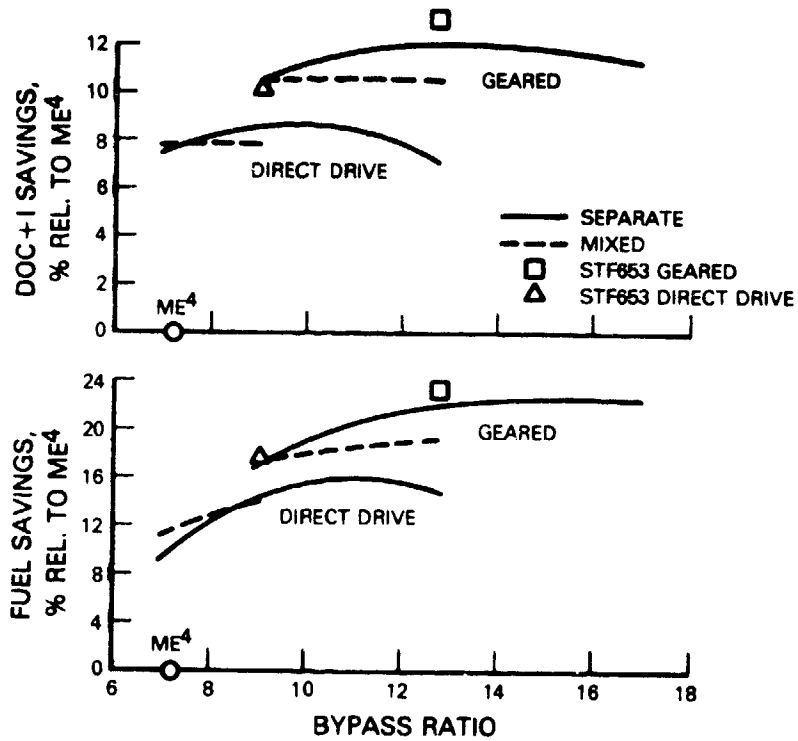
Figure 7.2-12   Bypass Ratio Effect on DOC+I and Fuel Burn: 350 Pax Twinjet
@ 1000NM, $0.40/1 ($1.50/gal.) Fuel (advanced technology
nacelles)
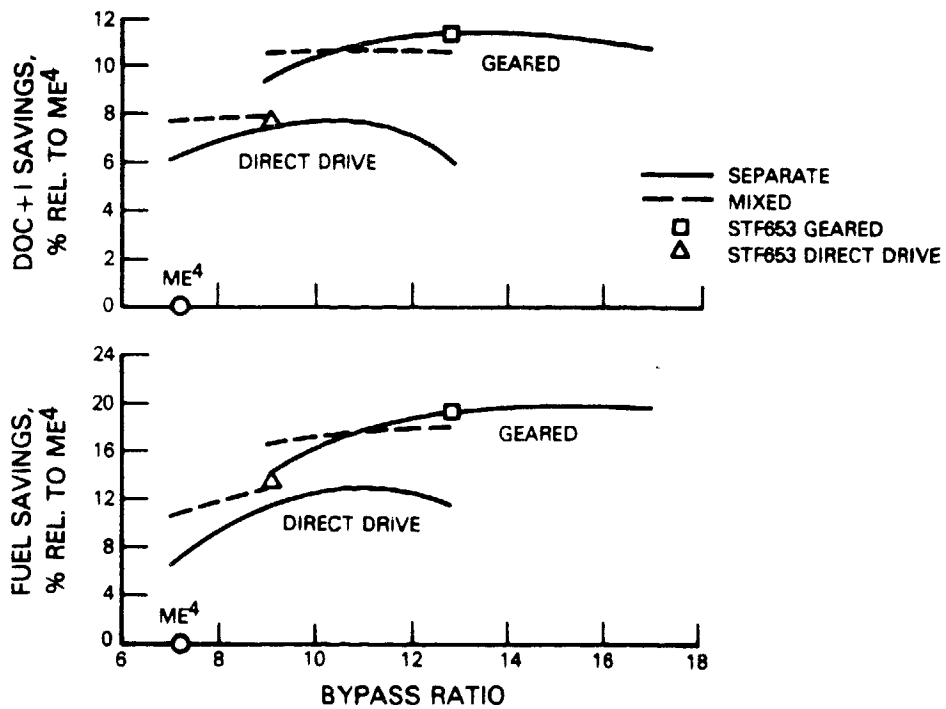
Figure 7.2-13   Bypass Ratio Effect on DOC+I and Fuel Burn: 440 Pax Trijet @
2000 NM, $0.40/1 ($1.50/gal.) Fuel (current technology
nacelles)

92
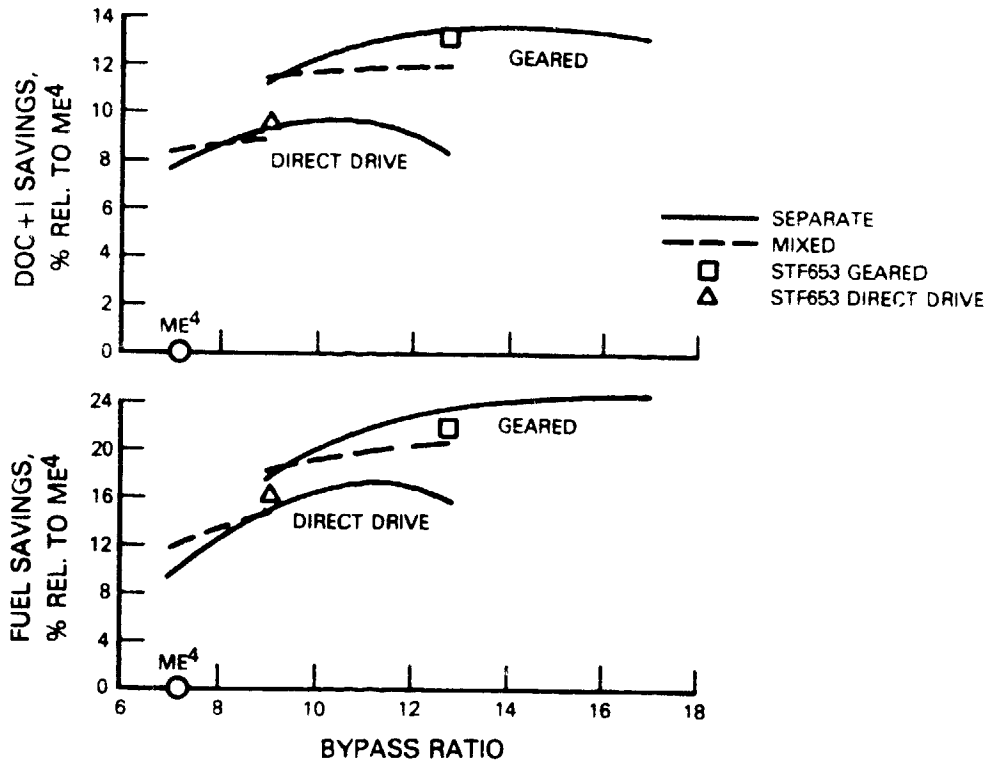
Figure 7.2-14   Bypass Ratio Effect on DOC+I and Fuel Burn: 440 Pax Trijet @ 2000 NM, $0.40/1 ($1.50/gal.) Fuel (advanced technology nacelles)

In conclusion, the advanced nacelle concepts evaluated in this Task offer substantial fuel burn and economic benefits over current technology nacelles.

SECTION 8.0   TECHNOLOGY CONCEPTS AND BENEFITS UPDATE

Designing thin cowl, tightly wrapped, short nacelles contributes to weight reduction and minimizes skin friction drag by reducing wetted surface area. In addition, transonic analysis has shown that contours can be formulated to keep the fan cowls virtually shock and separation free at cruise. Hence, skin friction drag reductions will not be compromised with other forms of wave drag increase. Also, the interference drag threat is lessened because the nacelle is shorter and features a smaller maximum diameter. The potential benefit is a 3 to 4.5 percent fuel burn savings relative to nacelle installations incorporating current technology. To realize this overall benefit certain technological challenges must be addressed; many of them require verification through test programs. Those advanced technologies assumed in the current study effort and their respective benefits are addressed in the following paragraphs.

Reduced Nacelle Skin Friction -- Proper contouring of the fan cowl can produce a favorable pressure gradient on the inlet. This can delay the boundary layer transition from laminar to turbulent flow. The lower skin friction coefficient of the laminar boundary layer reduces friction drag. Also, the use of 'riblets' has demonstrated the potential of reducing skin friction from turbulent boundary layers. These concepts can offer reductions in drag that equate to a 0.25 to 0.5 percent improvement in net thrust.

Cambered Inlet/Fan Coupling -- The standard method of drooping the inlet to align it with the wing produced upwash creates an internal upwash and circumferential gradients at the fan face. JT9D-7R4 tests have demonstrated that elimination of the distortion at the fan face can improve TSFC 0.7% at a sea level static condition. The coupling concept consists of cambering the internal inlet contours with a curved centerline that is tangential to the engine centerline, far enough in front of the fan face to eliminate the flow distortions. The external inlet contour is drooped in the usual way, and blends with the internal contour at or near the inlet highlight. The potential benefit is a 0.3% decrease in TSFC at cruise.

Optimized Pylon/Nacelle Integration -- JT9D-7R4 and PW2037 testing has shown that flow over the nacelle afterbody produces thrust on those portions of the afterbody where a favorable static pressure gradient exists. However, on the top 90° segment of the afterbody, in the vicinity of the pylon, low static pressures produce drag. Pylon/Nacelle integration can establish the afterbody offset required to reduce the projected low-pressure area in the vicinity of the pylon influence. The rate of close-out of the pylon sides is also an important area for examination. Optimized pylon/nacelle integration can result in 0.4% improvement in isolated nacelle net thrust.

Improved Fan Exit Guide Vane/Fan Duct Combination -- Guide vane losses are reduced by using low aspect ratios and reduced numbers of vanes. This approach also offers substantial weight and cost reductions. However, the duct radial total pressure profiles turned through a large cascade passage introduce secondary flows that create vorticity. This, in turn, generates a loss in nozzle thrust coefficient (C_v) because of the loss of axial momentum

associated with angular flow. There is a need to understand better the loss mechanisms and to quantify the penalties for various combinations of duct offset, nozzle throat angle, and afterbody angle. Adressing this challenge will result in the aerodynamic optimization of the guide vane and exhaust system. The potential benefit is a 0.25% improvement in TSFC.

Improved Off-Design Capability -- Realization of the payoff for slim nacelles will require developing the technology to operate stably and efficiently at off-design conditions. The two threats to stable operation are related to flow separation. The first threat is an internal phenomenon. Internal distortion threatens engine stability and fan blade stress. It is most likely to occur at high angles of attack, cross wind conditions, and high power, static operation. There are many methods for reducing this threat, though their effectiveness must be demonstrated. These methods include:

o   utilization of engine bleed;

o   development of fans with increased surge margins;

o   short inlet/fan coupling;

o   translatable inlet or blow-in-doors;

o   inflatable inlet lip;

o   active boundary layer control.

External separation occurs during second segment climb and is the second threat to stable operation. It can produce sufficient drag on a windmilling engine's nacelle to dictate the thrust size of the engine. This is particularly true for twin-engine aircraft. Concepts that need verification are:

o   engine thrust scheduling;

o   translatable inlet;

o   inflatable inlet lip;

o   local glove or blister to reduce separations.

The concepts that improve off-design capability may also offer increased engine stability and reduced stress (reduced internal separation) as well as reduced airplane takeoff gross weight or engine thrust size (if external separation is dictating engine size).

Noise Prediction With Inlet Distortion -- Even with a well designed cambered inlet, fan face distortions can be generated during operations at an angle of attack or with cross-wind. The fan also experiences distortion from downstream obstructions such as struts, pylons, and bifurcations. Noise generated by the acoustic interaction of the fan with these obstructions can be the dominant noise generated by high bypass ratio engines at certain operating conditions.

Therefore, a reliable distortion noise prediction model is needed for the evaluation of candidate advanced nacelle designs to assure that selected configurations do not adversely affect noise. The benefit will be the reduction of design constraints on acoustic treatment requirements.

Low Volume Reverser Concepts -- The slim nacelle constrains the structural depth that the reverser system can occupy. With high bypass ratios, though, the ram drag is large enough, and the thrust of the core flow is small enough, that the reverser need not be highly effective. The present study took advantage of these characteristics to investigate two unique, cascadeless reverser designs. This design concept needs further investigation and verification. The re-ingestion and foreign object damage threat should also be examined. The benefit is reduced weight and increased nacelle performance which approximates a 0.25 percent improvement in TSFC.

Additional Concepts -- Several additional suggestions came into being too late for inclusion in the current study effort but warrant mentioning. These are:

- o utilization of variable area nozzles for increased stability margin at take off and optimum performance match at cruise;

- o integration of engine/nacelle design, rather than merely wrapping a nacelle around pre-determined fan and engine cases;

- o further reduction of engine accessory size and weight: discussions with vendors indicate that a 40% reduction is feasible;

- o particle separators to reduce deterioration.

These concepts will require configuration studies and system analyses in order to quantify their potential benefits.

9.0 TECHNOLOGY VERIFICATION PROGRAM PLANS

To realize the potential benefits identified in sections 6.0 and 7.0, a four-phase technology development program was formulated (figure 9.1). Technologies and demonstration vehicles required to bring the concepts of slim-line nacelles and low volume thrust reversers to a state of technical readiness were identified, and a schedule of activities for each phase was formulated and integrated into the overall plan as shown. Each phase of the overall plan is described briefly below.

Phase I -- Design Definition Studies

This phase comprises the more detailed aerodynamic and mechanical design analysis required to 1) establish the preliminary design definition of the most promising concepts identified in the current study, 2) further define engine/airframe integration requirements, and 3) formulate a preliminary plan for test verification of the technology concepts. An airframe subcontractor will work with Pratt & Whitney to define the most promising nacelle aerodynamic configuration and low volume thrust reverser/spoiler configuration for use as a base for test model definition. This will include consideration of accessories and accessory location, bleed and horsepower extraction requirements, and plumbing and maintainability considerations that might affect nacelle contours.

Phase II -- Isolated Nacelle Model Test Program

This phase comprises design, fabrication, and testing of the most promising nacelle configurations identified in Phase I in order to verify performance predictions and obtain benchmark data for code refinement and verification. Inlet tests will investigate drag variations as a function of cruise inlet Mach number and inlet mass ratio for each model configuration. These tests will also include investigations of potential inlet internal and external flow disturbances resulting from low Mach number, high angle of attack flow conditions. Nozzle tests will investigate afterbody drag variations as a function of cruise Mach number and nozzle pressure ratio for each model configuration. The effects of fan exit flow profile and swirl will also be investigated, along with active boundary layer control to eliminate or reduce afterbody flow separation. Inlet and nozzle drags will be added together through use of a reference nozzle. Testing will be conducted at suitable vendor or NASA facilities.

Phase III -- Integrated Nacelle Model Test Program

This effort builds upon the results obtained from the Phase II tests and comprises design, fabrication, and testing of selected integrated nacelle model designs to verify interference drag predictions and to obtain benchmark data for drag code verification and refinement. Testing will be conducted at suitable NASA facilities and will encompass flow conditions representative of critical segments of a transport aircraft flight envelope. Flow visualization techniques will be utilized to enhance results. Wing-pylon interference drag

investigations will include variations in nacelle mount location, pylon camber, and pylon length. Primary focus will be on arrangements that maintain adequate nacelle ground clearance and minimize interference drag without imposing weight penalties on the airframe. Simulated aft-fuselage, nacelle mount model tests will also be conducted with the primary variable being nacelle distance from the fuselage, although axial location and engine centerline orientation may also be investigated. Following testing, the most promising nacelle model hardware will be made available for the reverser targeting test program in Phase IV.

Phase IV -- Reverser Effectiveness Model Test Program

This effort comprises design, fabrication, and testing of thrust reverser/spoiler models to verify effectiveness and efflux pattern predictions and to obtain benchmark data for code refinement and verification. Testing will be conducted in suitable vendor or NASA test facilities and will be initiated with reverser effectiveness and flow coefficient model tests. Following reverser effectiveness testing, the most promising reverser/spoiler configuration will be fitted to the most promising nacelle configuration identified in Phase III. Integrated nacelle/reverser tests will be conducted to investigate reverser targeting requirements and the effects of reverser efflux on nacelle inlet flow conditions. Test variables will cover a range of 1) free-stream Mach numbers, 2) reverser areas, 3) blocker door heights, and 4) targeting efflux angles. All testing will be conducted at flow conditions representative of typical thrust reverser operating points in a transport aircraft flight envelope.

This program plan represents the logical sequence of events required to achieve concept technology readiness in a time frame permitting maximum benefit to emerging and advanced turbofan engines.
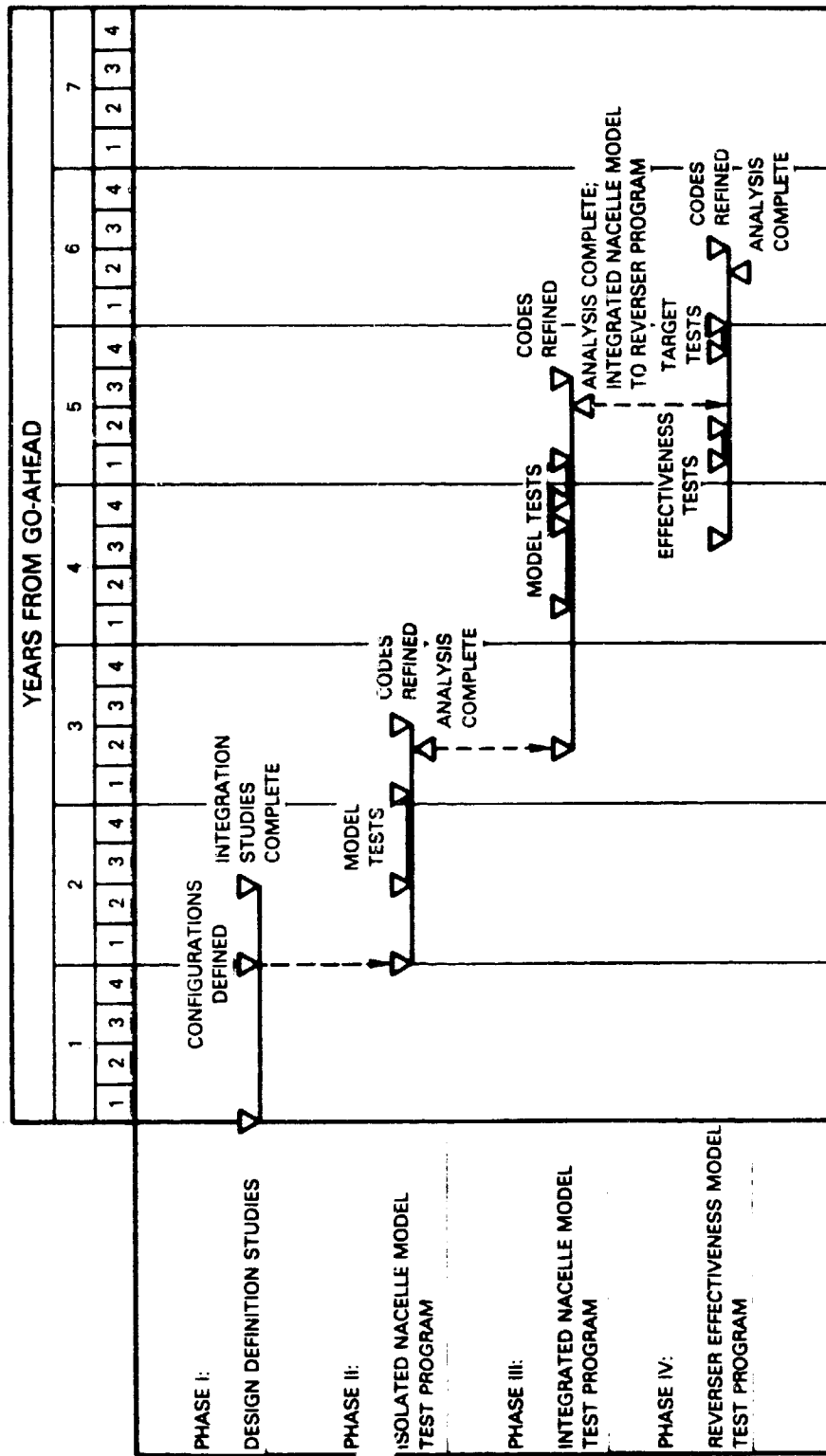
Figure 9.1   Technology Verification Program Plan

SECTION 10.0 CONCLUSIONS

The Advanced Turbofan Nacelle Definition Study established the design feasibility of advanced technology, slim-line nacelles applicable to advanced technology, high bypass ratio turbofan engines. Design feasibility was also established for two low volume thrust reverser/spoiler concepts that meet or exceed the required effectiveness for these engines. These nacelle and thrust reverser/spoiler designs were shown to be applicable in engines with takeoff thrust sizes ranging from 106,756 to 266,892 Newtons (24,000-60,000 lbs.). The reduced weight, drag, and cost of the advanced technology nacelle installations relative to current technology nacelles offer a mission fuel burn savings ranging from 3.0 to 4.5 percent (depending on mission) and direct operating cost plus interest improvements from 1.6 to 2.2 percent.

Douglas Aircraft Company evaluations utilized the advanced technology nacelle and engine concepts on advanced, wide body transport concepts. These evaluations indicated that up to 28 percent fuel burn savings on long range missions are attainable, relative to currently available production engines and nacelles.

A four-phase technology verification program was formulated to further define, fabricate, and test promising concepts identified in the study. Further evaluations should also address the following areas: 1) development of compact accessories and secondary power systems and 2) wing/pylon/nacelle aerodynamic integration.

100

LIST OF REFERENCES

1) Gray, D. E. et al, Energy Efficient Engine Preliminary Design and Integration Studies, NAS3-20628, November 1978

2) Gray, D. E., and Gardner, W. B., 'Energy Efficient Engine Technology Benefit/Cost Study,' Vol. II, NASA-CR-174766, October 1983

3) Ni, R. R., "A Multiple Grid Scheme for Solving the Euler Equations," AIAA 81-1025, and AIAA Journal, 20:1982

4) Kozlowski, H., and Usab, W. J., 'Final Report STOL Transport Thrust Reversing/Vectoring Program,' Pratt & Whitney Aircraft Subcontract Support: TBC P.O. G-794003-9563, January 26, 1973

APPENDIX A

McDonnell Douglas Corporation Final Report

APPENDIX A -- McDonnell Douglas Corporation Final Report

ADVANCED TURBOFAN NACELLE DEFINITION STUDY

Douglas Aircraft Company ACEE Project No. 33

December 1984

FORWARD

This study was conducted by the Douglas Aircraft Company for the Pratt & Whitney Aircraft Group under P.O. 20646. The study was conducted as a sub-contract to Pratt & Whitney under their prime contract with the NASA-Lewis Research Center on an E^3 Advanced Turbofan Nacelle Definition Study. This study was conducted from February to November 1984.

The study was conducted with the following contributors:

Aircraft Configuration Manager	M. F. Mossman
Aircraft Configuration Design	R. T. Cathers
Aerodynamics Configuration	D. G. MacWilkinson
Aerodynamics Performance	L. L. Hill
Propulsion Performance	J. G. McComb
Propulsion Installations	R. F. McCarthy
Weights	A. M. Maturkanich

The Douglas Project Manager was R. T. Kawai and Program Manager M. Klotzche. The Pratt & Whitney Task Manager was D. C. Howe.

TABLE OF CONTENTS

1.0 SUMMARY

A baseline advanced airplane configuration and performance was established using the Pratt & Whitney STF 631 Maximum Efficiency Energy Efficient Engine (ME^4). The STF 631 is a 40,000 lbs. thrust class turbofan with a bypass ratio of 7.2. The advanced tri-jet with this engine is designated the Douglas Model D967C-209. This study airplane incorporates advanced features that can be expected to be in future generation transports. The STF 631 engine and nacelle was then replaced with the STF 653 and STF 653DD with current technology and advanced technology nacelles. The STF 653 and STF 653DD are more advanced engines with a 12.8 bypass ratio geared fan, and a 9.1 bypass ratio direct drive fan, respectively.

The results show that a fuel savings of 22% to 23% is achievable from the advanced propulsion systems when compared to the ME^4 baseline. When based against the best currently available engine technology that is committed to production, there is a potential 28% reduction in fuel burned. Attainment of the full potential requires technology development for the engine and installation. The installation technology needs are the subject of this report.

PAGE 110 INTENTIONALLY BLANK

2.0 INTRODUCTION

This study has been conducted to assess the fuel burned savings potential of Pratt & Whitney Target Engines in advanced nacelles when installed in an advanced tri-jet transport in the time period near the year 2000. The Target Engines are study engines with advancements beyond that in the NASA-sponsored Energy Efficient Engine (E^3) technology program. The advanced nacelles are advanced concept designs employing means to reduce drag and weight. The advanced tri-jet is a long range, wide body transport employing advanced configuration, material, and system features.

The studies were conducted using engine installation data supplied by Pratt & Whitney for a baseline and for the advanced engines. The baseline was the STF 631. The more advanced engines were the STF 653 and STF 653DD. The STF 653 is a bypass ratio 12.8 geared fan. The STF 653DD is a bypass ratio 9.1 direct drive fan.

The studies were conducted using the Douglas airplane optimization program, CASE, to determine the aircraft size for minimum fuel burned.

3.0 STUDY RESULTS

3.1 BASELINE AIRPLANE DESCRIPTION

A baseline airplane was established in order to evaluate the advanced engines and nacelles. In order to assess improvements from only advanced engines, a conservative approach to advanced technology utilization in the airframe was used. Advanced features that are highly probable without feasibility demonstrations were used. The Douglas Aircraft Company (DAC) Model D967C-209 configuration with the baseline PWA STF 631 engines is shown in Figure 1. This advanced tri-jet has a maximum take-off gross weight of 645,200 lbs. with an overall length of 212 ft. 3 inches and wing span of 225 feet 3 inches. The STF 631 engines are sized for 48,400 lbs. thrust each. The characteristics are shown in Table I. The weight breakdown for the baseline is shown in Table II.

3.1.1. ADVANCED TECHNOLOGY WING

The Model D967C-209 incorporates an advanced technology wing based on supercritical airfoils. The wing characteristics were selected using the experience gained from extensive studies on the previous MDF-100 and D3300 airplane projects. The selected characteristics are:

Sweep Λ c/4 = 33°

Average Thickness Ratio, t/c = 12.64%

Aspect Ratio, A.R. = 10.8

Reference Area, Sw = 4700 Ft^2

The high lift system was derived from advanced aircraft studies and uses a full span, leading edge slat and an 80% span, trailing edge, single segment, high-extension fowler flap. Performance is based on an extensive data base developed under the NASA EET Program and DAC technology development programs.
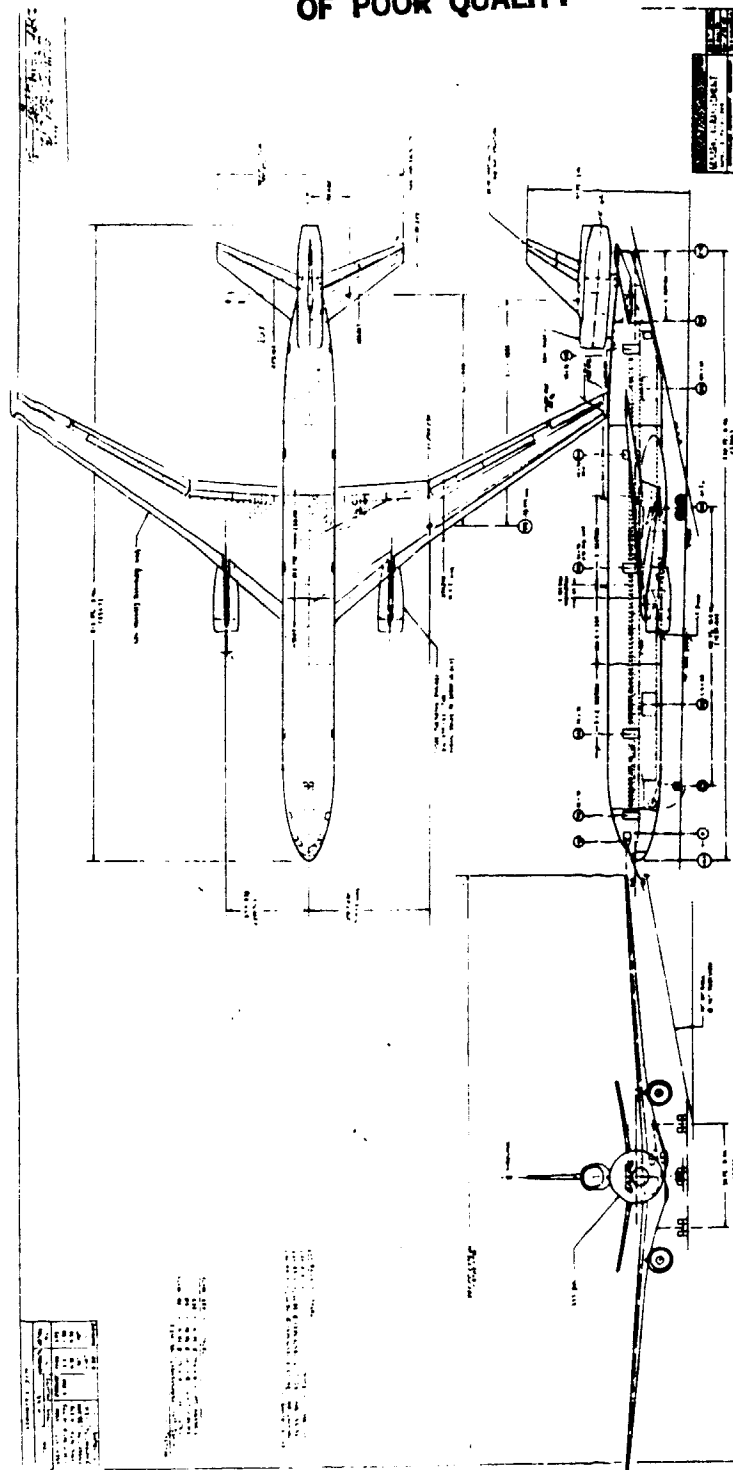
Figure 1   Study Transport Model D967C-209

114

TABLE I

MODEL 967C-209

CHARACTERISTICS

Aircraft Type	Advanced Tri-jet
Engines	P&W STF 631
Thrust, N (lbs)/Engine	215,292 (48,400)
Passenger Capacity	437
Design Range (NM)	5,800
Max Take Off Weight, kg (lbs)	292,656 (645,200)
Operating Empty Wgt, kg (lbs)	150,773 (332,400)
Wing Area, m^2 (Ft^2)	1,432 (4,700)
Horizontal Area, m^2 (Ft^2)	306 (1,007)
Vertical Area, m^2 (Ft^2)	184 (605)
Wing Aspect Ratio	10.8
Horizontal Aspect Ratio	5.0
Vertical Aspect Ratio	1.8
Fuselage Length, cm (in.)	7,025 (2,766)
Fuselage Width, cm (in.)	601 (237)

TABLE II

MODEL 967C-209

WEIGHT BREAKDOWN

	Weight, kg (lbs)
Max Take Off	292,656 (645,200)
Max Landing	229,970 (507,000)
Max Zero Fuel	218,630 (482,000
Wing	37,797 (83,329)
Horizontal	2,751 (6,067)
Vertical	2,599 (5,731)
Fuselage	27,733 (61,142)
Landing Gear	14,268 (31,457)
Airframe........................	85,150 (187,726)
Engines	13,198 (29,098)
Installation	6,561 (14,465)
Fuel System	1,387 (3,060)
Propulsion.....................	21,147 (46,623)
Controls	4,477 (9,871)
Avionics	1,031 (2,274)
Instruments	1,030 (2,271)
APU and Environmental	3,371 (7,433)
Electrical	3,401 (7,499)
Furnishings	20,859 (45,987)
Ice Protection	288 (635)
Aux Gear	25 (56)
Systems.......................	34,484 (76,026)
Max Empty Weight.................................	140,782 (310,375)
Operator Items...................................	9,990 (22,025)
Operating Empty Weight..........................	150,773 (332,400)

3.1.2 ADVANCED TAIL

In cruise, approximately six percent of the total airplane drag of a wide body tri-jet is due to parasite drag of the horizontal tail. Based on this, a 17 percent reduction in tail area would provide a one percent decrease in total drag, which would result on average in a 1.1 percent decrease in fuel burn. A smaller tail would also weigh less; a 1000-pound decrease in empty weight reduces the fuel burn by 0.3 percent.

The size of the horizontal tail is determined by its ability to provide (a) airplane nose-up (ANU) pitching moment for trim in landing configuration with a forward center of gravity (CG) and (b) adequate longitudinal stability at aft CG. Since the horizontal tail always carries a down load for steady 1 "g" flight, even when flying at aft CG, the trim capability can be increased by designing the tail with inverted camber, and the elevator as an inverted, slotted flap but with deflection capability in both directions. A further reduction in tail area is provided by having neutral elevator shift from zero at take-off flaps to several degrees trailing edge up (TEU) at maximum landing flaps. In this way the elevator provides part of the ANU trim for the critical landing case. For takeoff, the full throw of the powerful slotted elevator is still available for nose wheel liftoff. Further tail area reduction is possible if a stability augmentation system is used to provide artificial longitudinal stability, critical at the aft CG limit. The above rationale led to the current advanced tail design.

Cambered tails are in use on several transports, and a slotted elevator is currently in use on one transport aircraft. The Douglas advanced tail design is more refined due to (a) larger elevator deflections, (b) a slot cover/seal, and (c) the use of several degrees of elevator in the trim system. Current estimates predict that this tail will provide a 2.3 percent reduction in total airplane drag and a weight of 2083 pounds over the current long range tri-jet design.

3.1.3 α LONGITUDINAL STABILITY AUGMENTATION SYSTEM (α LSAS)

The study aircraft configuration includes a static stability augmentation system that allows operation at a center-of-gravity range aft of that of an unaugmented aircraft. The α LSAS system provides angle-of-attack stability characteristics similar to those of contemporary aircraft. The more aft center-of-gravity location reduces the aerodynamic balancing down load carried by the horizontal tail. This results in lower trim drag and a weight savings due to the smaller horizontal tail and wing. The α LSAS system provides positive stability for all flight conditions, ensuring the proper sense for control column motions and forces required for maneuvering the aircraft. The system employs pitch rate, pitch attitude and normal acceleration as feedback parameters to independent augmentation computers which provide control inputs in series with pilot commands to the four elevator segments and the horizontal stabilizer.

3.1.4 ADVANCED STRUCTURES

Major advanced material technology development activities have been underway at Douglas. Douglas composite programs, with major funding support from NASA, are leading to widespread application of composites in future transport aircraft.

Assumed application areas for composite materials in this study transport include control surfaces, floor beams, fairings, landing gear doors and carbon brakes.

Douglas is also conducting research and technology development on advanced metallics. The study airplane weights are based on using aluminum-lithium alloys in the wing and fuselage primary structures.

3.1.5 SYSTEMS

Improvements in aircraft systems are also included. Some of these are:

- o   Digital Avionics -- improved reliability and capability
- o   Flight Performance Management -- reduced aircraft operations fuel consumption
- o   Air Conditioning -- reduced engine bleed requirements and improved materials

- o   APU -- reduced fuel consumption
- o   Advanced Cockpit Displays -- reduced weight and improved performance
- o   Advanced Hydraulic System -- 8000 psi system
- o   Advanced Electrical System -- rare earth magnets, light weight wiring and high power transistors

3.2. CONFIGURATION ANALYSES

3.2.1. AIRPLANE SIZING

Detailed performance sizing runs were made for the study engines. These engines were assumed to be installed on the Model D967C-209 airplane with a capacity of 437 passengers and a supercritical, aspect ratio 10.8 wing designed for a cruise Mach number of 0.82. Constraints included an initial cruise altitude capability of 33000 feet, a take-off field length of 11000 feet, and an approach speed of 150 knots. The airplanes were sized for a range capability of 5800 nautical miles with a full passenger and bag payload. The wing area and engine sizes were selected to minimize the fuel burned for an average 2000 nautical mile mission.

Sizing was done using the Douglas CASE program. Results for the baseline using the STF 531 are shown in Figure 2. The critical sizing point for the engine was the 33000 feet initial cruise altitude capabilty and the airplane wing area was selected for minimum fuel burned.

The results for the STF653 with the advanced technology nacelle are shown in Figure 3. The STF653 has a bypass ratio of 12.8 compared to the bypass ratio of 7.2 for the STF631. Even though the higher bypass ratio STF653 has a greater thrust lapse than the STF631, when the airplane is resized and optimized for minimum fuel burned for the typical or average 2000 nautical miles mission, the optimum wing loading is lower and the engine and wing are sized for minimum fuel burned.

3.2.2 MISSION ANALYSIS

The fuel burned by mission segment for the design range mission of 5800 nautical miles and a typical mission of 2000 nautical miles are shown for the baseline in Tables III and IV. The case shown uses current technology secondary power extraction and current aerodynamic performance applied to the compact nacelle. Block fuel savings of 20.9% for a typical 2000 nautical mile mission and 22.4% for the design range of 5800 nautical miles are predicted. These analyses did not include the lower drag for the shock free lines assessed by Pratt & Whitney or the efficiency improvement expected by use of a more efficient advanced environmental control system. Inclusion of these features would provide an additional improvement of 0.9%, resulting in a block fuel savings of 21.8% for the typical 2000 nautical mile mission and 23.3% for the 5800 nautical mile design range mission.

Figure 2   Airplane Sizing for STF 631

120

Figure 3 -- Airplane Sizing for STF 653

TABLE III
Mission Analysis for STF 631

D967C-209 Stretch, S) REF = 4000, STF-631, RSS HOR., T3HO
AR = 10.7950, T/C = 0.1264, Sweep = 33.10, Taper = 0.2750

Range (NM)	5800	2000
Engine Size, kg (lb)	21,962 (48,420)	21,962 (48,420)
Wing Area, m^2 (ft^2)	1,431 (4,698)	1,431 (4,698)
Takeoff Gross Wgt, kg (lb)	292,151 (644,087)	226,985 (500,420)
Operating Empty Wgt, kg (lb)	150,738 (332,323)	150,738 (332,323)
Total Taxi Fuel, kg (lb)	629 (1,387)	544 (1,201)
Takeoff Fuel, kg (lb)	850 (1,874)	625 (1,378)
Climb Fuel, kg (lb)	7,445 (16,415)	5,038 (11,109)
Climb Distance, NM	269.0	185.7
Cruise Fuel, kg (lb)	79,638 (175,574)	21,892 (48,266)
Cruise Distance, NM	5414.0	1,698
Descent Fuel, kg (lb)	284 (623)	282 (622)
Descent Distance, NM	117.1	116.1
Approach Fuel, kg (lb)	229 (505)	223 (492)
Block Time (hr)	12.837	4.740
Block Fuel, kg (lb)	89,076 (196,381)	28,606 (63,067)
Cruise CL	0.4748 -- 0.4954	0.5241 -- 0.4717
Cruise Mach Number	0.8200 -- 0.8200	0.8300 -- 0.8304
Cruise L/D	18.785 -- 18.805	18.580 -- 18.364
Cruise SFC	0.5480 -- 0.5379	0.5408 -- 0.5398
Cruise Range Factor	16493. -- 16443.	16357. -- 16205.

TABLE IV
Mission Analysis for STF 653

Above with STF-653 with Advanced Technology Nacelles,
T3HO, AR = 10.7950, T/C = 0.1264, Sweep = 33.10, Taper = 0.2750

Range (NM)	5800	2000
Engine Size, kg (lb)	23,586 (52,000)	23,586 (52,000)
Wing Area, m^2 (ft^2)	1,463 (4,800)	1,463 (4,800)
Takeoff Gross Wgt, kg (lb)	264,874 (583,952)	214,521 (472,942)
Operating Empty Wgt, kg (lb)	145,884 (321,623)	145,884 (321,623)
Total Taxi Fuel, kg (lb)	414 (913)	346 (764)
Takeoff Fuel, kg (lb)	571 (1,260)	440 (972)
Climb Fuel, kg (lb)	5,994 (13,216)	4,007 (8,836)
Climb Distance, NM	288.9	189.0
Cruise Fuel, kg (lb)	61,780 (136,203)	17,447 (38,465)
Cruise Distance, NM	5363.8	1685
Descent Fuel, kg (lb)	215 (475)	213 (471)
Descent Distance, NM	127.4	126.6
Approach Fuel, kg (lb)	164 (362)	160 (354)
Block Time (hr)	12.872	4.743
Block Fuel, kg (lb)	69,184 (152,527)	22,616 (49,862)
Cruise CL	0.5081 -- 0.4667	0.4868 -- 0.4459
Cruise Mach Number	0.8200 -- 0.8200	0.8300 -- 0.8305
Cruise L/D	19.675 -- 19.293	19.214 -- 18.854
Cruise SFC	0.4658 -- 0.4647	0.4675 -- 0.4665
Cruise Range Factor	19965. -- 19526.	19566. -- 19253.

3.3   EVALUATION OF ADVANCED PROPULSION SYSTEMS

The advanced propulsion systems were evaluated to: (1) determine the fuel burned improvement, (2) determine the impact on installability, and (3) assess the impact of more advanced technology on airframe requirements.

3.3.1   FUEL SAVINGS

The fuel savings of the STF653 and STF653DD with current technology and advanced technology nacelles were determined from mission analyses with these propulsion systems installed on the model D967-209 advanced wide body tri-jet. The analyses were done using the Douglas CASE program with the aircraft resized to match the same payload and range capability.

The fuel savings for the typical 2000 nautical miles range typical mission are shown in Figure 4. The maximum fuel savings of 22% results from use of the STF653 with the advanced nacelle. A current technology installation would result in a 4% smaller fueled savings. These savings are relative to the STF631. The STF631 is about 5% better than the best currently available production technology.

The TARGET engine with advanced nacelle technology, therefore, offers a 27% improvement for the 2000 nautical mile mission and 28% improvement at the design range when compared to the best available engine and installation.

The analyses were conducted assuming an interference drag level of 3% of the nacelle drag in all installations. This level was based on a proprietary data correlation which shows this level is potentially achievable for the nacelle positioning used in this study. As discussed in Section 3.4.1, an experimental program is needed to determine the means to install the very high bypass ratio engines to minimize the interference drag.

Figure 5 shows the improvement potential from achieving a high efficiency nacelle configuration. The interference drag potential of 3% total airplane drag is based on data correlations. These data show the interference drag could be 6% of airplane drag unless the necessary data base is developed. The drag reduction also requires a short, sharp, leading edge inlet. The means to achieve a suitable design, particularly during off-design-point operating conditions, needs to be developed.

In addition to the need to minimize interference drag, the performance difference resulting from achieving a tightly wrapped, minimum length cowling versus a current technology installation is shown. The advanced installation also results in a fuel savings from weight reduction.

The fan reverser/nozzle improvement requires minimizing the volume needed by the reverser. This need as well as the others described above are described further in Section 3.4.

124
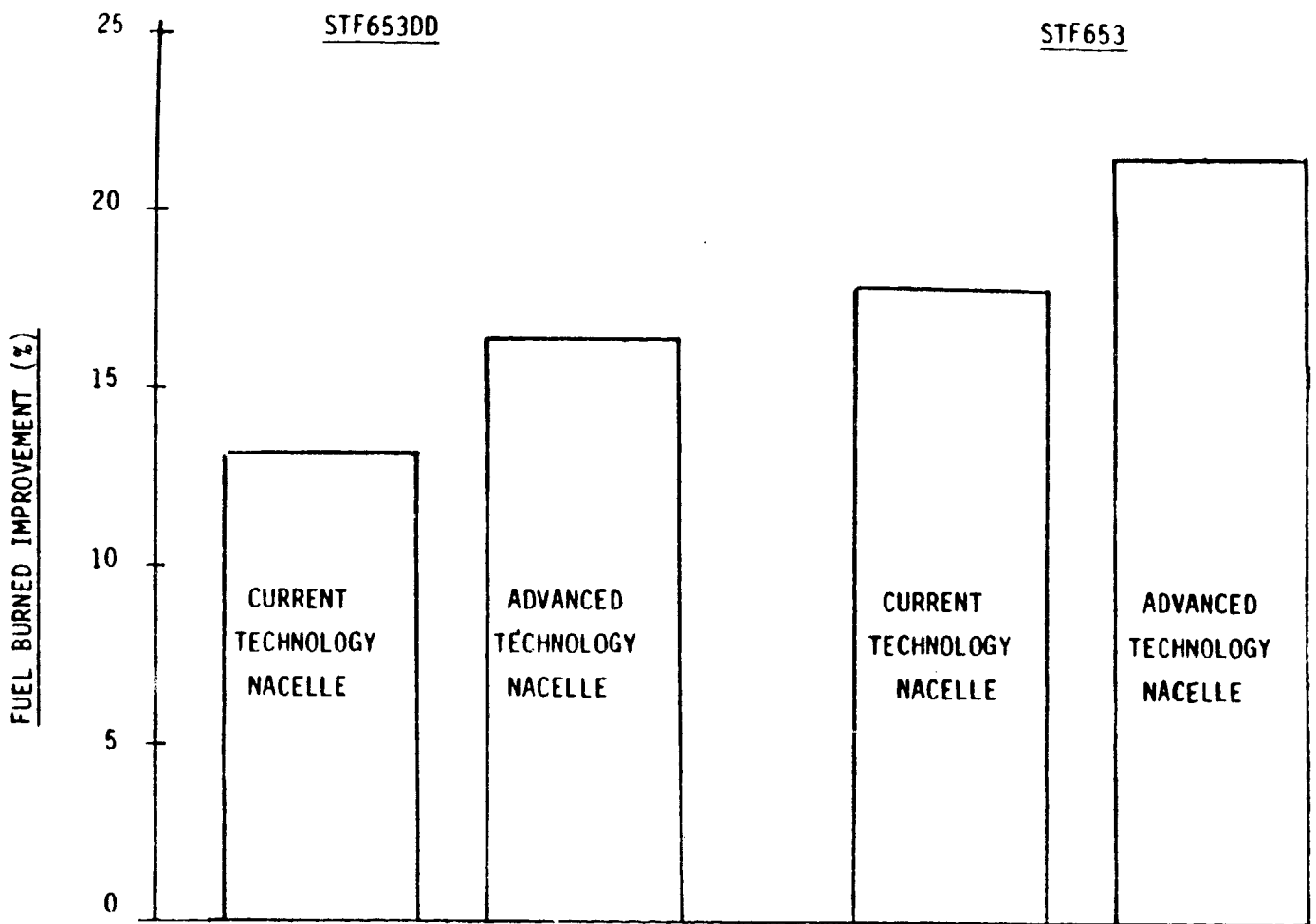
Figure 4   Improvements from Advanced Propulsion Systems Relative to STF 631
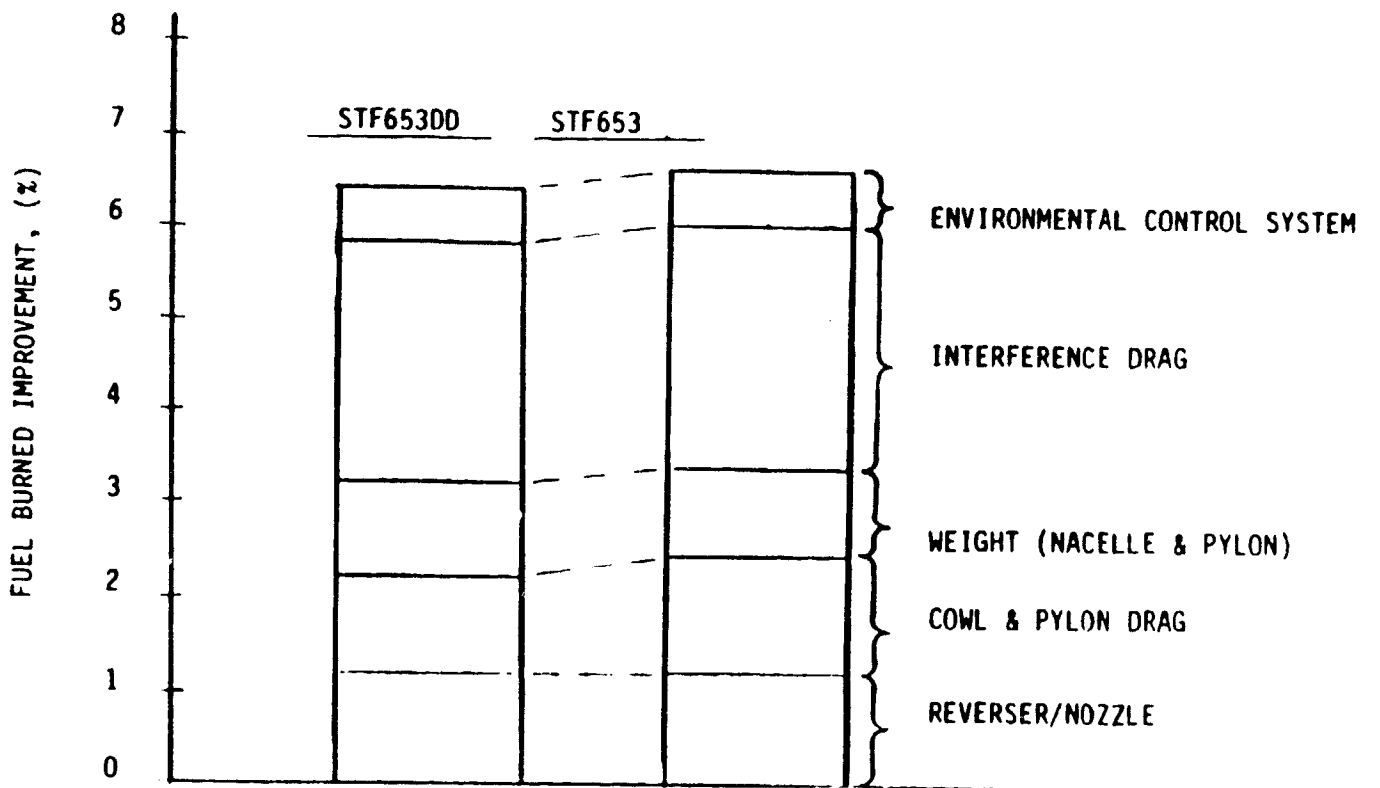
Figure 5 Installation Integration Technology Perspective Relative to Current
         Technology

126

3.3.2 INSTALLABILITY

Installation studies were conducted for the baseline STF631, the STF653 with current and advanced technology nacelles, and the STF653DD with current and advanced technology nacelles. The studies were conducted for the wing and tail locations. The installation characteristics are summarized on Table V for the wing position installations and on Table VI for the aft position.

The installation study drawings are shown in Figures 6 through 10 for the wing locations and in Figures 11 through 15 for the aft installations.

The mechanical installation studies of the nacelles show they can be installed in an advanced wide body tri-jet. However, the tightly wrapped nacelles require advanced approaches to accommodate the airframe systems in consonance with current maintainability standards.

Use of current technology pneumatic systems creates a number of problems. The simple bleed precoolers currently used do not integrate satisfactorily. With the short fan reverser/nozzle there is insufficient space for the fan cooling flow offtake and ducting.

With the advanced technology nacelles, the reverser concepts do not incorporate the use of cascades for directing reverse flow efflux patterns to the extent current designs achieve. Further investigations are needed in this area. The advanced technology requirements are described in the next section.

TABLE V
Installation Characteristics: Wing Mounted Engines

INSTALLATION CHARACTERISTICS – WING MOUNTED ENGINES

ENGINE IDENTITY & INSTL. DWG. NO.	NACELLE Max Dia Inches	NACELLE LENGTH Inlet to Fan Exh.	NACELLE LENGTH Inlet to Pri Exh	EXH LOCATION % WING CORD Fan	EXH LOCATION % WING CORD Primary	PRIMARY CRITERION FOR NACELLE LOCATION	C O M M E N T S
STF 631 CURRENT TECH MIXED EXHAUST FLOW NACELLE J015980	113.9	—	293.5	—	11.9	Aerodynamic	Determination of most suitable Wing/Pylon/Nacelle configuration requires further effort.
STF 653 CURRENT TECH. NAC. J015982	124.6	153.9	221.0	-9.4 (Fwd of Wing L.E.)	10.7	Separation of Reverser Efflux and Wing L.E.	Further airframe systems integration evaluations required because of restricted space provisions.
STF 653 ADV.TECH. NAC. J015984	115.4	102.8	188.0	-14.6 (Fwd of Wing L.E.)	10.7	Separation of Reverser Efflux with Wing L.E.	Same as above.
STF 653 DD CURRENT TECH. NAC. J015986	117.4	164.9	249.4	-8.3 (Fwd of Wing L.E.)	16.6	Separation of Reverser Efflux with Wing L.E.	Same as above.
STF 653 DD ADV. TECH. NAC J015988	106.0	115.0	218.9	-14.3 (Fwd of Wing L.E.)	16.0	Separation of Reverser Efflux with Wing L.E.	Same as above.

TABLE VI
Installation Characteristics: Tail Mounted Engines

INSTALLATION CHARACTERISTICS - TAIL MOUNTED ENGINES

ENGINE IDENTITY & INSTL. DWG. NO.	INLET DUCT DIMENSIONS		NACELLE LENGTH RELATIVE to DC-10-40 - JT9D-59 (Overhang Aft of #4 Banjo)		COMMENTS
	Length Aft of #4 Banjo Inches	Dia Rel to DC-10-40-JT9D-59 Fwd of #4 Banjo % and Δ Inches	Fan Exhaust Δ Inches	Pri.Exhaust Δ Inches	
STF 631 CURRENT TECH. MIXED EXHAUST FLOW NACELLE J015981	27.1	+2.1% (18 inches larger)	Not Applicable	28.6 inches Aft	Nacelle trailing edge is 4.5 inches aft of DC-10 type trailing edge.
STF 653 CURRENT TECH. NAC. J015983	27.1	+7.2% (6.2 inches larger)	36.8 inches Fwd	48.7 inches Fwd	Further airframe systems integration evaluations required because of restricted space provisions.
STF 653 ADV. TECH. NAC. J015985	27.1	+7.2% (6.2 inches larger)	54.6 inches Fwd	48.7 inches Fwd	Same as above. Requires development of new reverser concepts.
STF 653 DD CURRENT TECH. NAC J015987	27.1	+0.5% (0.4 inches larger)	22.1 inches Fwd	16.5 inches Fwd	Same as for STF653 with current technology nacelle.
STF 653 DD ADV. TECH. NAC. J015989	27.1	-0.5% (0.4 inches larger)	41.5 inches Fwd	16.5 inches Fwd	Same as for STF 653 with advanced technology nacelle.
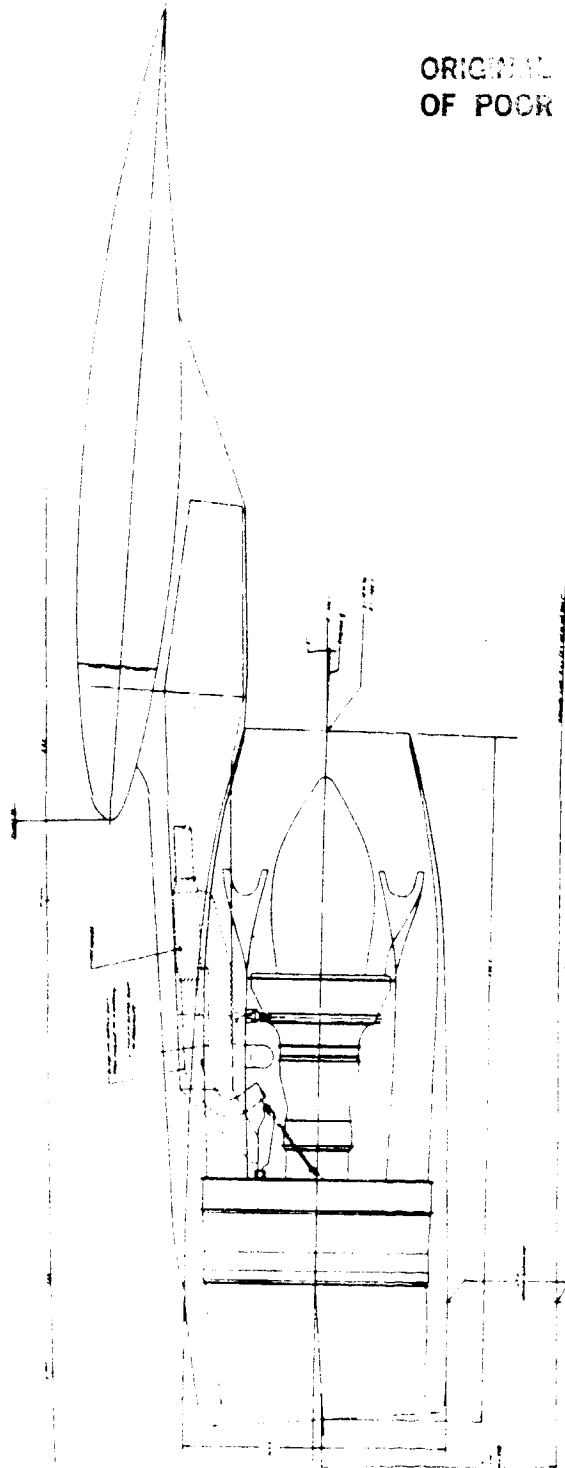
Figure 0   STF631 Reference Engine with Current Technology, Mixed-Flow Nacelle
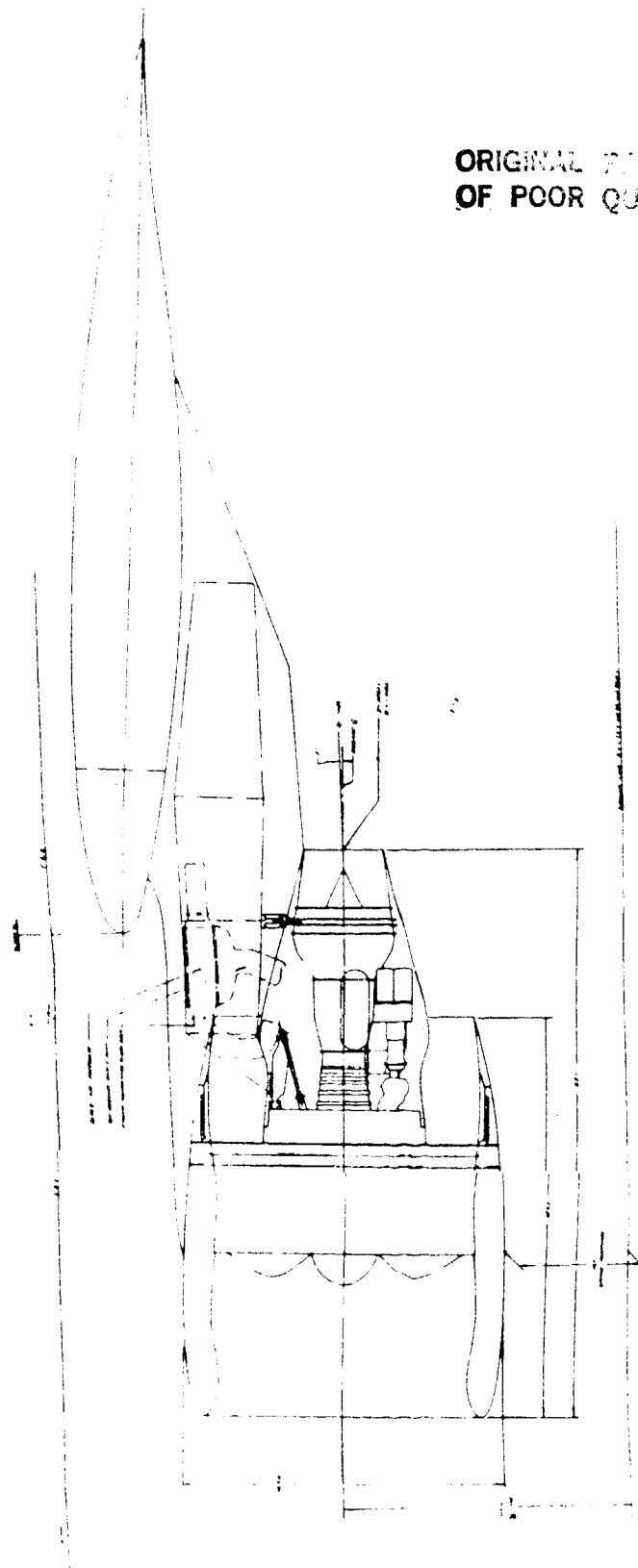
Figure 7   STF653 Advanced Technology Engine with Current Technology,
Separate-Flow Nacelle

131
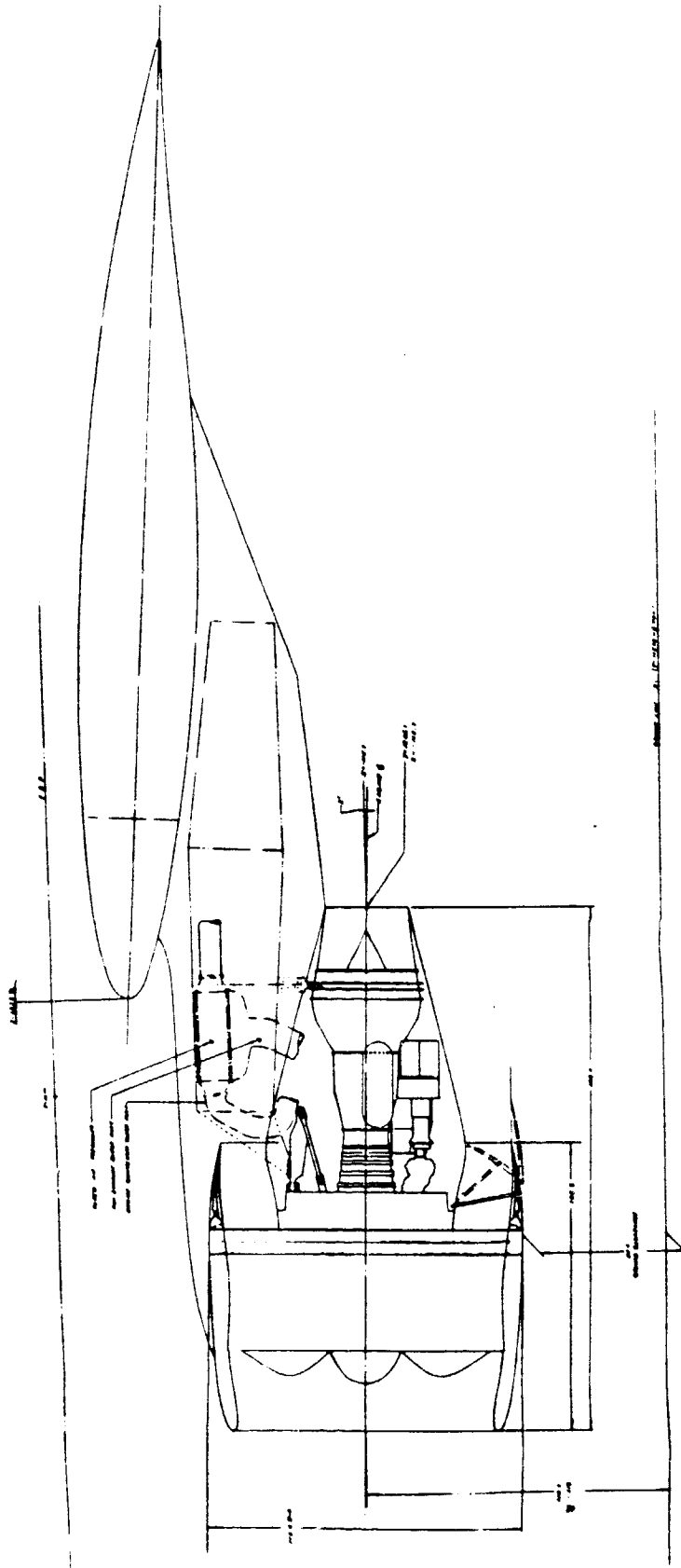
Figure 8   STF653   Advanced   Technology   Engine   with   Advanced   Technology,
Separate-Flow Nacelle

132
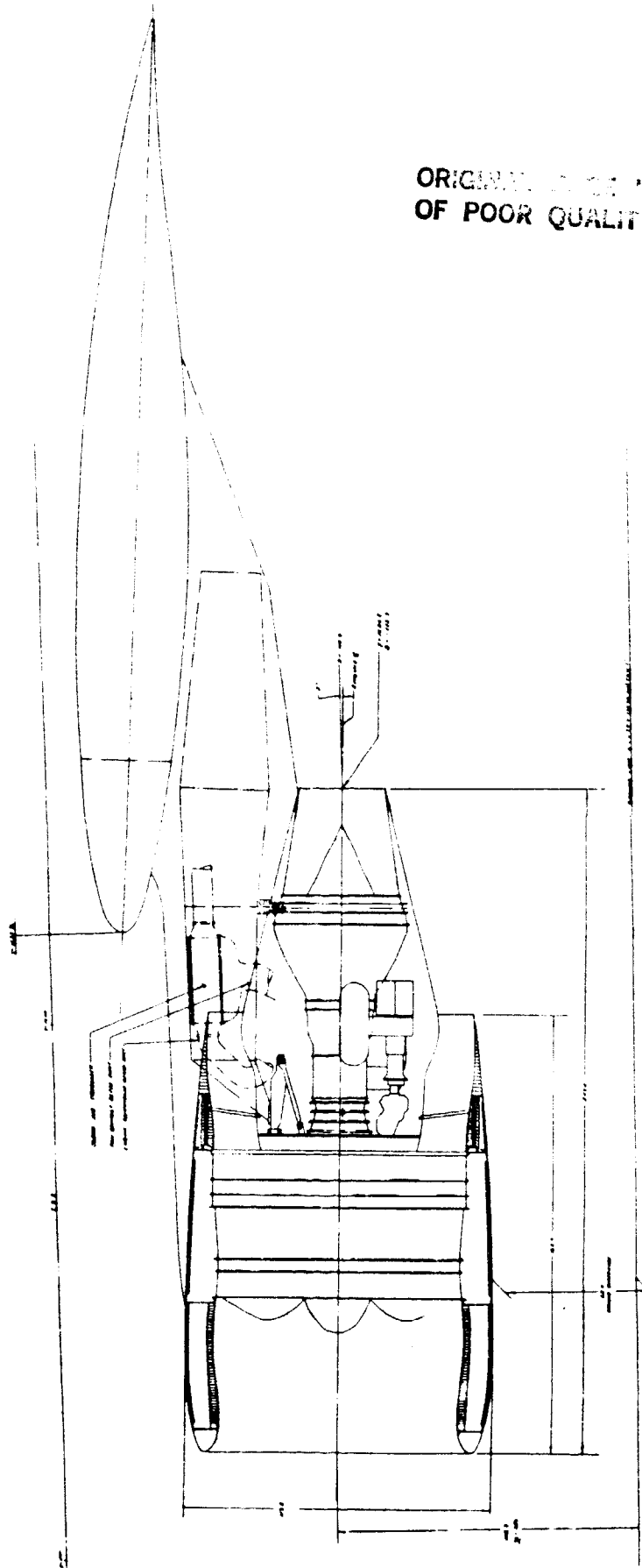
Figure 9   STF653-DD Advanced Technology Engine with Current Technology,
          Separate-Flow Nacelle
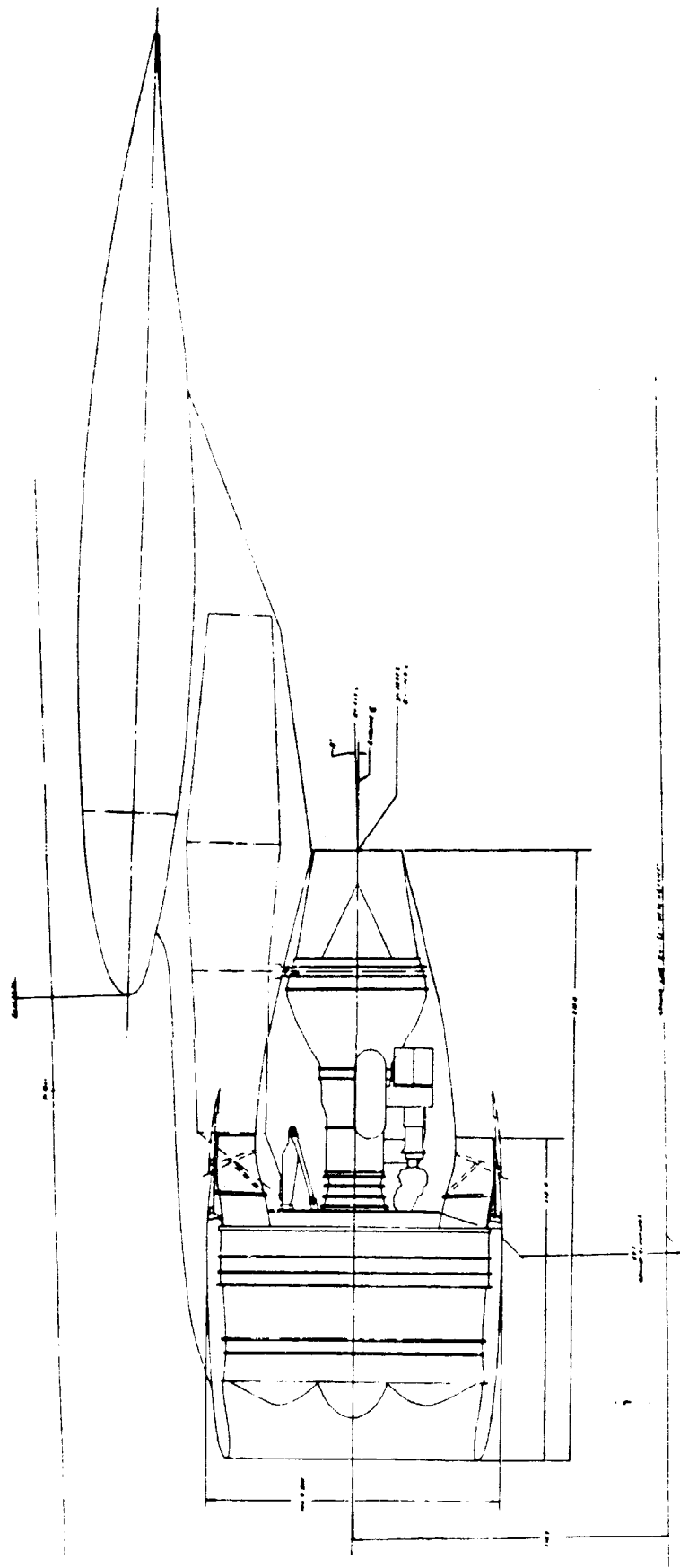
Figure 10   STF653 Advanced Technology Engine with Advanced Technology, Separate-Flow Nacelle
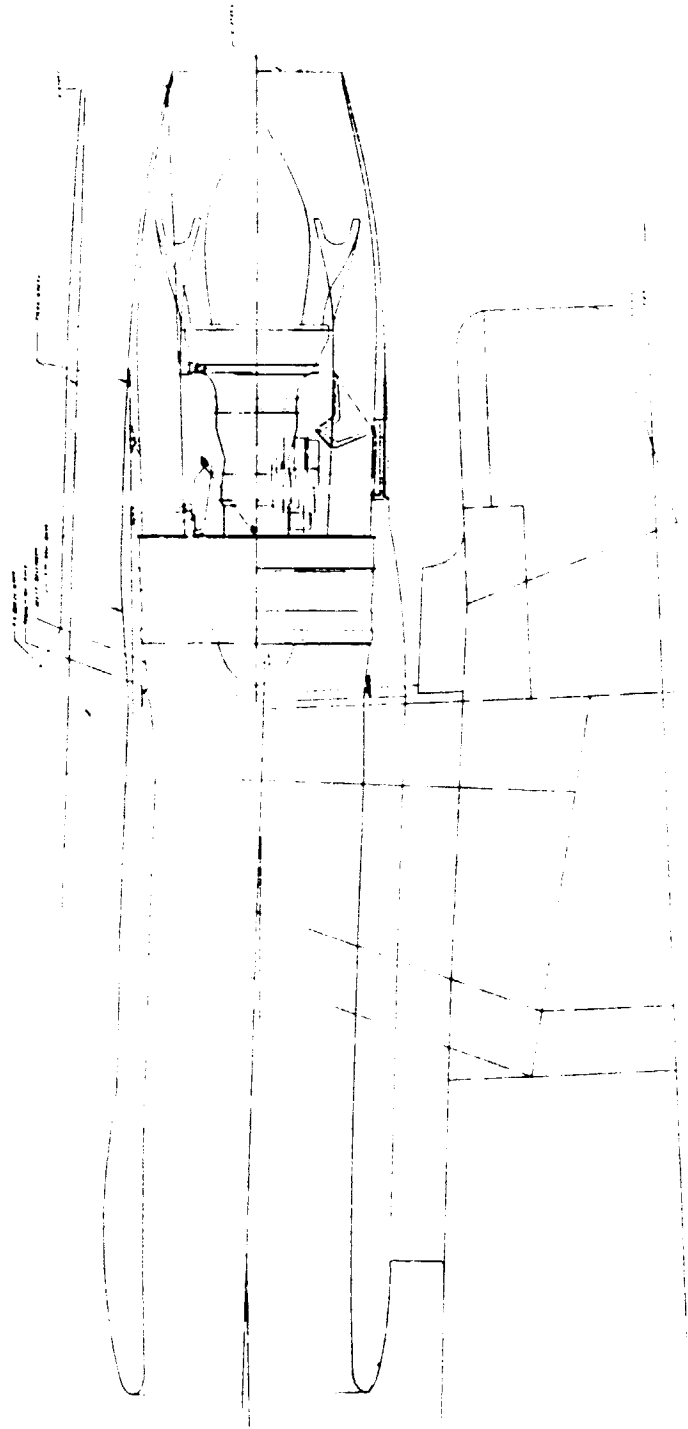
Figure 11   STF631 Reference Engine with Tail-Mounted, Mixed-Flow Configuration

135
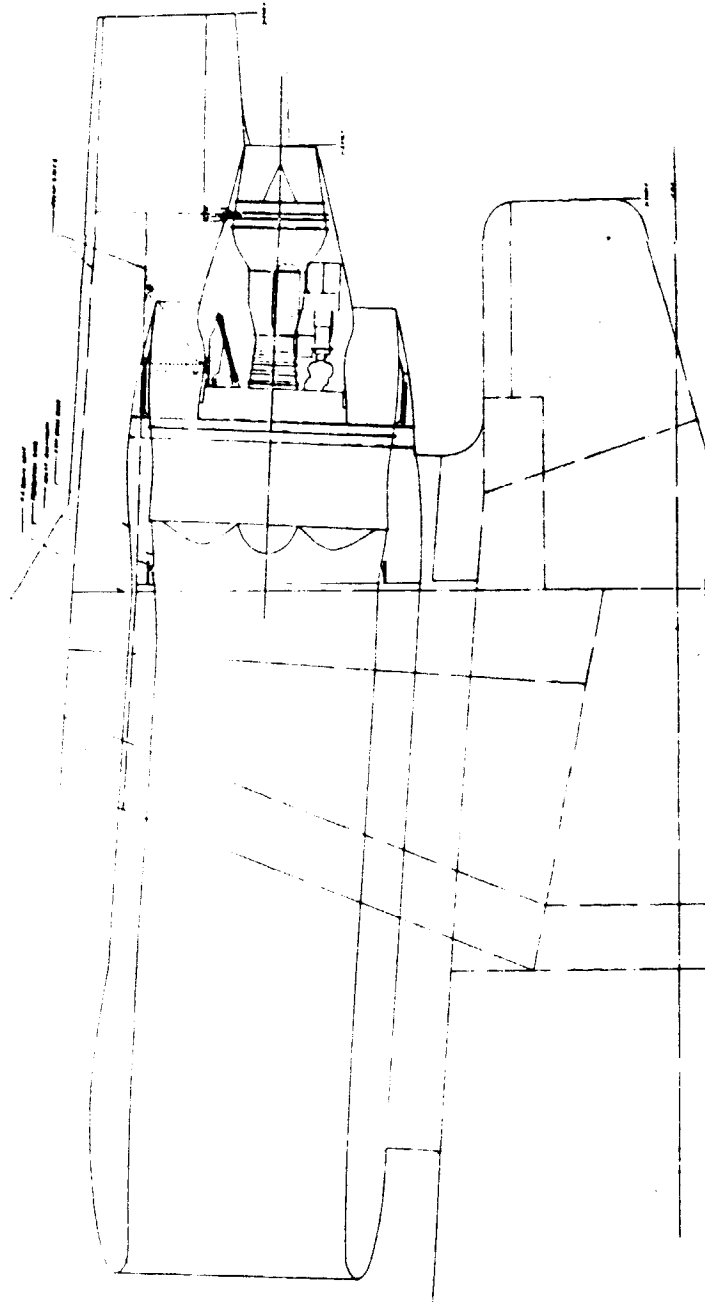
Figure 12 STF653 Advanced Technology Engine with Tail-Mounted, Current Technology, Separate-Flow Nacelle

136
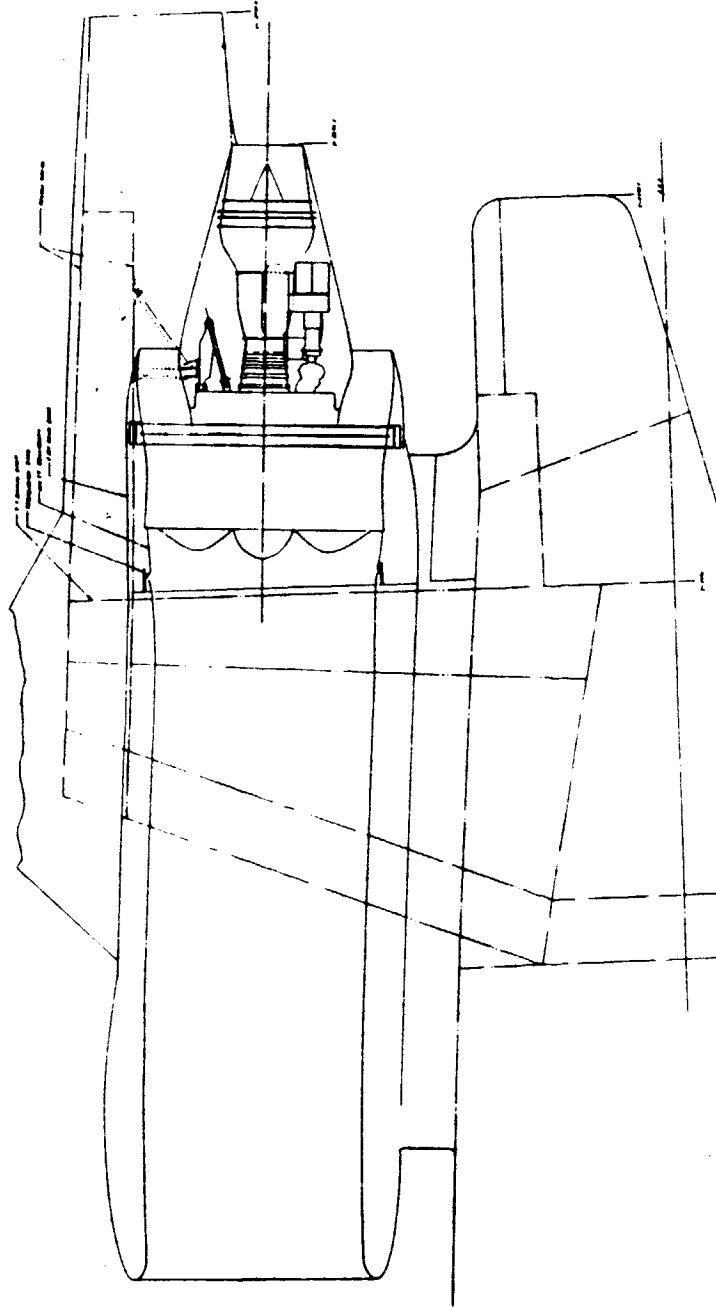
Figure 13   STF653   Advanced   Technology   Engine   with   Tail-Mounted,   Advanced
Technology, Separate-Flow Nacelle

137
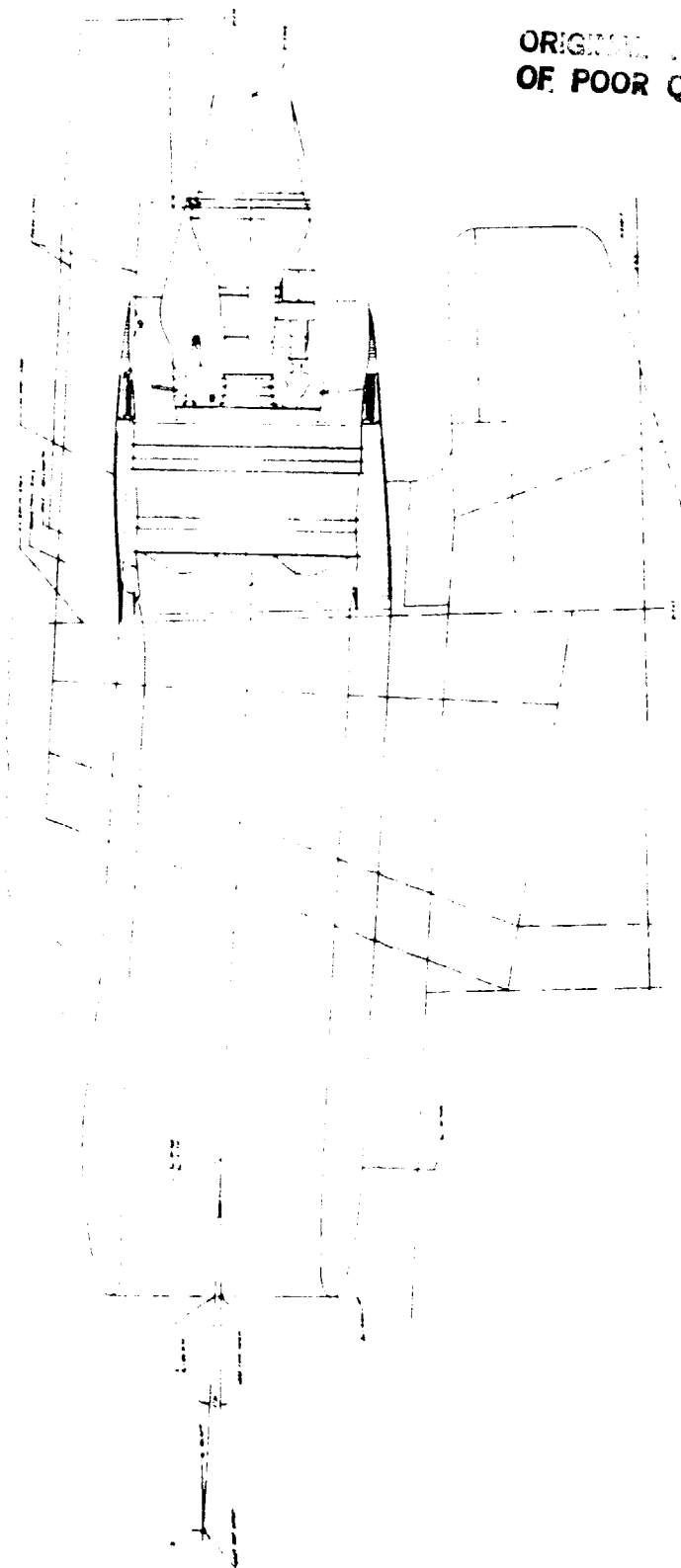
Figure 14   STF653-DD Advanced Technology Engine with Tail-Mounted, Current
Technology, Separate-Flow Nacelle

138
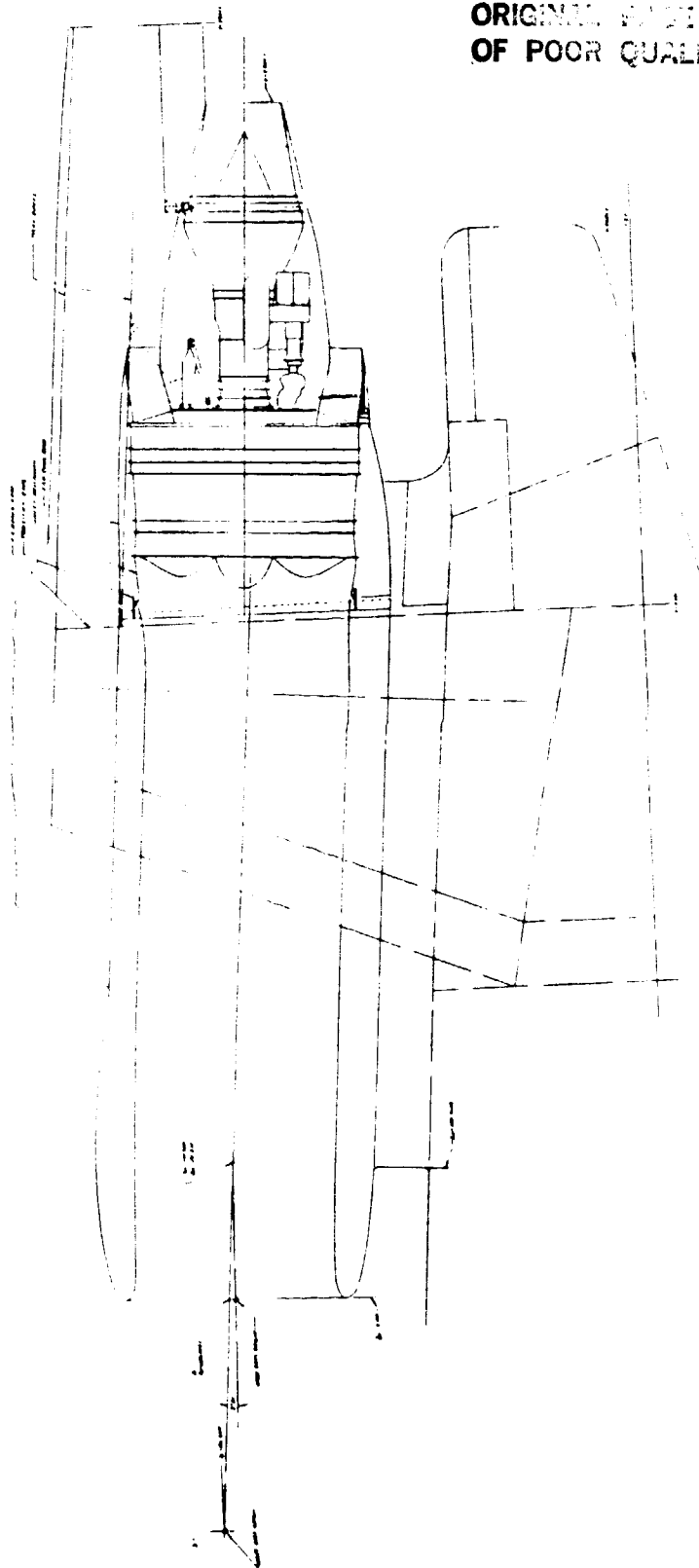
Figure 15 STF653-DD Advanced Technology Engine with Tail-Mounted, Advanced
Technology, Separate-Flow Nacelle

139

3.4. ADVANCED TECHNOLOGY REQUIREMENTS

Achieving the maximum benefit from target engines requires a high efficiency nacelle and high efficiency installation. This requires improved integration between the engine and airframe systems and requirements. A number of examples have been identified and described below.

3.4.1 INTERFERENCE DRAG

Figures 16 and 17 show the profile relationships of the study installations. With these higher bypass ratio installations, the fan exhaust flow effects will become larger than occurs with current high bypass ratio engines.

Figure 18 shows the positioning non-dimensionally comparing the study installations with current aircraft. The use of supercritical airfoils in advanced aircraft exacerbates the channel flow problem in the wing/pylon/nacelle intersection. Tests conducted by NASA have shown that use of a long duct with the supercritical wing results in higher drag levels for the same positioning. The higher bypass ratio of the STF653 introduces uncertainty because of the increased effect of the exhaust flow. Since the complex flow field cannot be accurately analyzed, an experimental data base needs to be established.

3.4.2 ADVANCED TECHNOLOGY INLETS

The inlets for the advanced nacelles have thin inlet cowls, thin inlet lips and short inlet duct lengths optimized for cruise conditions. Current designs are compromises for off-design-point operation. Current inlets are designed to maintain low pressure distortion on the fan face throughout the operating envelope including during static operation with cross wind, and with wing induced upwash during climb out. The use of protective devices such as blow-in-doors has been avoided in recent designs because of their adverse effects on noise. Cowling flow separation at low mass flow ratios and at high angles of attack also needs to be avoided because of the resultant buffeting and high drag levels. An analytical/experimental program is needed for the advanced nacelles to establish the means by which the high cruise efficiency designs will be made suitable for conditions which include:

     (1) Cross flow (upwash and crosswind)
     (2) Static operation
     (3) Buffet free operation throughout the operating envelope
     (4) Off-design drag
     (5) High noise environment
     (6) Inlet noise attenuation
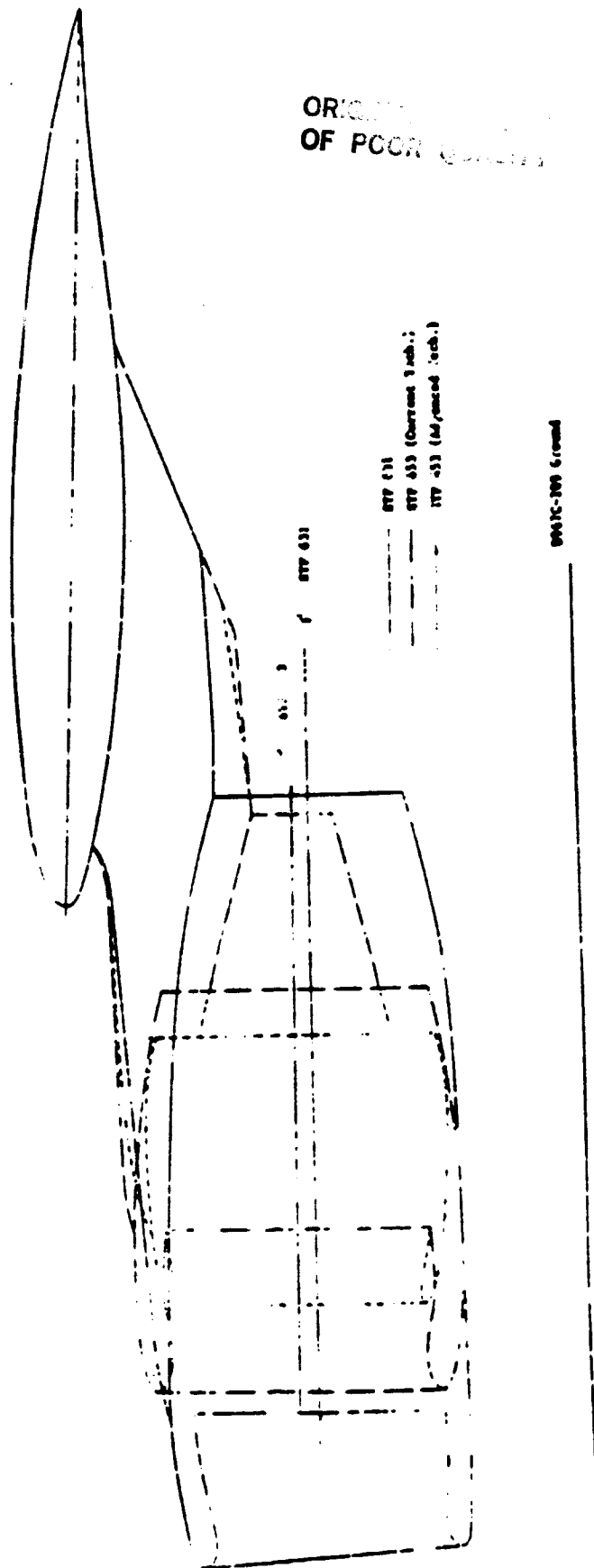
Figure 16 Wing Nacelle Comparison: STF 631 and STF 653
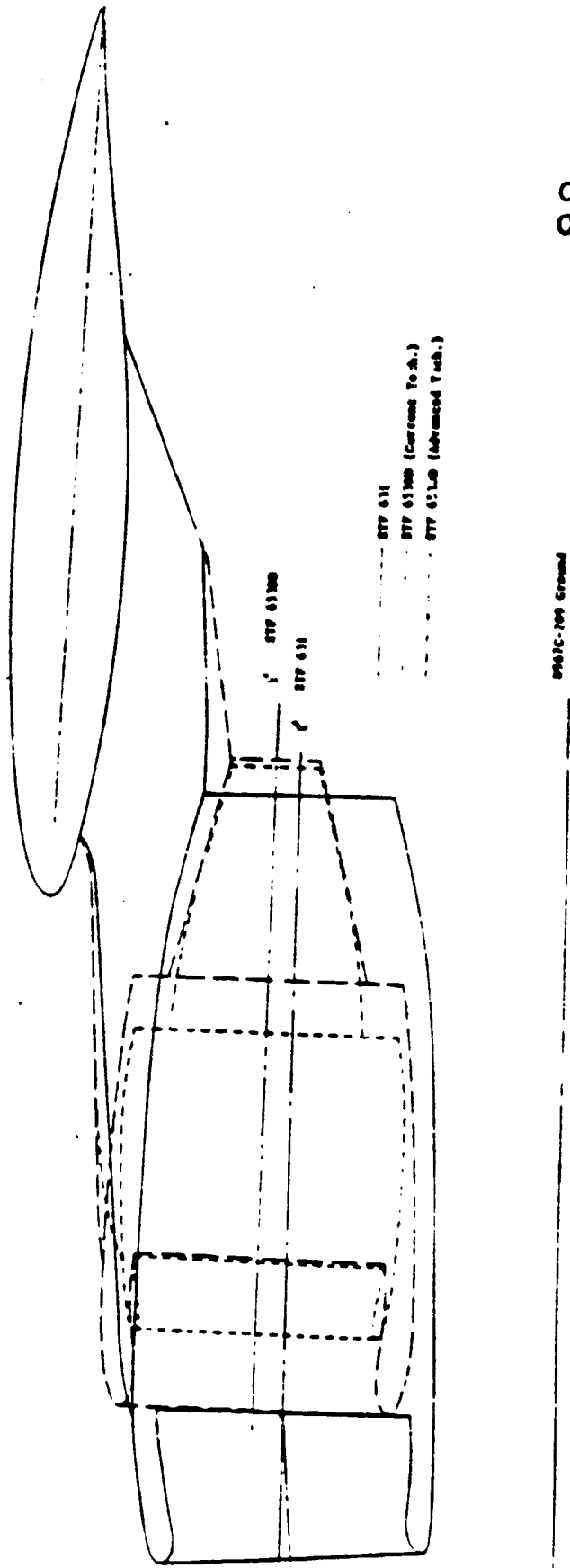
Figure 17 Wing Nacelle Comparison: STF 631 and STF 653DD
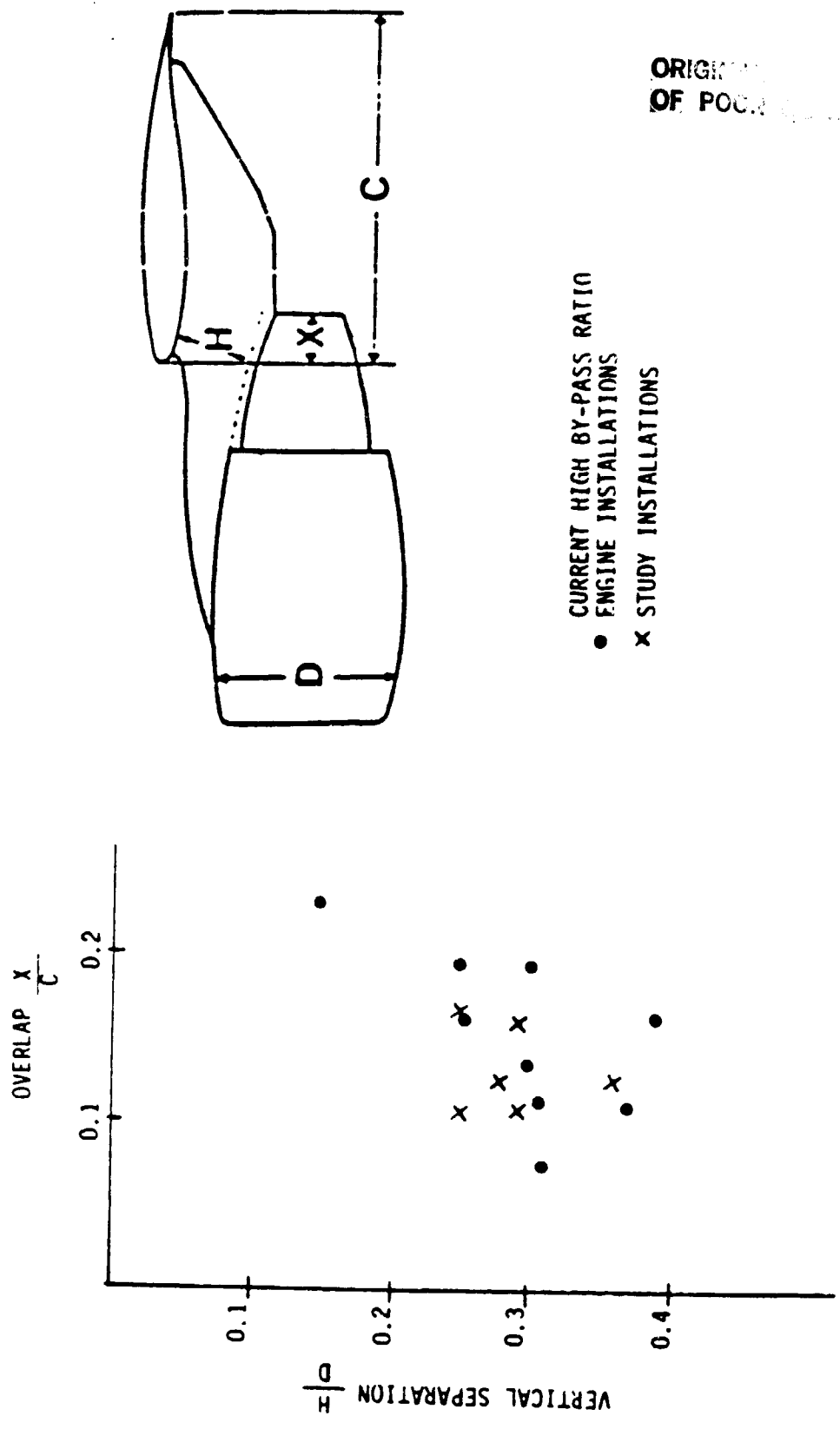
Figure 18   Wing/Engine Relationships

3.4.3 LOW VOLUME THRUST REVERSER

A key element in enabling use of higher bypass ratio engines most effectively is the short, tightly wrapped nacelle. The short nacelle in turn requires new thrust reverser concepts. The high bypass ratio engines, when first introduced in commercial transport aircraft, used fan flow reversers and core flow spoilers. Initial operational experience showed that the core flow spoilers, which were subjected to a high temperature environment, had poor reliability and high maintenance costs. The retarding capability of cascade type fan reversers was determined to be satisfactory without the core flow spoilers, and, subsequently, most operators removed the core flow spoilers. Later design high bypass ratio engine installations use fan-only reversing.

The cascade type of reverser allows a high degree of reverse flow directional tailoring while maintaining thrust reversing effectiveness at acceptable levels. Initially, translating cowl, fixed cascade, and translating cowl with translating cascade reversers were used. The translating cascade reverser allows a shorter fan cowl but does not lend itself to an installation where the engine is easily accessible and the engine can be removed with the reversers remaining on wing. Current maintainability standards require the easy access and engine removal features which have been included in all recent installations. An advanced reverser concept is needed which includes the necessary maintainability features and allows a short fan cowl.

A simple comparison of net reverse thrust, as shown in Figure 19, between a current engine with a bypass ratio of about 5 and an advanced engine with a bypass ratio of 10, shows that the fan reverser effectiveness can be significantly lower to produce the same retarding force. However, the advanced engine will be used on an advanced airframe and an assessment needs to be made of reversing characteristics needed for equal safety. The drag characteristics of an advanced airplane with the advanced engine on an icy runway need to be evaluated.

144
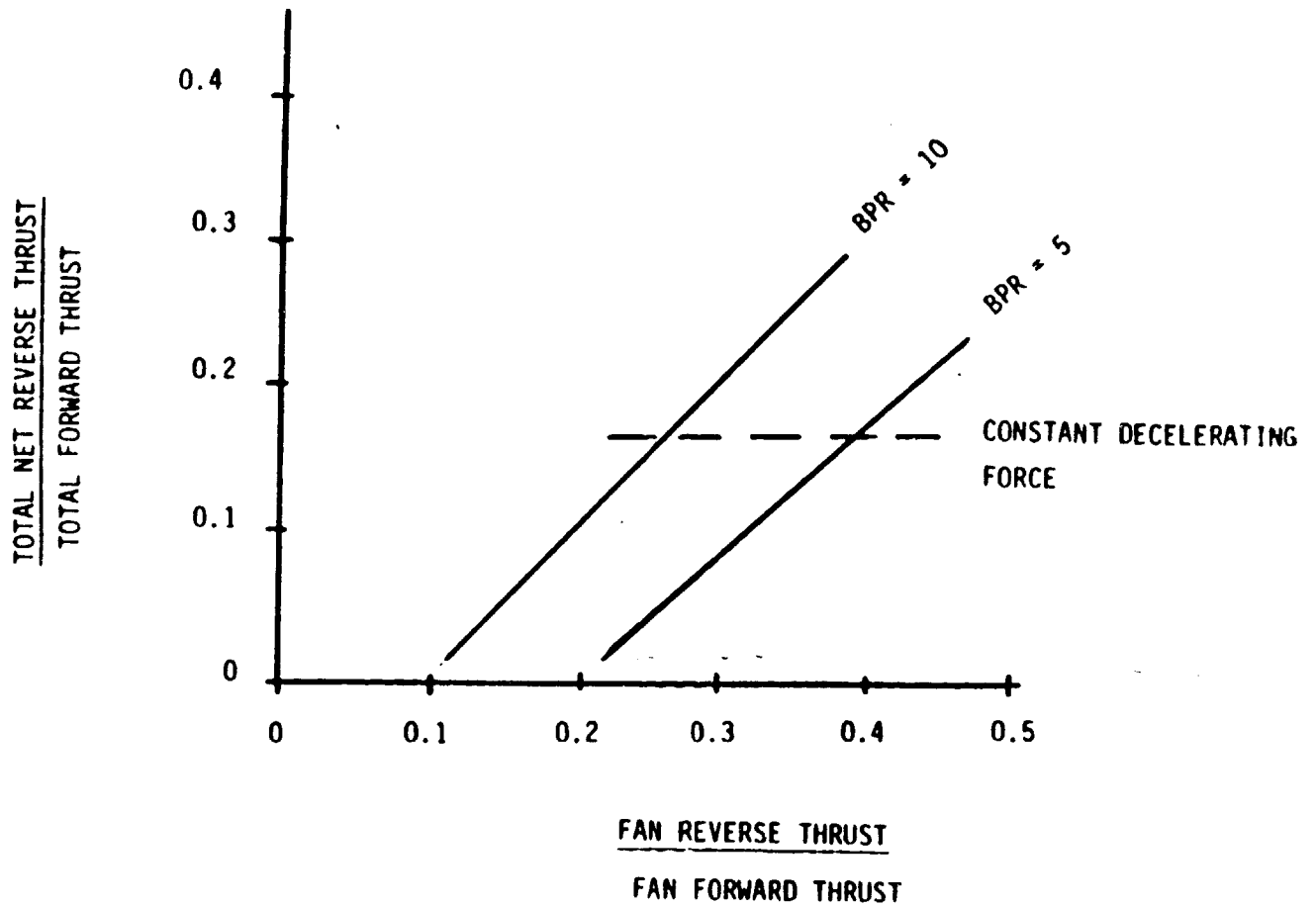
Figure 19 -- Overall Reversing Effectiveness

In current thrust reverser designs using cascades to control flow directivity, directivity is used to minimize re-ingestion, minimize F.O.D., avoid interference with fuselage mounted static taps used for air speed measurement, and to direct flow away from high lift devices since these also have high drag which is desirable during decelerations.

Minimizing nozzle length requires minimizing the length required for thrust reversers. The use of short thrust reversers requires minimizing the flow directivity control needed and minimizing the flow turning.

Since fan cowl lengths are determined by reverser configuration requirements, technology advancements for shorter reversers that occupy a minimum volume are needed. The low volume reverser would allow minimum length and cowl diameter. The initial phase of a reverser technology development needs to establish requirements. Advanced aircraft are expected to have higher lift to drag ratio during landing and, therefore, require additional retarding force for the same airplane deceleration. The higher bypass ratio engines have larger diameters with increased mass flows making F.O.D. considerations possibly more important. Improvements in predicting the occurrence of and developing criteria for re-ingestion and F.O.D. need to be included in the overall technology development.

Analytic method and experimental data base development are believed necessary. These efforts should be joint airframe and engine company activities.

3.4.4 INTEGRATED ENGINE/AIRFRAME POWER SYSTEMS

The advanced engines require improved integration of the non-propulsive power systems. Improvements are needed to adapt non-propulsive systems to tightly wrapped nacelles and reduce power extraction penalties while addressing the characteristics of the advanced engine cycles. For example, current auxiliary power units (APU's) are sized by the pneumatic power required by the environmental control system on the ground. These systems, however, are expected to be more efficient on future aircraft resulting in a lower power demand on the APU. On the other hand, the power required for starting the main engines is increasing. The trend with engine cycle pressure ratio is shown in Figure 20. It is expected that the advanced turbofans with overall cycle pressure ratios greater than 50 will result in the APU being sized by the power required for engine starting. The usage for engine starting is for a relatively short time. This means that most of the usage time for the APU would be at reduced power for operation of the environmental control system. Current APU's have a relatively poor specific fuel consumption at the design point but are much worse at reduced power.

Another consideration is the effect of higher cycle pressure ratios on the windmill start envelop. A number of incidents of all engine shutdowns followed by re-lights have occurred. In some cases, windmill starting resulted in restoration of engine thrust. For future installations, as a minimum, the current safety levels must be maintained. The inflight starting characteristics must therefore be investigated. Figure 21 shows trend data on the minimum speed for windmill starting versus engine pressure ratio. A continuation of this trend could result in the need for in-flight starter assist following all in-flight flame-outs.

146

The specific technology development requirements need to be determined. An initial requirements evaluation would be a joint engine/airframe company study. The engine company first estimates the ground and in-flight starting characteristics of advanced engines. Improved prediction method development may be required as an initial step. These data then are reviewed by an airframe company and the suitability evaluated. The engine and airframe companies then identify improvement approaches, if necessary.
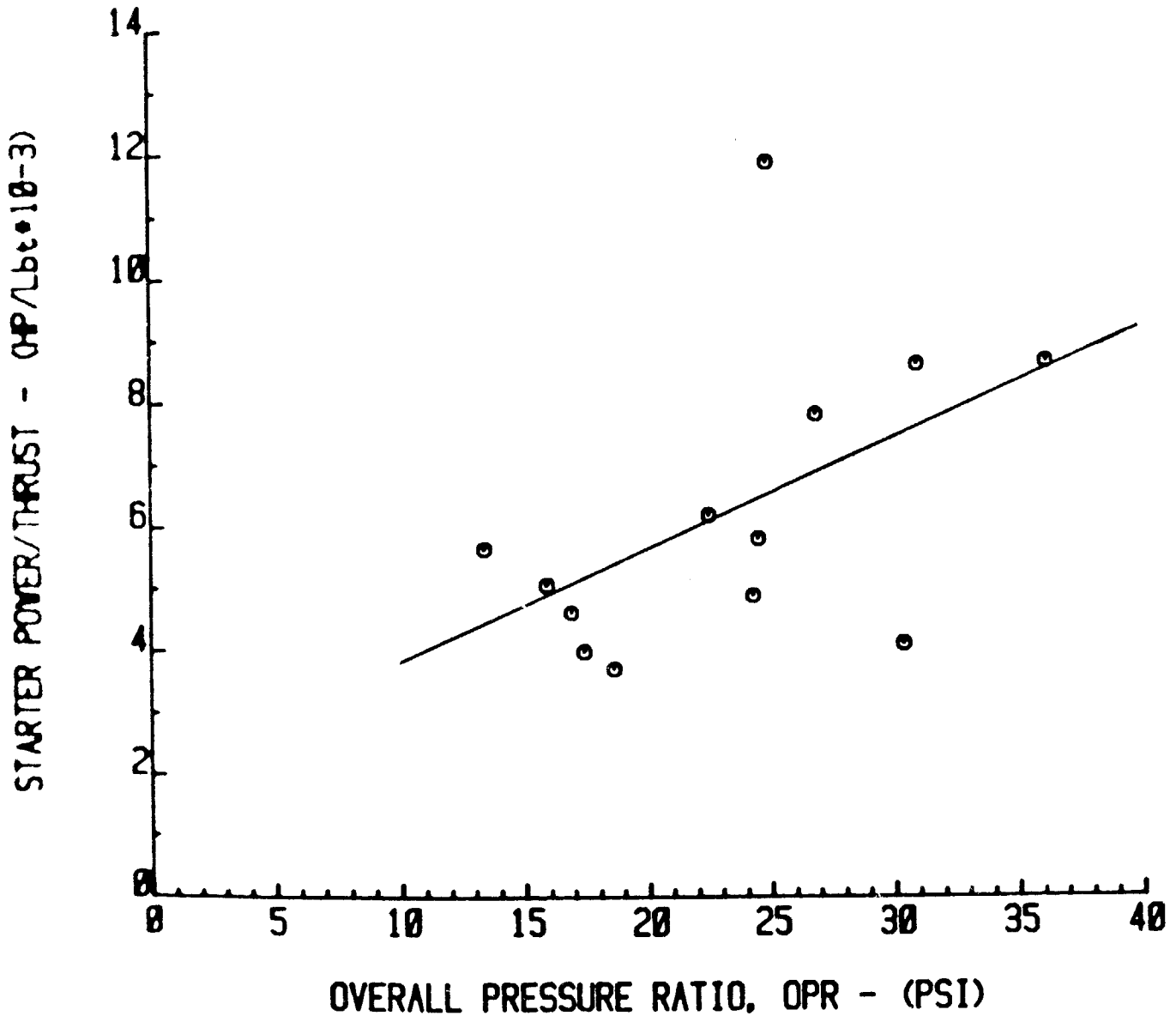
Figure 20 Effect of Overall Pressure Ratio on Engine Starting Power Requirement: 45 Second Start
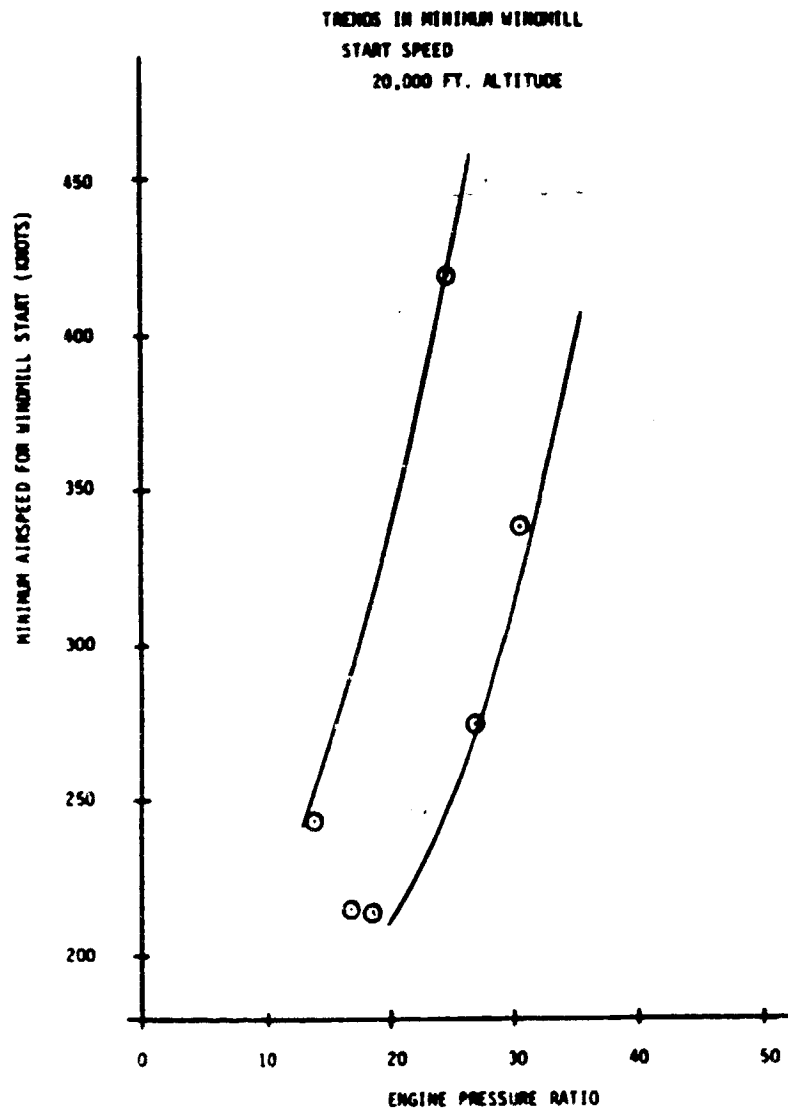
Figure 21   Trends in Minimum Windmill Start Speed: 20,000 Feet Altitude

3.4.5 ENERGY EFFICIENT ENVIRONMENTAL SYSTEMS

Electric, hydraulic and pneumatic power is needed to operate aircraft systems. Electric and hydraulic power are generated by shaft power from the engine while pneumatic power is derived from engine bleed. The time average power usage for a current wide body tri-jet is shown in Figure 22.

The electrical power usage is twice that for hydraulic power. The pneumatic power usage, however, is almost an order of magnitude larger than the electrical power usage. Clearly, the area for efficiency improvement is pneumatic power. In addition to efficiency considerations, as the bypass ratio increases, the quantity of bleed available decreases. Advanced aircraft studies show that a bleed availability problem occurs for ice protection which is exacerbated by the higher aspect ratio wing and larger diameter inlets with lower thrust levels at low speeds during icing conditions. Because current technology aircraft secondary power systems impose excessive performance penalties and the installations requirements are not compatible with the advanced nacelles, alternative improvement approaches need to be explored, and the technology base to allow use of the advanced engines in the most efficient way needs to be developed.

The largest in-flight pneumatic power usage is for cabin environmental control. The air cycle machine is currently used for this purpose. The air cycle machine is driven by engine bleed air. Engine bleed flow is compressed, cooled, and then expanded in a turbine which drives the compressor. The cold air from the expansion turbine discharge is mixed with hot bypass bleed air to provide the desired flow temperature. The air cycle machine provides cabin ventilation and temperature control on the ground and in flight. The air cycle machine is very efficient in terms of multi-function utilization of hardware but has a poor energy efficiency.

	TIME AVERAGE HORSEPOWER PER ENGINE	PERCENT OF TOTAL
HYDRAULIC	23	0.19
ELECTRICAL	49	0.41
PNEUMATIC	300	3.0
ENGINE THRUST POWER	11,592	96.4
TOTAL	11,964	

Figure 22   Wide Body Transport Cruise Secondary Power Usage

At a typical cruise condition, the flow path of the environmental control system starts from ambient air which undergoes a ram pressure rise and then is compressed by the engine compressor. The engine has a highly efficient compressor, but the bleed extraction process is not efficient. In order to minimize the quantity of contaminants in the bleed flow, the bleed is extracted, and only the static pressure is recovered. A further pressure drop is introduced by going through a pressure regulator. The regulated flow then is processed by the air cycle machine, which compresses part of the flow, removes heat, and then lowers the temperature by going through an expansion turbine. This cold flow is mixed with hot bleed flow that bypasses the air cycle.

Relative to the end requirement for a cabin at 11 psia pressure and a temperature in the 70's, the flow is overpressurized and over heated and then partially overcooled with numerous pressure loss processes introduced. Use of a digitally controlled active system in which only the necessary flow conditioning is done should be much more energy efficient.

Alternative means to achieving a more efficient system should be explored, including a more efficient means to derive pneumatic power from the engine. Improving bleed extraction efficiency reduces the temperature for a given pressure and should reduce the size or eliminate the need for a precooler. This is very desirable with the advanced nacelle, because the volume is not available for extracting the fan flow for cooling, and because the precooler volume is excessive.

For ice protection, the NASA electro-impulse de-icing activities should continue. However, other means of ice protection are also possible, such as use of freeze point depressants, thermo heating and pneumatic boots. The concepts that use the least energy without adding another fluid-on-board that requires servicing are the electro-impulse and pneumatic boot methods. These are de-icing methods as compared to anti-icing. De-icing introduces additional considerations. If used on the inlet, or on the aircraft with engines downstream of surfaces employing ice protection, the limitations of ice ingestion by the engine are not known.

An assessment needs to be conducted and the technology developed for ice protection systems for use with advanced engines. The evaluation should give consideration to the effects of using laminar flow control or shock free aerodynamic concepts. The data base is needed to evaluate use of de-icing systems, and the technology development for reduced or no bleed ice-protection systems must be developed. The NASA electro-impulse de-icing activity should be continued, but additional areas need to be addressed. In addition, other technology options should be developed. A list of candidate items is shown below.

De-Icing Data Base

- o Ice particle characteristics from de-icing systems
- o Criteria/requirements/limitations for ice ingestion by engines
- o Effects of ice build up on inlet performance
- o Effects of Ice build up on nacelle drag
- o Effects of ice build up on aerodynamic characteristics of advanced wings.

4.0 CONCLUSIONS

The evaluation of the Pratt & Whitney Target Engines in both Current Technology and Advanced Technology Nacelles shows that major reductions in fuel burned are achievable. The larger diameter, higher bypass ratio engines can be installed in both wing and aft positions of wide body transports. Achieving the full benefit, however, requires improving aerodynamic, mechanical, and subsystem integration between the airframe and engine. Technology developments in these areas for the Target Engines would result in 23% improvement in fuel burned on long range missions when compared to the ME^4 baseline. Compared to currently available production engines, a 28% improvement would result.

Specific areas needing advancements include inlets and thrust reversers, secondary power systems and accessories. The installations must be made more compact and integrated with the engine more efficiently. The following areas require technology advancements:

HIGH EFFICIENCY NACELLE CONFIGURATIONS

o Wing/Pylon/Nacelle Configurations For Minimum Interference Drag
o Inlets for Very High Bypass Ratio Engines
o Low Volume Reverser/Nozzles for Very High Bypass Ratio Engines

HIGH EFFICIENCY INSTALLATION INTEGRATION

o Integrated Engine/Airframe Power Systems
o Energy Efficient Environmental Systems.

5.0 RECOMMENDATONS

Historically, the major improvements in transport aircraft have been paced by propulsion system developments. In the 1950's, the introduction of the jet engine brought increased speed, comfort (from higher altitude flight) and reliability. There were then step-wise improvements from using low and then high bypass ratio engines. The introduction of new engine technology has occurred from application to new, large, long range transports, where the cost for improvements in fuel consumption could be absorbed by increased passenger capacity -- fuel costs being a major fraction of the direct operating costs.

While considerable research and technology efforts are currently underway for advanced turboprops, including counter-rotating versions, these efforts are directed towards applications in small and medium size transports. The very large turboprops needed with static thrust levels greater than 50,000 lbs. are not foreseen until the moderate, 25,000 lbs. thrust level systems have established proven reliability over extended periods of service. Continuing turbofan technology advancements are therefore needed to maintain a U.S. technology advantage for large commercial and military aircraft into the 21st century.

In order to achieve the major reductions in fuel consumption potentially attainable for turbofan engines, broad technology advancements are needed. The necessary technologies should be aggressively developed through a focused effort such as the TARGET engine propulsion system. Engine component technology advancements are needed. Equally important is the need to develop high efficiency installation technologies.

APPENDIX B

List of Symbols and Abbreviations

APPENDIX B

LIST OF SYMBOLS AND ABBREVIATIONS

Symbol	Definition
AERO.	Aerodynamic
A_{FAN}	Fan Area
A_{HI}	Highlight Area
Alpha (α)	Angle, Angle of Attack
ALT	Altitude
$(AJCD)_{FAN}$	Fan Nozzle Effective Area
A_{JR}	Reverser Effective Area
ANU	Airplane Nose-up
A_{PRIM}	Primary Jet Area
APU	Auxiliary Power Unit
A_{TH}	Throat Area
Aux	Auxiliary
A_{WET}	Wetted Area
Beta (β)	Flow Angle or Discharge Angle
BPR	Bypass Ratio
C	Cascade Chord
C_D	Discharge Coefficient
CET	Combustor Exit Temperature
Cf	Surface Friction Coefficient
C.G.	Center of Gravity

Symbol	Definition (cont.)
cm	Centimeters
C_V	Nozzle Thrust Coefficient
DAC	Douglas Aircraft Company
D_C	Cascade Diameter
DD	Direct Drive (turbofan)
D_{EQUIV}	Equivalent Diameter
D_{FAN}	Fan Tip Diameter
D_{FCI}	Fan Exit Inside Diameter
D_{FCO}	Fan Exit Outside Diameter
D_{HI}	Highlight Diameter
DIA	Diameter
D_{MAX}	Maximum Diameter
D_{MAXCLR}	Maximum Diameter for Nacelle Clearance
DOC	Direct Operating Cost
DOC plus I	Direct Operating Cost plus Interest
D_{TI}	Low-Pressure Turbine Exit Inner Diameter
D_{TMR}	Mount Ring Diameter
D_{TO}	Low-Pressure Turbine Exit Outside Diameter
E^3	Energy Efficient Engine
EFF	Efficiency
EPNdB	Effective Perceived Noise-Decibels
FAR	Federal Air Regulation
F_G	Gross Thrust

156

Symbol	Definition (cont.)
FOD	Foreign Object Damage
F_u	Crew Utilization Factor
F_w	Airplane Speed/Gross Weight Factor
ft	Feet
h'	Radial Offset from the Fan Duct Inner Diameter at the Downstream End of the Reverser Throat Plane
H	Radial Offset from the Fan Duct Inner Diameter at the Upstream End of the Reverser Throat Plane
FPR	Fan Pressure Ratio
FN	Net Thrust
FN_{REV}	Net Reverse Thrust
gal.	Gallon
G/B	Gearbox
GW	Gross Weight
HPC	High-Pressure Compressor
HR	Hour
HYD	Hydraulic
ICAC	Initial Cruise Altitude
IDGS	Integrated Drive Generator System
in.	Inches
I.D.	Inside Diameter
ISO.	Isolated
K	Factor to Account for Compressor Bleed Margin and Blockage
km	Kilometers

Symbol	Definition (cont.)
L	Cascade Reverser Length
$L_{A/B}$	Afterbody Length
lbs.	Pounds
L_{CLR}	Location of Clearance Point
L_{COWL}	Cowl Length
L_{DUCT}	Fan Duct Length
L_{ENG}	Total Engine Length
L_{FAN}	Fan Case Length
L_{IN}	Inlet Length
L_{MAX}	Maximum Length
L_{NAC}	Nacelle Length
L_{MR}	Location of Mount Ring
LSAS	Longitudinal Stability Augmentation System
L_{TOT}	Total Length
L_R	Reverser Length
m	Meters
MAX.	Maximum
ME^4	Maximum Efficiency Energy Efficient Engine
MGTOW	Maximum Gross Takeoff Weight
M_{CR}	Cruise Mach Number
mi.	Miles
Mn	Mach number
N	Newtons
NACPERF	Nacelle Geometry and Performance

Symbol	Definition (cont.)
NASA	National Aeronautics and Space Administration
No.	Number
NM	Nautical Miles
N_R	Reverser Effectiveness
O.D.	Outside Diameter
OEW	Operating Empty Weight
OWE	Operating Weight Empty (same as OEW)
OPR	Overall Pressure Ratio
P_{AMB}	Ambient Pressure
PAX	Number of Passengers
PTD	Fan Duct Exit Total Pressure
PTE	Core Engine Exit Total Pressure
P_T	Total Pressure
q	Free Stream Dynamic Pressure
R	Radius
RAD	Radius
REL.	Relative
Rev.	Revision
R_{FAN}	Fan Radius
R_{HI}	Highlight Radius
R_{HUB}	Hub Radius
R_{MAX}	Maximum Radius
S/C	Cascade Pitch/Chord Ratio
STA	Station

Symbol	Definition (cont.)
st.	statute (mile)
STD	Standard
TEU	Trailing Edge Up
Theta (Θ)	Reverser Angle
TOFL	Takeoff Field Length
TSFC	Thrust Specific Fuel Consumption
V_J	Jet Velocity
VJD	Fan Duct Jet Velocity
VJE	Core Engine Jet Velocity
W_A	Actual Flow
W_C	Corrected Flow
W_{AF}	Fan Airflow
WAF	Airframe Weight
W_{AP}	Primary Airflow
W_{AT}	Total Airflow
W_{AT2}	Maximum Corrected Flow
WGT.	Weight

APPENDIX C

Distribution List

Distribution List

NASA Scientific and Technical Information
Facility
P.O. Box 8757
B.W.I. Airport, Maryland   21240
(10 copies)

NASA Headquarters
600 Independence Ave. SW
Washington, D. C. 20546
Attention: R/R.S. Colladay   RT-6

NASA Headquarters
600 Independence Ave. SW
Washington, D. C. 20546
Attention: RT/C.C. Rosen   RTP-6

NASA-Lewis Research Center
21000 Brookpark Road
Cleveland, Ohio 44135
Attention: RJP/L. Wright

NASA Headquarters
600 Independence Ave. SW
Washington, D. C. 20546
Attention: J. Facey   RTP-6

NASA-Lewis Research Center
21000 Brookpark Road
Cleveland, Ohio 44135
Attention: J.A. Ziemianski   MS 49-6

NASA-Lewis Research Center
21000 Brookpark Road
Cleveland, Ohio 44135
Attention: C.C. Ciepluch   MS 100-3

NASA-Lewis Research Center
21000 Brookpark Road
Cleveland, Ohio 44135
Attention: P.G. Batterton   MS 301-4

NASA-Lewis Research Center
21000 Brookpark Road
Cleveland, Ohio 44135
Attention: G.M. Sievers   MS 301-2

NASA-Lewis Research Center
21000 Brookpark Road
Cleveland, Ohio 44135
Attention: E.T. Meleason   MS 49-6
(10 Copies)

NASA-Lewis Research Center
21000 Brookpark Road
Cleveland, Ohio 44135
Attention: M.A. Beheim   MS-3-5

NASA-Lewis Research Center
21000 Brookpark Road
Cleveland, Ohio 44135
Attention: N.T. Saunders   MS-3-8

NASA-Lewis Research Center
21000 Brookpark Road
Cleveland, Ohio 44135
Attention: M.J. Hartmann   MS-3-7

NASA-Lewis Research Center
21000 Brookpark Road
Cleveland, Ohio 44135
Attention: J.C. Williams   MS-500-211

NASA-Lewis Research Center
21000 Brookpark Road
Cleveland, Ohio 44135
Attention: L.J. Kaszubinski   MS-86-2

NASA-Lewis Research Center
21000 Brookpark Road
Cleveland, Ohio 44135
Attention: L.J. Kiraly   MS 23-2

NASA-Lewis Research Center
21000 Brookpark Road
Cleveland, Ohio 44135
Attention: D.C. Mikkelson   MS 86-1

NASA-Lewis Research Center
21000 Brookpark Road
Cleveland, Ohio 44135
Attention: L.J. Thomas   MS 500-305

NASA-Lewis Research Center
21000 Brookpark Road
Cleveland, Ohio 44135
Attention: J.F. Groeneweg   MS 54-3

NASA-Lewis Research Center
21000 Brookpark Road
Cleveland, Ohio 44135
Attention: R.L. Davies   MS 105-1

NASA-Lewis Research Center
21000 Brookpark Road
Cleveland, Ohio 44135
Attention: R. H. Johns   MS 49-6

NASA-Lewis Research Center
21000 Brookpark Road
Cleveland, Ohio 44135
Attention: J.R. Mihaloew   MS 100-1

NASA-Lewis Research Center
21000 Brookpark Road
Cleveland, Ohio 44135   MS 5-9
Attention: L. Reid

NASA-Lewis Research Center
21000 Brookpark Road
Cleveland, Ohio 44135   MS 86-2
Attention: D.W.Drier

NASA-Lewis Research Center
21000 Brookpark Road
Cleveland, Ohio 44135
Attention: R.W. Niedzwiecki   MS 86-6

NASA-Lewis Research Center
21000 Brookpark Road
Cleveland, Ohio 44135
Attention: AFSC Liaison Office
                MS 501-3

NASA-Lewis Research Center
21000 Brookpark Road
Cleveland, Ohio 44135   MS 302-2
Attention: Army R&T Propulsion

NASA Ames Research Center
Moffett Field, CA 94035
Attention: 202-7/M. H. Waters
                        (2)

NASA Langley Research Center
Langley Field, VA 23365
Attention: Bob James
          Neil Driver
          L.J. Williams   (3)

NASA Dryden Flight Research Center
P.O. Box 273
Edwards, CA 93523
Attention: J. A. Albers

Department of Defense
Washington, D.C. 20301
Attention: R. Standahar 3D1089 Pentagon

Wright-Patterson Air Force Base
Dayton, Ohio 45433
Attention: APL Chief Scientist AFWAL/PS

Wright-Patterson Air Force Base
Dayton, Ohio 45433
Attention: E.E. Abell ASD/YZE

Wright-Patterson Air Force Base
Dayton, Ohio 45433
Attention: H.I. Bush AFWAL/POT

Wright-Patterson Air Force Base
Dayton, Ohio 45433
Attention: E.E. Bailey (NASA Liaison)
                AFWAL/NASA

Wright-Patterson Air Force Base
Dayton, Ohio 45433
Attention: R.P. Carmichael ASD/XRHI

Wright-Patterson Air Force Base
Dayton, Ohio 45433
Attention: R. Ellis ASD/YZN

Wright-Patterson Air Force Base
Dayton, Ohio 45433
Attention: W.H. Austin, Jr. ASD/ENF

Eustis Directorate
U.S. Army Air Mobility
R&D Laboratory
Fort Eustis, VA 23604
Attention: J. Lane, SAVDL-EU-Tapp

Navy Department
Naval Air Systems Command
Washington, D. C. 20361
Attention: W. Koven AIR-03E

Navy Department
Naval Air Systems Command
Washington, D. C. 20361
Attention: J.L. Byers AIR-53602

Navy Department
Naval Air Systems Command
Washington, D. C. 20361
Attention: E.A. Lichtman AIR-330E

Navy Department
Naval Air Systems Command
Washington, D. C. 20361
Attention: G. Derderian AIR-5302C

NAVAL AIR Propulsion Test Center
Trenton, NJ 08628
Attention   J. J. Curry
            A. A. Martino   (2)

USAVRAD Command
PO Box 209
St. Louis, MO 63166
Attention: Robert M. Titus (ASTIO)

Department of Transportation
NASA/DOT Joint Office of Noise Abatement
Washington, D.C. 20590
Attention: C. Foster

Federal Aviation Administration
12 New England Executive Park
Burlington, MA 18083
Attention: Jack A. Sain, ANE-200

Curtiss Wright Corporation
Woodridge, NJ 07075
Attention: S. Lombardo
           S. Moskowitz   (2)

Detroit Diesel Allison Div. G.M.C.
P.O. Box 894
Indianapolis, IN 46206
Attention: W. L. McIntire

AVCO/Lycoming
550 S. Main Street
Stratford, CT 06497
Attention: H. Moellmann

The Garrett Corporation
AIResearch Manufacturing Co.
Torrance, CA 90509
Attention: F. E. Faulkner

The Garrettt Corportion
AIResearch Manufacturing Co.
402 S. 36 Street
Phoenix, AZ 85034
Attention: Library

General Electric Co./AEG
One Jimson Road
Evendale, Ohio 45215
Attention: R.W. Bucy (3 copies)
           T. F. Donohue
                                    (4)

Pratt & Whitney Aircraft Group/UTC
Government Products Division
P.O. Box 2691
West Palm Beach, Fl 33402
Attention: B. A. Jones

AIResearch Manufacturing Co.
111 South 34th Street
P.O. Box 5217
Phoenix, AZ 85010
Attention: C. E. Corrigan
           (93-120/503-4F)

Williams Research Co.
2280 W. Maple Road
Walled Lake, MI 48088
Attention: R. VanNimwegen
           R. Horn   (3)
           Library

Teledyne CAE, Turbine Engines
1330 Laskey Road
Tolendo, Ohio 43612
Attention: R. H. Gaylord

General Electric Co./AEG
1000 Western Ave.
Lynn, MA 01910
Attention: R. E. Neitzel

Pratt & Whitney Aircraft Group/UTC
Commercial Products Division
East Hartford, Ct 06108
Attention: D. Gray

                MS-118-26

Douglas Aircraft Company
McDonnell Douglas Corp.
3855 Lakewood Boulevard
Long Beach, CA 90846
Attention: R. T. Kawai Code 36-41
           M. Klotzsche   (2)

Lockheed California Co.
Burbank, CA 91502
Attention: J. F. Stroud, Dept. 75-42
         R. Tullis, Dept. 75-21
                (2)

Federal Aviation Administration
Noise Abatement Division
Washington, D. C. 20590
Attention: E. Sellman AEE-120

Detroit Diesel Allison Div. G.M.C.
333 West First St.
Dayton, OH 45402
Attention: F.H. Walters

Boeing Commercial Airplane Co.
P.O. Box 3707
Seattle, WA 98124
Attention: P.E. Johnson   MS-9H-46

Boeing Commercial Airplane Co.
P.O. Box 3707
Seattle, WA 98124
Attention: D.C. Nordstrom MS-73-4F

Drexel University
College of Engineering
Philadelphia, PA 19104
Attention: A.M. Mellor

Brunswick Corporation
2000 Brunswick Lane
Deland, FL 32720
Attention: A. Erickson

166

END

DATE

FILMED

NOV 5 1990